FINAL REPORT

PROJECT A-770

PART I - THE EFFECT OF DUNES UPON LOCALIZED SCOUR

By: M. R. Carstens

Contract No. N600(24)-59885

31 December 1965

Engineering Experiment Station
GEORGIA INSTITUTE OF TECHNOLOGY
Atlanta, Georgia

FINAL REPORT

PROJECT A-770

PART I - THE EFFECT OF DUNES UPON LOCALIZED SCOUR

By: M. R. Carstens

Contract No. N600(24)-59885

31 December 1965

TABLE OF CONTENTS

LIST OF TABLES

LIST OF FIGURES

NOMENCLATURE

The following symbols have been adopted for use in this paper:

D = cylinder diameter;

D_g = mean grain diameter of sediment;

f = denotes "function of";

g = acceleration of gravity;

L = reference dimension to characterize flow pattern;

N_s = sediment number, $V/\sqrt{(s-1)gD_g}$;

N_{sc} = value of sediment number at limit of zero transport;

S = scour depth and settlement depth;

S_c = scour depth if the top of the cylinder is at dune-crest elevation;

S_t = scour depth if the bottom of the cylinder is at dune-trough elevation;

$S_{initial}$ = initial burial;

s = ratio of solids density to fluid density;

T = period of oscillatory motion;

t = time;

U_m = maximum velocity at bed level in oscillatory flow;

V = reference velocity;

γ = specific weight of fluid;

γ_s = specific weight of sediment;

η = dune amplitude;

λ = dune wave length;

ρ = fluid density;

ρ_s = bed-material density;

σ_g = geometric standard deviation (sediment diameter); and

ϕ = angle of repose.

INTRODUCTION

This study is concerned with the effect of dunes upon localized scour which occurs as water is moved past an obstruction in the stream. Specifically this study is to determine the effect of dunes upon localized scour which occurs around a horizontal cylinder placed upon the bed under an oscillatory flow.

In a previously submitted report[1] similarity criteria for localized scour were developed and were demonstrated using the experimental results of five different scouring situations; namely, (a) in a defined scour hole, (b) by two-dimensional dunes, (c) by a two-dimensional jet, (d) around a vertical cylinder, and (e) around a horizontal cylinder. A common analysis was shown to apply in all five scouring situations provided that (1) the flow pattern in the scour hole was not influenced by the free surface; (2) sediment was not transported into the scour hole from a distance as for example by littoral drift; and (3) the flow pattern in the scour hole was not influenced by bed forms such as dunes (ripples). In this restricted sense the similarity criterion for depth of scour is presented as

$$\frac{S/L}{(N_s^2 - N_{sc}^2)^{5/2}\,(D_g/L)(Vt/L)} = f\,(\text{obstruction geometry, sediment-grain geometry}) \qquad (1)$$

in which S is scour depth;

L is a reference length of the obstruction;

$N_s = V/\sqrt{(s-1)\,gD_g}$ is called the sediment number;

N_{sc} is the value of the sediment number at zero-transport;

---

[1] "Similarity-Localized Scour," Technical Report, Project A-770, October 1965 is appended to this report as APPENDIX B.

V is reference velocity of the fluid;

s is the ratio of densities of bed material and fluid;

g is acceleration of gravity;

D_g is mean diameter of the bed material; and

t is time.

Equation (1) is a statement that the scour-depth parameter is a function of the obstruction geometry and the sediment-grain geometry. The function must be determined experimentally for each obstruction. In addition the value of the zero-transport sediment number N_{sc} has to be determined experimentally for the particular obstruction and bed material.

The experimentally determined function, equation (1), is shown in Figure 13 of APPENDIX B for a horizontal cylinder lying on the bed under an oscillatory flow. The length-to-diameter ratio of the cylinder is four.

The object of this investigation is to determine the effect of dunes (ripples) upon the localized scour around this same cylinder. The existence of dunes can be expected to alter the flow pattern and hence the localized scour around the cylinder. The problem is that the magnitude of the scour around an object is a function of the size of the object whereas the size of the dunes is not. In other words with a duned bed a scale effect is introduced. Prior to analyzing this scale effect a summary of the knowledge of dune geometry is presented.

GEOMETRY OF DUNES

The following qualitative description of dune geometry is related in terms of increasing values of the maximum velocity U_m of the oscillatory flow at the bed level. At some velocity the originally flat bed becomes unstable and a symmetrical two-dimensional system of dunes will cover the

bed. At some higher value of the velocity the two-dimensional dune system begins to be transformed into a three-dimensional system in which the dune crests are somewhat irregular in plan and in which the dune crests are uneven in elevation. With an even higher value of the velocity the dune system appears to be a system of sand hills of differing elevations. Finally at an elevated value of the velocity the sand hills (dunes) are completely gone and the bed is again flat.

As of this date no acceptable theory has been presented with which to predict dune geometry as a function of the fluid, flow, and sediment variables. Numerous experimental results are available. However, the range of variables of the various experiments has been quite spotty. Before attempting to present the experimental results which are pertinent to this study, a discussion of the variables and the dimensionless form of these variables will be undertaken in order to explain the manner of presentation of the pertinent experimental results.

The dependent variables of dune geometry are amplitude η and wave length λ. The fluid-property variables are fluid density ρ and the fluid specific weight γ. The fluid specific weight γ is a variable because the stabilizing force of the bed particles is a function of the submerged weight which is proportional to $\gamma_s - \gamma$ or $\Delta\gamma$ in which γ_s is the specific weight of the sediment. The fluid viscosity has been omitted as a variable by virture of the negligible boundary layer thickness anticipated in the flow occurring over dunes.[2] The fluid flow variables would be the maximum velocity U_m at the bed level and the period T of the oscillatory motion. Alternately one

[2] A more complete justification for the elimination of viscosity is found in APPENDIX B, page 11.

could use the amplitude of the fluid motion at bed level and the period. The sediment-property variables are mean diameter D_g, geometric standard deviation σ_g with regard to size, particle shape, and specific weight of the sediment γ_s. The omission of the sediment density ρ_s is founded upon the idea that the inertial reaction of the sediment particles is insignificant in the movement of the bed grains. Since the two specific weights are involved in a known way, that is, by submerged weight, γ and γ_s can be replaced with a single variable $\Delta\gamma$. Thus

$$\eta \text{ or } \lambda = f\,(U_m,\ T,\ \rho,\ \Delta\gamma,\ D_g,\ \sigma_g,\ \text{particle shape}) \tag{2}$$

In dimensionless form

$$\frac{\eta}{D_g},\ \frac{\lambda}{D_g},\ \text{or}\ \frac{\eta}{\lambda} = f\left(T\sqrt{\frac{(s-1)g}{D_g}},\ \frac{U_m}{\sqrt{(s-1)gD_g}},\ \sigma_g,\ \text{particle shape}\right) \tag{3}$$

Inasmuch as this study was performed with a single bed material (D_g = 0.297 mm) and with a constant period (T = 3.54 ± 0.02 seconds), the pertinent experimentally determined results can be presented in a simplified form of equation (3); namely

$$\eta = f_1\left(U_m/\sqrt{(s-1)g\ D_g}\right) \tag{3a}$$

and

$$\lambda = f_2\left(U_m/\sqrt{(s-1)g\ D_g}\right) \tag{3b}$$

as shown in Figures 1 and 2. The measured maximum and minimum values are shown in Figures 1 and 2. The dune characteristics were determined during

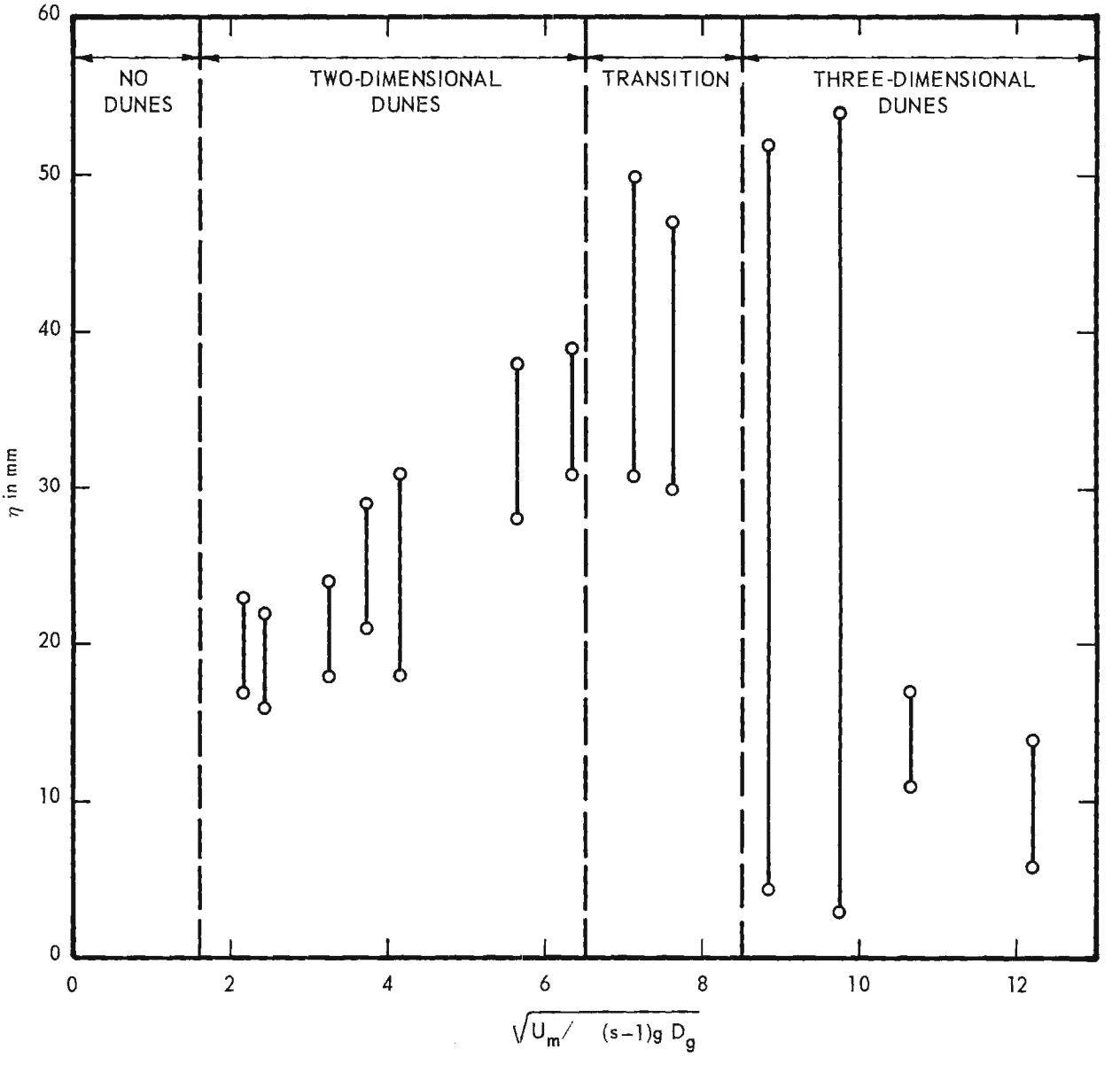

Figure 1. Amplitude of Dunes (D_g = 0.297 mm).

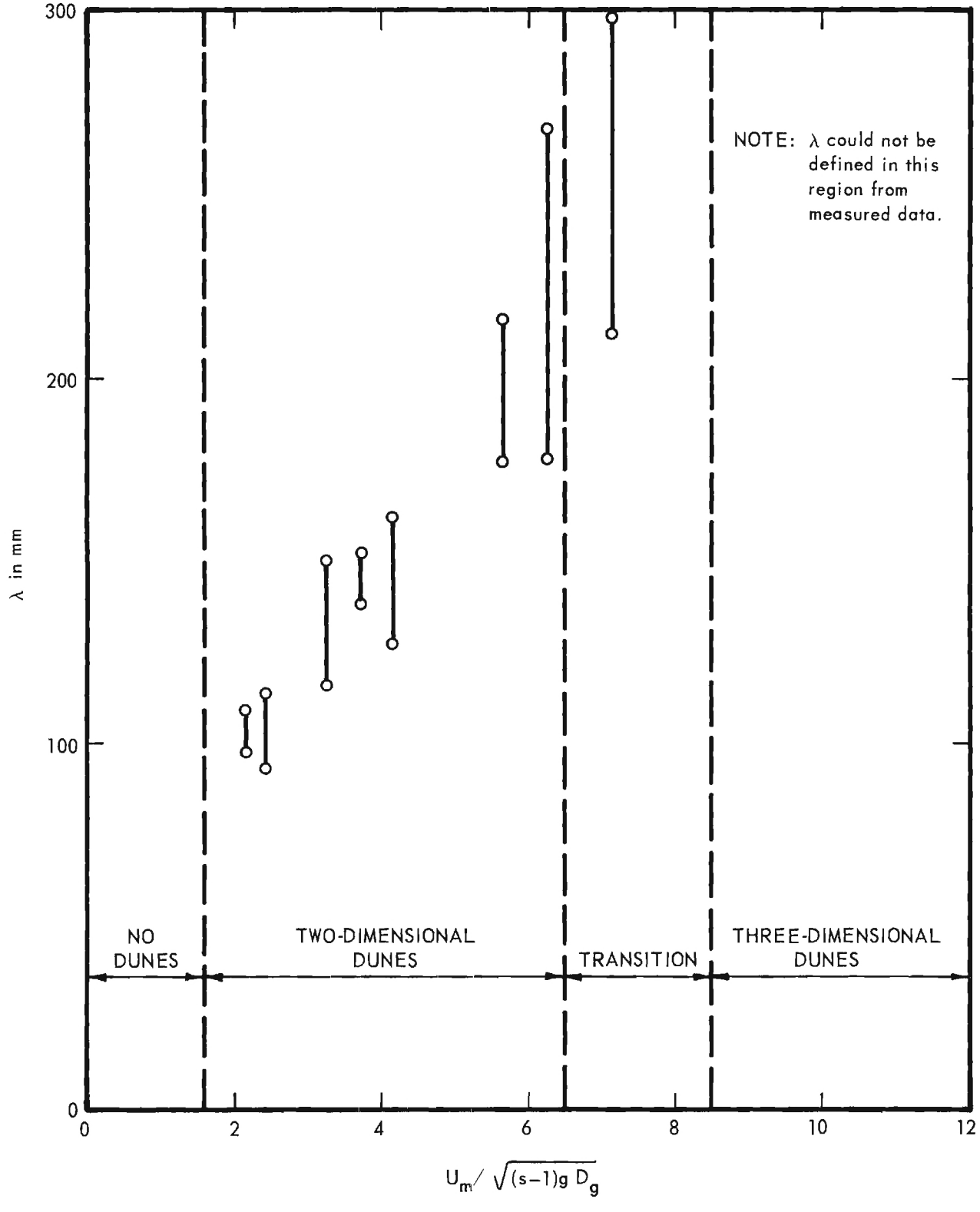

Figure 2. Wave Length of Dunes (D_g = 0.297 mm).

the execution of another study[3] currently being conducted in the Georgia Tech Hydraulics Laboratory. APPENDIX C is a description of the experimental apparatus and of the instrumentation. A description of the bed material is found on page 12 of APPENDIX B.

Other features of the dune system are noted in Figures 1 and 2 and are explained in the following. (A) No dune system will develop if $N_s < 1.6$. (B) In the range $1.6 < N_s < 6.5$ the dune system is two-dimensional with the dune crests being level, straight, and perpendicular to the direction of the water motion. Measured profiles of two-dimensional dunes are shown in Figure 3. (C) The range $6.5 < N_s < 8.5$ is designated as a transition region in which the two-dimensional dune system is progressively destroyed. (D) For $8.5 < N_s < 13$, the dune system is three-dimensional as shown in Figure 4. In the transition region and in the three-dimensional-dune region, the dune wave length is difficult to define. (E) For $N_s > 13$, the bed is flat with all of the uppermost bed particles in motion looking like a second fluid in motion underneath the moving water.

CYLINDER SCOUR PLUS DUNE SCOUR

Tests to determine the scour around a cylinder lying on a movable bed were performed in the U-tube water tunnel in the Georgia Tech Hydraulics Laboratory which is described in APPENDIX C. The test procedure is described on pages 28 and 29 of APPENDIX B. Test results of six runs in which the dunes were a negligible factor are shown in Figure 13 of APPENDIX B.

Inasmuch as the object of this study was to investigate the effect of dunes upon localized scour, a total of 35 tests were performed with cylinders

---

[3]The study of dunes is sponsored by the Coastal Engineering Research Center, Corps of Engineers, U.S. Army, Washington, D.C.--Contract No. DA-49-055-CIVENG-65-1.

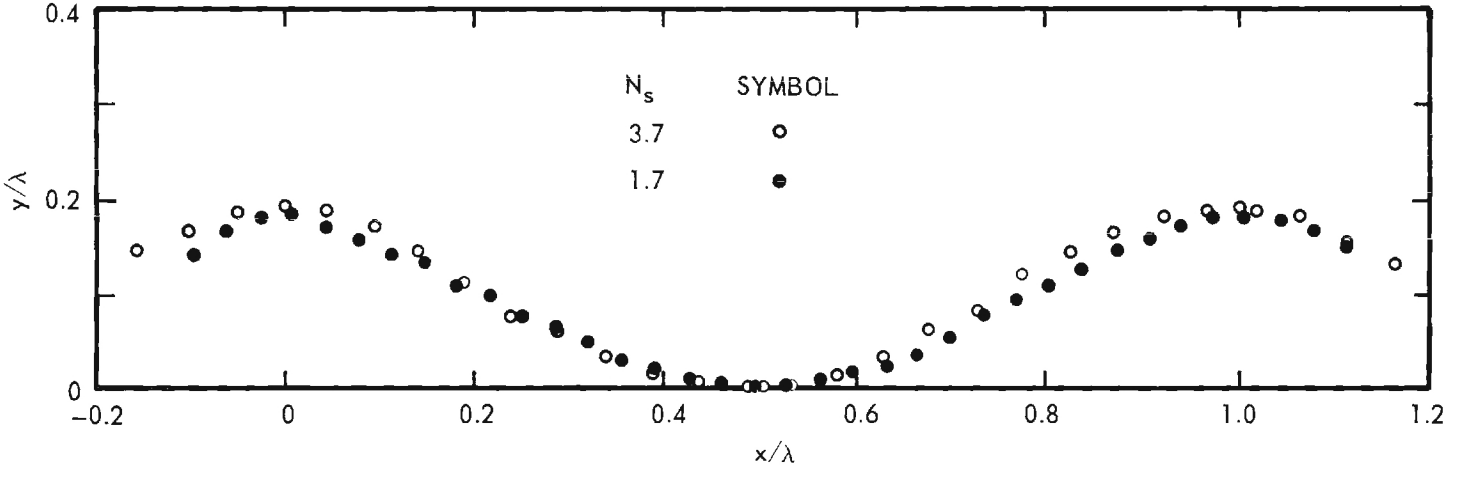

Figure 3. Cross Sections of Two-Dimensional Dunes (D_g = 0.297 mm)

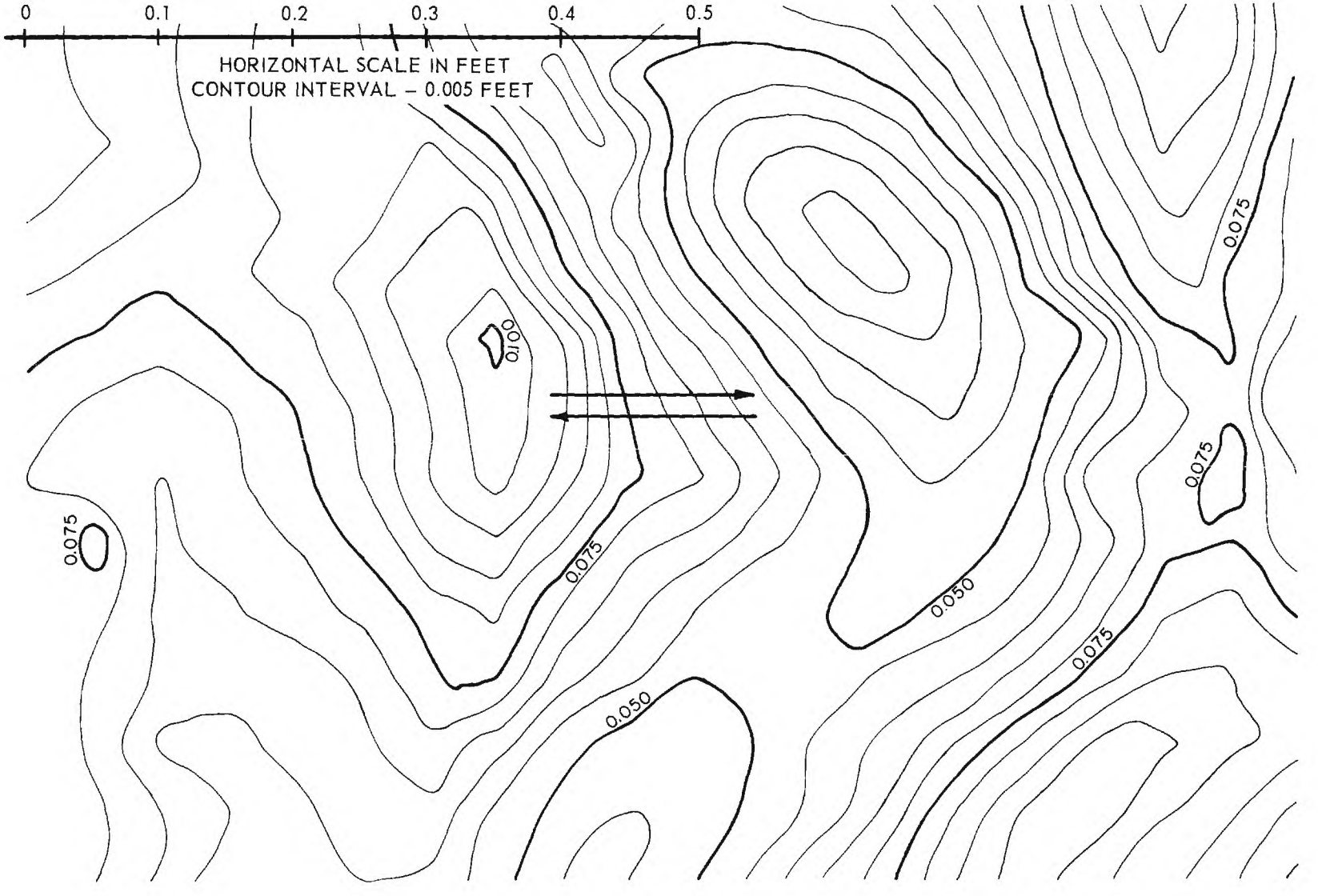

Figure 4. Topographic Map of Three-Dimensional Dunes (D_g = 0.297 mm, N_s = 10.5).

of three different diameters and throughout a range of duned bed conditions. The bed material was glass beads having the properties shown on page 12 of APPENDIX B. Each of the 35 tests was performed with an initially flat bed upon which the cylinder was placed. The same test procedure was followed in all of the 35 tests.

Results

The experimental results are shown in APPENDIX A as an Exhibit for each run. The right-hand ordinate of each Exhibit is a dimensionless parameter of burial in which S is the vertical distance from the initial bed level to the bottom of the cylinder. The left-hand ordinate is a measure of protrusion since D minus S is the vertical distance from the top of the cylinder to the initial bed level. The abscissa is a dimensionless time parameter which is derived in APPENDIX B. The values of the pertinent experimental variables and parameters are shown in the legend of each Exhibit. The other information shown in each Exhibit is for the purpose of analyzing the results.

The solid-line curve shown in each Exhibit is the empirically determined burial function for situations in which the dunes do not influence local scour around the cylinder. In other words, the solid-line curve shown in each Exhibit is the function shown graphically in Figure 13 of APPENDIX B.

The horizontal dashed line labelled S_c/D in each Exhibit is the burial that would exist <u>if</u> the top surface of the cylinder were at the same elevation as the crests of the dunes. This concept is clearly shown in Figure 5.

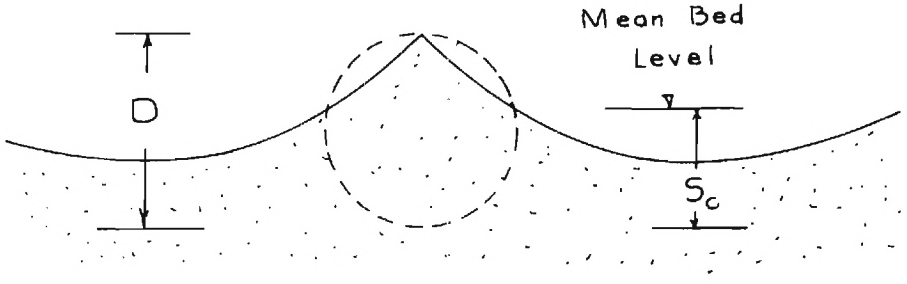

Figure 5. Definition Sketch of S_c

Dune crest elevation above mean bed level was determined from experimental results of the dune-geometry study mentioned previously.

The horizontal dashed line labelled S_t/D in each Exhibit is the burial that would exist <u>if</u> the bottom surface of the cylinder were at the same elevation as the troughs of the dunes. This concept is clearly shown in Figure 6.

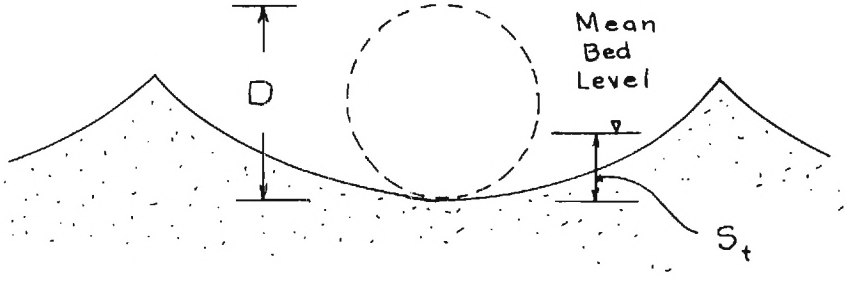

Figure 6. Definition Sketch of S_t

Dune-trough elevation below mean bed level was also obtained from experimental results of the dune-geometry study.

The vertical dashed line in the Exhibits (APPENDIX A) denotes the time required for the dunes to develop from the initially flat bed. The value for the time required for dunes to develop, t_d, was estimated from the data of the dune-geometry study. Values of t_d/T as a function of the sediment number N_s are shown in Figure 7. The data shown in Figure 7 were determined from the continuous amplitude record of each run. In each run the magnitude of the pressure pulse applied to the water surface in the west leg of the water tunnel (APPENDIX C) was fixed. Amplitude of the motion decreases as the dune system develops since resistance to the water motion increases as the dunes develop. The amplitude of the motion approaches a constant value when the dune system is completely developed. The time at which the amplitude of the water motion approached a constant value was taken as the time for dunes to develop, t_d.

Discussion of results

In order to discuss the test results shown in the Exhibits in an orderly manner, values of the significant parameters are summarized in Table 1.

Dune trough elevation. In column 9 of Table 1 the values of S/S_t are tabulated. This ratio is the scour depth below mean bed level divided by the vertical distance from mean bed level to the troughs of the dunes. In all tests with the largest cylinder, Exhibits 1 through 21, the value of S/S_t is greater than unity regardless of the value of N_s. The conclusion

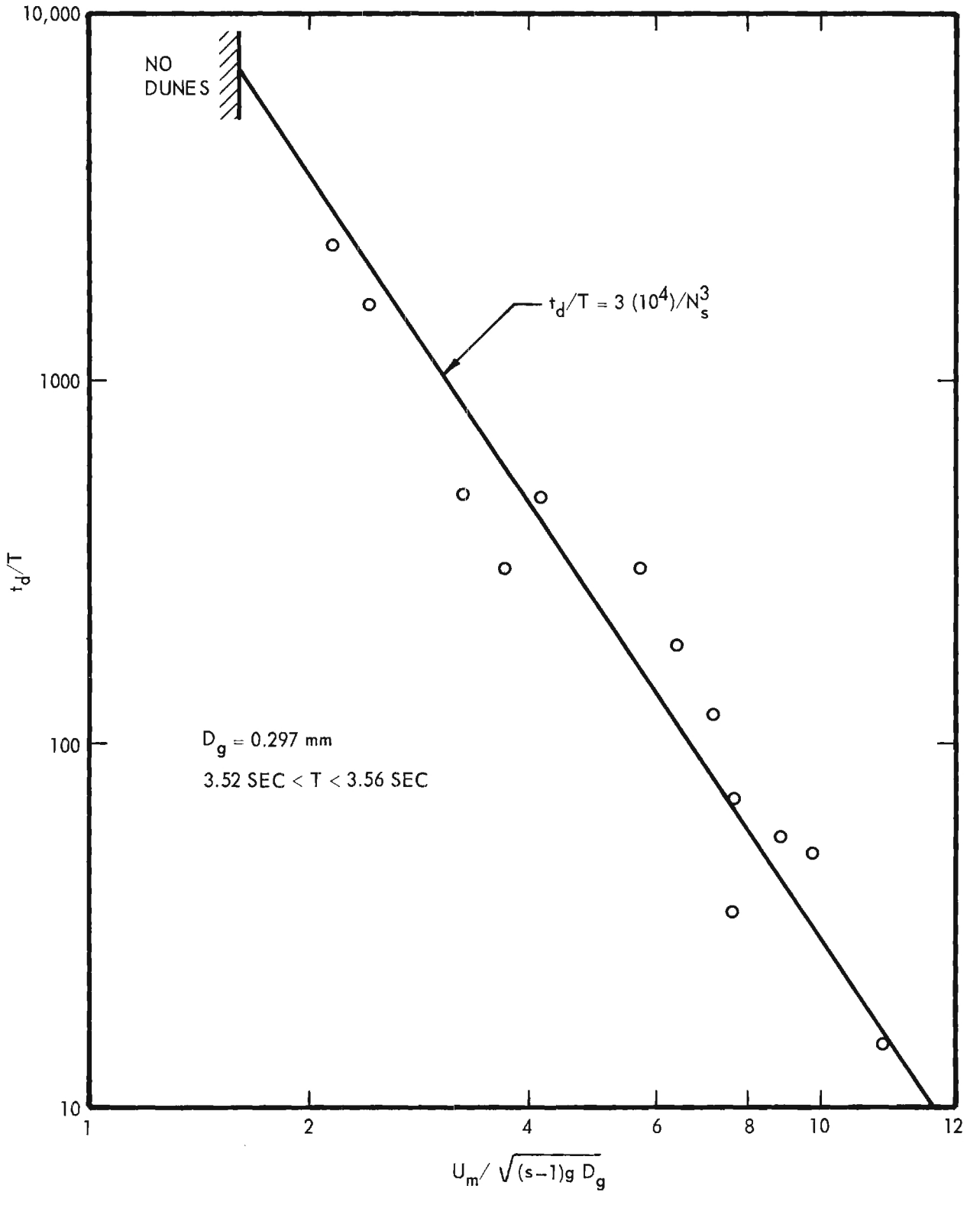

Figure 7. Time for Dune Development from an Initially Flat Bed.

Table 1. Parameters Used in Analysis

1	2	3	4	5	6	7	8	9	10	11
Exhibit No.	D_g (mm)	D (mm)	$S_{initial}$ / D	U_m / $(s-1)gD_g$	η_{max} / D	λ_{max} / D	Values at Final Settlement S/S_c	S/S_t	t/t_d	S(mm)
1	0.297	87.6	0.06	5.1	0.4	2.3	0.3	1.3	0.5	15
2	0.297	87.6	0.02	5.3	0.4	2.4	0.4	1.4	0.6	24
3	0.297	87.6	0.05	6.1	0.5	2.7	0.4	1.3	0.5	25
4	0.297	87.6	0.10	6.6	0.5	2.9	0.4	1.4	0.5	27
5	0.297	87.6	0.07	7.5	0.5	—	0.9	2.3	1.0	45
6	0.297	87.6	0.10	7.8	0.5	—	0.8	2.1	1.0	41
7	0.297	87.6	0.06	8.0	0.5	—	0.9	1.4	1.0	47
8	0.297	87.6	0.14	8.7	0.6	—	0.9	1.5	2.8	51
9	0.297	87.6	0.22	8.9	0.6	—	1.1	2.0	8.5	66
10	0.297	87.6	0.52	8.9	0.6	—	1.0	1.8	8.0	60
11	0.297	87.6	0.06	9.2	0.6	—	0.8	1.6	2.5	52
12	0.297	87.6	0.07	9.5	0.6	—	1.1	2.2	3.7	70
13	0.297	87.6	0.09	9.7	0.6	—	1.0	2.2	4.5	67
14	0.297	87.6	0.04	10.1	0.2	—	1.0	2.5	2.6	69
15	0.297	87.6	0.07	10.6	0.2	—	1.1	3.1	2.6	76
16	0.297	87.6	0.27	10.8	0.2	—	1.1	3.0	3.0	76
17	0.297	87.6	0.76	10.9	0.2	—	1.0	3.2	3.2	73
18	0.297	87.6	0.50	11.0	0.2	—	1.1	3.8	4.8	83
19	0.297	87.6	0.06	11.1	0.2	—	1.2	4.0	3.1	86
20	0.297	87.6	0.05	11.7	0.1	—	1.0	4.8	2.1	77
21	0.297	87.6	0.09	11.9	0.1	—	1.0	6.2	3.4	83
22	0.297	43.2	0.09	5.0	0.8	4.6	0.7	1.0	1.0	18
23	0.297	43.2	0.14	6.5	0.9	5.9	1.0	1.1	0.9	23
24	0.297	43.2	0.15	7.2	1.0	6.4	1.5	1.0	0.6	26
25	0.297	43.2	0.15	8.2	1.1	—	3.3	0.9	0.5	31
26	0.297	43.2	0.18	8.6	1.2	—	2.6	0.9	1.0	35
27	0.297	43.2	0.14	10.0	0.5	—	1.7	1.4	0.9	39
28	0.297	43.2	0.09	10.2	0.4	—	1.7	1.7	0.9	40
29	0.297	43.2	0.01	11.0	0.3	—	1.4	1.8	0.8	41
30	0.297	25.4	0.29	5.1	1.4	8.1	2.0	0.9	0.5	16
31	0.297	25.4	0.23	7.3	1.8	—	<0	0.8	0.4	17
32	0.297	25.4	0.18	8.3	1.9	—	<0	0.5	0.4	19
33	0.297	25.4	0.29	8.9	2.0	—	<0	0.5	0.2	25
34	0.297	25.4	0.26	9.8	2.2	—	<0	0.9	0.4	25
35	0.297	25.4	0.19	10.3	0.7	—	3.4	0.9	0.5	24

is that scour around a horizontal cylinder is independent of the elevation of the dune troughs. This conclusion is reinforced by the experimental observation that the axis of the cylinder coincided with the axis of the dune crest rather than with the axis of the trough.

Dune crest elevation. In column 8 of Table 1 the values of S/S_c are tabulated. If S/S_c is less than unity the top of the cylinder is higher than the elevation of the dune crests. Conversely if S/S_c is greater than unity the top of the cylinder is lower than the elevation of the dune crests. However, since the settlement of the cylinder was observed through the sidewall of the test section by means of a horizontal telescope, the cylinder could not be observed if S/S_c were appreciably greater than unity. Several exceptions are shown in column 8, for example Exhibit 25. In this test the top of the cylinder was observed to be lower than the elevation of the crests of the equilibrium dunes. Referring to column 10, the value of t/t_d is found to be 0.5. In other words, the settlement of the cylinder as shown in Exhibit 25 occurred before the dunes had developed to an equilibrium state. Because of the method of observation it is obvious that the dune crests were not appreciably higher than the top of the cylinder at the time this test was terminated. On account of the obstruction of the dunes in regard to observing settlement, no meaningful conclusion can be reached as to the effect of the elevation of the dune crests in relation to the scour around the cylinder.

Sediment number. A study of the Exhibits reveals that effect of dunes upon local scour is delineated by the value of the sediment number, N_s · (A) If

$N_s > 9$, the dunes have no discernible effect upon local scour as shown by the scour similarity in Exhibits 11-21, 27-29, and 34-35. Referring to Figure 1, this region is one of three-dimensional dunes of low amplitude. (B) If the dunes are definitely two-dimensional, scour will be small as shown in Exhibits 1-4. In this range, $1.6 < N_s < 6.5$, the cylinder joins the dune system with the top of the cylinder being aligned with a dune crest. The pseudo-dune (cylinder) can protrude well above the real dunes as demonstrated by the values of S/S_c of Exhibits 1-4. The rate of scour is greatly accelerated during the time that dunes are being formed. In other words, the scour which forms dunes appears to augment the scour around the cylinder. On the other hand, the writer suspects that the cylinder would not become part of the dune system if the cylinder diameter was equal to or greater than a dune length. Even the largest cylinder used in the test was only about 0.4 of the dune length. In other words, the tests are indicative that the cylinder will join the dune system if $N_s < 6.5$ and if $\lambda/D > 2.3$ but the tests are inadequate to show whether the cylinder would join the dune system if $N_s < 6.5$ and if $\lambda/D \leq 1$. (C) In the range $6.5 < N_s < 9$ the test results are indicative that the dunes do influence the scour around the cylinder. Exhibits 5-10 are indicative that the cylinder does join the dune system but that the cylinder settles until the cylinder protrusion is about equal to the protrusion of the dune crests. Settlement of the smaller cylinders, Exhibits 24-26 and Exhibits 31-32, was greater probably because the settlement of the smaller cylinders occurred before the equilibrium dune condition was attained.

Initial burial. Even though the cylinder was lowered carefully onto the bed some initial settlement occurred in all tests as shown in Column 4 of Table 1 and as shown by the initial point in each Exhibit. In five tests, Exhibits 9-10 and 16-18, the cylinder was partially buried by design prior to the test. As shown in Exhibits 16 and 18, the initially buried cylinder remains stationary until the normal scour hole develops. Thereafter the cylinder settles in a typical manner. As shown in Exhibits 16 and 18, the time required to reach a given scour depth is essentially the same regardless of whether the cylinder was initially buried or not. The previous statement is not true for exaggerated cases of initial burial as shown in Exhibit 17 in which the cylinder was 76 percent buried prior to the test. In this case a longer time was required to develop the scour hole. This result would be expected since the initial flow disturbance and resulting separation pattern would be considerably smaller with only 24 per cent of the cylinder protruding from the initially flat bed. On the basis of the three tests shown in Exhibits 16-18, the conclusion is that the cylinder will settle in the same time if the initial burial is less than 50 per cent. On the other hand, a longer time will be required for the cylinder to settle if the initial burial is greater than 50 per cent--about 60 per cent more time for 76 per cent initial burial. The initial times required to form the scour hole are shown in Exhibits 9 and 10. However in these two runs, the subsequent settlement was undoubtedly influenced by the presence of dunes.

Scour without the effect of dunes. Scour around the cylinder which is unaffected by dunes is discussed in Section E of APPENDIX B. Test results

are shown in Exhibits 11-21, 27-29, and 33-35. The similarity relationship for scour without dunes is given by equation (25) of APPENDIX B, that is,

$$(N_s^2 - N_{sc}^2)^{5/2}\left(\frac{D_g}{D}\right)\left(\frac{U_m t}{D}\right) = f\left(\frac{S}{D}, \phi, \sigma_g\right) \tag{4}$$

in which ϕ is the angle of repose of the bed material.

In the following the relative effect of individual variables will be evaluated by comparing two situations for which the RHS of equation (4) is identical. Hence, the parameter on the LHS of equation (4) must be equal in the two situations, that is

$$\left[1 - \left(\frac{U_{mc1}}{U_{m1}}\right)^2\right]^{5/2} \frac{U_{m1}^6 t_1}{(s_1-1)^{5/2} D_{g1}^{3/2} D_1^2} = \left[1 - \left(\frac{U_{mc2}}{U_{m2}}\right)^2\right]^{5/2} \frac{U_{m2}^6 t_2}{(s_2-1)^{5/2} D_{g2}^{3/2} D_2^2} \tag{5}$$

or

$$\frac{t_2}{t_1} = \left[\frac{1 - \left(\frac{U_{mc1}}{U_{m1}}\right)^2}{1 - \left(\frac{U_{mc2}}{U_{m2}}\right)^2}\right]^{5/2} \left(\frac{U_{m1}}{U_{m2}}\right)^6 \left(\frac{D_{g2}}{D_{g1}}\right)^{3/2} \left(\frac{D_2}{D_1}\right)^2 \left(\frac{s_2-1}{s_1-1}\right)^{5/2} \tag{6}$$

From equation (6), the time of settlement is seen to be most sensitive to changes in velocity and least sensitive to changes in sediment diameter.

CONCLUSIONS

Based upon the analysis of experimental results the following conclusions are presented

1. Localized scour around a horizontal cylinder is influenced by the dunes which form on the bed if the sediment number, $U_m/\sqrt{(s-1)g\,D_g}$, has a value less than about nine.

2. If the dune system is two-dimensional, that is, $1.6 < N_s < 6.5$, the cylinder will join the dune system with cylinder acting as a pseudo dune. In this range the scour will be quite small but the rate of scour is higher than without dunes. This conclusion is of doubtful validity if the cylinder diameter is greater than the dune wave length since the largest cylinder used in the experiments had a diameter which was only 0.4 of the dune wave length. For cylinders of diameter larger than the dune wave length the flow pattern around the cylinder is not likely to be influenced appreciably by the flow pattern over the dunes.

3. A similarity relationship for localized scour around a cylinder having a length-to-diameter ratio of 4 was developed for flow situations in which the flow pattern over the dunes does not influence the flow pattern around the cylinder. This similarity relation is graphically presented in Figure 13 of APPENDIX B. For the cylinders used in these experiments the similarity relationship is applicable if the sediment number, $U_m/\sqrt{(s-1)g\ D_g}$, is greater than about nine. The expectation is that the dunes would exert a negligible influence at any value of the sediment number if the cylinder diameter were greater than the dune wave length; however, this experimental study was too limited to verify this expectation. The similarity relation for elapsed time, t, to achieve a given state of settlement, S/D, is

$$t \propto \left[1 - (U_{mc}/U_m)^2\right]^{-5/2} U_m^{-6} D_g^{3/2} D^2 (s-1)^{5/2}$$

in which the predominant variable is the velocity at the bed.

APPENDIX A

EXHIBITS

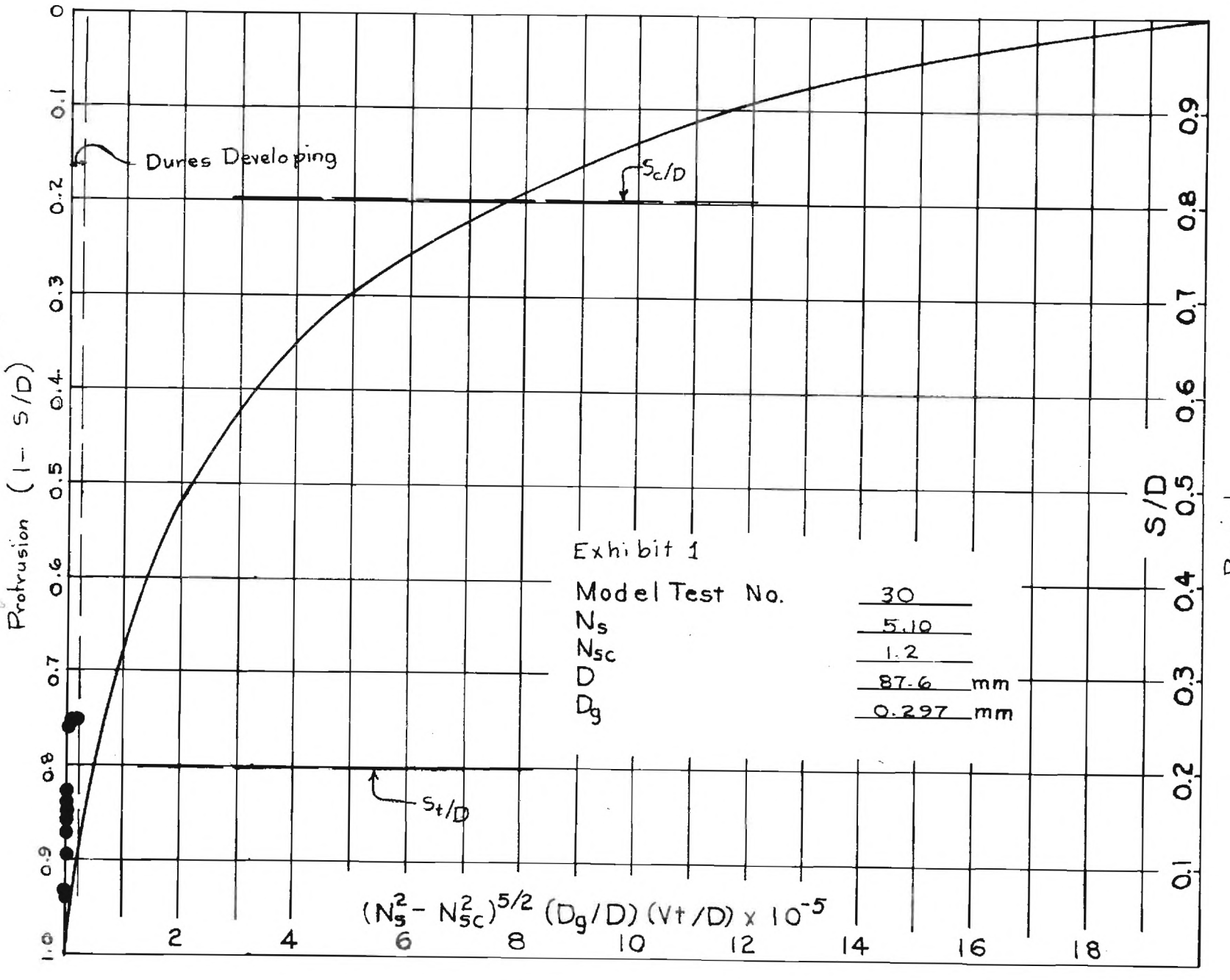
Protrusion (1 - S/D)
Burial S/D
Dunes Developing
S_c/D
S_t/D
Exhibit 1
Model Test No. 30
N_s 5.10
N_{sc} 1.2
D 87.6 mm
D_g 0.297 mm
$(N_s^2 - N_{sc}^2)^{5/2} (D_g/D) (Vt/D) \times 10^{-5}$
0
0.1
0.2
0.3
0.4
0.5
0.6
0.7
0.8
0.9
1.0
2
4
6
8
10
12
14
16
18

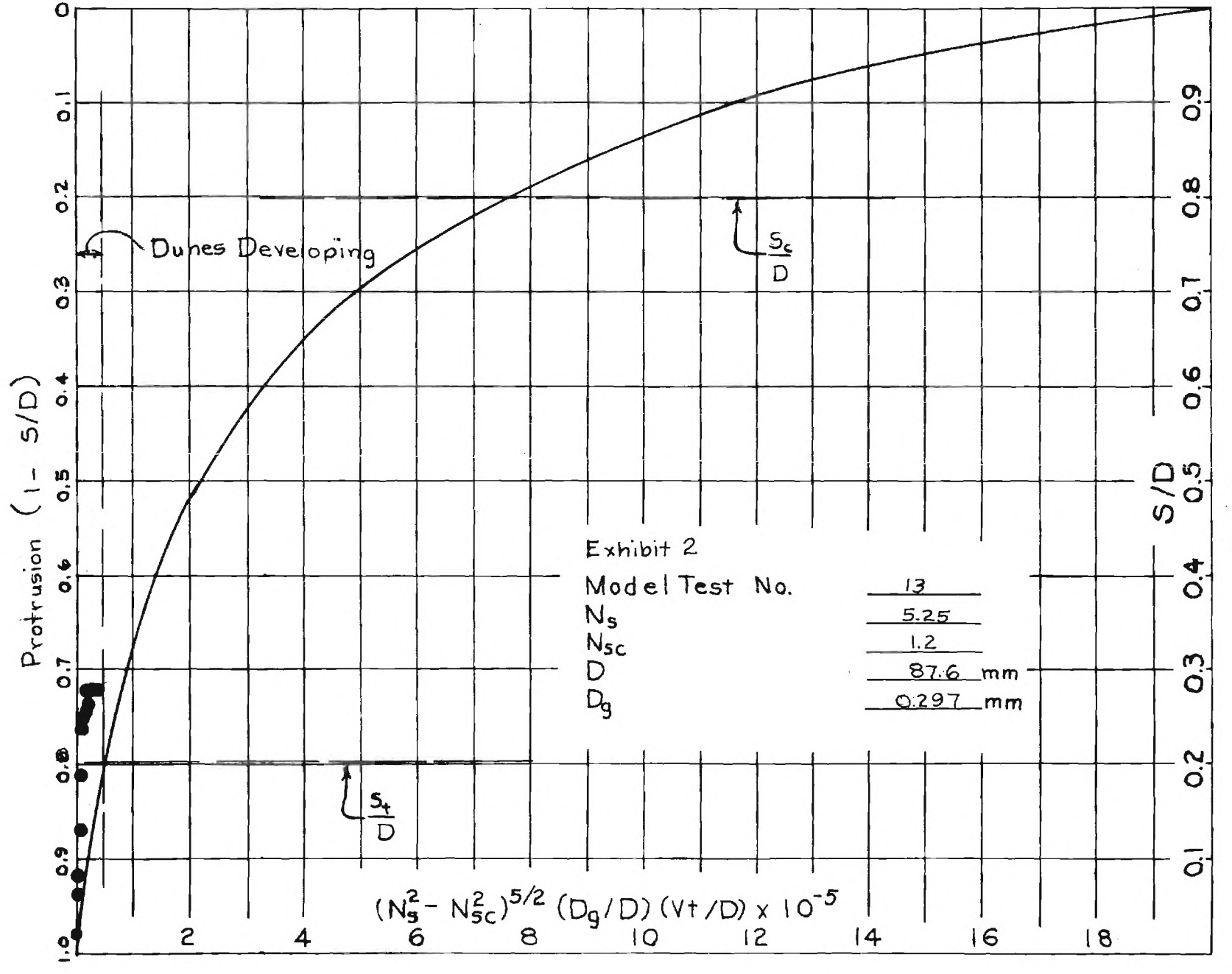
Protrusion (1 - S/D)
S/D
Burial
Dunes Developing
$\frac{S_c}{D}$
$\frac{S_t}{D}$
Exhibit 2
Model Test No. 13
N_s 5.25
N_{sc} 1.2
D 87.6 mm
D_g 0.297 mm
$(N_s^2 - N_{sc}^2)^{5/2} (D_g/D) (Vt/D) \times 10^{-5}$
0
0.1
0.2
0.3
0.4
0.5
0.6
0.7
0.8
0.9
1.0
2
4
6
8
10
12
14
16
18

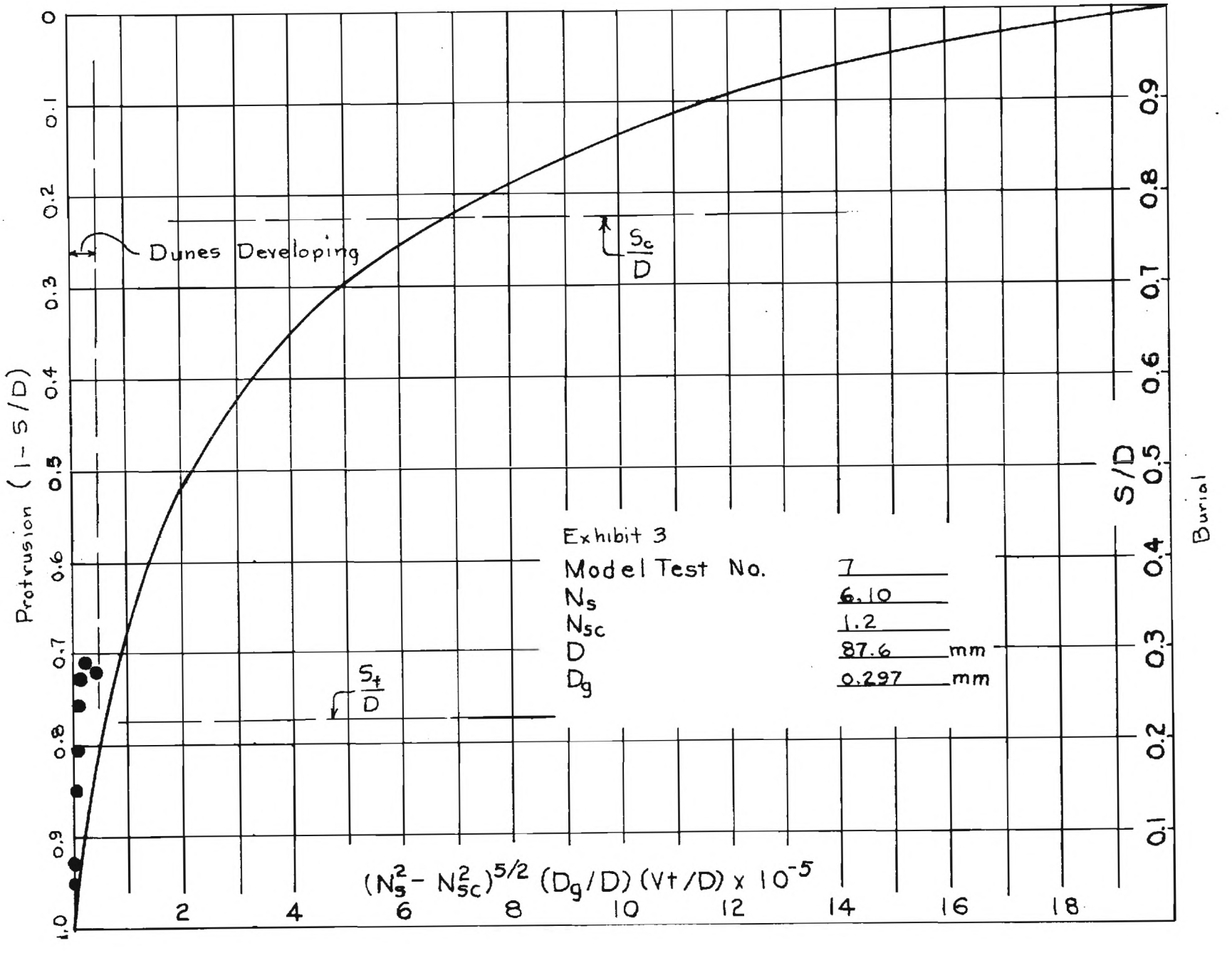
Protrusion (1 - S/D)
Burial S/D
0
0.1
0.2
0.3
0.4
0.5
0.6
0.7
0.8
0.9
1.0
Dunes Developing
$\frac{S_c}{D}$
$\frac{S_f}{D}$
Exhibit 3
Model Test No. 7
N_s 6.10
N_{sc} 1.2
D 87.6 mm
D_g 0.297 mm
$(N_s^2 - N_{sc}^2)^{5/2} (D_g/D) (Vt/D) \times 10^{-5}$
2
4
6
8
10
12
14
16
18

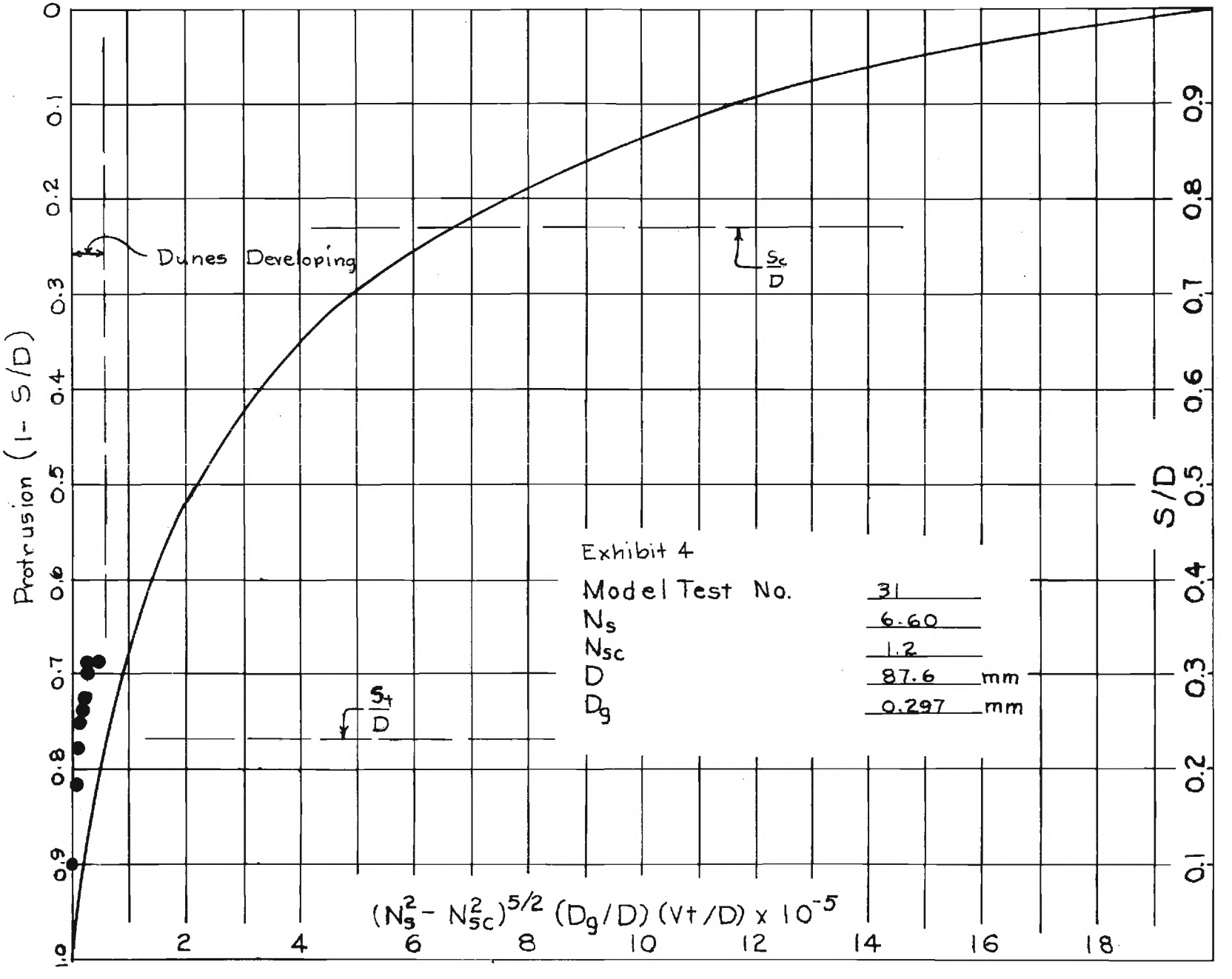
Protrusion (1 - S/D)
S/D
Burial
Dunes Developing
$\frac{S_c}{D}$
$\frac{S_f}{D}$
Exhibit 4
Model Test No. 31
N_s 6.60
N_{sc} 1.2
D 87.6 mm
D_g 0.297 mm
$(N_s^2 - N_{sc}^2)^{5/2} (D_g/D) (Vt/D) \times 10^{-5}$
0
0.1
0.2
0.3
0.4
0.5
0.6
0.7
0.8
0.9
1.0
2
4
6
8
10
12
14
16
18

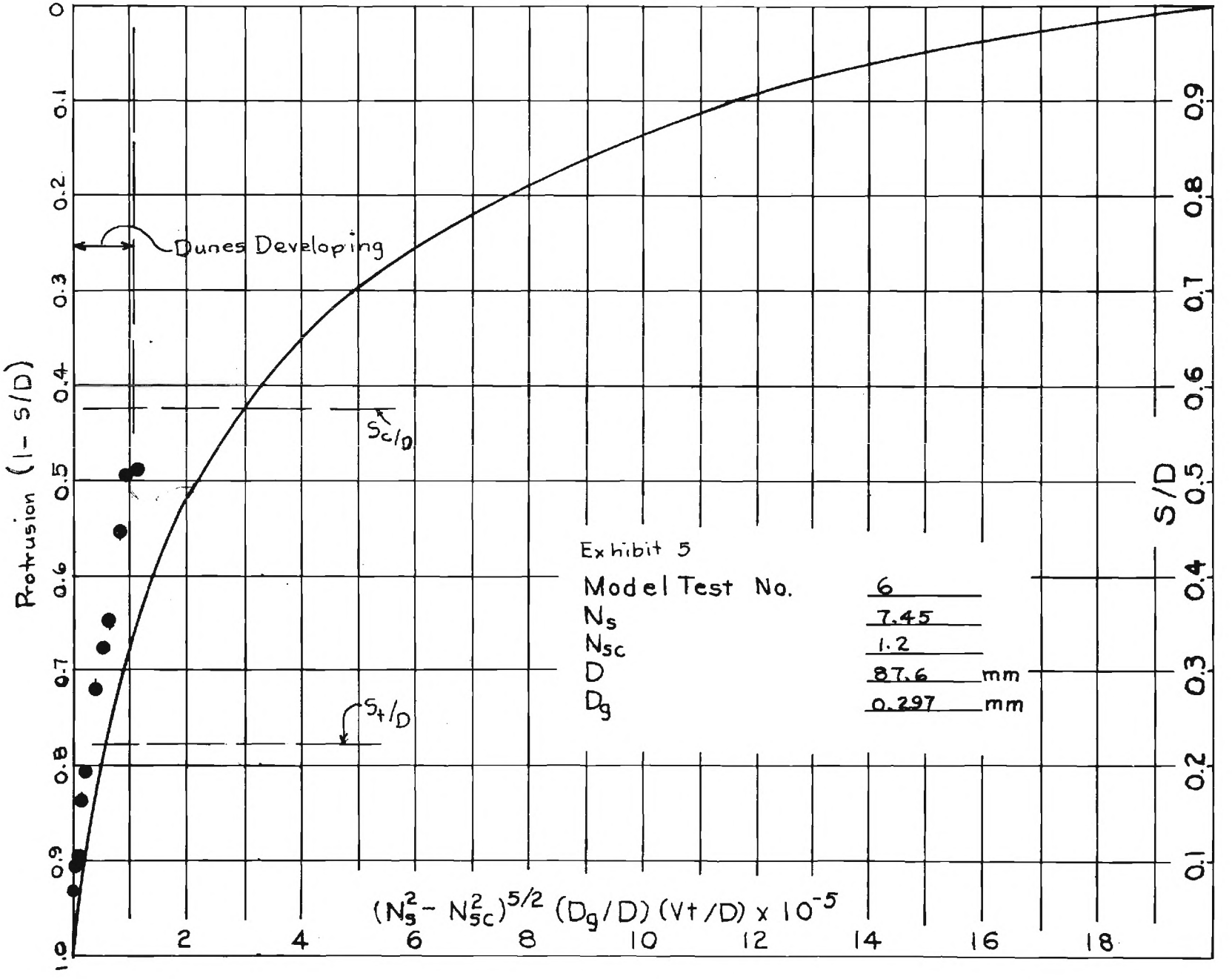
Protrusion (1 - S/D)
S/D
Burial
Dunes Developing
S_c/D
S_t/D
Exhibit 5
Model Test No. 6
N_s 7.45
N_{sc} 1.2
D 87.6 mm
D_g 0.297 mm
$(N_s^2 - N_{sc}^2)^{5/2} (D_g/D) (Vt/D) \times 10^{-5}$
0
0.1
0.2
0.3
0.4
0.5
0.6
0.7
0.8
0.9
1.0
2
4
6
8
10
12
14
16
18

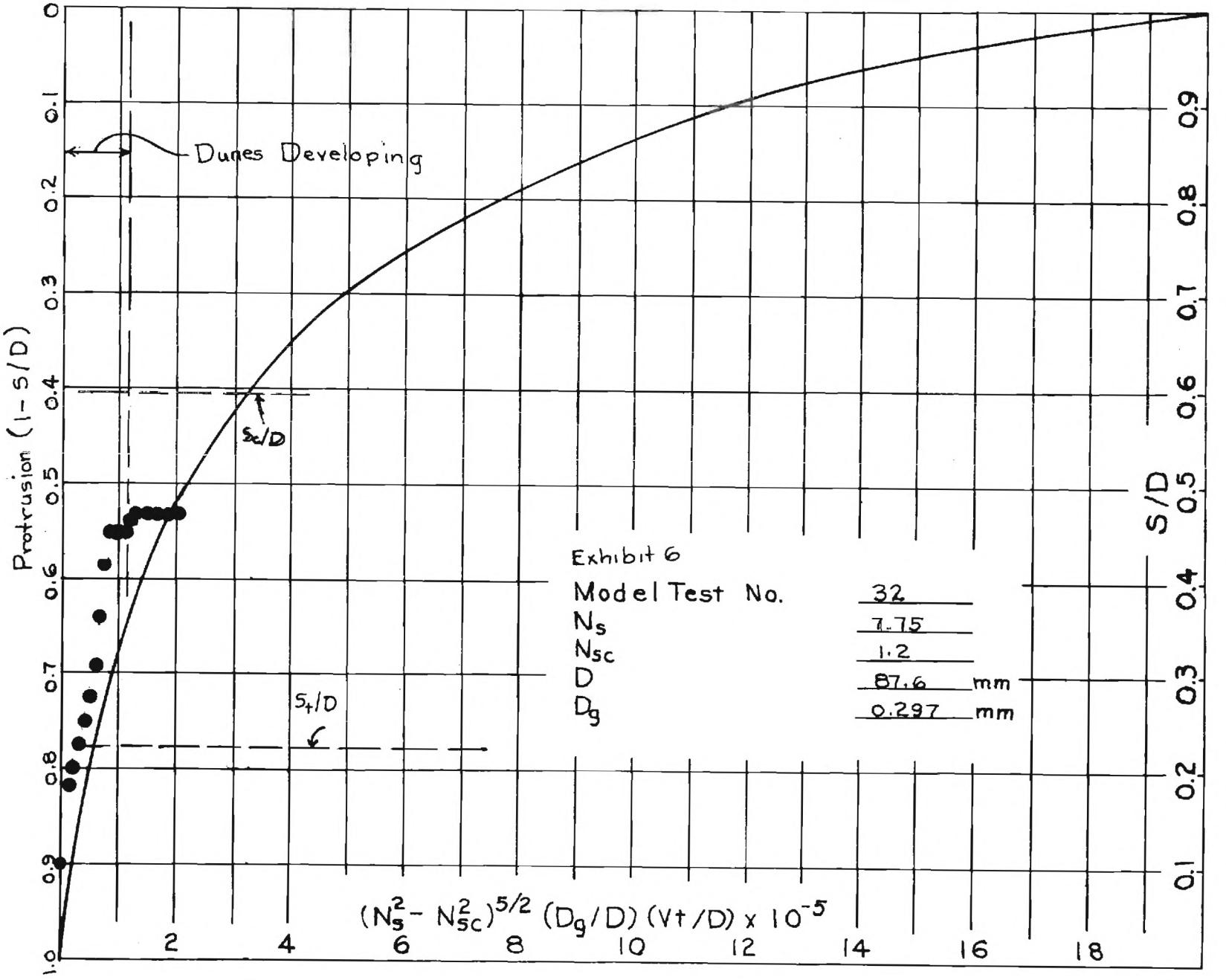
Dunes Developing
Sc/D
St/D
Exhibit 6
Model Test No. 32
Ns 7.75
Nsc 1.2
D 87.6 mm
Dg 0.297 mm
Protrusion (1 - S/D)
S/D
(Ns² - Nsc²)^5/2 (Dg/D) (Vt/D) x 10^-5
0
0.1
0.2
0.3
0.4
0.5
0.6
0.7
0.8
0.9
1.0
2
4
6
8
10
12
14
16
18

Burial

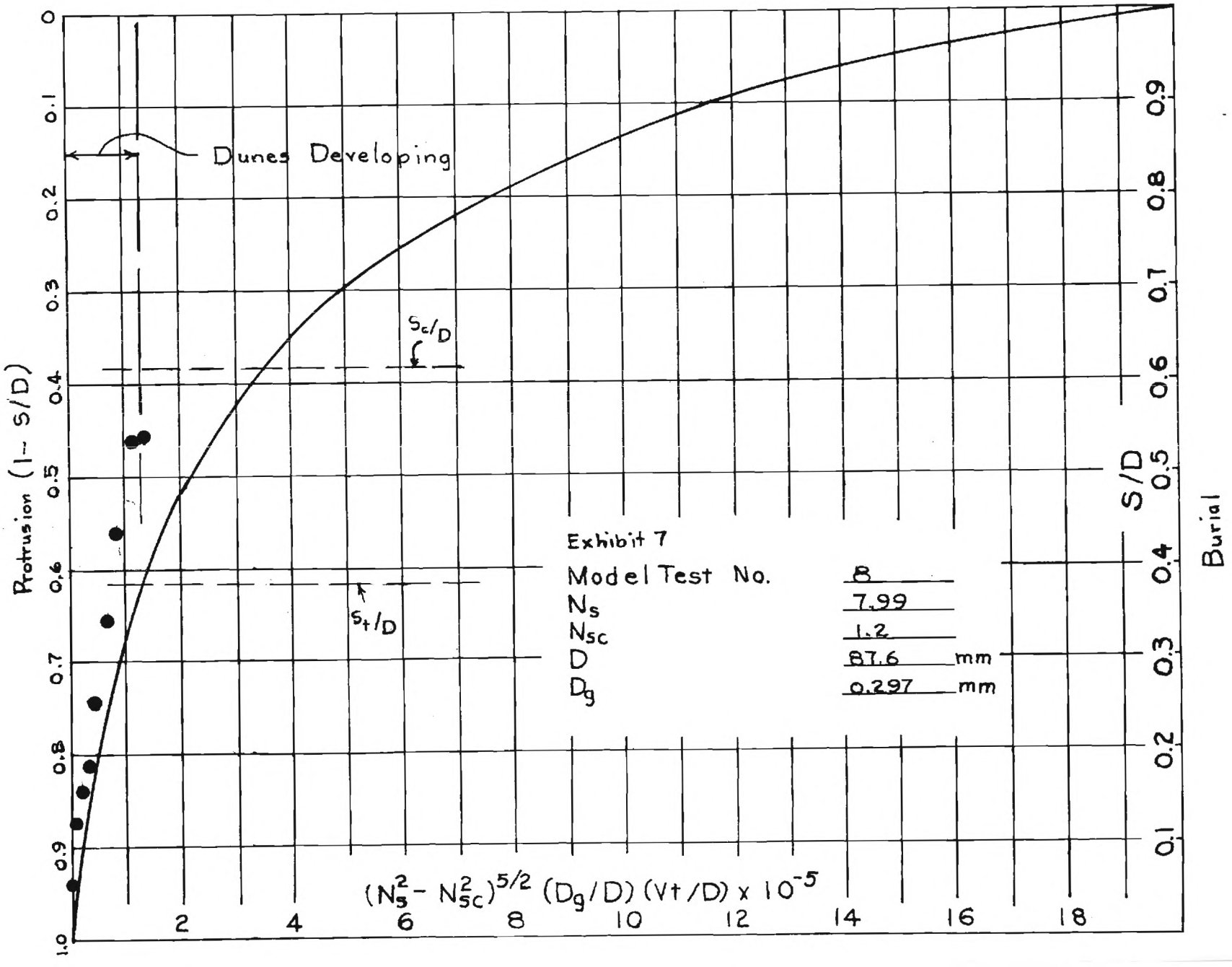
Dunes Developing
S_c/D
S_t/D
Exhibit 7
Model Test No. 8
N_s 7.99
N_{sc} 1.2
D 87.6 mm
D_g 0.297 mm
Protrusion (1 - S/D)
Burial S/D
$(N_s^2 - N_{sc}^2)^{5/2} (D_g/D) (Vt/D) \times 10^{-5}$
0
0.1
0.2
0.3
0.4
0.5
0.6
0.7
0.8
0.9
1.0
2
4
6
8
10
12
14
16
18

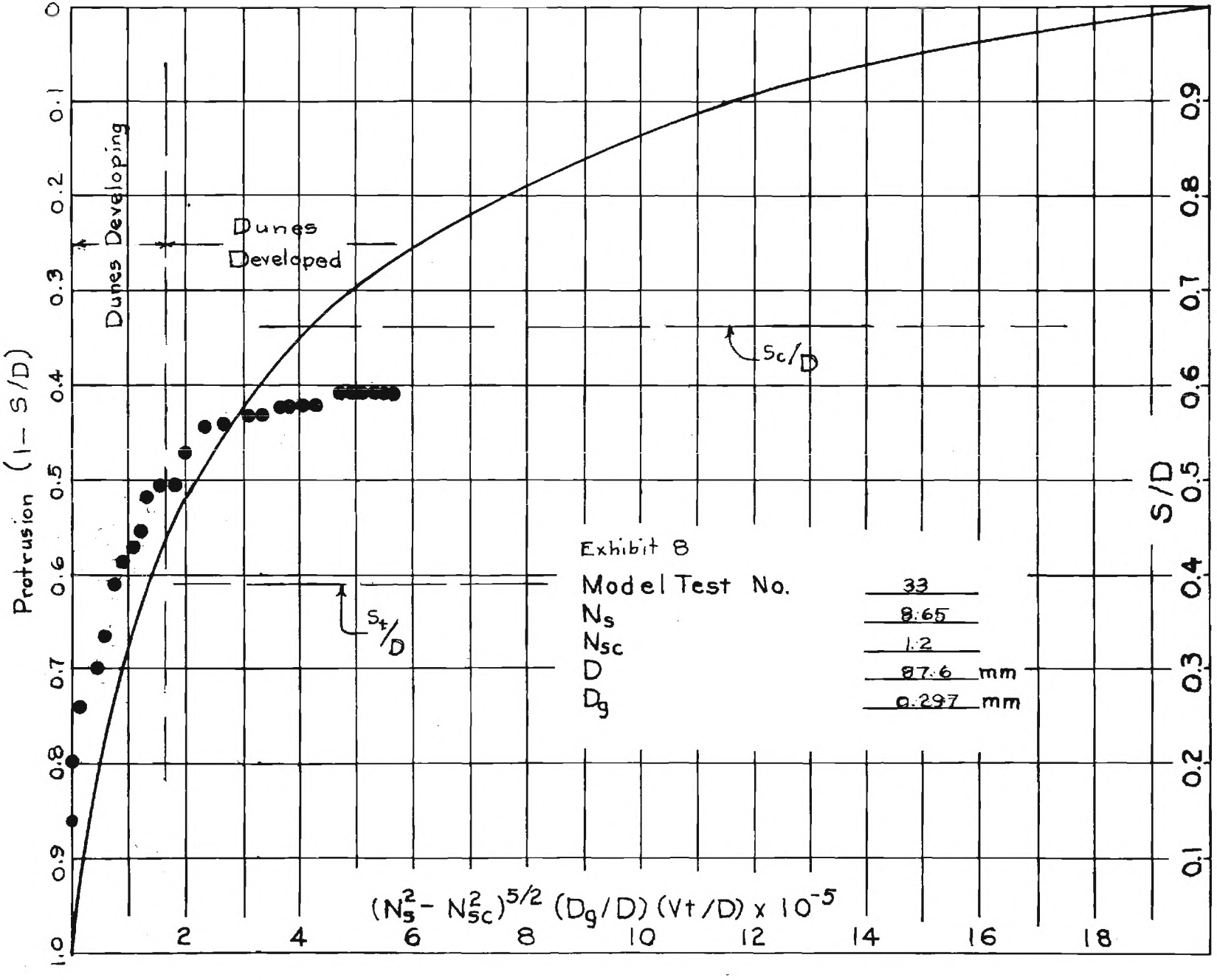
Protrusion (1 − S/D)
S/D
Burial
Dunes Developing
Dunes Developed
Sc/D
St/D
Exhibit 8
Model Test No. 33
Ns 8.65
Nsc 1.2
D 87.6 mm
Dg 0.297 mm
(Ns² − Nsc²)^5/2 (Dg/D) (Vt/D) x 10⁻⁵
0
0.1
0.2
0.3
0.4
0.5
0.6
0.7
0.8
0.9
1.0
2
4
6
8
10
12
14
16
18

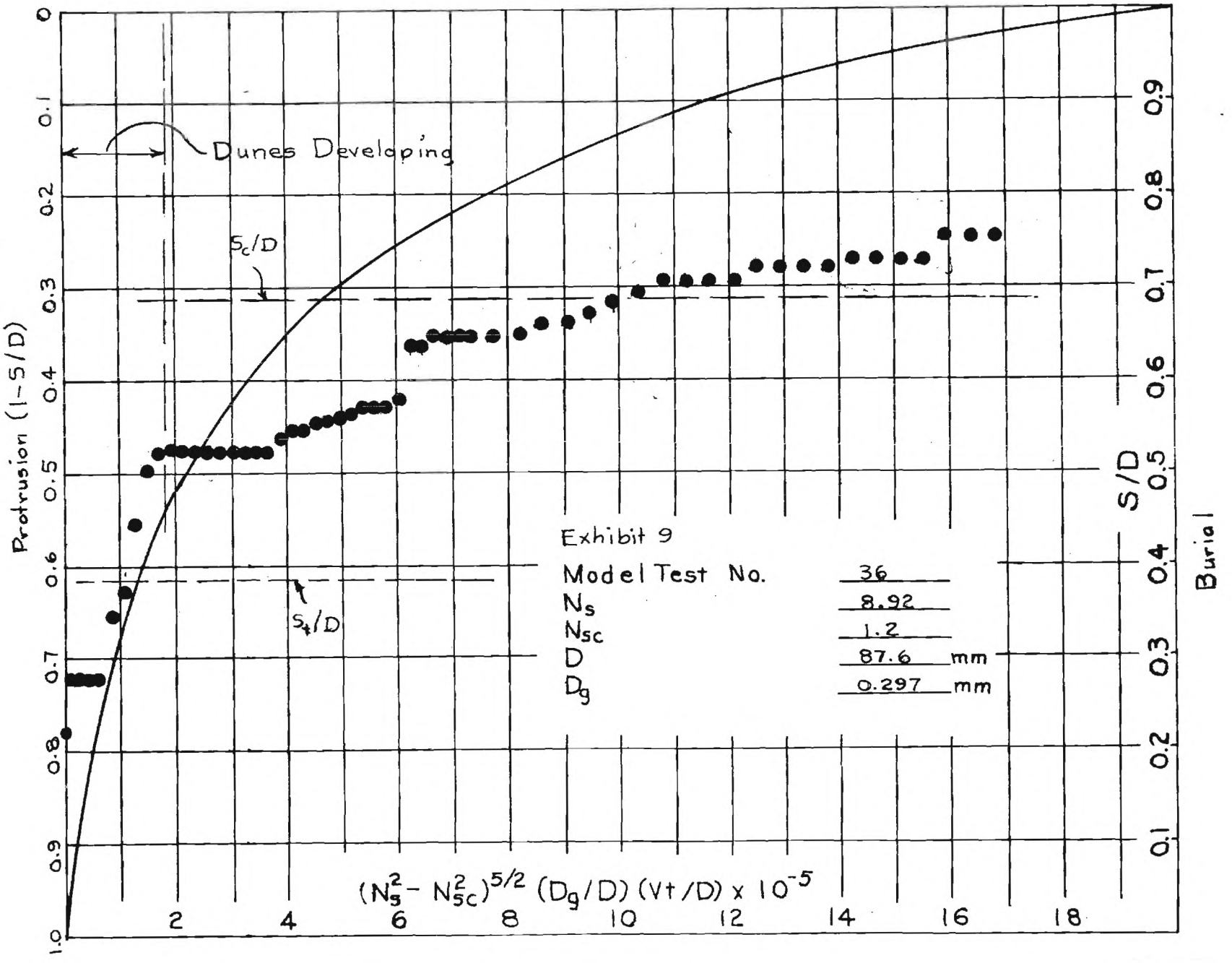
Dunes Developing
S_c/D
S_t/D
Exhibit 9
Model Test No. 36
N_s 8.92
N_{sc} 1.2
D 87.6 mm
D_g 0.297 mm
Protrusion (1-S/D)
Burial S/D
$(N_s^2 - N_{sc}^2)^{5/2} (D_g/D) (Vt/D) \times 10^{-5}$
0
0.1
0.2
0.3
0.4
0.5
0.6
0.7
0.8
0.9
1.0
2
4
6
8
10
12
14
16
18

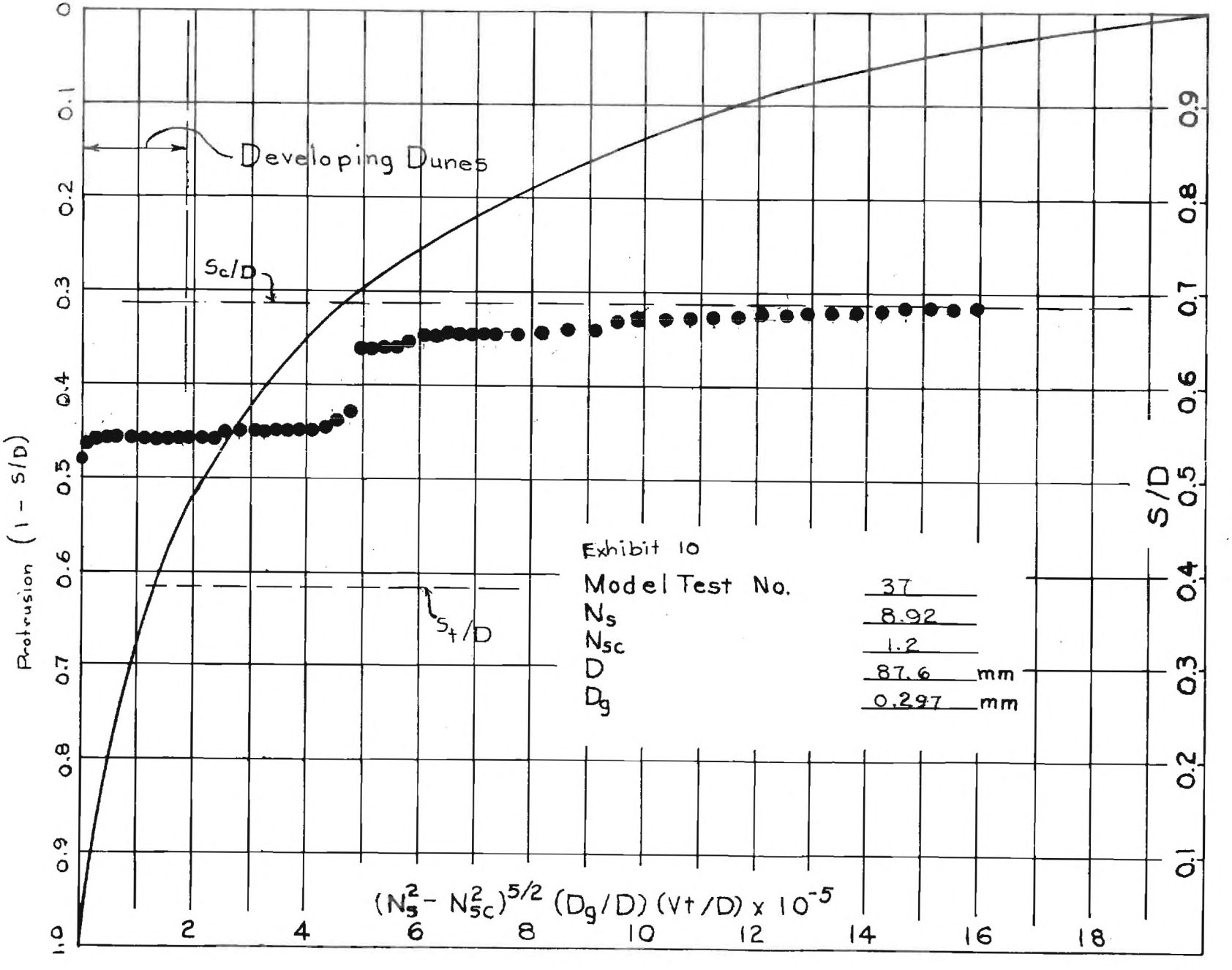
Developing Dunes
S_c/D
S_t/D
Exhibit 10
Model Test No. 37
N_s 8.92
N_{sc} 1.2
D 87.6 mm
D_g 0.297 mm
Protrusion (1 - S/D)
Burial S/D
$(N_s^2 - N_{sc}^2)^{5/2} (D_g/D) (Vt/D) \times 10^{-5}$
0
0.1
0.2
0.3
0.4
0.5
0.6
0.7
0.8
0.9
1.0
2
4
6
8
10
12
14
16
18

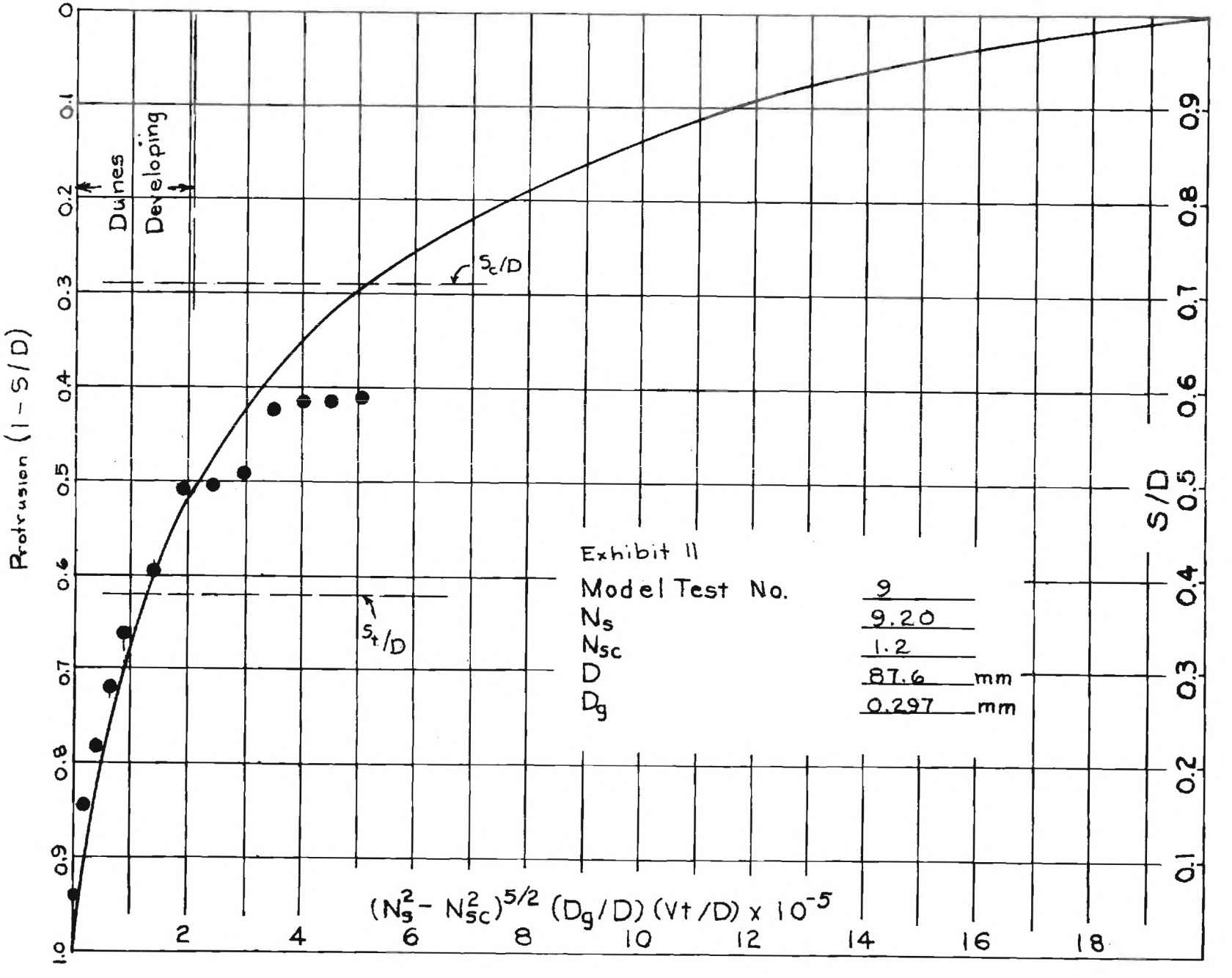
Protrusion (1 - S/D)
Burial
S/D
Dunes
Developing
S_c/D
S_t/D
Exhibit 11
Model Test No. 9
N_s 9.20
N_{sc} 1.2
D 87.6 mm
D_g 0.297 mm
$(N_s^2 - N_{sc}^2)^{5/2} (D_g/D) (Vt/D) \times 10^{-5}$
0
0.1
0.2
0.3
0.4
0.5
0.6
0.7
0.8
0.9
1.0
2
4
6
8
10
12
14
16
18

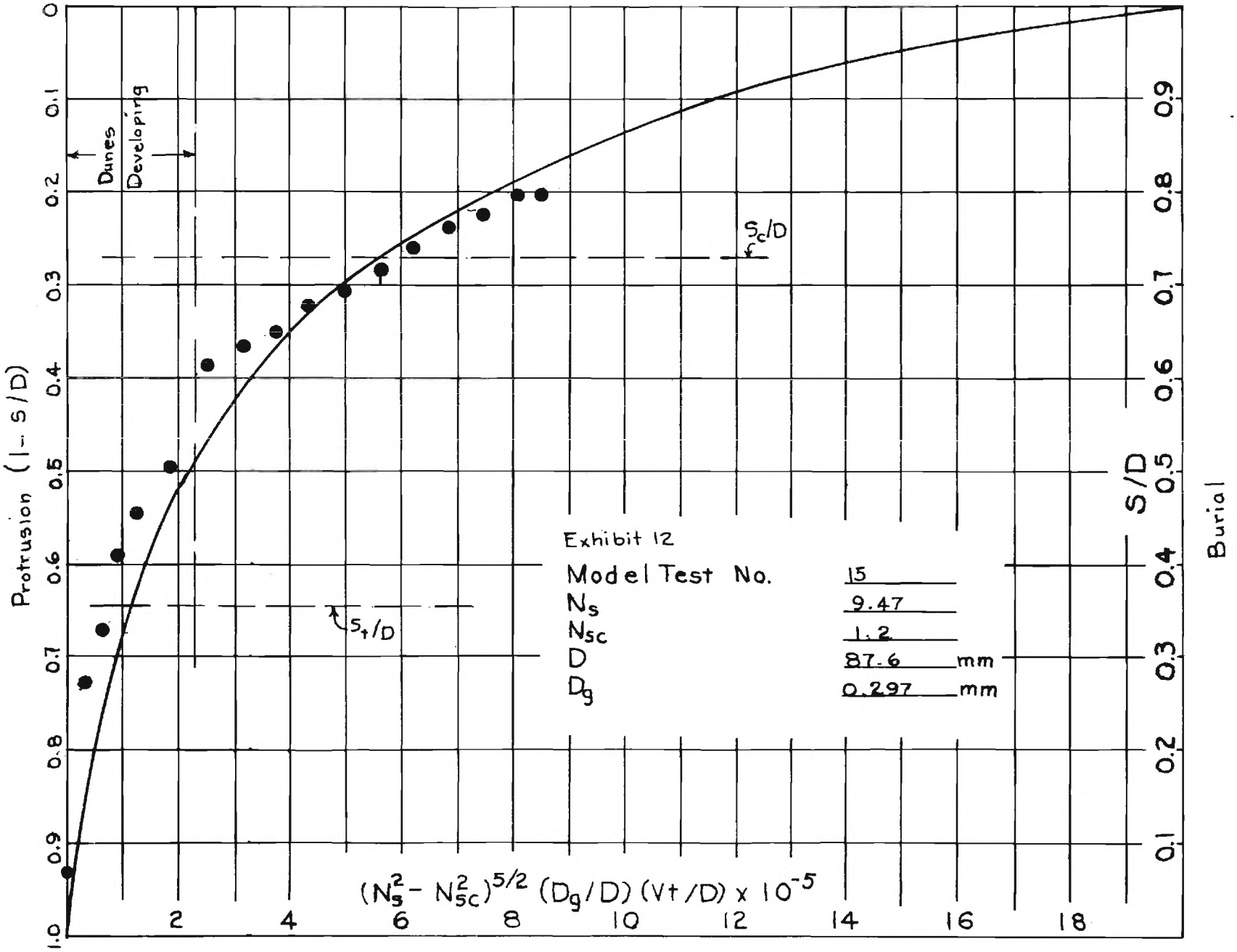
Protrusion (1 - S/D)
S/D
Burial
Dunes Developing
S_c/D
S_t/D
$(N_s^2 - N_{sc}^2)^{5/2} (D_g/D) (Vt/D) \times 10^{-5}$
Exhibit 12
Model Test No. 15
N_s 9.47
N_{sc} 1.2
D 87.6 mm
D_g 0.297 mm

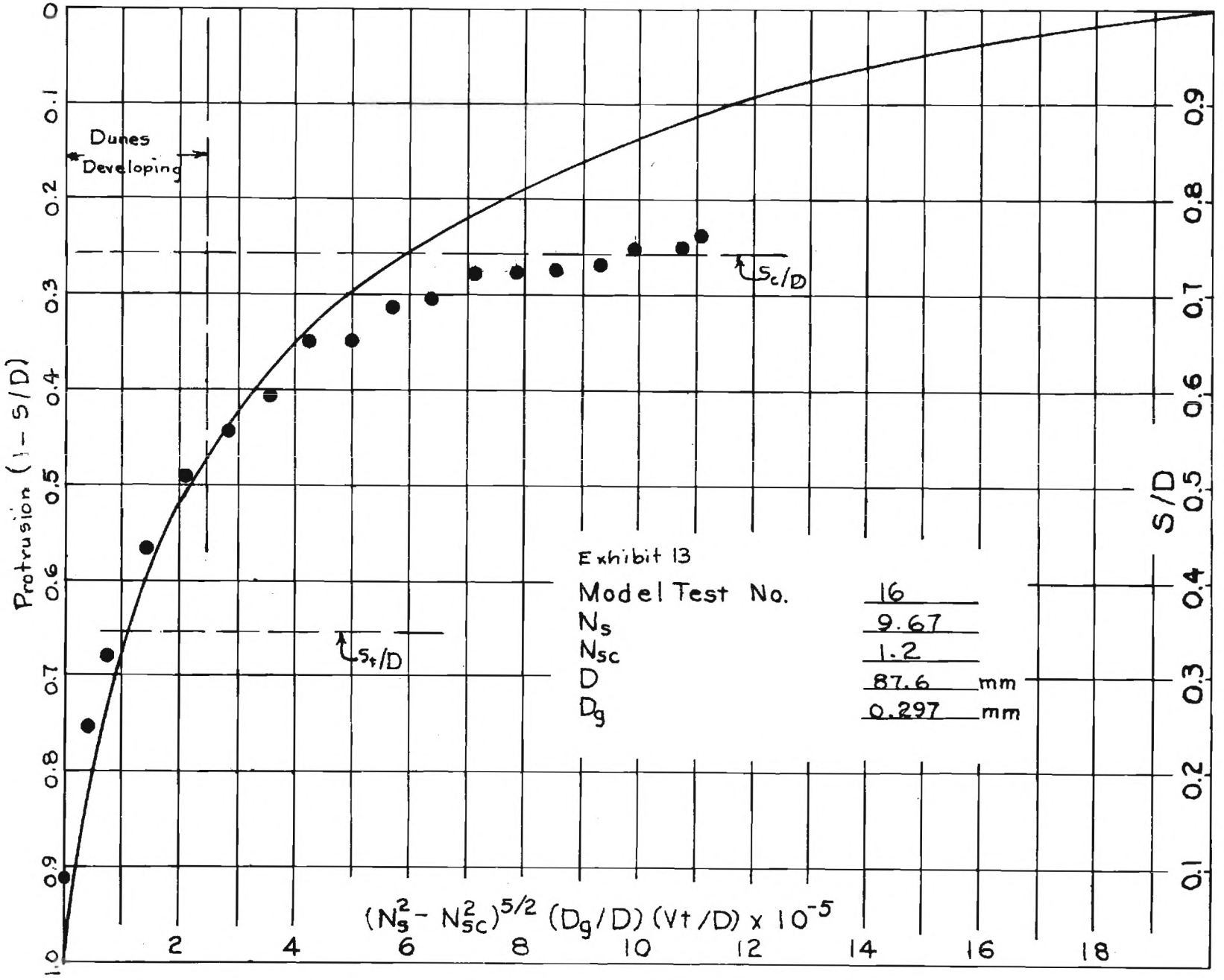
Protrusion (1 - S/D)
S/D
Burial
Dunes Developing
S_c/D
S_t/D
Exhibit 13
Model Test No. 16
N_s 9.67
N_{sc} 1.2
D 87.6 mm
D_g 0.297 mm
$(N_s^2 - N_{sc}^2)^{5/2} (D_g/D) (Vt/D) \times 10^{-5}$
0
0.1
0.2
0.3
0.4
0.5
0.6
0.7
0.8
0.9
1.0
2
4
6
8
10
12
14
16
18

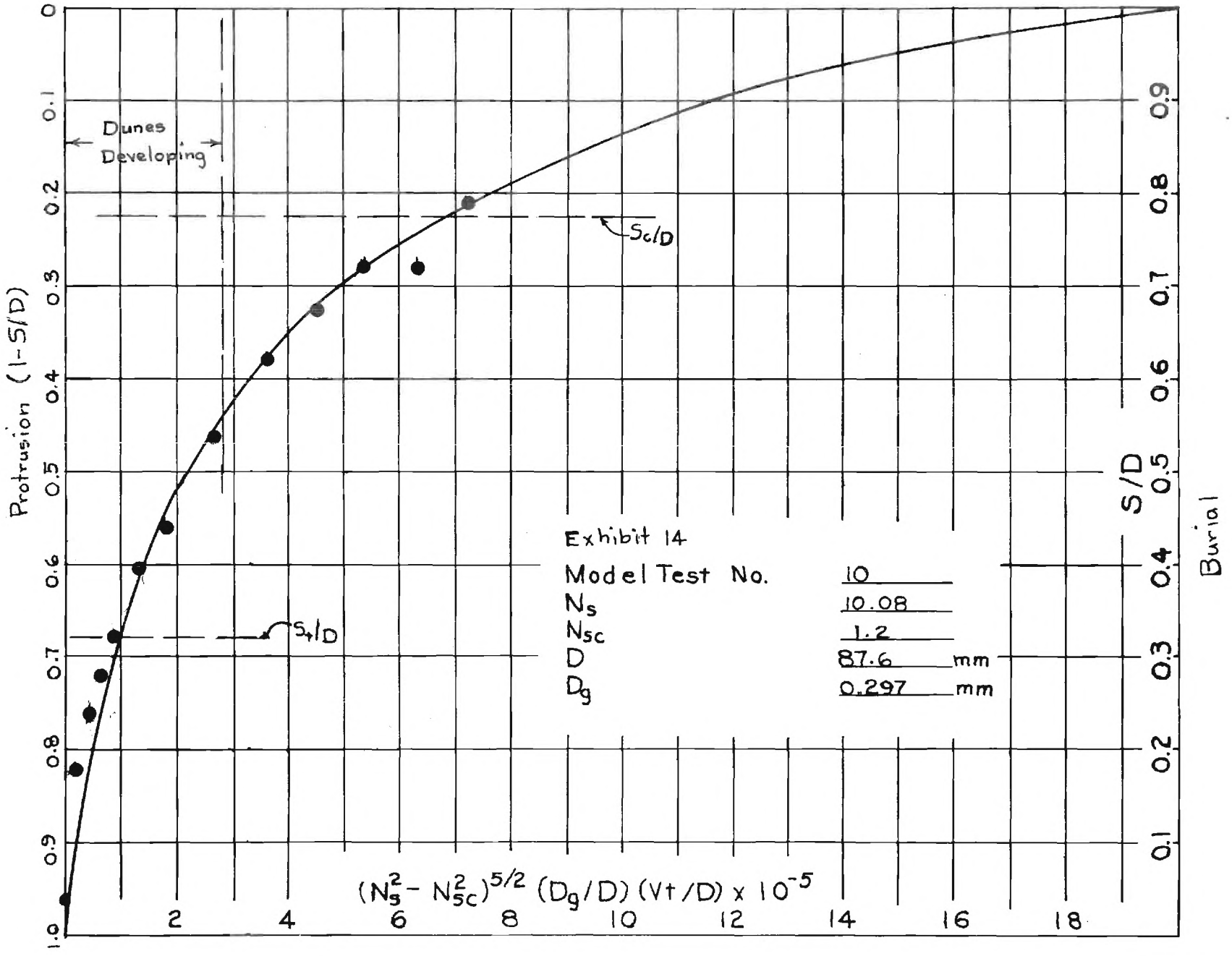
Protrusion (1-S/D)
S/D
Burial
Dunes Developing
S_c/D
S_t/D
Exhibit 14
Model Test No. 10
N_s 10.08
N_{sc} 1.2
D 87.6 mm
D_g 0.297 mm
$(N_s^2 - N_{sc}^2)^{5/2} (D_g/D) (Vt/D) \times 10^{-5}$
0
0.1
0.2
0.3
0.4
0.5
0.6
0.7
0.8
0.9
1.0
2
4
6
8
10
12
14
16
18

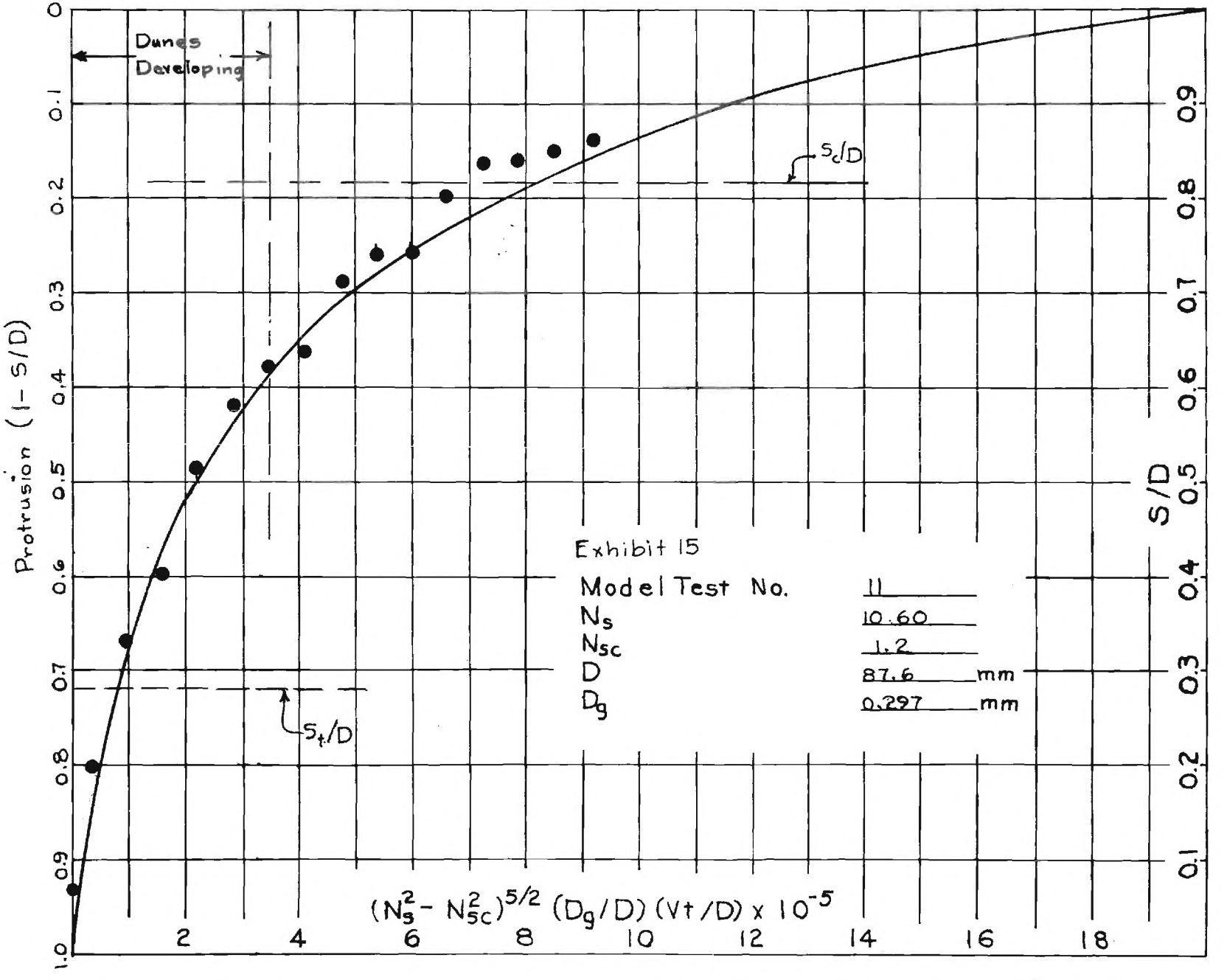
Dunes Developing
S_c/D
S_t/D
Exhibit 15
Model Test No. 11
N_s 10.60
N_{sc} 1.2
D 87.6 mm
D_g 0.297 mm
Protrusion (1 - S/D)
S/D
$(N_s^2 - N_{sc}^2)^{5/2} (D_g/D) (Vt/D) \times 10^{-5}$
0
0.1
0.2
0.3
0.4
0.5
0.6
0.7
0.8
0.9
1.0
2
4
6
8
10
12
14
16
18

Burial

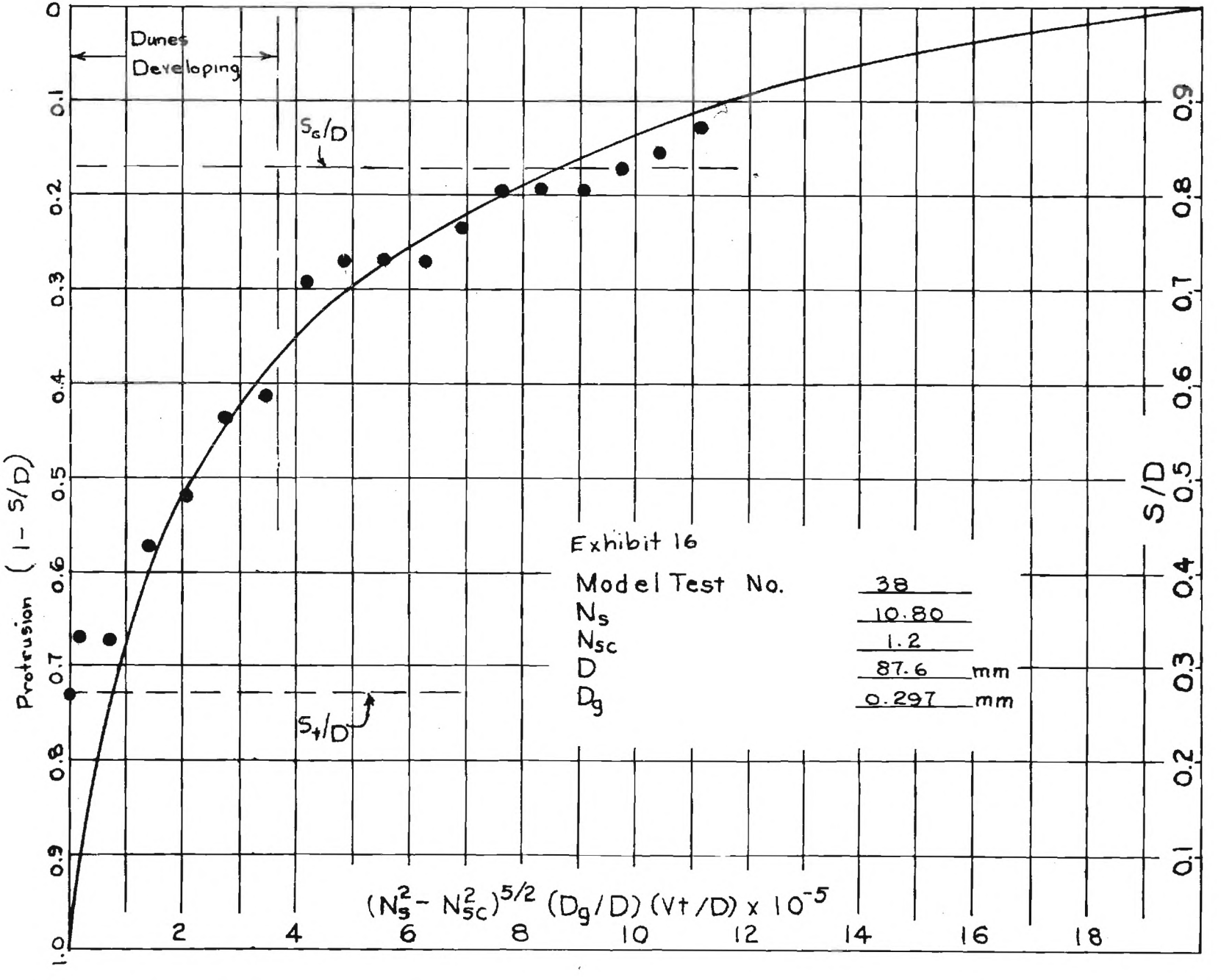
Dunes Developing
S_c/D
S_t/D
Exhibit 16
Model Test No. 38
N_s 10.80
N_{sc} 1.2
D 87.6 mm
D_g 0.297 mm
Protrusion (1 - S/D)
S/D
Burial
$(N_s^2 - N_{sc}^2)^{5/2} (D_g/D) (Vt/D) \times 10^{-5}$
0
0.1
0.2
0.3
0.4
0.5
0.6
0.7
0.8
0.9
1.0
2
4
6
8
10
12
14
16
18

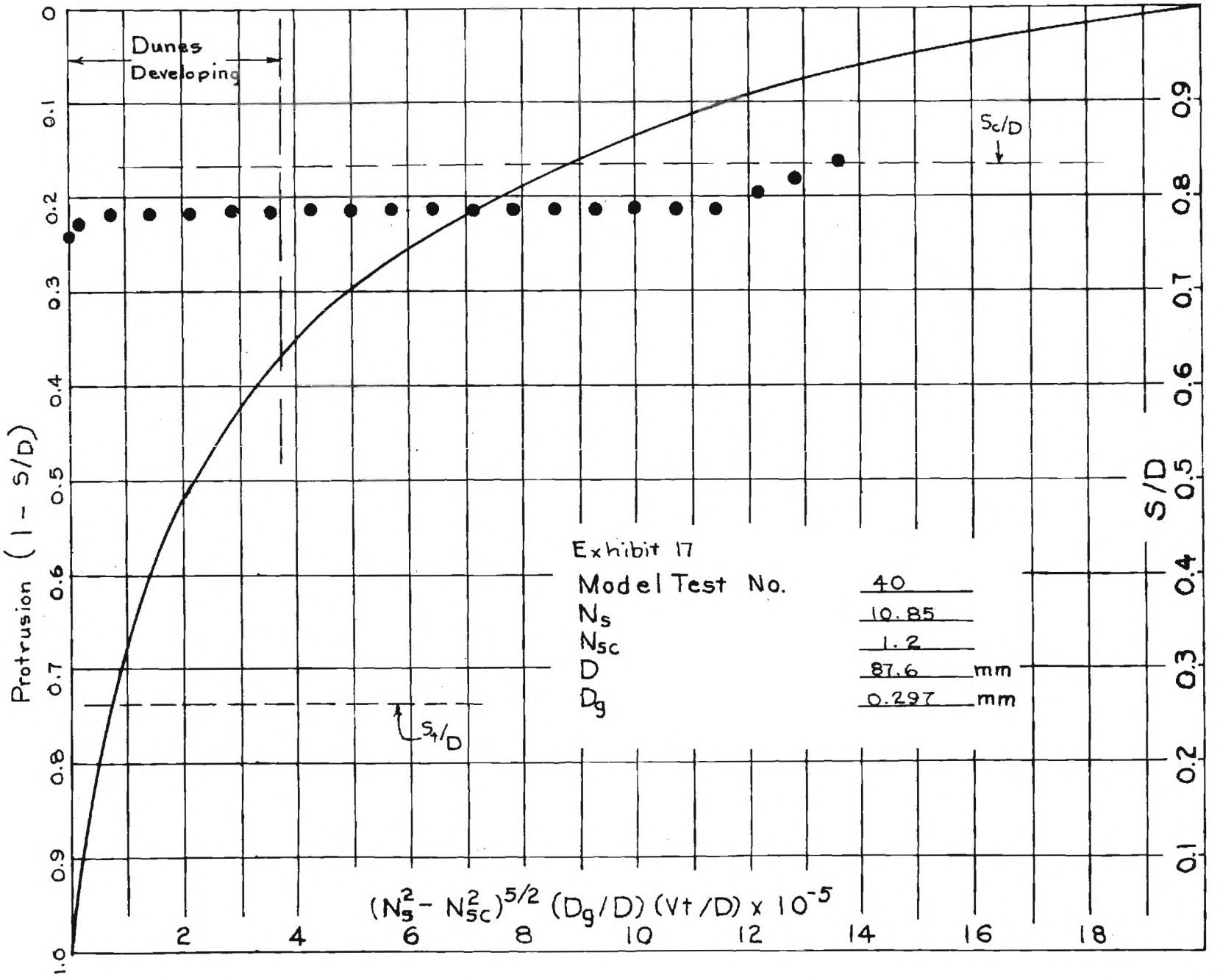
Dunes
Developing
S_c/D
S_f/D
Exhibit 17
Model Test No. 40
N_s 10.85
N_{sc} 1.2
D 87.6 mm
D_g 0.297 mm
Protrusion (1 - S/D)
S/D
$(N_s^2 - N_{sc}^2)^{5/2} (D_g/D) (Vt/D) \times 10^{-5}$
0
0.1
0.2
0.3
0.4
0.5
0.6
0.7
0.8
0.9
1.0
2
4
6
8
10
12
14
16
18

Burial

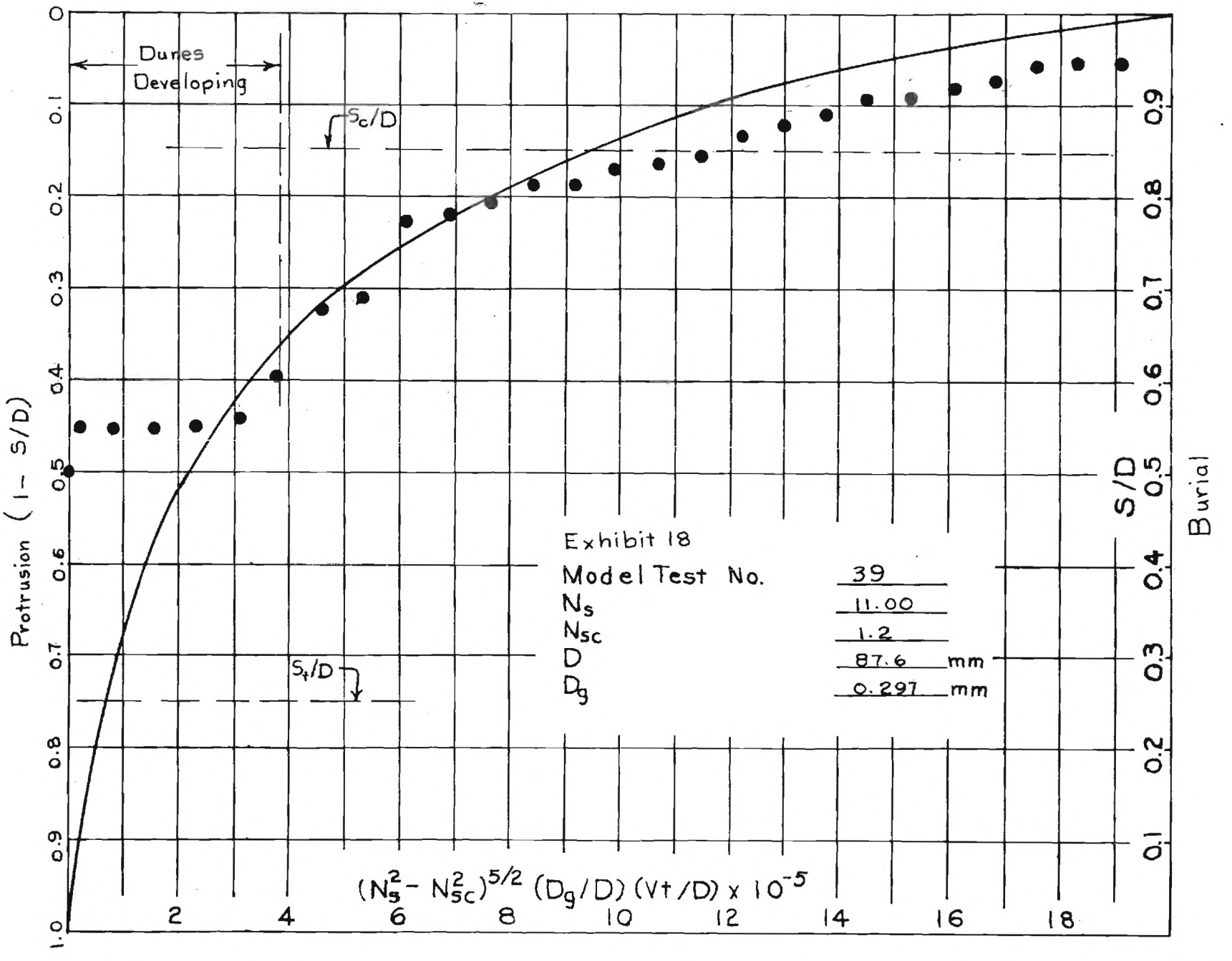
Dunes Developing
S_c/D
S_t/D
Exhibit 18
Model Test No. 39
N_s 11.00
N_{sc} 1.2
D 87.6 mm
D_g 0.297 mm
Protrusion (1 - S/D)
S/D
Burial
$(N_s^2 - N_{sc}^2)^{5/2} (D_g/D) (Vt/D) \times 10^{-5}$
0
0.1
0.2
0.3
0.4
0.5
0.6
0.7
0.8
0.9
1.0
2
4
6
8
10
12
14
16
18

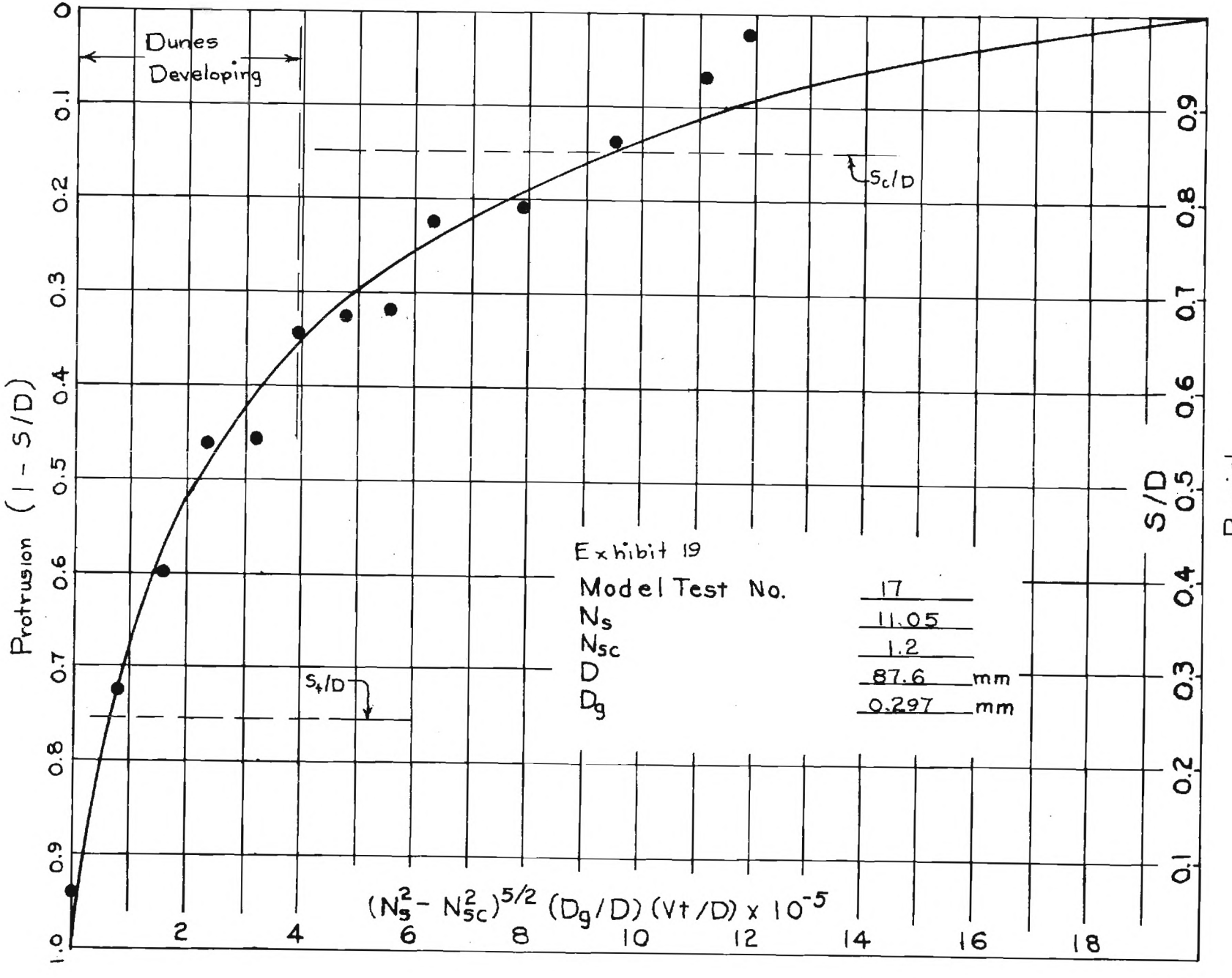
Dunes
Developing
S_c/D
S_t/D
Exhibit 19
Model Test No. 17
N_s 11.05
N_{sc} 1.2
D 87.6 mm
D_g 0.297 mm
Protrusion (1 - S/D)
Burial S/D
$(N_s^2 - N_{sc}^2)^{5/2} (D_g/D) (Vt/D) \times 10^{-5}$
0
0.1
0.2
0.3
0.4
0.5
0.6
0.7
0.8
0.9
1.0
2
4
6
8
10
12
14
16
18

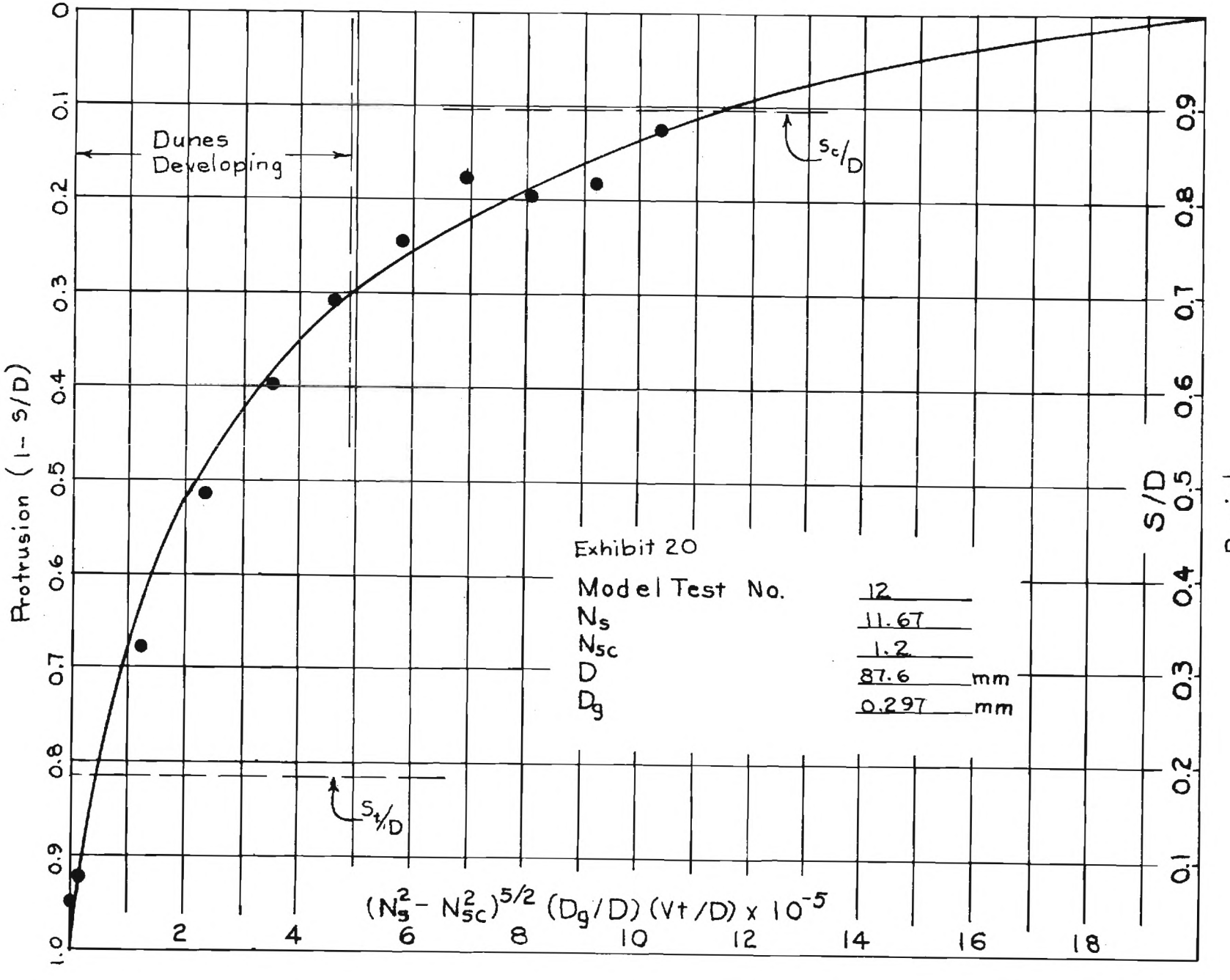
Protrusion (1 - S/D)
Burial S/D
Dunes Developing
S_c/D
S_t/D
Exhibit 20
Model Test No. 12
N_s 11.67
N_{sc} 1.2
D 87.6 mm
D_g 0.297 mm
$(N_s^2 - N_{sc}^2)^{5/2} (D_g/D) (Vt/D) \times 10^{-5}$
0
0.1
0.2
0.3
0.4
0.5
0.6
0.7
0.8
0.9
1.0
2
4
6
8
10
12
14
16
18

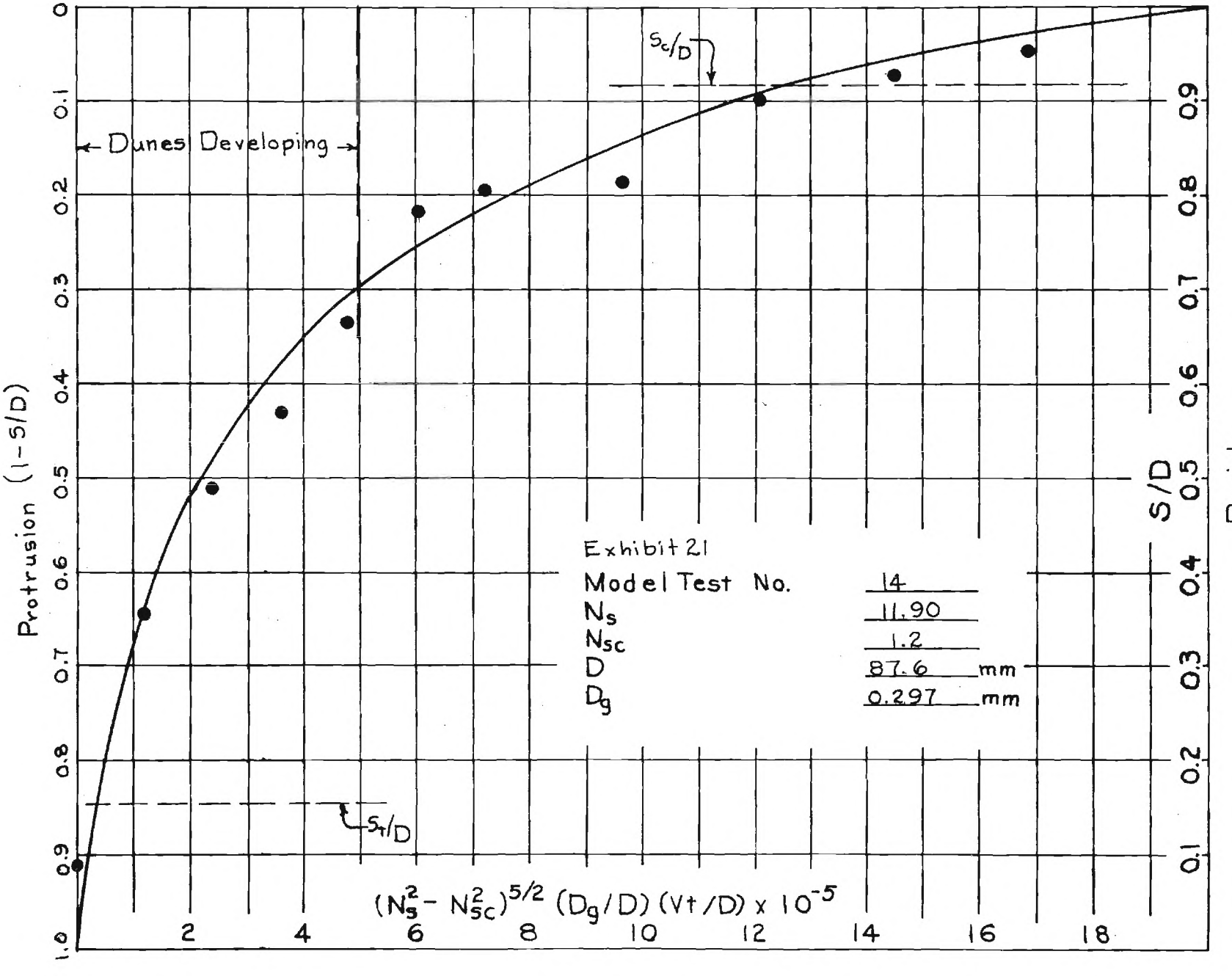
Protrusion (1-S/D)
Burial S/D
← Dunes Developing →
S_c/D
S_t/D
Exhibit 21
Model Test No. 14
N_s 11.90
N_{sc} 1.2
D 87.6 mm
D_g 0.297 mm
$(N_s^2 - N_{sc}^2)^{5/2} (D_g/D) (Vt/D) \times 10^{-5}$
0
0.1
0.2
0.3
0.4
0.5
0.6
0.7
0.8
0.9
1.0
2
4
6
8
10
12
14
16
18

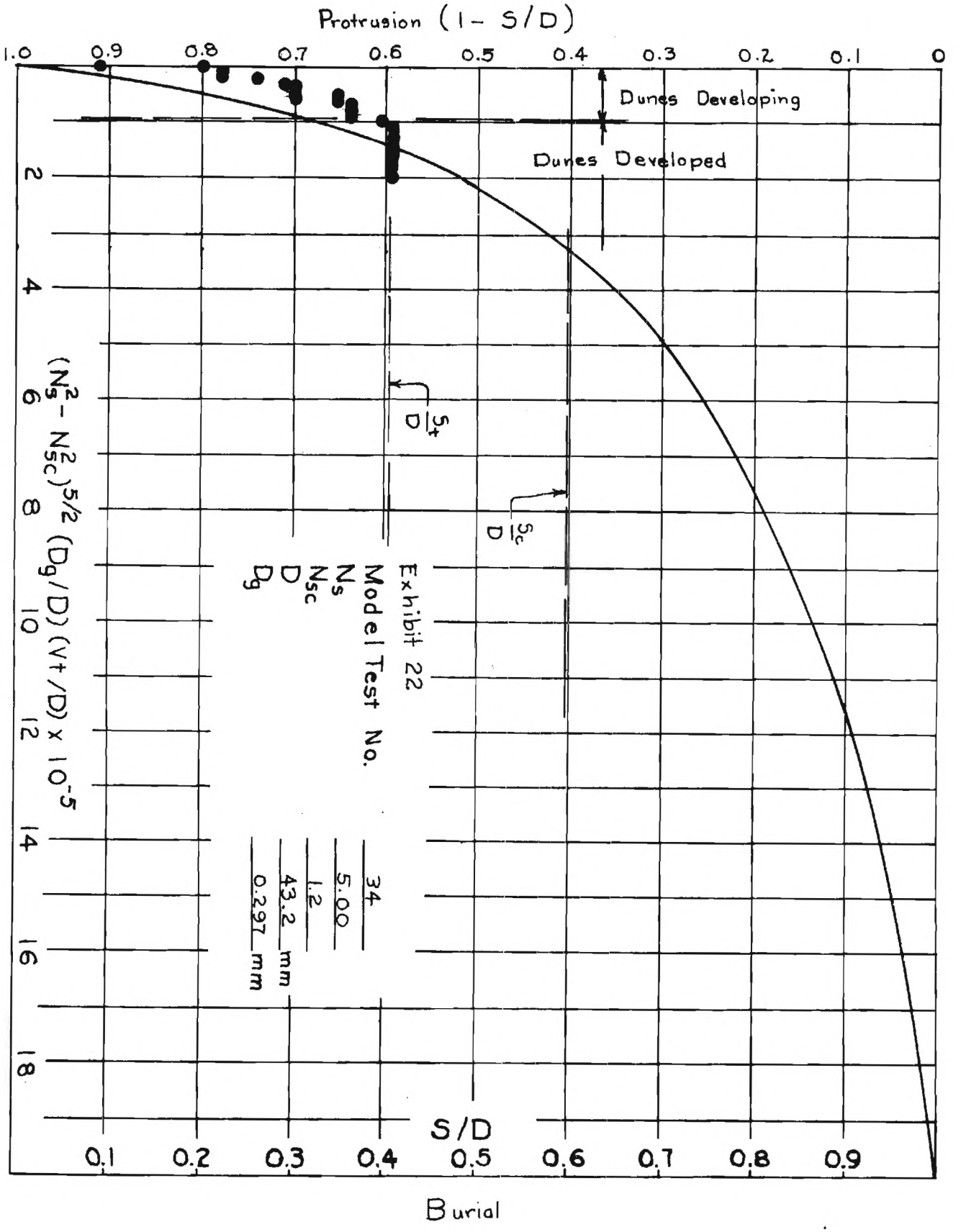
Protrusion (1 - S/D)
1.0
0.9
0.8
0.7
0.6
0.5
0.4
0.3
0.2
0.1
0
Dunes Developing
Dunes Developed
$\frac{S_t}{D}$
$\frac{S_c}{D}$
Exhibit 22
Model Test No.
N_s
N_{sc}
D
D_g
34
5.00
1.2
43.2 mm
0.297 mm
$(N_s^2 - N_{sc}^2)^{5/2} (D_g/D) (V_t/D) \times 10^{-5}$
2
4
6
8
10
12
14
16
18
S/D
0.1
0.2
0.3
0.4
0.5
0.6
0.7
0.8
0.9
Burial

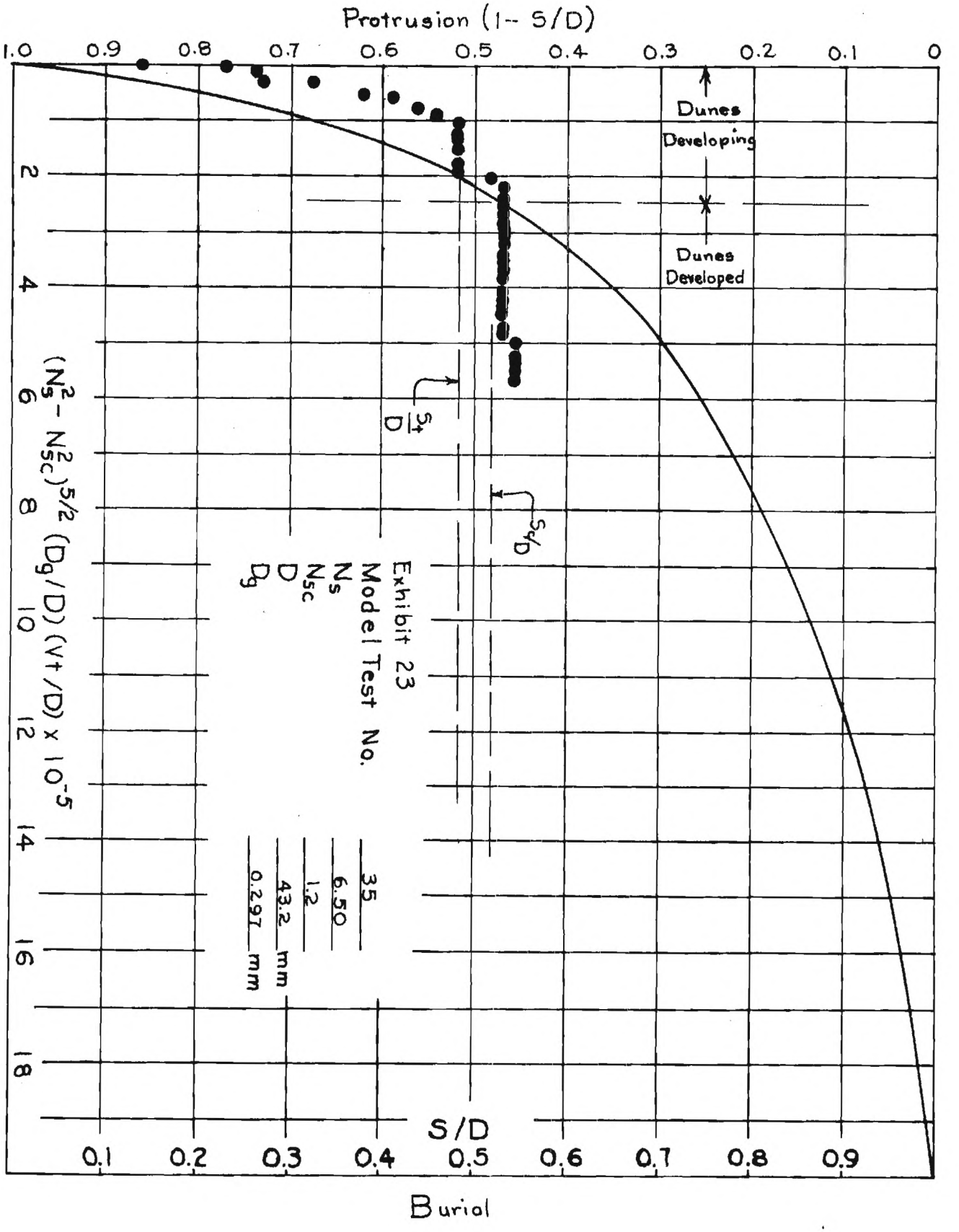
Protrusion (1- S/D)
1.0
0.9
0.8
0.7
0.6
0.5
0.4
0.3
0.2
0.1
0
Dunes Developing
Dunes Developed
$\frac{S_t}{D}$
$\frac{S_{sc}}{D}$
$(\frac{N_s^2}{6} - N_{sc}^2)^{5/2} (D_g/D) (V_t/D) \times 10^{-5}$
2
4
6
8
10
12
14
16
18
Exhibit 23
Model Test No.
N_s 35
N_{sc} 6.50
D 1.2
D_g 43.2 mm
0.297 mm
S/D
0.1
0.2
0.3
0.4
0.5
0.6
0.7
0.8
0.9
Burial

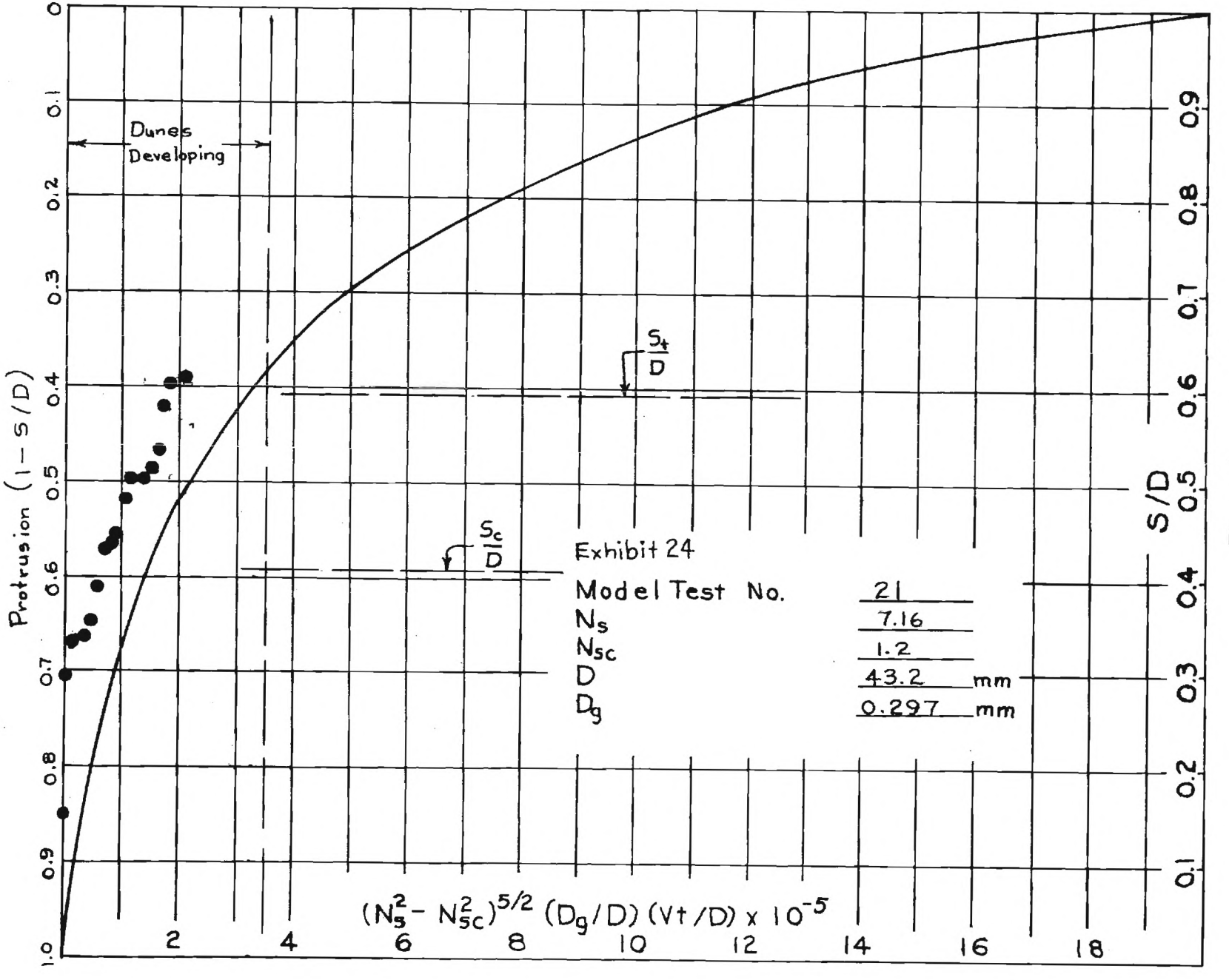
Dunes Developing
$\frac{S_t}{D}$
$\frac{S_c}{D}$
Exhibit 24
Model Test No. 21
N_s 7.16
N_{sc} 1.2
D 43.2 mm
D_g 0.297 mm
Protrusion (1 − S/D)
S/D
Burial
$(N_s^2 - N_{sc}^2)^{5/2} (D_g/D) (Vt/D) \times 10^{-5}$
0
0.1
0.2
0.3
0.4
0.5
0.6
0.7
0.8
0.9
1.0
2
4
6
8
10
12
14
16
18

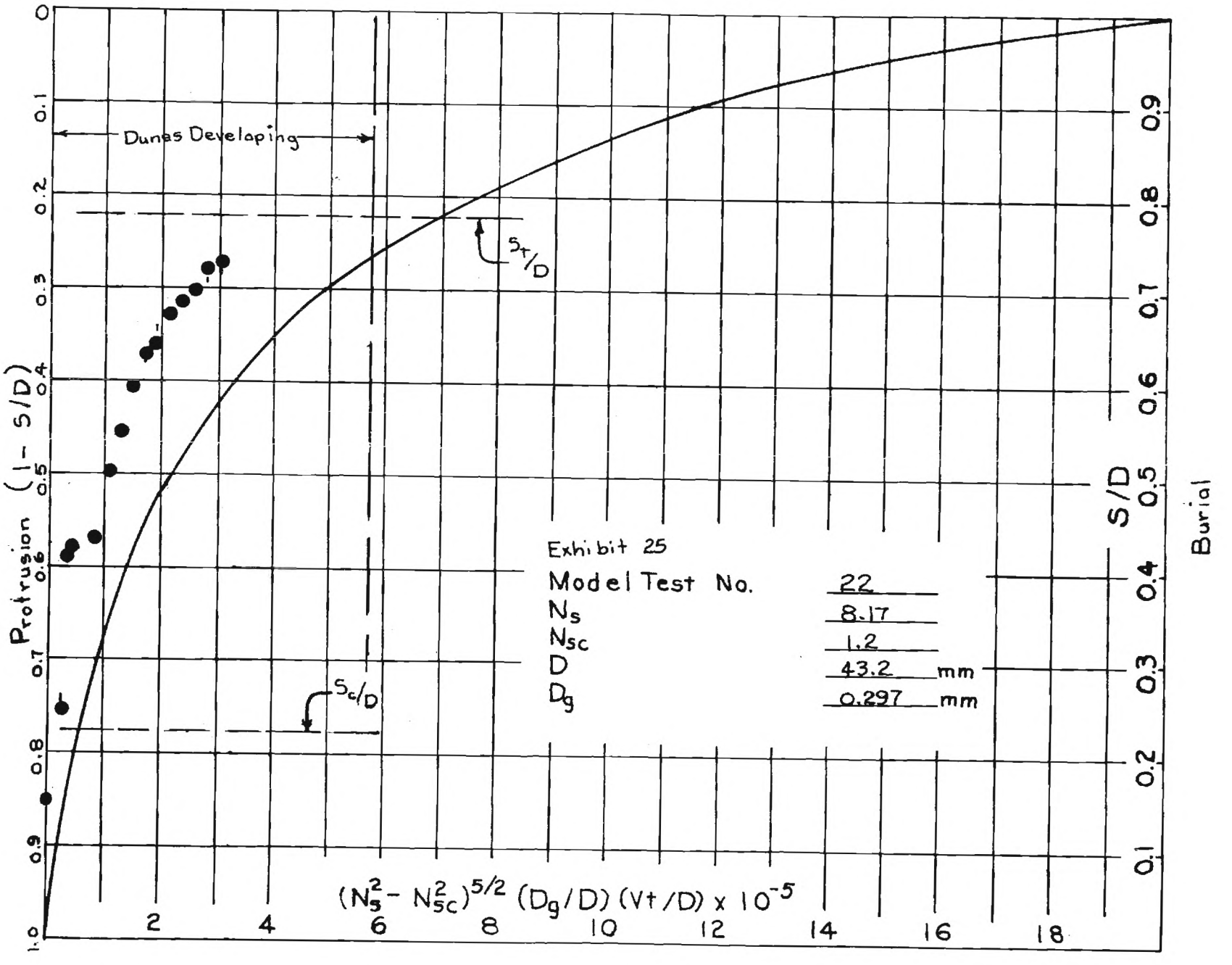
Dunes Developing
S_t/D
S_c/D
Exhibit 25
Model Test No. 22
N_s 8.17
N_{sc} 1.2
D 43.2 mm
D_g 0.297 mm
Protrusion (1 - S/D)
Burial S/D
$(N_s^2 - N_{sc}^2)^{5/2} (D_g/D) (Vt/D) \times 10^{-5}$
0
0.1
0.2
0.3
0.4
0.5
0.6
0.7
0.8
0.9
1.0
2
4
6
8
10
12
14
16
18

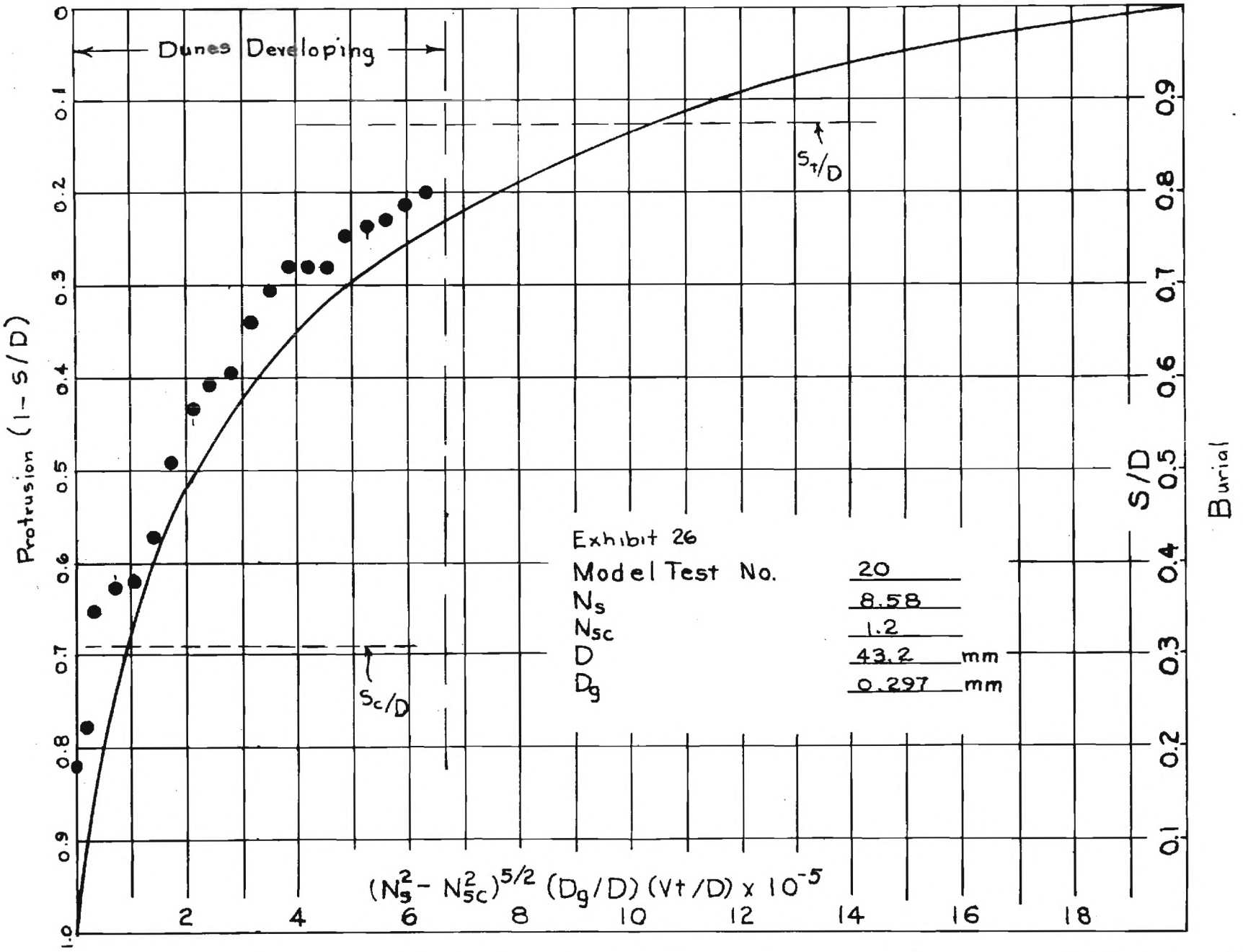
Dunes Developing
S_T/D
S_c/D
Exhibit 26
Model Test No. 20
N_s 8.58
N_{sc} 1.2
D 43.2 mm
D_g 0.297 mm
Protrusion (1 - S/D)
Burial S/D
$(N_s^2 - N_{sc}^2)^{5/2} (D_g/D) (Vt/D) \times 10^{-5}$
0
0.1
0.2
0.3
0.4
0.5
0.6
0.7
0.8
0.9
1.0
2
4
6
8
10
12
14
16
18

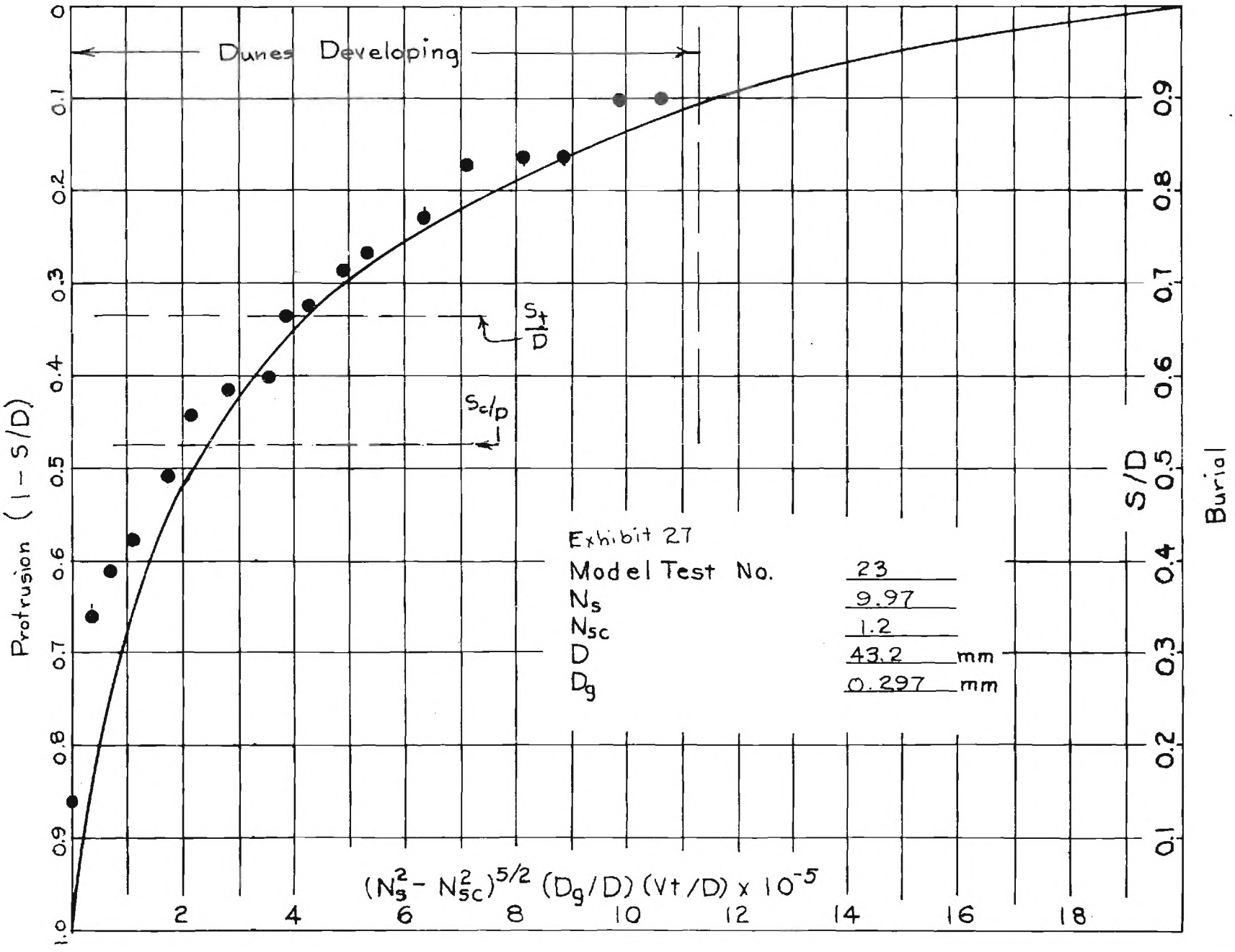
Dunes Developing
Protrusion (1 − S/D)
S/D
Burial
$(N_s^2 - N_{sc}^2)^{5/2} (D_g/D) (Vt/D) \times 10^{-5}$
S_t/D
$S_{c/p}$
Exhibit 27
Model Test No. 23
N_s 9.97
N_{sc} 1.2
D 43.2 mm
D_g 0.297 mm

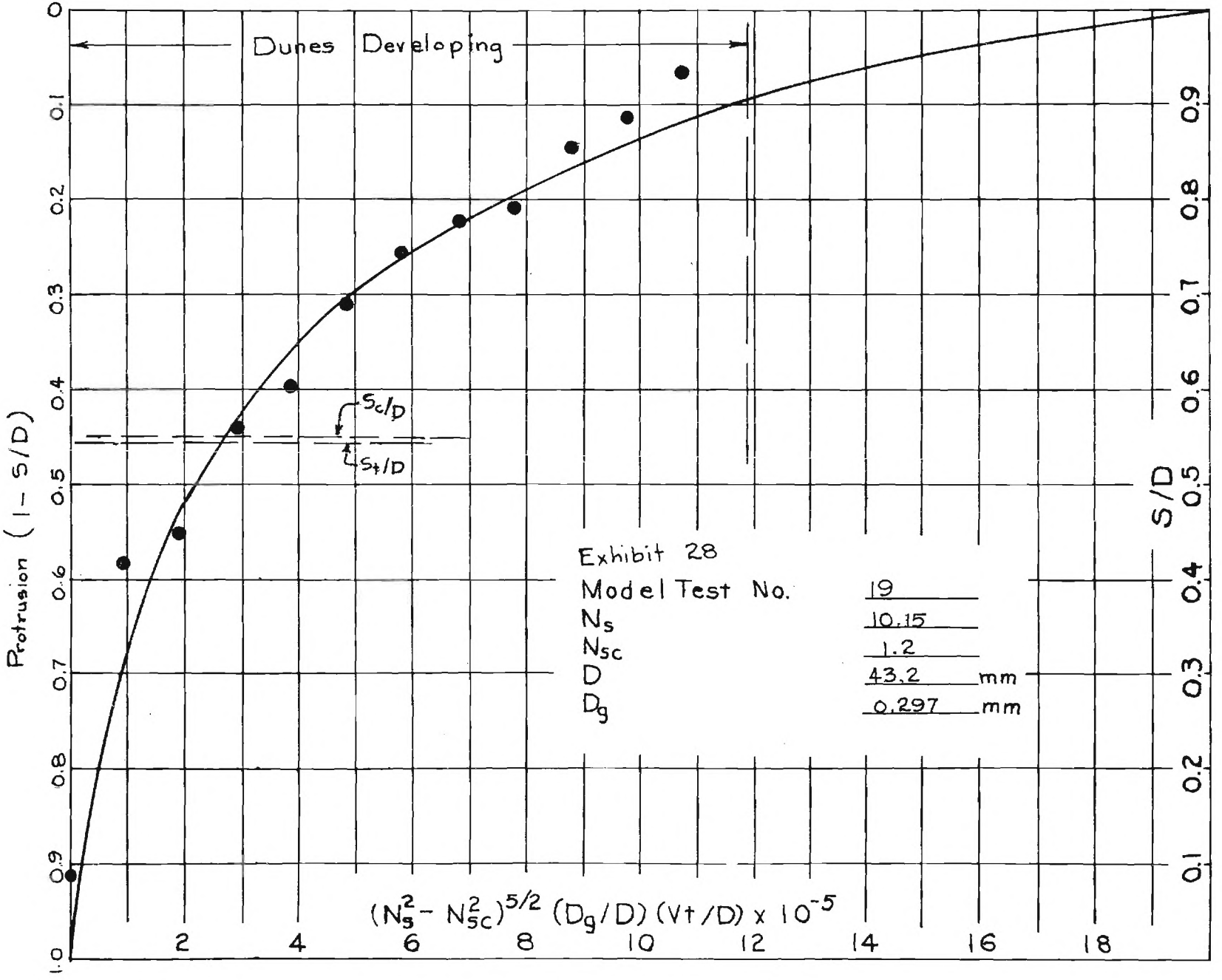
Dunes Developing
Protrusion (1 - S/D)
S/D
Burial
S_c/D
S_t/D
Exhibit 28
Model Test No. 19
N_s 10.15
N_{sc} 1.2
D 43.2 mm
D_g 0.297 mm
$(N_s^2 - N_{sc}^2)^{5/2} (D_g/D) (Vt/D) \times 10^{-5}$
0
0.1
0.2
0.3
0.4
0.5
0.6
0.7
0.8
0.9
1.0
2
4
6
8
10
12
14
16
18

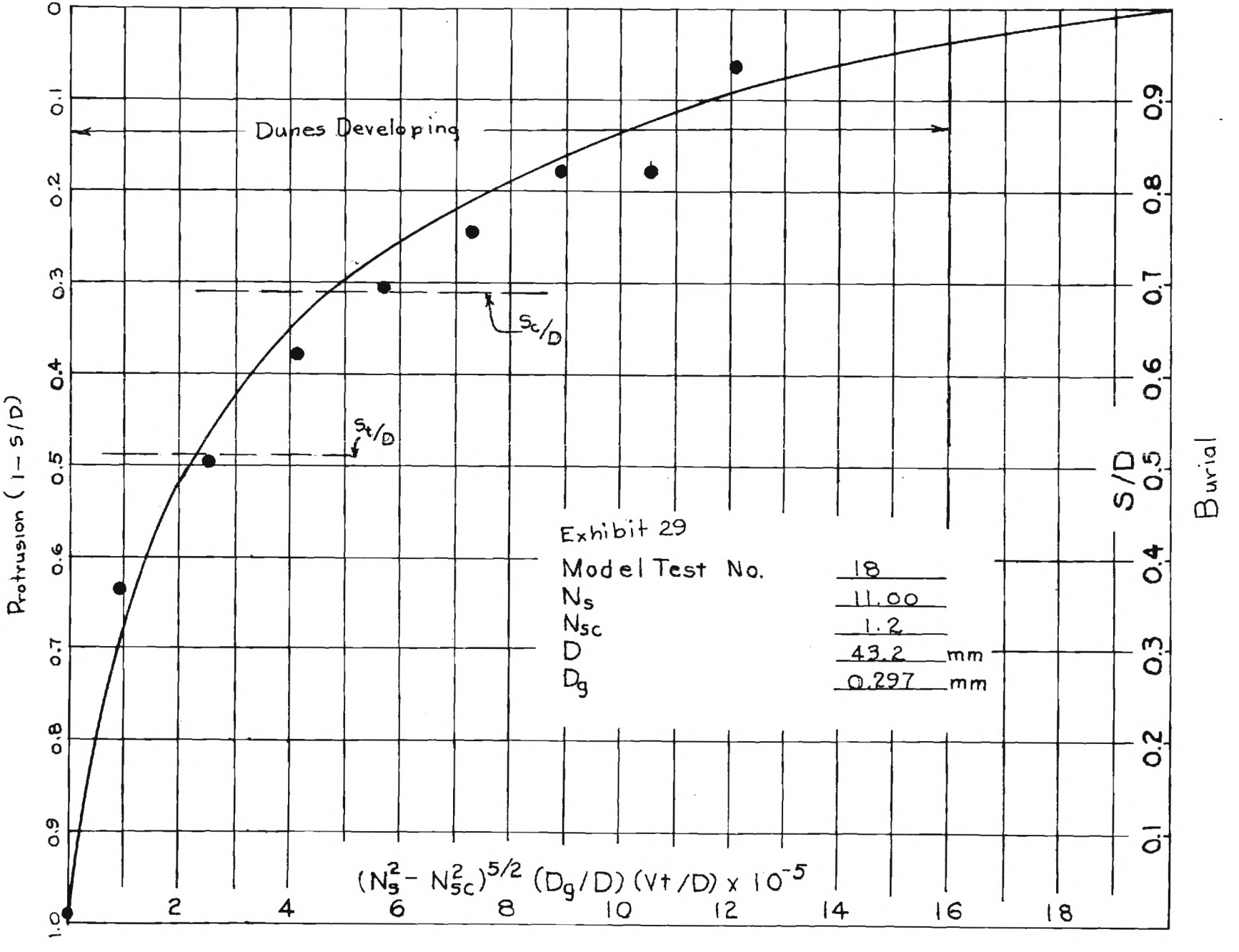
Dunes Developing
S_c/D
S_t/D
Exhibit 29
Model Test No. 18
N_s 11.00
N_{sc} 1.2
D 43.2 mm
D_g 0.297 mm
Protrusion (1 − S/D)
S/D
Burial
$(N_s^2 - N_{sc}^2)^{5/2} (D_g/D) (Vt/D) \times 10^{-5}$
0
0.1
0.2
0.3
0.4
0.5
0.6
0.7
0.8
0.9
1.0
2
4
6
8
10
12
14
16
18

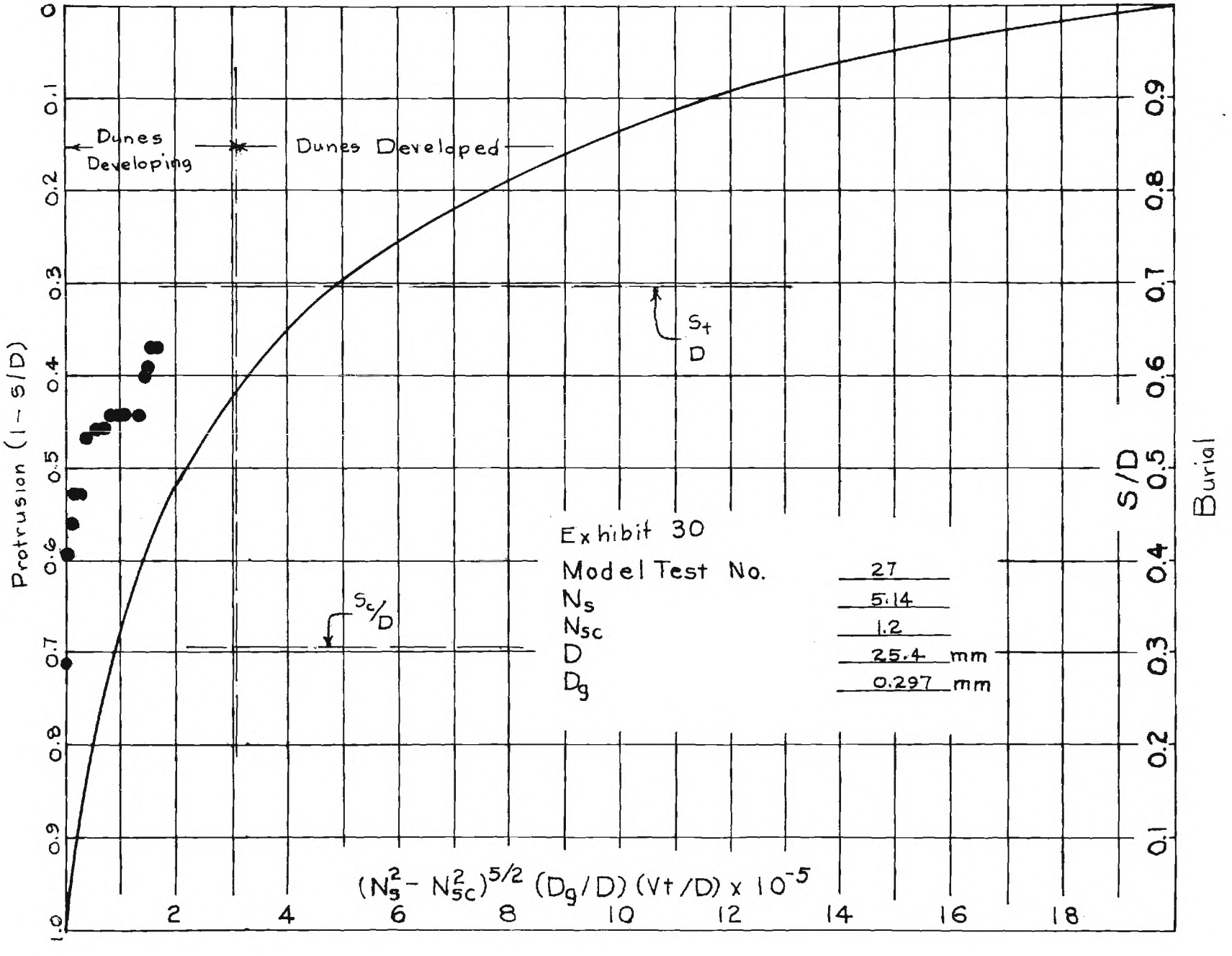
Dunes Developing
Dunes Developed
S_t
D
S_c/D
Exhibit 30
Model Test No. 27
N_s 5.14
N_{sc} 1.2
D 25.4 mm
D_g 0.297 mm
Protrusion (1 - S/D)
S/D
Burial
$(N_s^2 - N_{sc}^2)^{5/2} (D_g/D) (Vt/D) \times 10^{-5}$
0
0.1
0.2
0.3
0.4
0.5
0.6
0.7
0.8
0.9
1.0
2
4
6
8
10
12
14
16
18

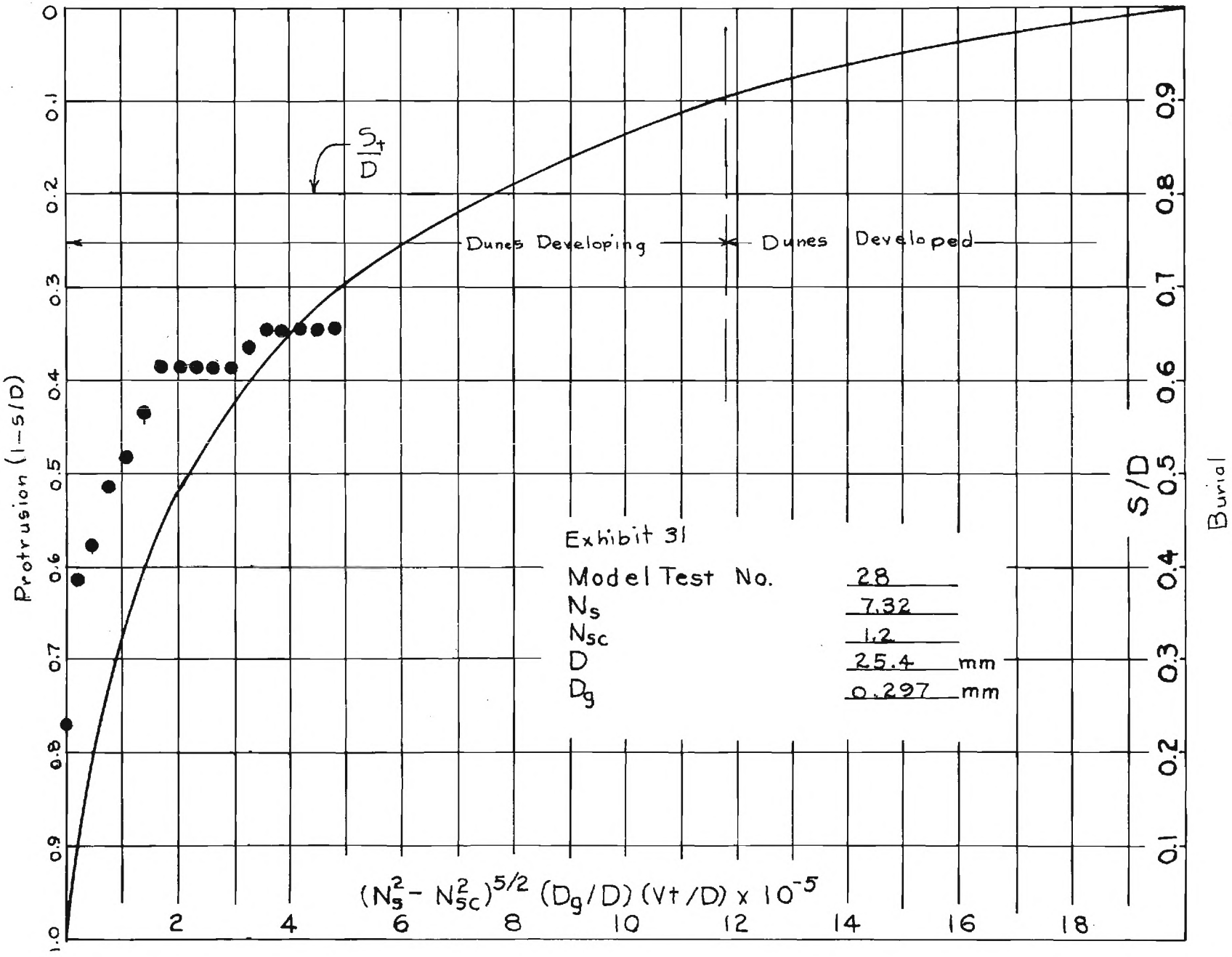
Protrusion (1-S/D)
S/D
Burial
$\frac{S_t}{D}$
Dunes Developing
Dunes Developed
$(N_s^2 - N_{sc}^2)^{5/2} (D_g/D) (Vt/D) \times 10^{-5}$
Exhibit 31
Model Test No. 28
N_s 7.32
N_{sc} 1.2
D 25.4 mm
D_g 0.297 mm

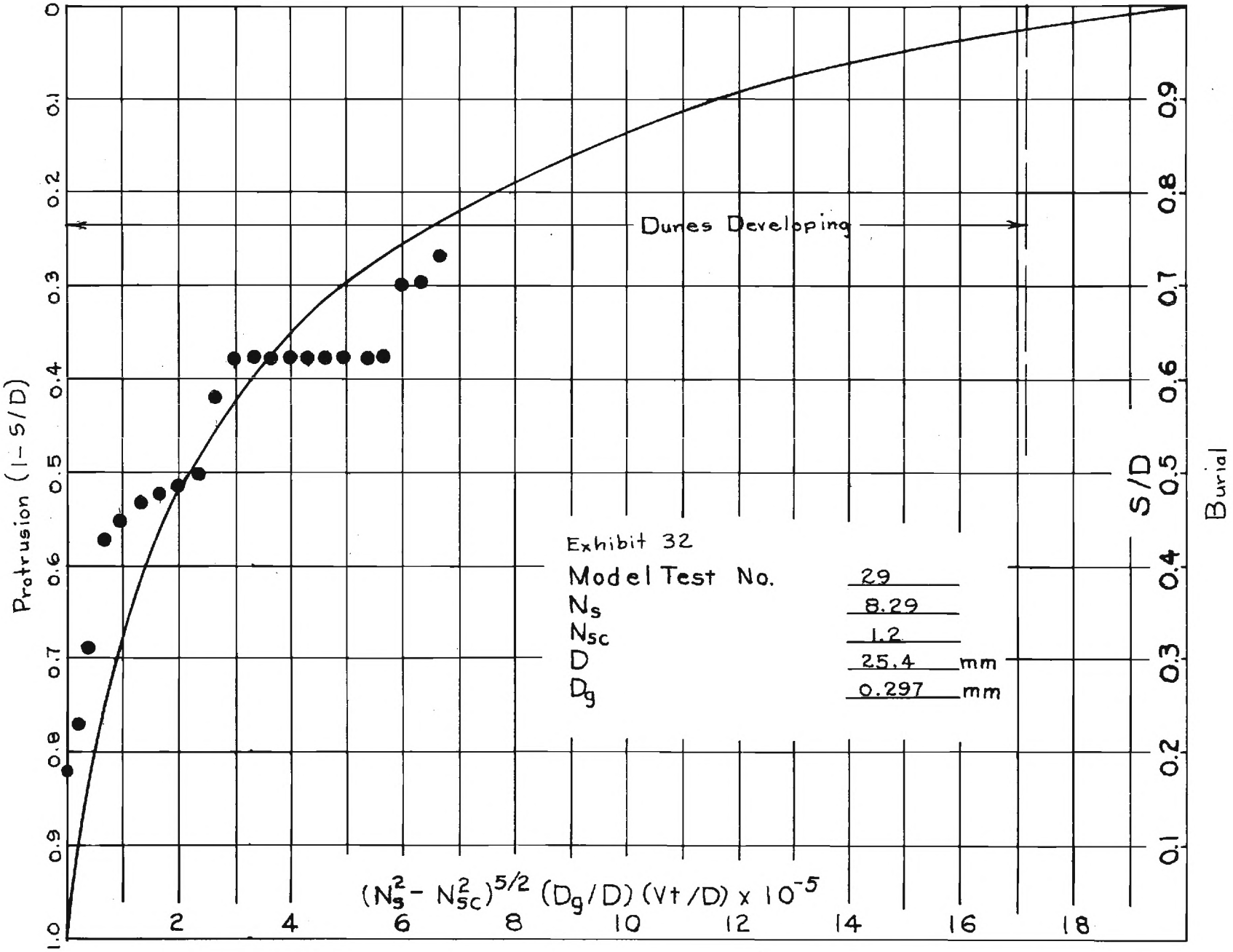
Protrusion (1 - S/D)
Burial S/D
Dunes Developing
Exhibit 32
Model Test No. 29
N_s 8.29
N_{sc} 1.2
D 25.4 mm
D_g 0.297 mm
$(N_s^2 - N_{sc}^2)^{5/2} (D_g/D) (Vt/D) \times 10^{-5}$
0
0.1
0.2
0.3
0.4
0.5
0.6
0.7
0.8
0.9
1.0
2
4
6
8
10
12
14
16
18

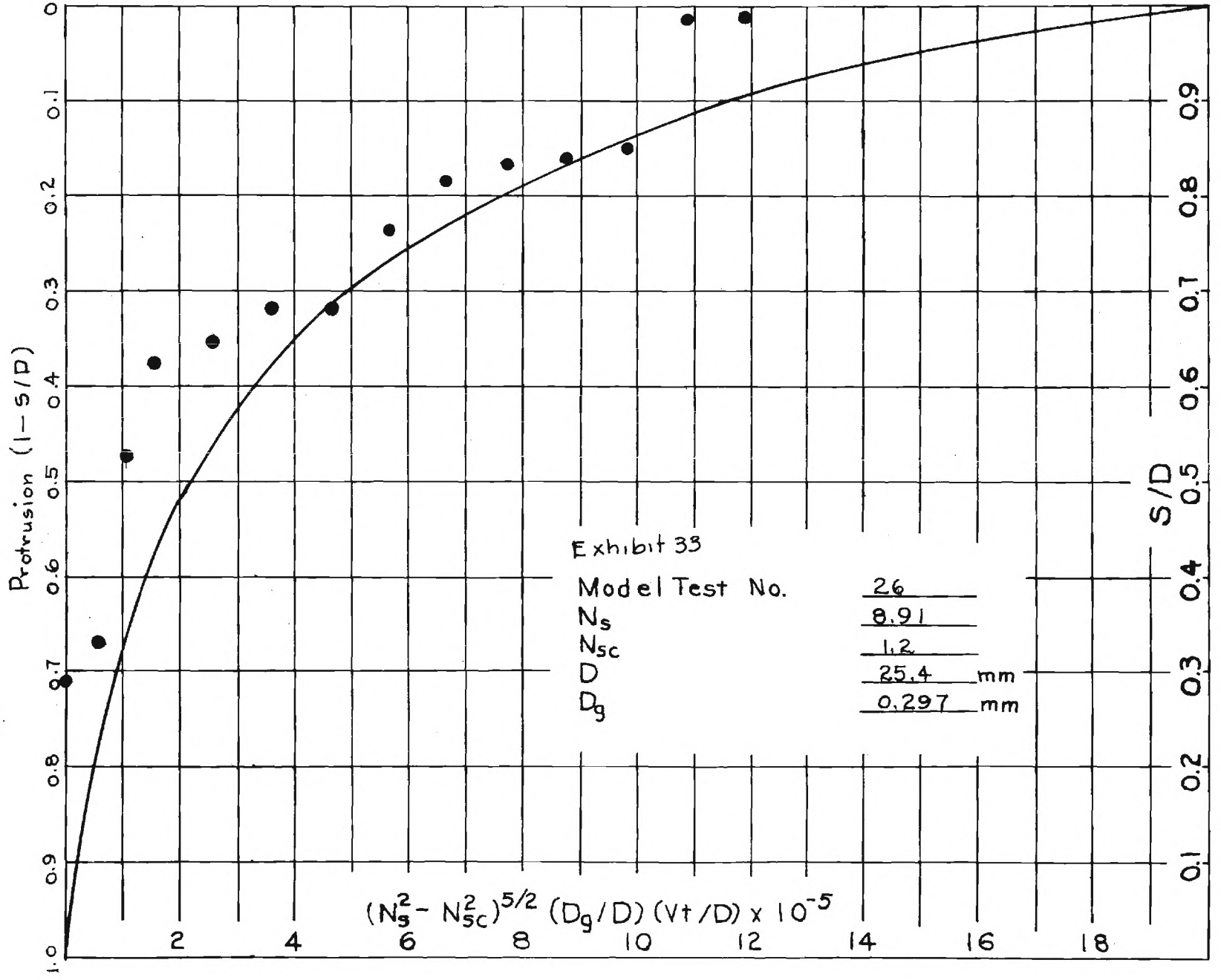
Protrusion (1 − S/D)
0
0.1
0.2
0.3
0.4
0.5
0.6
0.7
0.8
0.9
1.0
S/D
0.9
0.8
0.7
0.6
0.5
0.4
0.3
0.2
0.1
$(N_s^2 - N_{sc}^2)^{5/2} (D_g/D) (Vt/D) \times 10^{-5}$
2
4
6
8
10
12
14
16
18
Exhibit 33
Model Test No. 26
N_s 8.91
N_{sc} 1.2
D 25.4 mm
D_g 0.297 mm
Burial

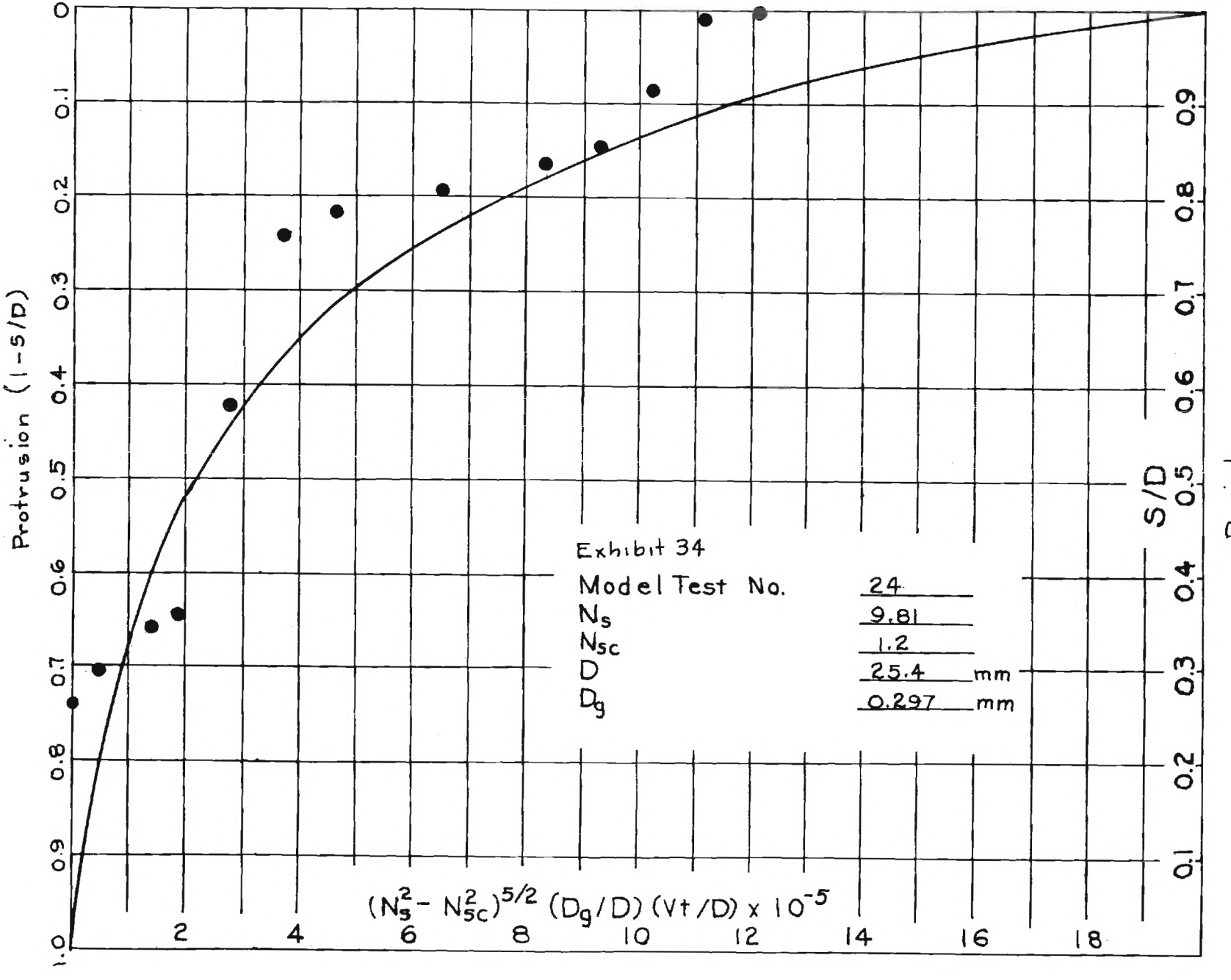
Protrusion (1-S/D)
0
0.1
0.2
0.3
0.4
0.5
0.6
0.7
0.8
0.9
1.0
S/D
Burial
Exhibit 34
Model Test No. 24
N_s 9.81
N_{sc} 1.2
D 25.4 mm
D_g 0.297 mm
$(N_s^2 - N_{sc}^2)^{5/2} (D_g/D) (Vt/D) \times 10^{-5}$
2
4
6
8
10
12
14
16
18

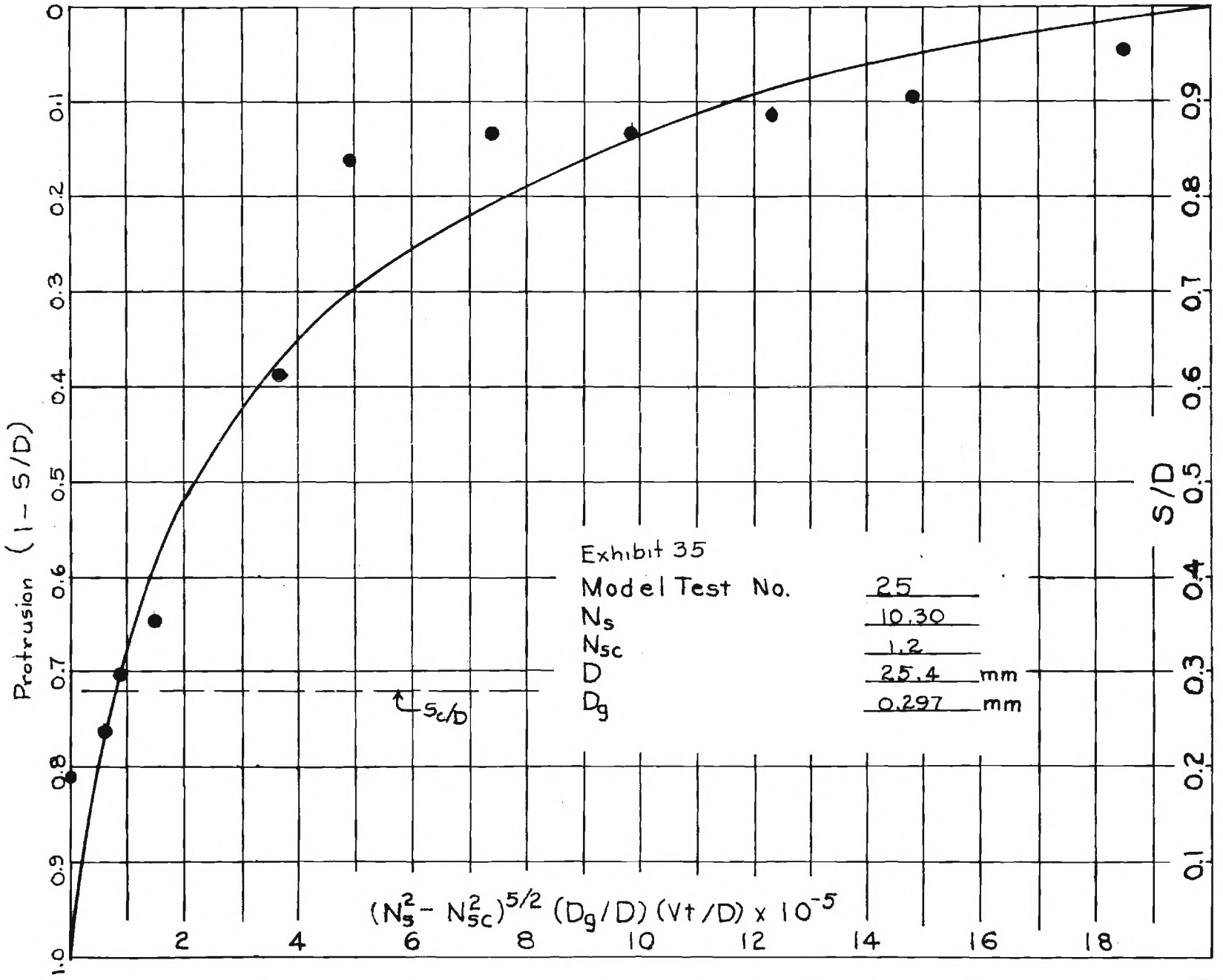
Protrusion (1 − S/D)
S/D
$(N_s^2 - N_{sc}^2)^{5/2} (D_g/D) (Vt/D) \times 10^{-5}$
S_c/D
Exhibit 35
Model Test No. 25
N_s 10.30
N_{sc} 1.2
D 25.4 mm
D_g 0.297 mm
Burial

APPENDIX B

SIMILARITY--LOCALIZED SCOUR

SIMILARITY--LOCALIZED SCOUR

By M. R. Carstens[1], M. ASCE

SYNOPSIS

Similarity criteria are developed for rate of sediment transport and for scour depth of localized scour. The similarity relations are demonstrated for the following localized-scour situations: (A) in a defined scour hole, (B) by two-dimensional dunes, (C) by a two-dimensional jet, (D) around a vertical cylinder, and (E) around a horizontal cylinder.

[1]Professor of Civil Engineering, Georgia Institute of Technology, Atlanta, Georgia.

INTRODUCTION

The object of this study is to formulate similarity criteria for localized scour. An intermediate step is to formulate sediment-transport functions of localized scour which are then integrated to obtain scour-depth functions. Inasmuch as localized scour occurs in non-uniform flow regions resulting from obstructions placed in the flow, any sediment-transport function for localized scour will be strongly dependent upon the geometry of the obstruction. Obviously, then, a general sediment-transport function for localized scour is quite unobtainable. Rather the hope would be in analyzing localized-scour experimental results that the fluid, sediment, and flow variables could be grouped separately from the geometric variables. The functional relation between sediment-transport parameter and the geometric parameters would be expected to vary from one scouring situation to another. On the other hand, the functional relation between the sediment-transport parameter and the parameter containing fluid, sediment, and flow variables should be similar from one scouring situation to another.

Localized scour will occur where the water has been accelerated as the water is moved past the obstruction in the stream or where large vortices are generated as the flow separates from the obstruction. In either event the boundary-layer thickness adjacent to the bed where maximum scouring is occurring can be expected to be negligible. The following analysis is predicated upon the assumption that the boundary layer is of negligible thickness in areas of active localized scour. In other words the velocity and velocity distribution in areas of active local scour are assumed to be functions only of the geometry of the obstruction and of the scour hole.

Also the following analysis is based upon the assumption that no sediment is transported into the hole other than the sediment which would slide into the hole down the sides and down the upstream slope. Situations in which sediment is transported into the scour-hole area from upstream are subsequently analyzed by mass-transport continuity assuming that the incoming sediment does not affect the localized scouring process, per se.

The rate of sediment transport can be expected to be a function of the forces on a typical particle on the surface of the bed. The disturbing force on a typical particle is the resultant of the drag and lift forces resulting from the flow around and over the surface particle, that is,

$$\Sigma F_M = C_D K_1 D_g^2 \frac{\rho V^2}{2} + C_L K_1 D_g^2 \frac{\rho V^2}{2} \qquad (1)$$

in which

ΣF_M is the disturbing force on the particle;

C_D is the coefficient of drag of the particle;

C_L is the coefficient of lift of tne particle;

K_1 is a dimensionless particle-shape factor (projected area);

D_g is the typical grain diameter of the surface particles;

ρ is the density of water; and

V is the fluid velocity adjacent to the bed.

The stabilizing force on a typical particle is the effective weight, that is,

$$\Sigma F_R = (\gamma_s - \gamma) K_2 D_g^3 \qquad (2)$$

in which

ΣF_R is the effective weight of the particle;

γ_s is the specific weight of the particles;

γ is the specific weight of water; and

K_2 is a dimensionless particle-shape factor (volume).

The force ratio is

$$\frac{\Sigma F_M}{\Sigma F_R} = \frac{K_1\sqrt{C_L^2 + C_D^2}}{K_2} \frac{V^2}{(s - 1) gD_g} \tag{3}$$

The particle shape factors, K_1 and K_2, are sediment-geometry variables which are independent of the flow situation. The coefficients of lift and drag, C_L and C_D, would, in general, be functions of (a) the particle geometry and geometric arrangement of the surface particles, (b) the Reynolds number, and (c) the velocity distribution in the vicinity of the particle. Since the particles are unstreamlined, since the velocity is large in areas of localized scour, since the fluid (water) has a low viscosity, and since the boundary layer is expected to be of negligible thickness in areas of active scour, a reasonable assumption is that C_L and C_D are also sediment-geometry variables which are independent of the flow situation. In light of these considerations equation (3) is indicative that

$$\frac{\Sigma F_M}{\Sigma F_R} = \left[f \text{ (sediment-grain geometry)}\right] N_s^2 \tag{3a}$$

in which N_s is $V/\sqrt{(s-1)gD_g}$. Hereafter N_s will be referred to as sediment number.

The local rate of scour will vary over the surface of the scour hole. The greatest rate of scour will occur where the fluid velocity is greatest. At this location the scour hole will be the deepest. Since the capacity for pickup and transport will decrease away from the position of greatest depth much of the sediment scoured at the bottom will deposit on the downstream slope of the scour hole. The deposition of the sediment on the downstream slope of the scour hole and the sliding of the sediment down the upstream slope and side of the scour hole results in the wall slope of the scour hole being nearly equal to the angle of repose ϕ of the cohesionless sediment (sediment-grain geometry). The net rate of transport out of the hole Q_s is the transport over the downstream edge. As the scour hole deepens, the lateral limit of the hole is moved further from the flow disturbance. Hence, the rate of transport out of the hole can be expected to decrease drastically as the depth of scour S increases.

Utilizing these geometric concepts as well as the assumption that the sediment transport rate is a function of the force ratio $\Sigma F_M/\Sigma F_R$, equation (3a), a dimensionless form of the sediment-transport function can be hypothesized as follows

$$\frac{Q_s}{VBD_g} = f\left((N_s^2 - N_{sc}^2), \frac{S}{L}, \text{disturbance geometry, sediment-grain geometry}\right) \quad (4)$$

in which

N_{sc} is the lowest value of the sediment number for which scour will occur;

V is a reference velocity;

B is the width of the scour hole; and

L is a pertinent dimension of the obstruction.

In equation (4), the sediment-grain geometry includes not only the variables involving the shape of the bed material but also the gradation. The geometric variable S/L is necessary to establish the stage of the scour-hole development. The reference discharge VBD_g used in the discharge ratio, LHS of equation (4), can be visualized as the approaching water discharge through an area having a width B equal to the scour-hole width and having a height D_g equal to a grain diameter (or some multiple of the grain diameter). The choice of the height D_g rather than the depth of flow is based upon the idea that the pickup and transport of sediment in the active scour area is a function of the flow conditions close to the bed and is essentially independent of the flow conditions in the water some distance above the bed. Of course, this concept is invalid if the water depth is small or if the Froude number is large resulting in appreciable changes in elevation of the water surface which has the effect of changing the flow pattern in addition to the changes resulting from the obstruction and the scour-hole.

If one were to include all of the possible variables upon which the sediment transport rate is dependent, the object of this study would appear hopeless at the outset. Lacking a mathematical model for sediment pickup and transport in non uniform flow, the writer has been forced to use physical reasoning in order to eliminate many variables having a second-order effect. The validity of the result, equation (4), can only be determined by analyzing the data from different experiments in which the localized scour results from different types of flow obstructions. In the following, localized scour experiments with (A) a defined scour hole, (B) scour associated with dunes, (C) two-dimensional jet scour, (D) scour around a vertical cylinder, and (E) scour around a cylinder lying on the bed, are analyzed in order to formulate sediment-transport functions associated with

localized scour. Subsequent integration involving the sediment-transport functions leads to the relationship of the dependent variables with which to express scour depth as a function of time.

A. DEFINED SCOUR HOLE

In order to study a steady-state localized scour situation, LeFeuvre[2] studied sediment transport from a scour hole of fixed geometry. The top of the scour hole was the opening formed by the junction of a two-inch diameter transparent plastic pipe with the bottom of the main-flow section which was a three-inch diameter transparent plastic pipe as shown in Figure 1. A machined plastic wedge was fastened inside the vertical two-inch diameter pipe forming a defined scour hole with a sloping (60-degree) upstream wall and with vertical sidewalls. Sediment was forced into the bottom of the scour hole by means of a piston which was moved upward at a uniform rate by means of a system of gears powered by a synchronous motor. By means of various combinations of gears the sediment-feed rate could be varied in finite steps with a total range of 126.5 to 1. During a run, the water discharge through the main-flow section was adjusted by means of a downstream pinch valve until the horizontally oriented vortex within the scour hole could pick up and transport the sediment being forced into the bottom at a uniform rate. In all runs the water discharge was adjusted until the sediment bed was stabilized at the same equilibrium level. A total of 148 runs were made involving variation of sediment-transport rate Q_s^1 and six different sediments.

In LeFeuvre's experiments, the scour depth S and the dimensions of vortex-generating system were fixed with the result that equation (4) is simplified as follows

---

[2] LeFeuvre, A. R., "Sediment Transport Functions with Special Emphasis on Localized Scour," Ph.D. Dissertation, Georgia Institute of Technology, Atlanta, Georgia, 1965.

$$\frac{Q_s^1}{VBD_g} = f\left[(N_s^2 - N_{sc}^2),\ \text{sediment grain geometry}\right] \qquad (4a)$$

The reference velocity V used is the mean velocity in the main flow section since the velocity at a given point within the vortex would be proportional to the velocity of the flow which generates the vortex. The width of the scour hole B is simply the two-inch dimension of the vertical tube.

LeFeuvre determined the zero-transport limit for each of the six sediments. At zero transport the value of N_s is equal to N_{sc}. Values of N_{sc} and sediment properties are listed in TABLE 1.

TABLE 1. PROPERTIES OF SEDIMENTS USED BY LEFEUVRE[2]

Sediment	Material	Specific Gravity (s)	Diameter D_g(mm)	Standard Deviation σ_g	Angle of Repose ϕ	Porosity P	N_{sc}
1	Nickel	8.75	0.570	1.10	35°	0.501	10.27
2	Sand	2.62	0.585	1.04	47°	0.499	8.70
3	Sand	2.63	0.185	1.24	48°	0.512	8.12
4	Glass	2.47	0.297	1.08	37°	0.513	8.52
5	Glass	2.46	0.106	1.05	40°	0.512	9.64
6	Lucite	1.20	0.250	1.31	40°	0.517	8.81

The experimental results of LeFeuvre's study are presented in Figure 2 in the form of equation (4a). The line shown in Figure 2 is a simple and reasonable approximation of the experimental results for all sediments and for all values of N_s.

$$\frac{Q_s^1}{VBD_g} \propto \left(N_s^2 - N_{sc}^2\right)^{5/2} \qquad (5)$$

Equation (5) will be utilized in the following sections in analyzing more complicated scouring situations. Reliance upon LeFeuvre's experiment is based upon (a) the absence of free-surface effects, (b) the existence of a steady-state scour hole, (c) the absence of superposed effects such as dunes, and (d) the accuracy with which the variables could be measured (particularly sediment-transport rate). In other scour experiments one or more of the complicating factors listed above occur which makes the task of separating the effect of the sediment number quite difficult.

B. SCOUR BY DUNES

Bed-load transport of sediment by means of a moving dune system is an example of localized scour. Scour occurs on the upstream face of the dune with the scoured material being deposited on the downstream face. The repeating flow pattern of separation at the crest, reattachment in the trough, and contracting flow over the upstream face is a flow situation in which the boundary layer would tend to be of negligible thickness in the area of active scour. Hence a reasonable expectation is that the analysis leading to equation (4a) and that the experimental results leading to equation (5) are likewise applicable to bed-load transport by dunes.

Neither the reason for the existence nor the sequence of development of dunes is well understood at the present time. However, a current study being conducted in the Georgia Tech Hydraulics Laboratory is revealing as to the principal features of the sequence of dune development.

Geometric characteristics and energy dissipation of dunes on a movable bed under oscillatory flow of water are being studied in the Georgia Tech Hydraulics Laboratory. These studies are being conducted in a large U-tube in which the test section is the bottom horizontal leg of the U. The test section is 10 ft. long, 1 ft. high, and 4 ft. wide. The central section of the floor is depressed in order to form a container for the erodible bed material. The erodible bed is 6 ft. long, 4 ft. wide, and 4 in. deep. The sidewalls and top of the test section are transparent plastic in order to permit visual observation of the phenomena occurring within the test section. The vertical legs of the U-tube are also 1 ft. by 4 ft. in dimension. The vertical legs are joined to the horizontal leg so as to form a streamlined flow passage. The free surface of the water in one of the vertical legs serves as a piston. Air is continuously forced into the con-

fined volume above the water. Two large, solenoid-actuated, piston-operated, exhaust valves are used to quickly relieve the excess pressure in the air above the water surface. The exhaust valves are closed for about one-quarter cycle during the time when the water surface is falling in that leg. A float gage in the other vertical leg is joined to a direction-sensing switch which is the first element in a feedback-control system used to close and to open the exhaust valves at the proper time during the cycle. This system oscillates the water in the U-tube with simple harmonic motion at resonant frequency. Equilibrium amplitude can be controlled by adjustment of the air pressure. Air pressure is controlled by means of a bypass valve in the air-supply conduit from the blower. Initial transients are eliminated by means of a separate air system whereby the water levels are initially unbalanced to the desired equilibrium amplitude. Upon release of the initial unbalance, the water oscillates at equilibrium amplitude. The U-tube is also equipped with a mechanism for eliminating the final transient (oscillatory decay) at the end of a run.

As of the present time, the experimental study has been limited to only one bed material, glass beads, having the following properties:

D_g (geometric mean diameter) - 0.297mm,

σ_g (geometric standard deviation) - 1.06,

s (specific gravity) - 2.47, and

ϕ (angle of repose) - 24°.

Amplitude and period of oscillation are recorded on a direct-writing oscillograph. The float-elevation sensor system consists of an endless, small-diameter, stainless-steel cable which passes over pulleys at the top and bottom in one vertical leg of the U-tube. The endless cable is fastened to a wooden

float. A three-turn potentiometer, which is connected to the axle of the upper pulley, is one leg of a wheatstone bridge. Bridge unbalance is sensed and recorded. The recorder is also equipped with a timing marker which marks pips at one-second intervals on the record. In all runs, the float elevation system is calibrated just before and immediately following a run by making short records at several elevations of the float.

Dune geometry is recorded photographically. After the dune system has attained an equilibrium geometry, a photograph is taken through the transparent sidewall of the test section in order to record the dune configuration of the bed material adjacent to the sidewall.

The traditional concept of incipient motion is of doubtful relevance in relation to the formation of dunes. Incipient-motion condition is normally considered to exist when an appreciable number of particles on the surface of an initially flat bed are moved by the overlying moving fluid. In the oscillatory tests, incipient motion occurred at a sediment number N_s of about 3.9. The maximum velocity is used in computing the sediment number in oscillatory flow. An embryo dune system would spontaneously occur over the entire flat bed when the sediment number attained a value of 4.9. However a dune system would propagate outward from a disturbance placed in the bed when the sediment number was less than 3.9--the incipient motion condition. In fact a dune system was generated during one run in which the sediment number was 1.6. For all runs in which the sediment number was less than 4.9, a half-round bar with a radius of 1/4 in. and a length of 4 ft. was used as the disturbance element. Prior to a run, the disturbance was placed on the bed perpendicular to the direction of the water motion and in the center of the 6 ft. long bed. Inasmuch as all natural stream channels and ocean beds would have disturbance elements on the bed, the conclusion is that

the incipient-motion criterion as determined in the laboratory is probably irrelevant. Generation of the dunes from a disturbance element was noted by Bagnold[3]. In fact Bagnold also utilized a disturbance element for generating dunes in his experiments. The effect of disturbance elements is mentioned by Simons and Richardson[4] as being used during one run in an experimental program involving sediment transport in a flume.

The principal features of dunes are shown in Figure 3 in which the dune amplitude η is plotted as a function of the sediment number. The period of the simple harmonic motion was essentially constant, that is 3.52 sec < T < 3.56 sec.

If the value of N_s is less than about 6.5 the dune system is two-dimensional. The crests of the dunes are unbroken and are essentially constant in elevation. The crest of the dunes are perpendicular to the direction of the fluid motion. In this range the fluid motion appears to be two-dimensional with line vortices being formed in the lee of the dune crests. Two vortices are formed each cycle in the trough between a pair of adjacent crests. Upon reversal of motion the previously formed vortex is moved back toward the crest upon which it was formed and is ejected into the main flow above the dune system. Being a symmetrical and cyclic motion, the dunes are essentially symmetrical with the crests moving slightly to and fro as scour and deposition occur alternately on each side of the crest. Two-dimensional dunes are geometrically similar as evidenced by the

---

[3]Bagnold, R. A., "Motion of Waves in Shallow Water--Interaction between Waves and Sand Bottom," Proceedings, Royal Society, A, Vol. 187, Oct. 8, 1946, pp. 1-18.

[4]Simons, D. B., and E. V. Richardson, "Studies of Flow in Alluvial Channels--Basic Data from Flume Experiments," Colorado State University Report, CER61EVR31, May, 1961, 13 pp. plus 9 figures plus 17 tables.

constancy of the ratio of amplitude to wave length η/λ. For the runs shown in Figure 3 the ratio η/λ was 0.174.

If the value of N_s is greater than 6.5, the flow pattern is no longer two-dimensional. The breakdown of the two-dimensional dune system is progressive. When N_s is about 9 the dunes can be described as sand hills with valleys both across and along the bed. As N_s is increased to greater than 9 the elevation of the peaks of the dunes (sand hills) decrease as shown in Figure 3. At values of N_s greater than 10 the entire surface of the bed is in motion resembling a second fluid under the water. Extrapolation of the measured points shown in Figure 3 is indicative that the flat-bed condition is attained when N_s is about 13.

Similar characteristics between the dunes under oscillatory flow and dunes under uni-directional flow are shown by comparison of Figure 3 with Figure 4. Figure 4 has been prepared from the data of Stein[5]. Stein's experiments were conducted in a 4 ft. wide flume having a length of 100 ft. The bed material was sand having a mean diameter D_g of 0.40 mm and geometric standard deviation σ_g of 1.50. The data shown in Figure 4 are from runs in which the depth of flow was essentially constant, that is, 0.98 ft. $< y <$ 1.02 ft. The mean velocity is used in computing the value of the sediment number, N_s. The comparison of the two figures reveals that dune amplitude η increases linearly with increasing values of the sediment number N_s at low values of N_s. In oscillatory flow this region is characterized by two-dimensional dunes with unbroken crests and by geometric similarity. Presumably these key features of the dune system also exist in the dune system generated in uni-directional flow. That two-dimensional

[5]Stein, Richard A., "Laboratory Studies of Total Load and Apparent Bed Loads," Journal of Geophysical Research, Vol. 70, No. 8, April 15, 1965, pp. 1831-1842.

dunes have not been noted by experimenters in uni-directional flow might be the result of the curved crests. In oscillatory flow a new boundary layer forms twice each cycle from the sidewalls. This boundary layer is thin at the maximum stage of development. Consequently the effect of the sidewalls is negligible in oscillatory flow. In contrast, the sidewalls cause a retardation of the flow for an appreciable distance into the main stream of uniform, steady, open-channel flow. In this retarded zone the dune crest would lag behind that in the central zone and the dune amplitude would tend to decrease as the wall is approached. Thus an observer might observe a central region in which the dunes were truly two-dimensional with the crest being curved in plan view as the wall is approached. Simons and Richardson[4] classify dunes as being ripples and dunes. In reviewing their data, the writer has concluded that the "ripples" of Simons and Richardson are probably equivalent to "two-dimensional dunes" as designated by the writer.

The preceding observations are indicative that a sediment-transport function could be formulated for transport by dunes which are geometrically similar. Geometric similarity of the scour hole is a requisite condition, that is, two-dimensional dunes. Data of Simons and Richardson[4] were used in preparing Figure 5. The analogy between Figure 2 for a defined scour hole and Figure 5 for dunes is obvious. In preparing Figure 5 only the runs in which the sediment number N_s was less than 6.5 were used in order to be certain that geometrically similar dunes were being considered. The properties of the eight different sediments are listed in TABLE 2.

TABLE 2. BED MATERIAL USED IN THE COLORADO STATE UNIVERSITY STUDIES

Sediment No.	Material	Mean Diameter D_g (mm)	Geometric Standard Deviation σ_g
1	Sand	0.19	1.30
2	Sand	0.27	1.54
3	Sand	0.28	1.67
4	Sand	0.32	1.57
5	Sand	0.45	1.60
6	Sand	0.47	1.54
7	Sand	0.54	1.52
8	Sand	0.93	1.54

In preparing Figure 5 using the similarity relationship, equation (5), judgement was required in the selection of a value of N_{sc}. The basis of selection is illustrated in TABLE 3. Values of the zero-transport sediment number N_{sc} were selected as being slightly less than the values for which some transport was observed. No attempt was made to explain or to smooth out the somewhat erratic values at N_{sc} as determined from observations.

TABLE 3. SELECTION OF N_{sc}

Sediment	D_g (mm)	Values of the sediment number N_s: Lowest Recorded Movement	Lowest Recorded Dunes	N_{sc}
1	0.19	4.03	4.03	3.9
2	0.27	3.66	3.88	3.6
3	0.28	4.00	4.00	3.9
4	0.32	5.25	5.25	3.8 (?)
5	0.45	2.50	2.50	2.4
6	0.47	—	3.91	3.6 (?)
7	0.54	2.90	2.90	2.8
8	0.93	3.28	3.98	3.1

From Figure 5, the sediment-transport rate by dunes (if the sediment number is less than 7 or 8) can be approximated by

$$\frac{Q_s^1}{VBD_g} = 4\ (10^{-5})(N_s^2 - N_{sc}^2)^{5/2} \qquad (6)$$

The data are scattered considerably about the function, equation (6), which is shown as a solid line in Figure 5. Considerable scatter of experimental data is to be expected inasmuch as the sediment-transport rate is extremely small. Relative errors of measurement are likely to be large under such conditions. In spite of the scatter, the writer believes that the similarity relationship, equation (5), is shown to be valid for sediment transport by two-dimensional dunes.

C. TWO-DIMENSIONAL JET-SCOUR

Laursen[6] performed an experiment in which a two-dimensional jet of water was directed over a two-dimensional bed of sand which was initially flat. Laursen observed the development of the scour-hole depth, S, with elapsed time t. The scour-hole geometry remained constant with time. The scour hole had essentially the configuration shown in Figure 6. Three different sizes of quartz sand were used with the properties as listed in TABLE 4.

TABLE 4. SANDS USED IN LAURSEN'S EXPERIMENTS

D_g(mm)	σ_g	ϕ
0.24	1.14	33°
0.69	1.11	33°
1.60	1.25	33°

Each run was executed with a constant value of the jet velocity V.

A study of Laursen's results of scour depth S as a function of time indicates a difference between the early periods and the later periods. The writer's interpretation of this difference is that since the bed was initially flat some material transport (and elapsed time) occurred before the scour-hole geometry was established in the form shown in Figure 6. Only data obtained with established scour-hole geometry are used in the following analysis.

The rate of sediment transport Q_s out of the scour hole shown in Figure 6 is equal to the rate of change of the scour-hole volume $\forall$, that is,

$$Q_s = \frac{d\forall}{dt} \tag{7}$$

[6] Laursen, E. M., "Observations on the Nature of Scour," Proceedings, 5th Hydraulics Conference, University of Iowa Studies in Engineering, Bulletin 34, 1952.

For Laursen's experiment, Figure 6,

$$\frac{Q_s}{B} = \frac{4}{\tan \phi} S \frac{dS}{dt} \tag{8}$$

Using the experimental results of S as a function of t, the sediment-transport rate Q_s out of the scour hole was calculated.

Laursen's results are shown in Figure 7 in the form of equation (4). The reference velocity V is taken to be the velocity of the water issuing from the nozzle. The pertinent dimension L in equation (4) is taken as the thickness of the jet b as shown in Figure 6. The scour-hole width B is simply the channel width since the scour-hole was two-dimensional. Considering the wide range of sediment numbers ($4.6 < N_s < 25.9$) and sediment sizes (D_g of 0.24 mm, 0.69 mm, and 1.6 mm), the similarity relationship, equation (5) appears to apply to the jet-scour study. The function

$$\frac{Q_s}{VBD_g} = 1.9\,(10^{-3})\,(N_s^2 - 4)^{5/2} \left(\frac{S}{b}\right)^{-4} \tag{9}$$

is a reasonable empirical approximation for the sediment transport rate. The value of N_{sc} was chosen as being two. Since Laursen's jet was directed slightly downward by a lip on the upper flow boundary, the writer felt that the value of N_{sc} would be somewhat lower than for a parallel stream over a flat bed as given in TABLE 3. Detailed study of the 16 individual runs in indicative that equation (9) is a better approximation for the 0.69-mm size than for the smallest and largest sizes. For the 0.24-mm size and for the 1.6-mm size the function appears to be more complex than a simple variation with S^{-4}. In spite of this observation, the similarity criterion of scour, equation (5), appears to be substantiated by the jet-scour experiment.

Finally the scour depth-versus-time function can be formulated. Substituting equation (9) into equation (8),

$$\frac{(S/b)^5}{\tan \phi} \frac{d(S/b)}{d(V_o t/b)} = 4.75\ (10^{-4})\ (N_s^2 - 4)^{5/2}\ (D_g/b) \qquad (10)$$

Integrating equation (10)

$$\left(\frac{S}{b}\right)^6 = 2.85\ (10^{-3})\ (N_s^2 - 4)^{5/2} \tan \phi \left(\frac{D_g}{b}\right)\left(\frac{V_o t}{b}\right) + C \qquad (11)$$

in which the constant of integration, C, is determined by initial conditions and by the time required for the scour hole to be scoured from the flat bed to the geometry shown in Figure 6. Since the time of adjustment was short this period is ignored and the initial condition that S = 0 when t = 0 is used to determine that C = 0. An example of Laursen's data of scour-depth versus time is shown in Figure 8 for comparison with equation (11).

Finally the scour depth-versus-time function can be formulated. Substituting equation (9) into equation (8),

$$\frac{(S/b)^5}{\tan \phi} \frac{d(S/b)}{d(V_o t/b)} = 4.75\ (10^{-4})\ (N_s^2 - 4)^{5/2}\ (D_g/b) \qquad (10)$$

Integrating equation (10)

$$\left(\frac{S}{b}\right)^6 = 2.85\ (10^{-3})\ (N_s^2 - 4)^{5/2} \tan \phi \left(\frac{D_g}{b}\right)\left(\frac{V_o t}{b}\right) + C \qquad (11)$$

in which the constant of integration, C, is determined by initial conditions and by the time required for the scour hole to be scoured from the flat bed to the geometry shown in Figure 6. Since the time of adjustment was short this period is ignored and the initial condition that S = 0 when t = 0 is used to determine that C = 0. An example of Laursen's data of scour-depth versus time is shown in Figure 8 for comparison with equation (11).

D. SCOUR AROUND A VERTICAL CYLINDER

As a part of an extensive study of scour around bridge piers, Chabert and Engeldinger[7] studied scour around single vertical cylinders placed in a recirculating flume. The cylinders were placed at midwidth of a rectangular channel which was 0.8m wide and 21.0m long. The bed of the channel was covered with sand to a depth of 0.3m for a length of 15 m along the channel. Three piles each having a different diameter were placed in the channel during each run with an axial separation of 6.5m along the channel between adjacent cylinders. Runs were made with depths of flow of 100mm, 200mm, and 350mm. The channel slope and discharge were adjusted to obtain uniform flow with the mean velocity ranging from 0.25m/sec to 1.25m/sec. Depths of the scour holes were measured at 15-minute intervals. Tests were made with four different sizes of sands, that is, D_g of 3.08mm, 1.52mm, 0.52mm, and 0.26mm. Measured values of depth of scour S as a function of time t are presented graphically for 75 runs.

Since this analysis is based upon the determination of the sediment-transport rate Q_s out of the scour hole, runs in which bed material was carried into the hole from upstream at an unknown rate could not be utilized. From the data presented only Run 204 could be identified as having no sediment-transport into the hole from upstream.

Study of contour maps of the scour holes is indicative that the scour hole can be closely approximated by an inverted frustum of a right circular cone having a base diameter equal to the pile diameter D and having a side

---

[7]Chabert, J. and P. Engeldinger, "Etude des Affouillements Autour des Piles de Ponts," Report of the National Hydraulic Laboratory (Chatou, France), Series A, October, 1956.

slope equal to the angle of repose ϕ. The volume $\forall$ of such a frustum is

$$\forall = \frac{\pi}{3 \tan \phi} \left(\frac{S^3}{\tan \phi} + \frac{3 DS^2}{2} \right) \tag{12}$$

Differentiating equation (12) and substituting into equation (7)

$$Q_s = \frac{\pi}{\tan \phi} \left(\frac{S}{\tan \phi} + D \right) S \frac{dS}{dt} \tag{13}$$

Using the experimental results of S as a function of t, the sediment-transport rate Q_s was calculated.

The calculated values from Chabert and Engeldinger's results are shown in Figure 9 in the form of equation (4). The reference velocity V is taken as the mean velocity of the approaching flow. The pertinent dimension L in equation (4) is taken as the pile diameter D. The scour-hole width B is D + (2S/tan ϕ). The sediment-transport function as shown in Figure 9 can be represented as

$$\frac{Q_s}{V(D + 2S/\tan \phi) D_g} = 1.3(10^{-5}) (N_s^2 - N_{sc}^2)^{5/2} (S/D)^{-3} \tag{14}$$

Equation (14) is an approximation of the experimentally determined results of Run 204 for D of 50mm and 100mm but not for the pile having a diameter of 150mm. The implication is that free-surface effects are significant if $y/D < 2$.

Scour depth as a function of time can be reconstructed by substituting equation (14) into equation (13).

$$\left(\frac{1}{\tan\phi}\left(\frac{S/D + \tan\phi}{2S/D + \tan\phi}\right)\left(\frac{S}{D}\right)^4\right)\frac{d(S/D)}{d(Vt/D)} = 4.14\ (10^{-6})\ (N_s^2 - N_{sc}^2)^{5/2}\left(\frac{D_g}{D}\right) \qquad (15)$$

Integrating equation (15) and letting S = 0 when t = 0

$$4.14\ (10^{-6})(N_s^2 - N_{sc}^2)^{5/2}\left(\frac{D_g}{D}\right)\left(\frac{Vt}{D}\right) = \frac{(S/D)^5}{\tan\phi} + \frac{(S/D)^4}{16}$$

$$- \frac{(\tan\phi)(S/D)^3}{24} + \frac{(\tan\phi)^2(S/D)^2}{32} - \frac{(\tan\phi)^3(S/D)}{32}$$

$$+ \frac{(\tan\phi)^4}{64}\ \ln\left(\frac{2(S/D)}{\tan\phi} + 1\right) \qquad (16)$$

The integrated scour-depth function, equation (16), as well as the experimentally determined results of Run 204 are shown in Figure 10.

The above analysis, which pertains to a limited range of velocities at which scour occurs around the cylinder but does not occur in the bed material away from the pile, can be extended to include the typical case in which sediment is carried into the scour hole from upstream. The principal assumption is that the incoming sediment does not affect the localized scouring process adjacent to the pile. With sediment inflow into the scour hole equation (7) is modified as follows

$$Q_s(\text{out}) - Q_s(\text{in}) = \frac{d\forall}{dt} \qquad (17)$$

The rate of sediment transport out of the scour hole, Q_s (out), is evaluated from equation (14). The rate of sediment transport into the scour hole, Q_s (in), would have to be evaluated by means of a bed-load transport equation such as equation (6). Substituting equations (6), (12), and (14) into equation (17)

$$1.3\ (10^{-5})(N_s^2 - N_{sc1}^2)^{5/2}\ VD_g \left(\frac{2S}{\tan\phi} + D\right)\left(\frac{S}{D}\right)^{-3}$$

$$- \frac{4\ (10^{-5})(N_s^2 - N_{sc2}^2)^{5/2}}{P}\ VD_g \left(\frac{2S}{\tan\phi} + D\right) = \frac{\pi}{\tan\phi}\left(\frac{S}{\tan\phi} + D\right) S \frac{dS}{dt} \qquad (18)$$

in which P is the porosity of the bed material. In equation (18) the sediment number N_s for the pile and for the bed would be identical. However the zero-transport sediment number N_{sc1} of the pile would be less than N_{sc2} of bed by virtue of higher velocities around the sides of the pile. For irrotational flow, the velocity at the sides of the cylinder is twice the approach velocity. Therefore a reasonable approximation is that

$$N_{sc1} = \frac{N_{sc2}}{2} \qquad (19)$$

A further reasonable approximation for use in equation (18) is that P = 0.5 for all bed materials.

In order to illustrate the various aspects of scour around a pile with sediment inflow, the following discussion will be restricted to the experiments of Chabert and Engeldinger[7] with bed material having a mean diameter D_g of 3.08mm. From a study of the data, the value of N_{sc2} appears to be 2.24.

The first topic of discussion is that of terminal scour depth S_T for which the RHS of equation (18) would be zero. In this case and with the previously stated numerical values equation (18) reduces to

$$1.3\ (N_s^2 - 1.64)^{5/2}\left(\frac{S_T}{D}\right)^{-3} - 8\ (N_s^2 - 5.02)^{5/2} = 0 \qquad (20)$$

Solving for the terminal-depth-of-scour ratio

$$\frac{S_T}{D} = 0.546\left(\frac{N_s^2 - 1.64}{N_s^2 - 5.02}\right)^{5/6} \qquad (21)$$

Equation (20) is displayed in Figure 11. Figure 11 is a graph of the depth of scour around the vertical cylinder. The maximum and minimum depths were obtained from data. The oscillation of scour depth for sediment numbers greater than 2.24 is undoubtedly the result of dunes moving downstream past the cylinder. As shown in Figure 11, equation (20) appears to bear some relation to the minimum scour depth but not to the maximum. In any event, the oscillating scour depth resulting from dune passage illustrates a major problem of movable-bed model studies. Namely, the magnitude of scour around an object is related to the size of the object whereas the dune amplitude and flow pattern over the dunes are not. Yet the flow pattern over the dunes can result in significant alteration of the flow pattern within the scour hole as illustrated in Figure 11.

The region of localized scour shown in Figure 11 is restricted to the range of sediment numbers between 1.12 and 2.24. In other words, with this bed material, model tests would have to be conducted within a narrow range of sediment numbers in order to avoid the complications introduced by dunes. The other alternative would be to conduct the tests at a high value of the sediment number, say 15, where the bed is again flat. Model testing at a high value of the sediment number would not only involve sediment transport into the hole but may introduce a flow-pattern disturbance resulting from gravity-waves. These difficulties enhance the value of the studies of LeFeuvre[2] and Laursen[6] in which neither the problem of incoming sediment, gravity waves, nor passage of dunes through the scour area existed.

A terminal scour depth is unquestioned when sediment is being transported into the scour hole from upstream. In fact an expression for terminal scour was derived, equation (21), by simply equating the transport rate out of the hole by localized scour to the transport rate into the hole by bed-load movement. On the other hand, in the absence of transport into the hole, equation (16) is indicative that no terminal depth exists. The nature of the scour function as shown in Figure 10 is such that scour depth increases at a progressively slower rate as time passes. Run 204 shown in Figure 10 was continued for 40.5 hours yet there is no indication of a terminal condition. The writer is of the opinion that terminal scour depth is too poorly defined to be useful as an experimental variable as has been suggested by some.

E. SCOUR AROUND A HORIZONTAL CYLINDER

Scour around a cylinder lying on a movable bed and in oscillatory flow is being studies in the Georgia Tech Hydraulics Laboratory. These studies are being performed in the large U-tube described previously in B. SCOUR BY DUNES. The cylinders are aluminum with a length-to-diameter ratio of four. Three different cylinders are used having diameters of 8.76 cm, 4.32 cm and 2.54 cm. The bed material is the 0.297-mm diameter glass beads which were described previously.

Scour-hole development is determined by visual observation of the settlement of the cylinder into the scour hole. The telescope of a cathetometer is attached to a traversing mechanism such that an observer can raise or lower the telescope by operating a crank. The telescope is attached to a differential transformer in order that the elevation of the axis of the telescope can be recorded on a direct-writing oscillograph.

The transient data are recorded by means of a two-channel direct-writing oscillograph. One channel is utilized to record the elevation of the telescope of the cathetometer. The other channel is utilized to record the water-surface elevation (actually float elevation) in one of the vertical legs. The recorder is also equipped with a timing marker which marks pips at one-second intervals on the record.

Immediately prior to a run, both the telescope-elevation and water-level-elevation systems were calibrated directly by making short records at several elevations of the telescope and of the float.

During a run, one observer would start the oscillatory motion at the preset equilibrium amplitude while the other observer maintained the crossed hairs of the telescope on the top of the cylinder as seen through the sidewall of the test section.

Immediately following a run the elevation-recording instruments were again calibrated.

The cylinder settles into the scour hole in a stepwise manner. The region of greatest scour is at the ends of the cylinder. The scour hole is enlarged under the cylinder from the ends. This action continues until the central support is insufficient to support the cylinder at which time the cylinder drops suddenly. The process is repetitive. The cylinder axis always remains perpendicular to the direction of water motion.

In order to avoid the effect of dunes upon the flow pattern within the scour hole, settlement runs are made with a high value of the sediment number. Referring to Figure 3, the sediment number should be about 13 in order for the bed to be flat. A sediment number of 13 could not be achieved in these tests by virtue of an equipment limitation which corresponds to a total amplitude of oscillation of about 35 in. Thus the maximum attainable sediment number was about 12. Visual inspection of the scour holes was indicative that the effect of dunes was negligible if N_s was greater than 9. In the following, only runs for which $10.3 < N_s < 11.9$ are utilized in order to avoid the effects of dunes. Since the flow is oscillatory, the net rate of sediment-transport from the area away from the hole into the hole is zero even at the high values of N_s at which the surface layer of the bed material is in motion.

Scour hole geometry was determined from contour maps prepared from point-gage surveys and from pairs of stereophotographs.

The contour maps of the scour holes are indicative that the scour hole can be closely approximated by an inverted frustum of a right circular cone having a base diameter of $\ell + 0.24D$ in which ℓ is the length of the cylinder and D is the diameter and having a side slope equal to the angle of repose ϕ. The volume $\forall$ of such a frustum is

$$\Psi = \frac{\pi}{3}\left(\frac{S^3}{\tan^2\phi} + \frac{3D\,(\ell/D + 0.24)\,S^2}{2\tan\phi} + \frac{3D^2}{4}(\ell/D + 0.24)^2\,S\right) \qquad (22)$$

and

$$\frac{d\Psi}{dt} = Q_s = \pi\left(\frac{S^2}{\tan^2\phi} + \frac{D\,(\ell/D + 0.24)\,S}{\tan\phi} + \frac{D^2}{4}(\ell/D + 0.24)^2\right)\frac{dS}{dt} \qquad (23)$$

Using the experimental results of S as a function of t and equation (23), the sediment-transport rate Q_s out of the scour holes was calculated.

A separate experiment was performed to determine the value of N_{sc}. The cylinder was placed on the flat bed. The amplitude of oscillation was increased until movement was observed at the ends of the cylinder. The corresponding sediment number is the zero-transport sediment number, N_{sc}. The value of N_{sc} was found to be 1.2 for the 0.297 mm glass beads.

The calculated values are shown in Figure 12 in the form of equation (4). The reference velocity V is taken to be the maximum velocity of the uniform stream in the test section. The diameter D of the cylinder is taken as the reference dimension of the obstruction. The scour-hole width B is $\ell + 0.24D + (2S/\tan\phi)$. The data having the highest order of accuracy are obtained with the largest cylinder. The smallest cylinder settled out of sight in 15 cycles or in 53 seconds. The briefness of the observation time tends to decrease the accuracy of observation since the observer must follow the settlement with the telescope of the cathetometer. Recognizing the order of accuracy, the empirical function shown as a solid line in Figure 12 was selected by giving greater weight to the data for the runs with the largest cylinder.

$$Q_s = \left(f\left(\frac{S}{d}\right)\right)\left(V\ (\ell + 0.24D + 2S/\tan\phi)\ D_g\ (N_s^2 - N_{sc}^2)^{5/2}\right) \qquad (24)$$

Finally the scour-depth function can be formulated. Introducing equation (24) into equation (23) and integrating

$$(N_s^2 - N_{sc}^2)^{5/2}\ (D_g/D)(Vt/D) =$$

$$\pi \int_0^{(S/D)} \frac{\frac{1}{\tan^2\phi}\left(\frac{S}{D}\right)^2 + \frac{(\ell/D + 0.24)}{\tan\phi}\left(\frac{S}{D}\right) + \frac{(\ell/D + 0.24)^2}{4}}{\left(f\left(\frac{S}{D}\right)\right)\left(\frac{\ell}{D} + 0.24 + \frac{2\ (S/D)}{\tan\phi}\right)}\ d\left(\frac{S}{D}\right) \qquad (25)$$

Experimental data are shown in Figure 13 in the form indicated by equation (25). Equation (25) is identical in form to the previous examples of jet scour, equation (11), and of scour around a vertical cylinder, equation (16). All of these scouring functions are of the form

$$\frac{S}{L} = f\left((N_s^2 - N_{sc}^2)^{5/2}\ (D_g/L)(Vt/L)\right) \qquad (26)$$

CONCLUSIONS

The object of this study is to develop similarity criteria for sediment-transport rate and for scour depth in localized-scour situations. The principal assumption is that in an area of localized scour the velocity and velocity distribution are the result of the disturbance element around which scour was occurring. For flow situations which are free from (a) gravity waves, (b) sediment inflow from upstream, and (c) extraneous influences on the flow pattern such as dunes passing through the scour hole, the following criteria are presented. For sediment-transport rate

$$\frac{Q_s}{(N_s^2 - N_{sc}^2)^{5/2} VBD_g} = f \text{ (disturbance element, } S/L\text{, sediment-grain geometry)} \tag{27}$$

and for scour depth

$$\frac{S/L}{(N_s^2 - N_{sc}^2)^{5/2} (D_g/L)(Vt/L)} = f \text{ (disturbance element, sediment-grain geometry)} \tag{28}$$

In order to apply the similarity relation, equation (27) or equation (28), to a given situation of localized scour a minimum of two model tests is required. The first is an empirical determination of the sediment number with zero transport, N_{sc}. The second model test required is for the empirical determination of the RHS of equation (27) or equation (28). The procedure is demonstrated for the case of a horizontal cylinder settling into the scour hole in oscillatory flow.

ACKNOWLEDGMENTS

The writer wishes to acknowledge that the results obtained in the Georgia Tech Hydraulics Laboratory were obtained from sponsored research projects. Appreciation is expressed to Capt. R. T. Miller, Director of the U. S. Navy Mine Defense Laboratory and to Col. F. O. Diercks, Director of the Coastal Engineering Research Center (U. S. Army, Corps of Engineers) for permission to use a portion of their data. The writer particularly wishes to thank Dr. Jasper and Dr. Hogge of the Mine Defense Laboratory for their initial and continuing encouragement for the investigation of similarity criteria. Based upon their initial encouragement, the writer was able to obtain the necessary funds from Georgia Tech for the construction of the unique water tunnel. The assistance of the following colleagues and students is likewise acknowledged: C. S. Martin, F. M. Neilson, H. Majumdar, and L. DeJarnette.

APPENDIX - NOTATION

The following symbols have been adopted for use in this paper:

B = width of scour hole;

b = jet thickness in Laursen's experiment;

C = constant of integration;

C_D = coefficient of drag of sediment particle on surface of bed;

C_L = coefficient of lift of sediment particle on surface of bed;

D = cylinder diameter;

D_g = mean grain diameter of sediment;

ΣF_M = resultant disturbing force on particle;

ΣF_R = resultant stabilizing force on particle;

f = denotes "function of";

g = acceleration of gravity;

K_1 = particle shape factor (projected area);

K_2 = particle shape factor (volume);

L = reference dimension to characterize flow pattern;

ℓ = length of cylinder;

N_s = sediment number, $V/\sqrt{(s-1)gD_g}$;

N_{sc} = value of sediment number at limit of zero transport;

P = porosity

Q_s = volume rate of sediment transport (solids plus voids);

Q_s^1 = volume rate of sediment transport (solids);

S = scour depth and settlement depth;

S_T = terminal scour depth;

s = ratio of solids density to fluid density;

T = period of oscillatory motion;

t = time;

V = reference velocity;

$\forall$ = volume of scour hole;

γ = specific weight of fluid;

γ_s = specific weight of sediment;

η = dune amplitude;

λ = dune wave length;

ρ = fluid density;

σ_g = geometric standard deviation (sediment diameter); and

ϕ = angle of repose.

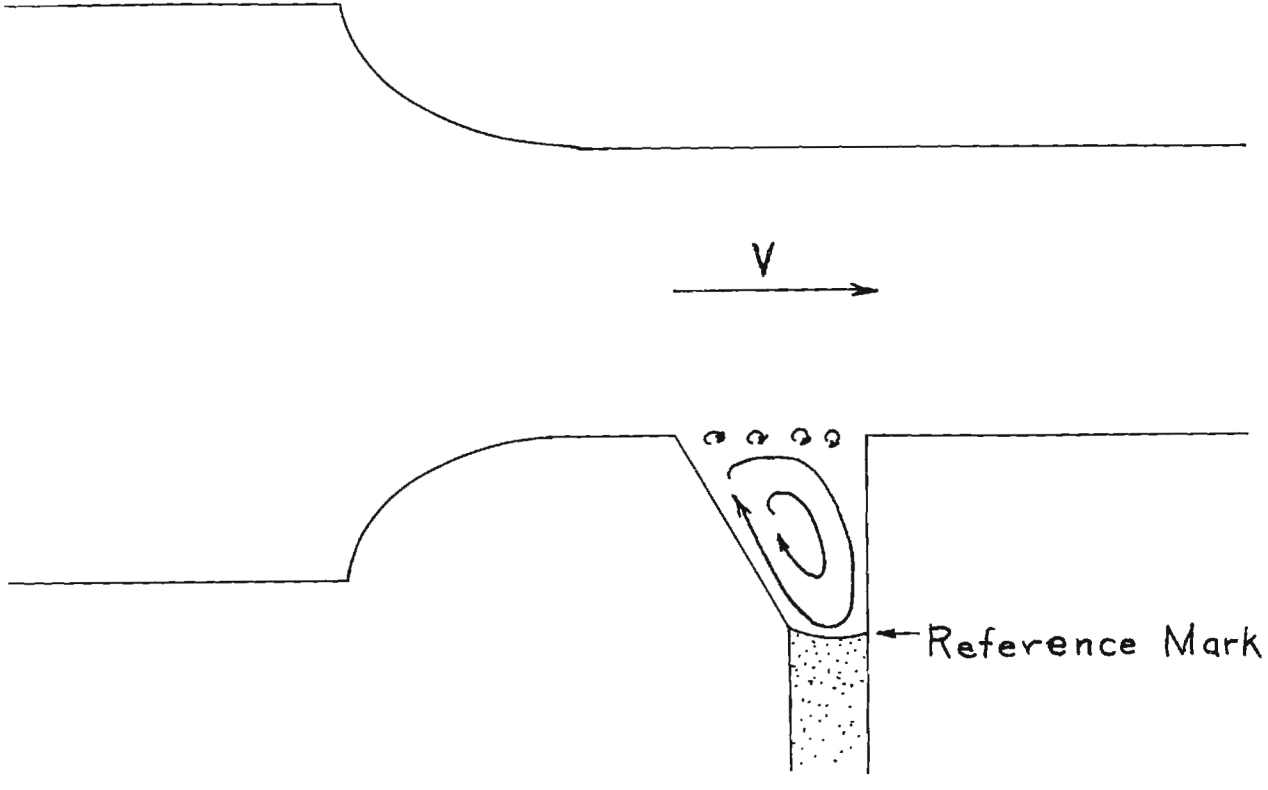

Figure 1. Defined Scour Hole.

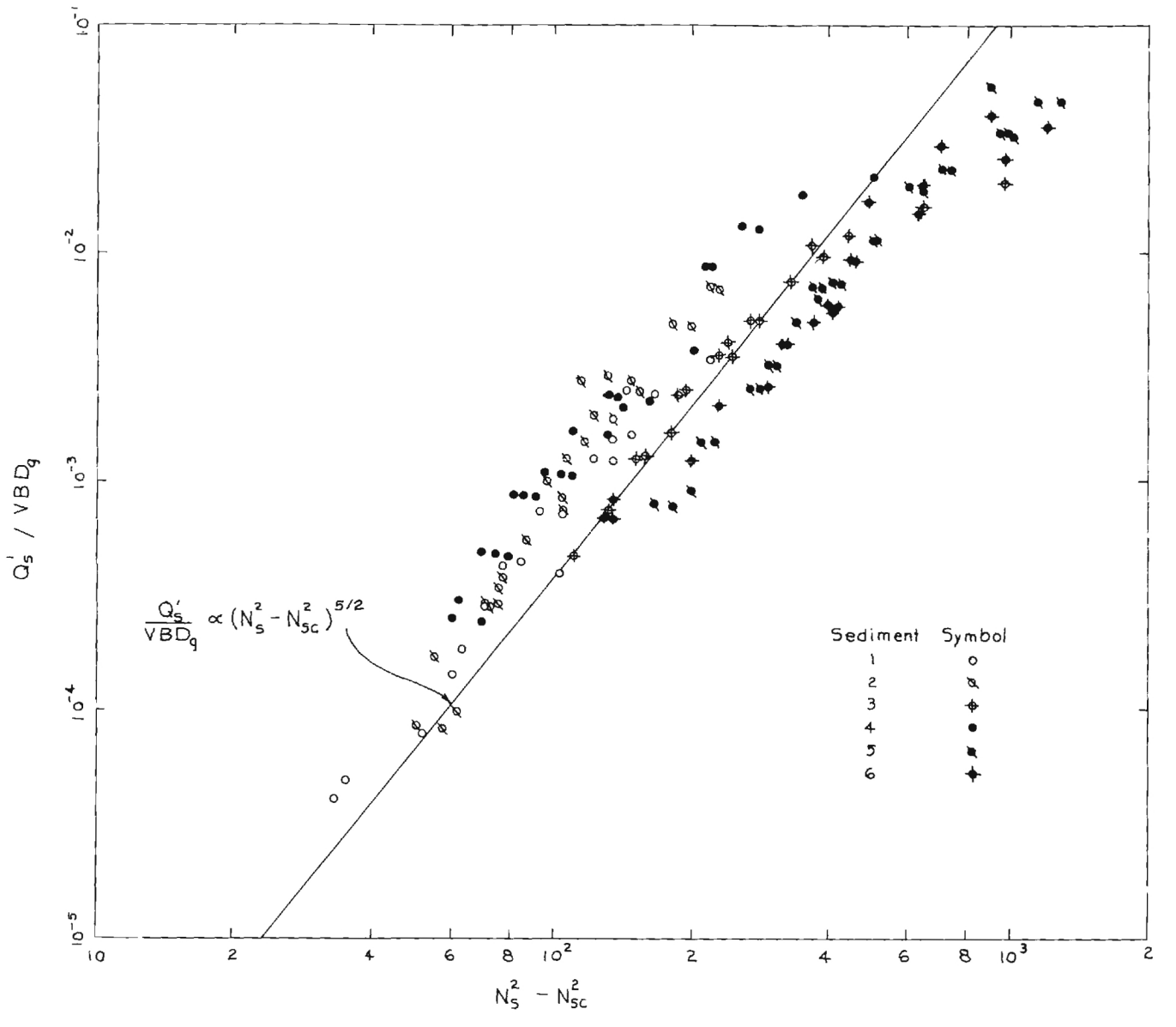

Figure 2. Sediment-Transport Rate (Defined Scour Hole).

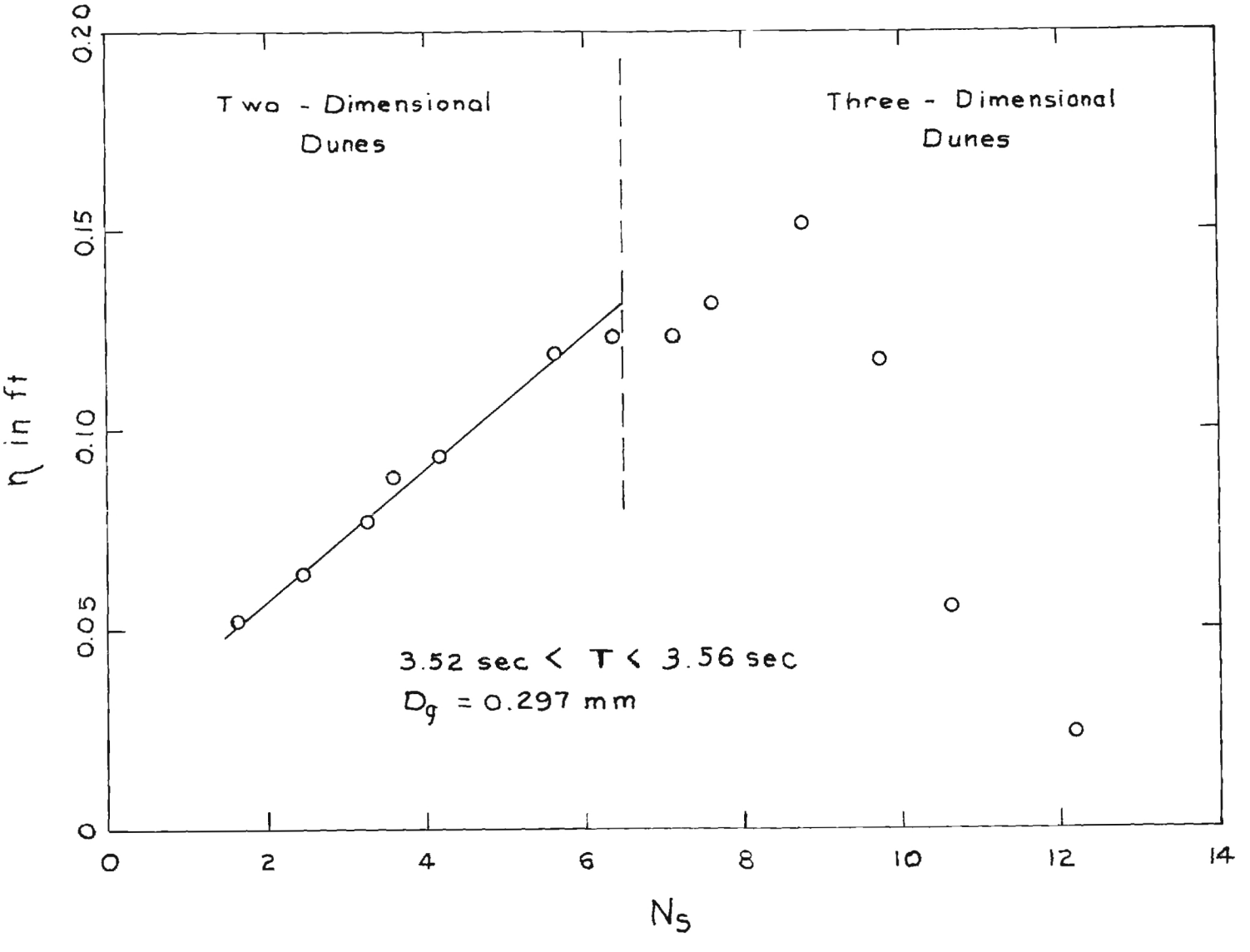

Figure 3. Dune Amplitude (Oscillatory Flow).

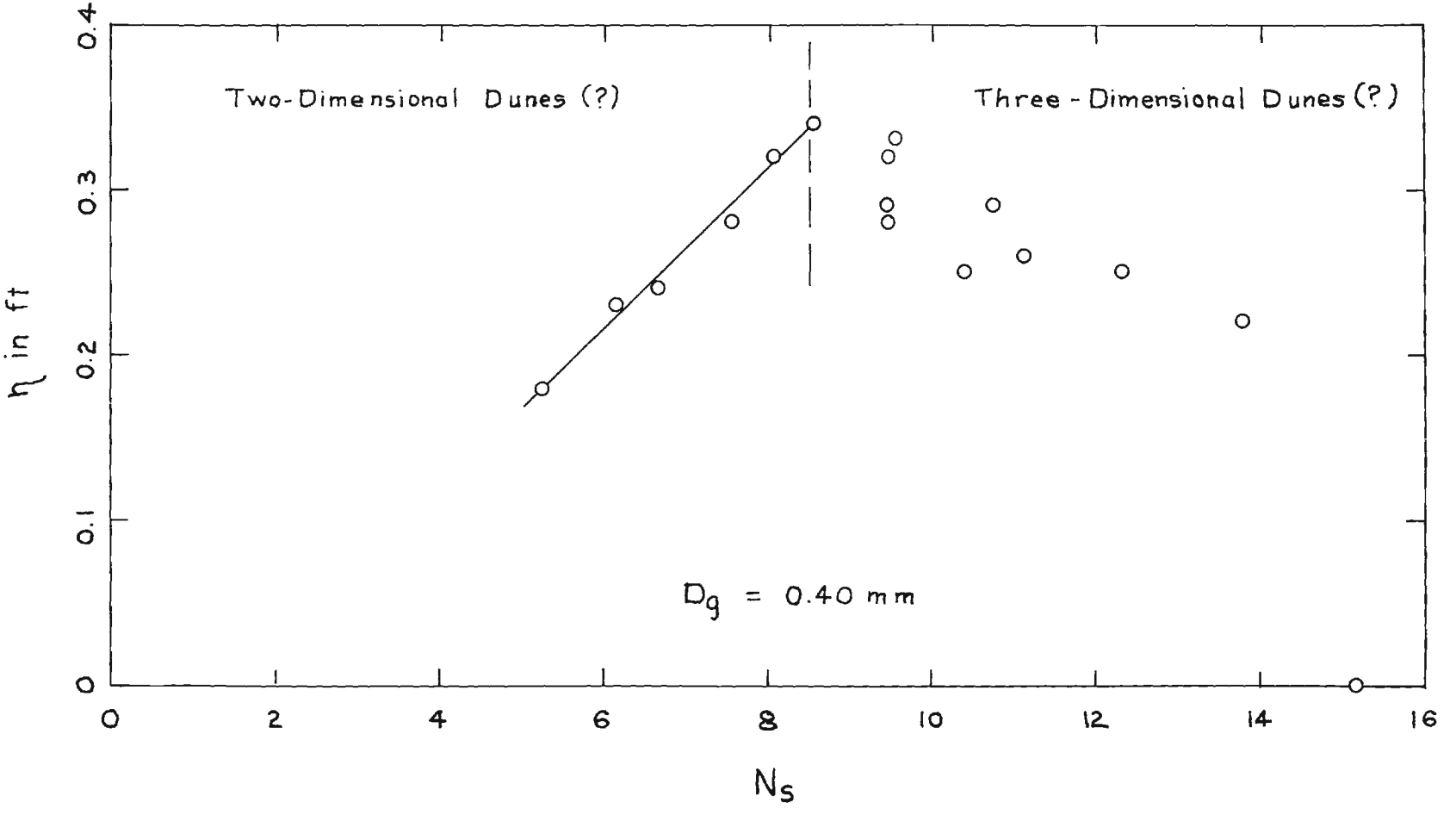

Figure 4. Dune Amplitude (Uni-directional Flow).

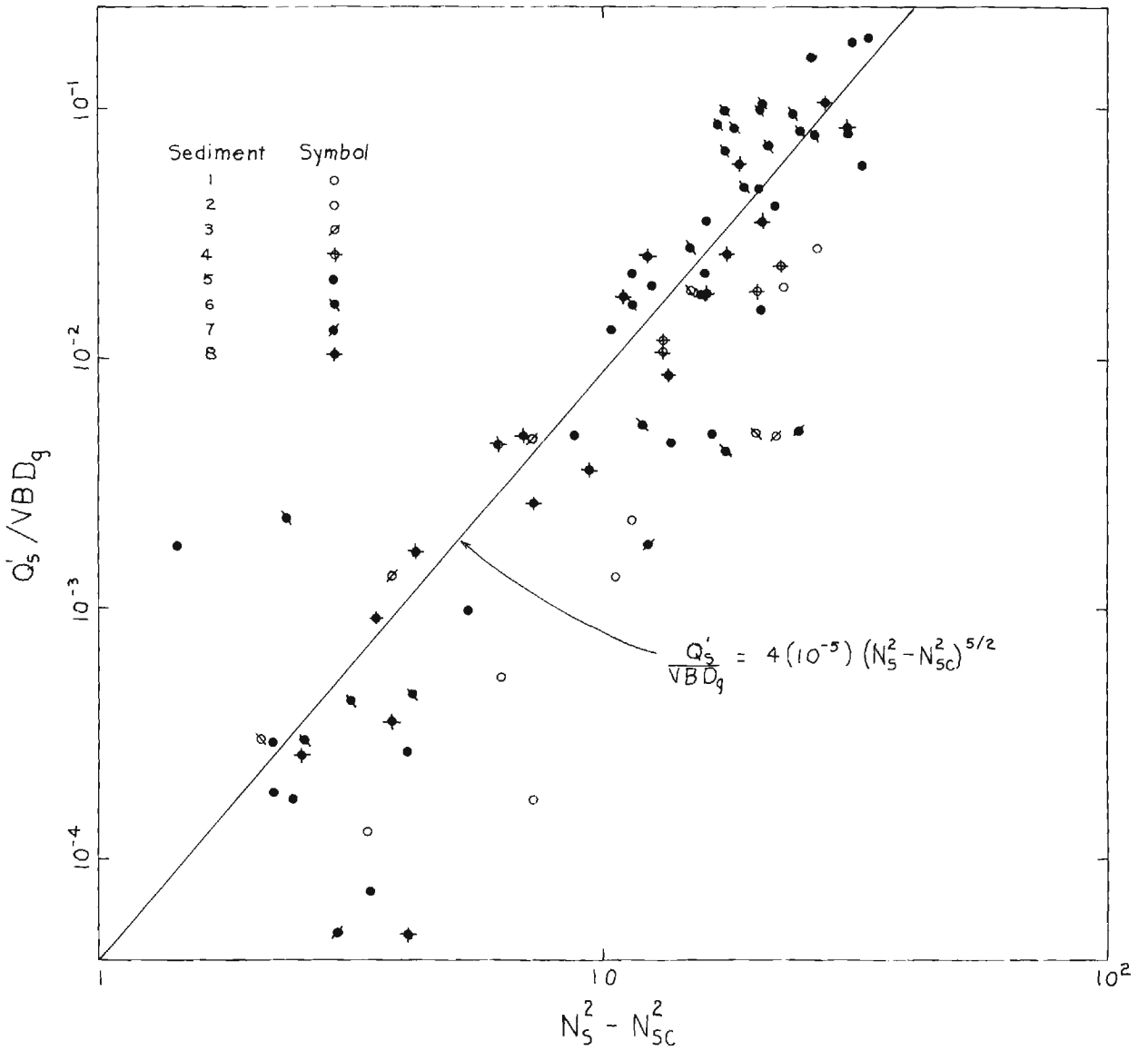

Figure 5. Sediment-Transport Rate (Dunes).

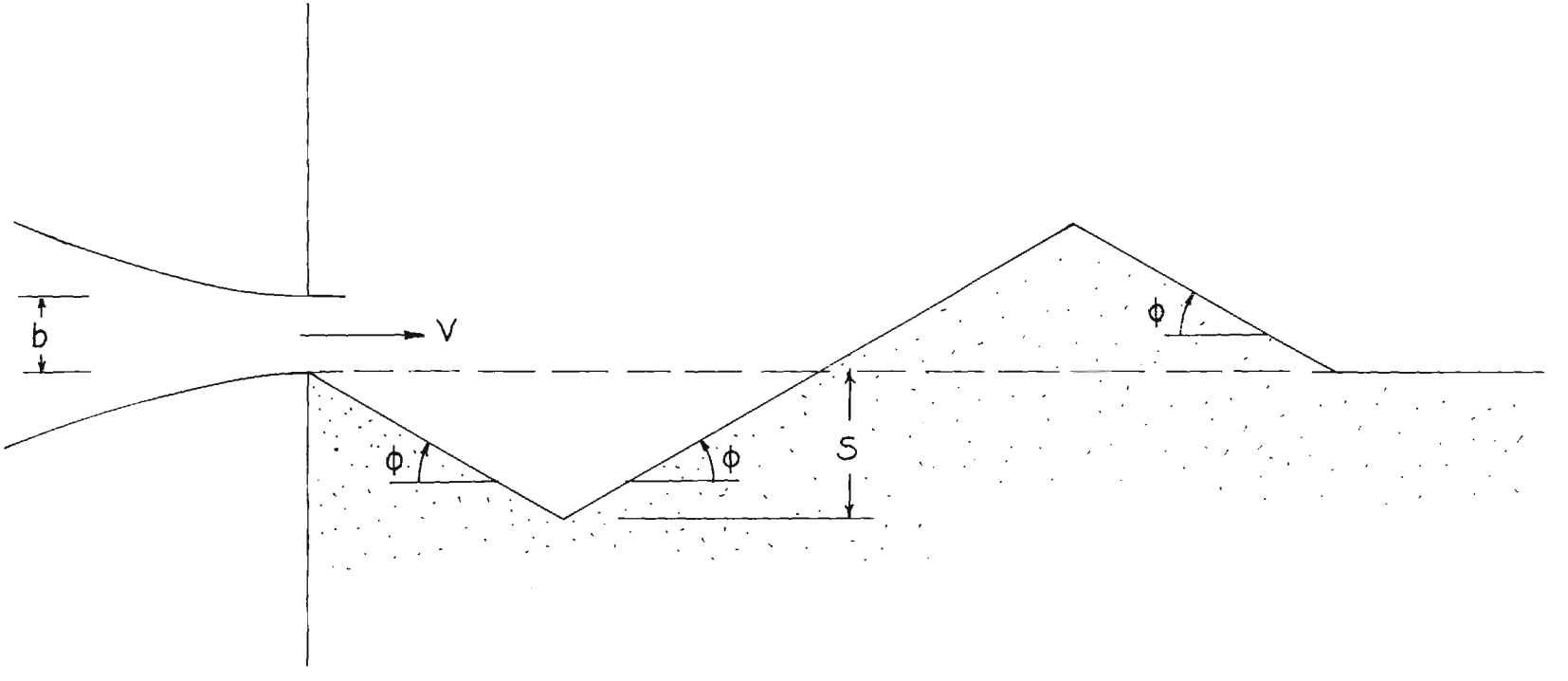

Figure 6. Scour Hole (Jet).

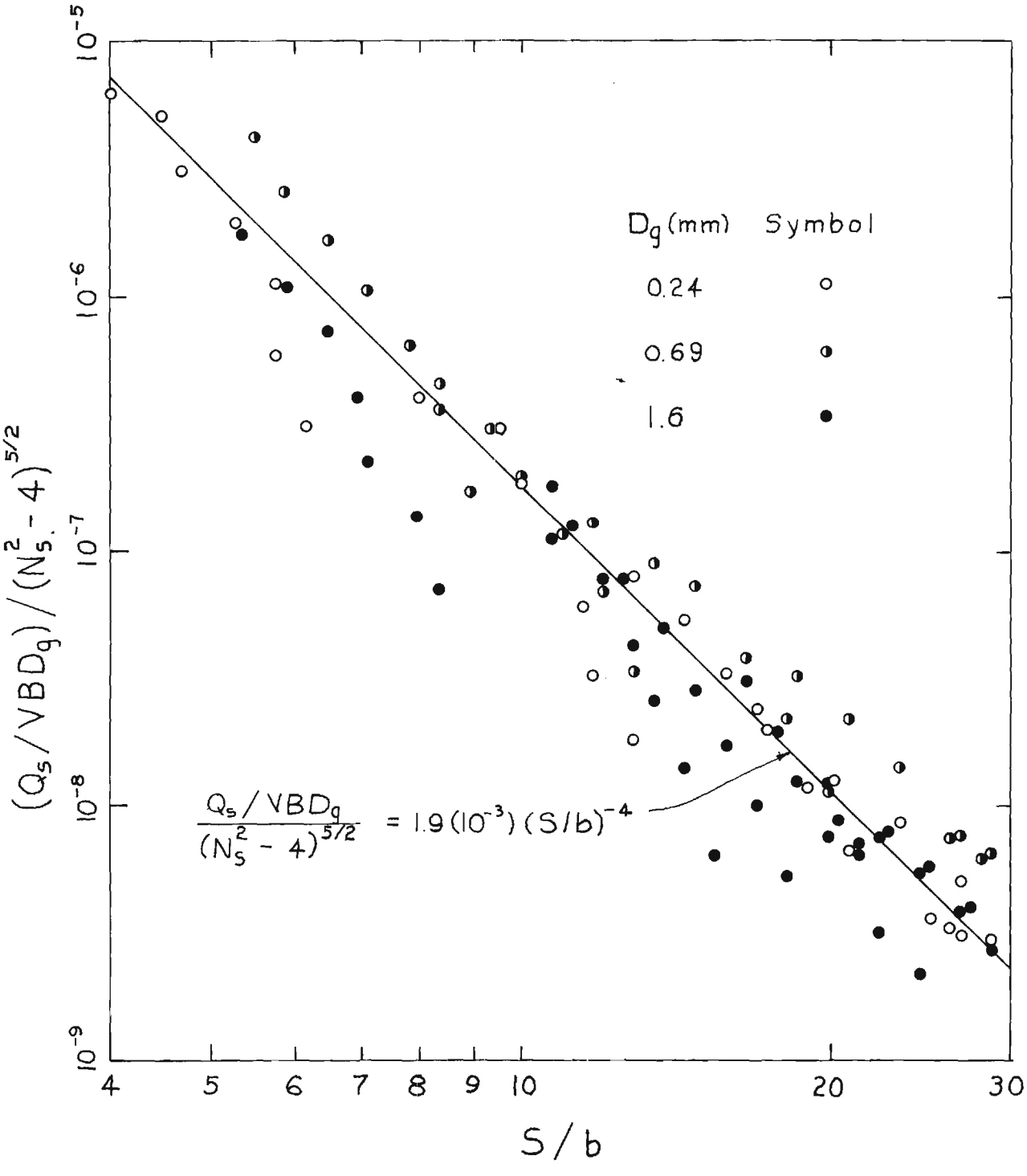

Figure 7. Sediment-Transport Rate (Jet).

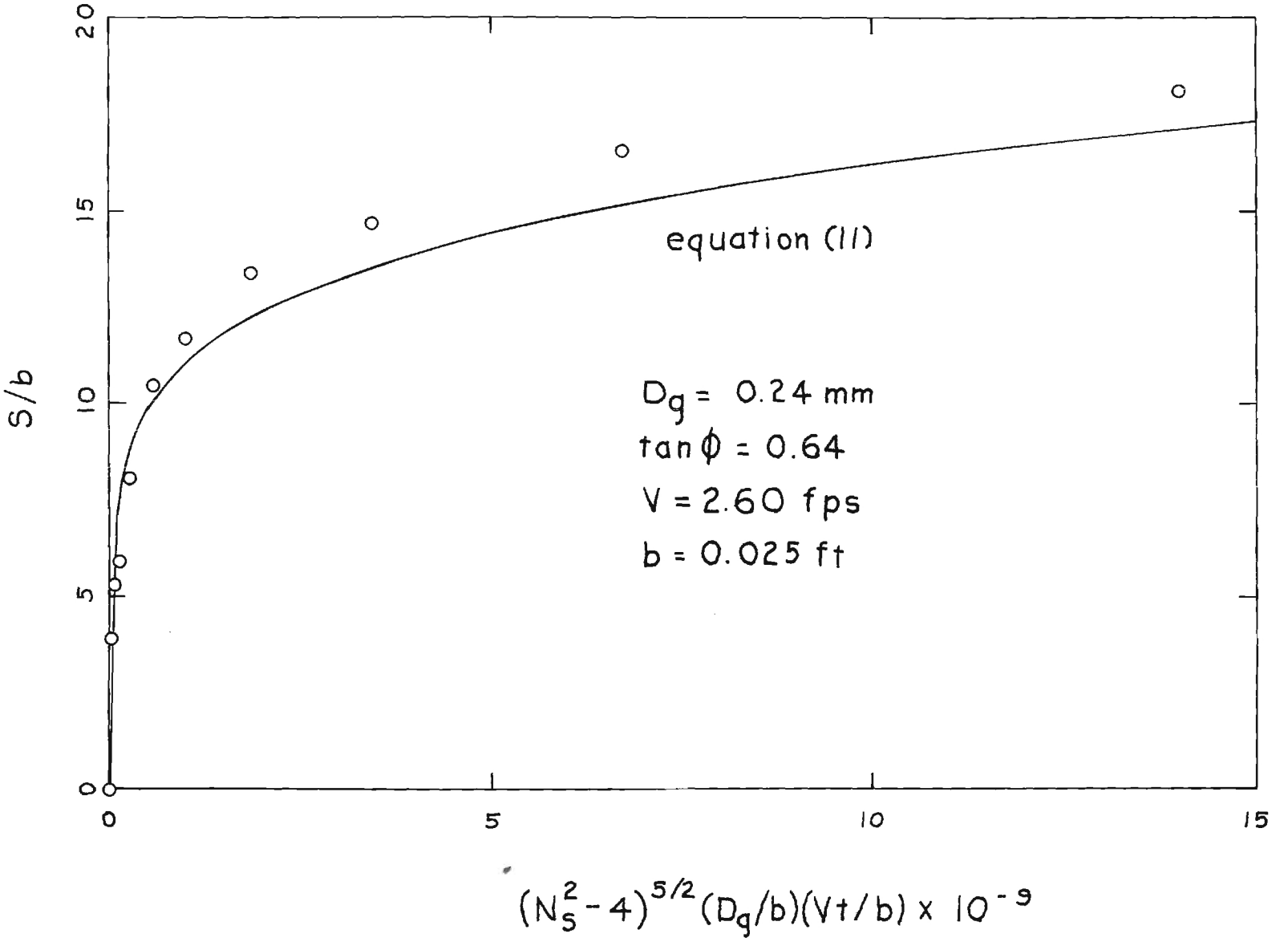

Figure 8. Scour Depth Versus Time (Jet).

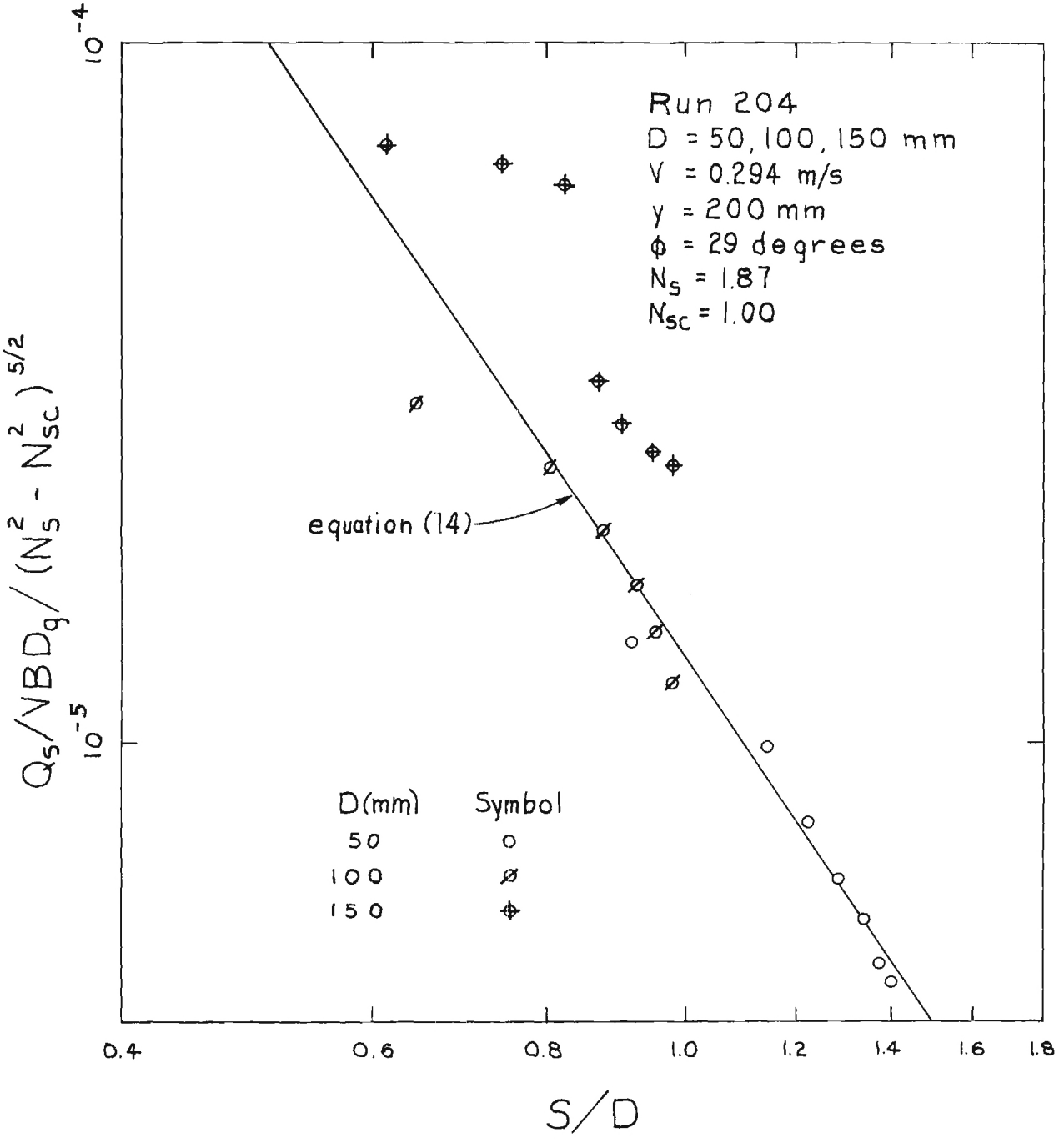

Figure 9. Sediment-Transport Rate (Vertical Cylinder).

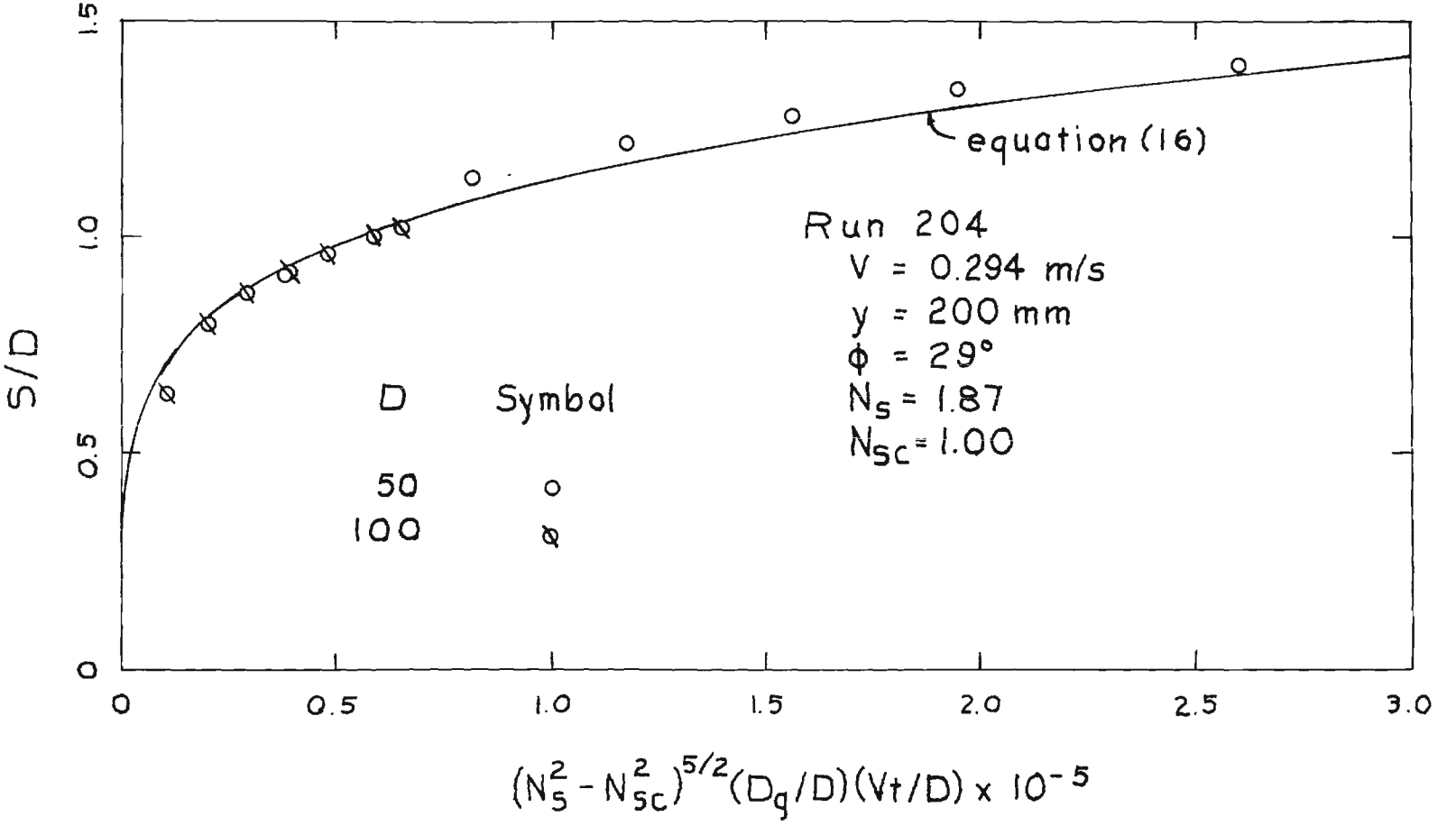

Figure 10. Scour Depth Versus Time (Vertical Cylinder).

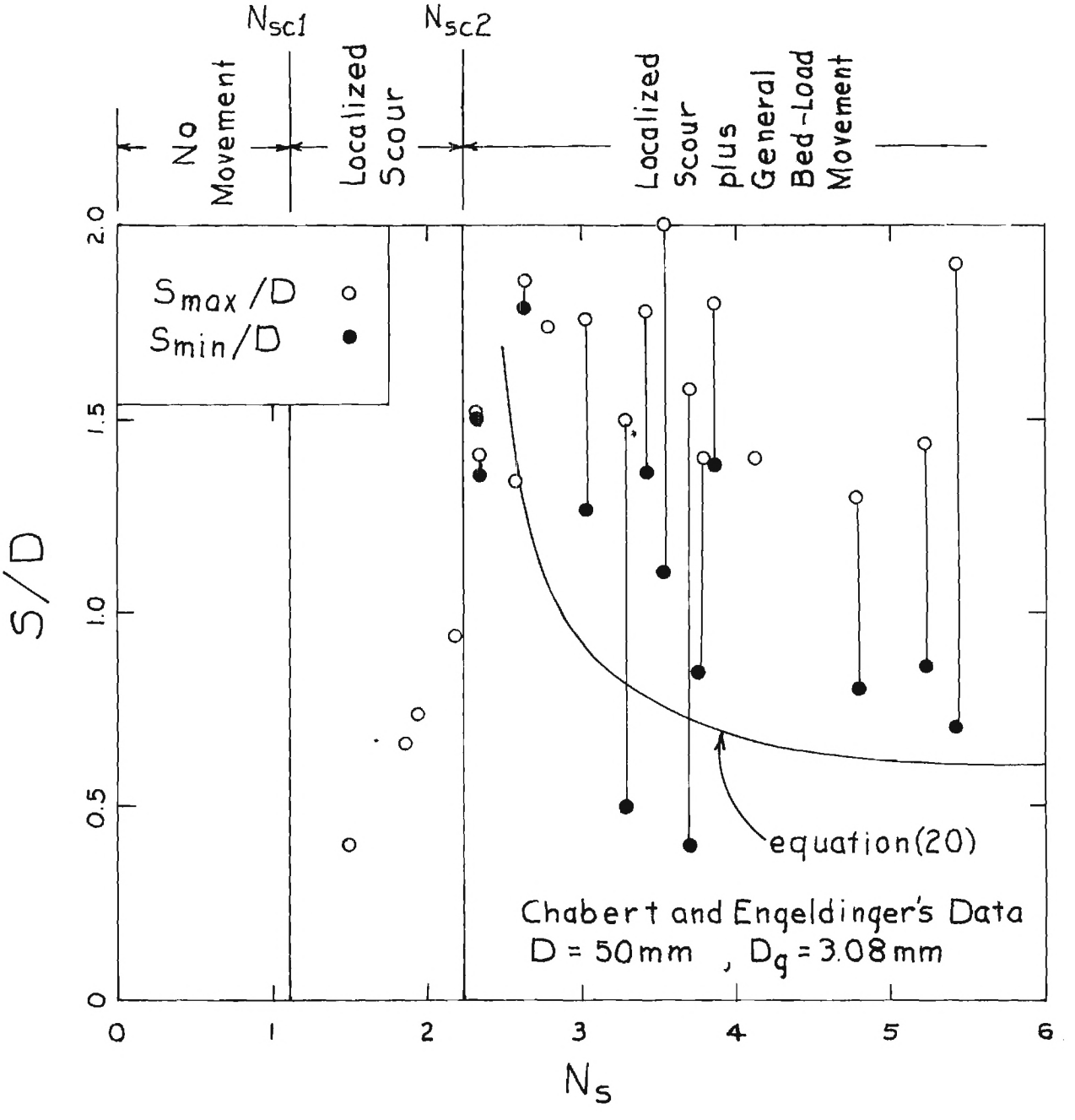

Figure 11. Maximum and Minimum Scour Depths (Vertical Cylinder).

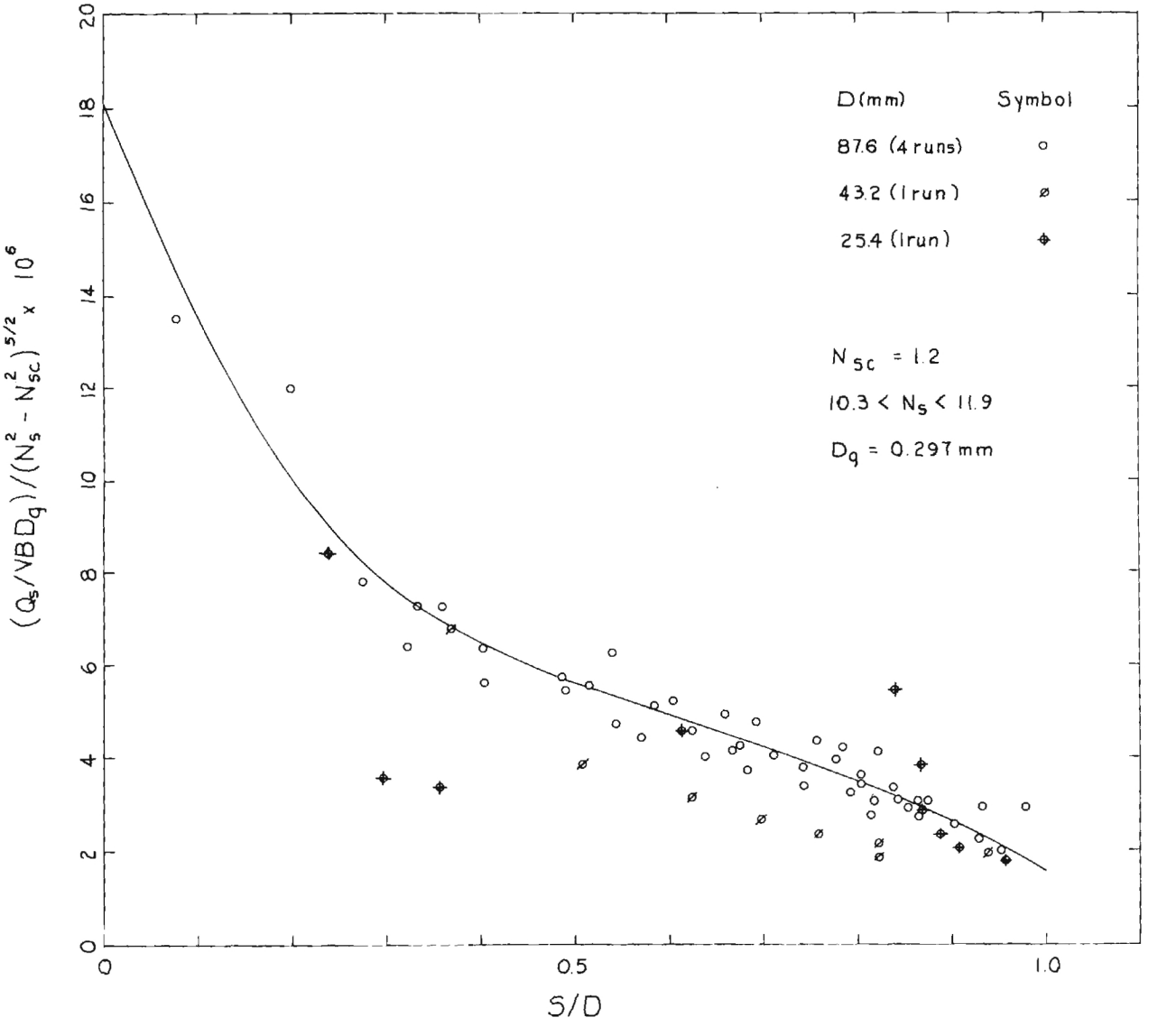

Figure 12. Sediment-Transport Rate(Horizontal Cylinder).

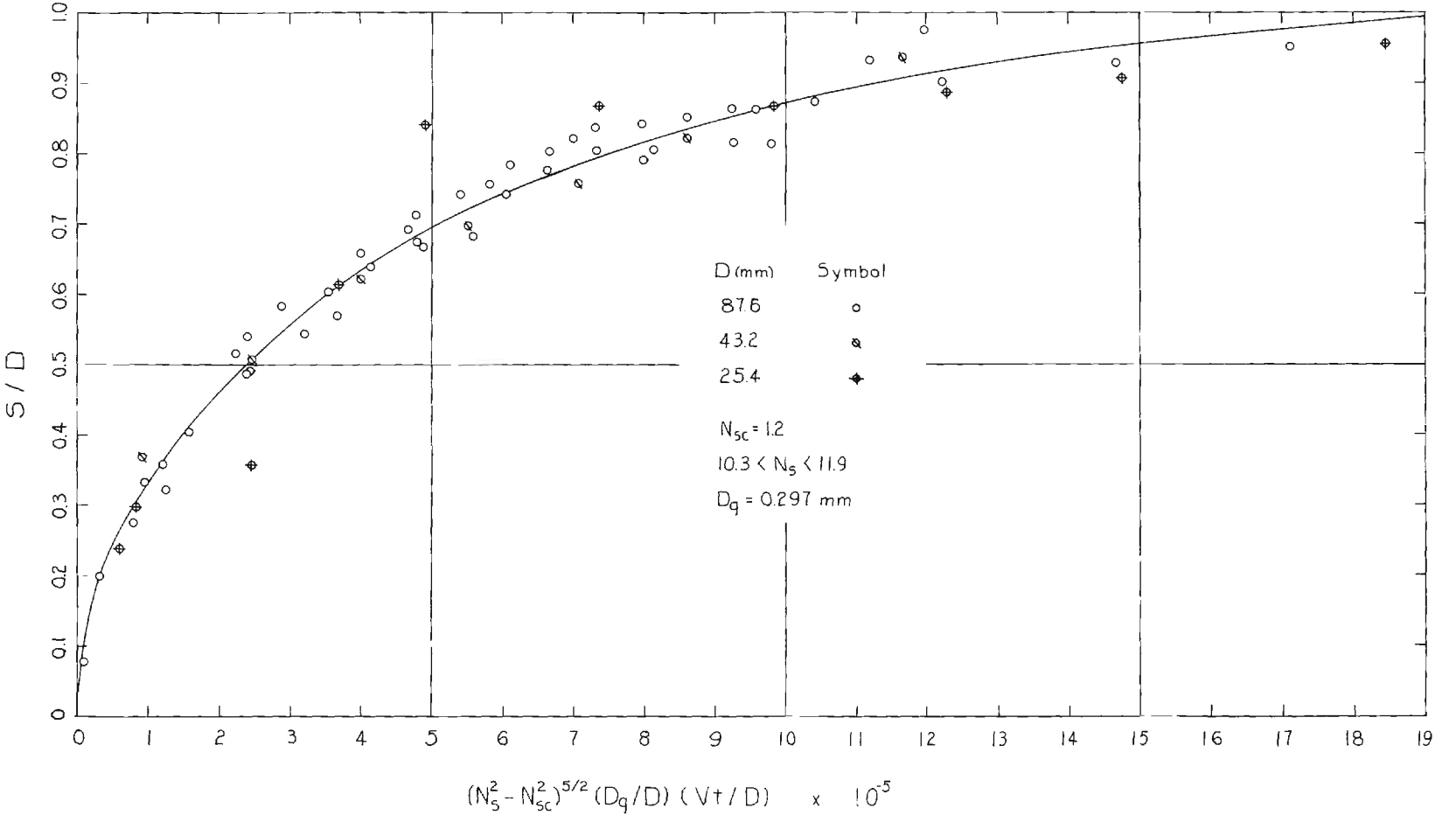

Figure 13. Settlement Versus Time (Horizontal Cylinder).

APPENDIX C

THE GEORGIA TECH OSCILLATING-FLOW WATER TUNNEL

THE GEORGIA TECH OSCILLATING-FLOW WATER TUNNEL

M. R. CARSTENS, M. ASCE, Professor, School of Civil Engineering
Georgia Institute of Technology, Atlanta, Georgia

A water tunnel in which the water is oscillated with simple harmonic motion through the test section has been installed in the Georgia Tech Hydraulics Laboratory and has been in operation since January 1963. The principal purpose for constructing the water tunnel was to study various physical phenomena at the sea bed under a system of first-order Stokian waves. To date, the water tunnel has been used to study ripple (dune) formations and to study localized scour around objects resting upon the sea bed. Other potential uses are for the study of boundary-layer transition and for the determination of forces on submerged bodies such as piles. The only other similar water tunnel (to the writer's knowledge) is located at the Technical University of Denmark in Copenhagen.

DESCRIPTION

The water tunnel is constructed as a large U-tube in which the bottom horizontal leg of the U is the test section as shown in Figures 1 and 2. The vertical legs of the U-tube are contained within steel tanks (A) which are 3 ft by 4 ft in cross section and are 11 ft tall. Streamlined flow passages are formed by inserts (C) fastened to the inner walls of the steel tanks. The water oscillates through the flow passage of the U-tube at the natural or resonant frequency. The free surface of the East leg, RHS of Figure 1, is utilized for water-surface-elevation measurement. The free surface of the West leg, LHS

of Figure 1, is utilized as a piston by which work is done on the oscillating system in an amount equal to the energy dissipated as the water moves back and forth through the U-tube.

The test section is 1 ft (vertical) by 4 ft (horizontal) in cross section and is 10 ft long. The roof and sidewalls are fabricated of 1/2-in transparent plastic and are framed on the exterior with steel angles and channels. A 3-ft square flush-mounted hatch is located in the center of the roof as an access into the test section. The central section of the floor is depressed in order to provide a container for erodible bed material. The depressed section is 6 ft long by 4 ft wide by 4 in deep. The entire test section rests upon three pre-fabricated steel trusses which span between the steel tanks.

The water in the U-tube is made to oscillate at the resonant frequency by applying a pressure pulse on the water surface in the West leg during the time the water surface is falling in that leg. The output of a centrifugal blower is discharged continuously in the air space above the water surface. Two 7 in diameter, pneumatically powered, poppet valves (E) in the top of the West leg are open except for a time during which the water level is falling in the West leg. The feedback mechanism by which the exhaust valves are sequentially operated is initiated by the change of direction of the water surface in the East leg. A float (F) in the East leg is attached to a steel rod (G) by means of a light flexible cable. The steel rod (G) slides easily past a permanent magnet which operates a microswitch. The combination of the steel rod, the magnet, and the switch constitute a direction-sensing switch (H). Whenever the steel rod (G) is falling the switch (H) is closed and vice versa. The closing of the switch (H) actuates a single-cycle timer. This timer makes one revolution in 2 seconds and then stops. A second microswitch is contained within the timer unit. By

means of an adjustable cam this second microswitch can be made to close during any portion of the two-second interval. Solenoid valves which control the pneumatically operated pistons on the exhaust valves are in the circuit with the timer microswitch. The timer microswitch is set such that the exhaust valves close when the timer starts and remain closed for about one-quarter cycle.

Initial and final transients of the oscillatory motion are eliminated by means of the blowdown and damping valve (I) in the East leg. The blowdown and damping valve is an 8 in diameter, pneumatically powered, poppet valve (I). In order to eliminate the initial transient, the blowdown valve (I) is closed and air is forced into the tank through (K). The water surface is forced downward to the desired equilibrium amplitude at which time the operator switches to the "run" position. As the operator switches to "run" the blowdown valve (I) opens, the air supply through air inlet (2) is stopped, and control of the tunnel reverts to the feedback mechanism described above. The terminal transient at the end of a run is eliminated by simply closing the damping valve (I). To start a run, the operator turns the masterswitch to "blowdown." When the water surface in the East leg is depressed to equilibrium amplitude, the operator turns the masterswitch to "run." To end a run, the operator turns the masterswitch to "stop."

VARIABLES

Since the tunnel is designed to operate at the resonant frequency of the water mass, only small changes in the period of the motion are possible without altering the flow passages. The tunnel was designed to be operated at different frequencies by changing the upper inserts (C) within the steel tanks.

Up to the present time only one set of inserts has been fabricated forming flow passages in the vertical legs which are 1 ft by 4 ft in cross section. With a normal water level the period of oscillation is 3.56 sec. By filling the tunnel to higher-than-normal level a period of 3.79 sec has been attained. By filling the tunnel to lower-than-normal level a period of 3.30 sec has been attained.

Total amplitude of the motion can be varied from 0 to 36 in by adjusting the magnitude of the pressure pulse which is applied to the water surface in the West leg of the U-tube. This pressure adjustment is accomplished by control of the angular velocity of the blower. By means of a mechanically variable V-belt drive, the blower can be operated at any speed from 400 to 3600 rpm. The motor, speed changer, and blower are shown in the foreground of Figure 2.

INSTRUMENTATION

The kinematics of the water are determined from the water-surface level in the East leg. The float-elevation sensor system consists of a small-diameter, stainless-steel cable which passes over 6-in diameter pulleys at the top and bottom of the East leg. The spring-tensioned endless cable is fastened to the wooden float (F). A three-turn potentiometer is connected to the axle of the upper pulley. The potentiometer is series connected in one leg of a Wheatstone bridge. Bridge unbalance is amplified and recorded by means of a Sanborn direct-writing oscillograph. The float-elevation sensor system is calibrated just before and just after a run by making short records at several elevations of the float. An example of the recorded motion curve is the uppermost trace in Figure 3. In addition to the continuous measurements of float-level, the maximum and minimum levels can be directly read from the position of the steel rod (G) which has a stationary scale fastened parallel to the rod.

A dual system of time measurement is provided. A timing marker in the recorder produces pips at one-second intervals as shown by the lowermost trace in Figure 3. In addition, an electrically operated digital counter is placed in the circuit with the direction-sensing switch (H). The readout of the counter is the integer number of cycles since the beginning of a run.

Work input to maintain the oscillation is calculated from the water-motion curve and the measured air pressure in the volume above the water surface in the West leg. Pressure measurement is accomplished by means of a Statham pressure transducer (± 0.15 psid). Bridge unbalance in the transducer is amplified and recorded. The pressure measuring and recording system is calibrated just before and just after a run by making short records at several pressures applied to the transducer diaphragm. The middle trace in Figure 3 is the pressure record.

Additional measurements of phenomena within the test section have been measured and recorded by optical devices. Photographs through the transparent sidewall and coordinate grid have been used extensively for the measurement of ripple (dune) geometry. Figure 4 is a photograph of a ripple system developed in the tunnel. A cathetometer has been employed to determine and record the scour depth in localized-scour studies involving objects resting on the bed. For this purpose, the telescope of the cathetometer was attached to a traversing mechanism such that an observer can raise or lower the telescope by turning a crank. The telescope was attached to a differential transformer which served as a transducer for the recording of the elevation of the telescope axis by means of a direct-writing oscillograph.

Plans are being formulated to incorporate a force-transducer system for the measurement of forces on bodies which are submerged in the oscillatory flow.

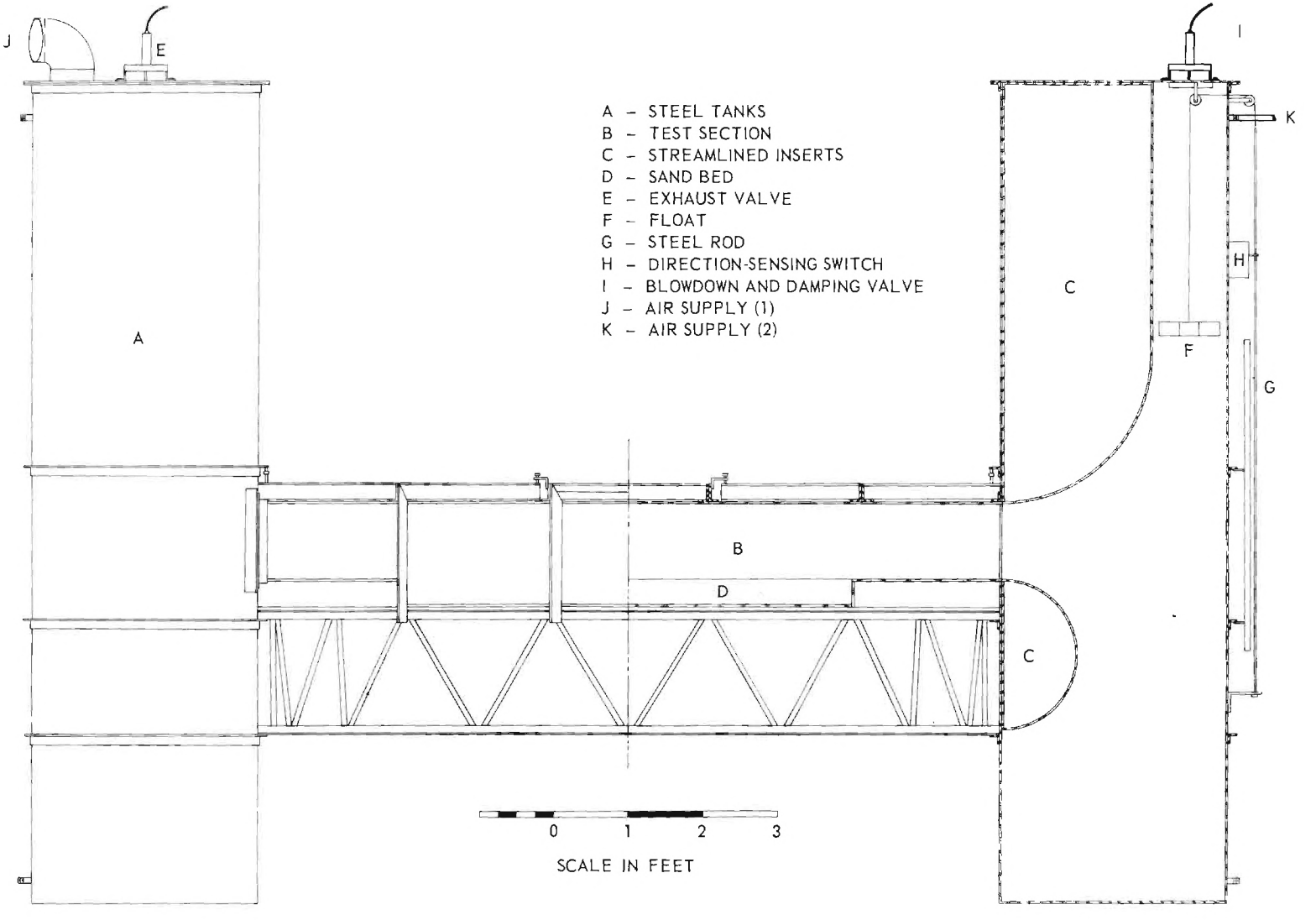

Figure 1. Side Elevation of Oscillatory-Flow Water Tunnel.

Figure 2. Photograph of Oscillatory-Flow Water Tunnel.

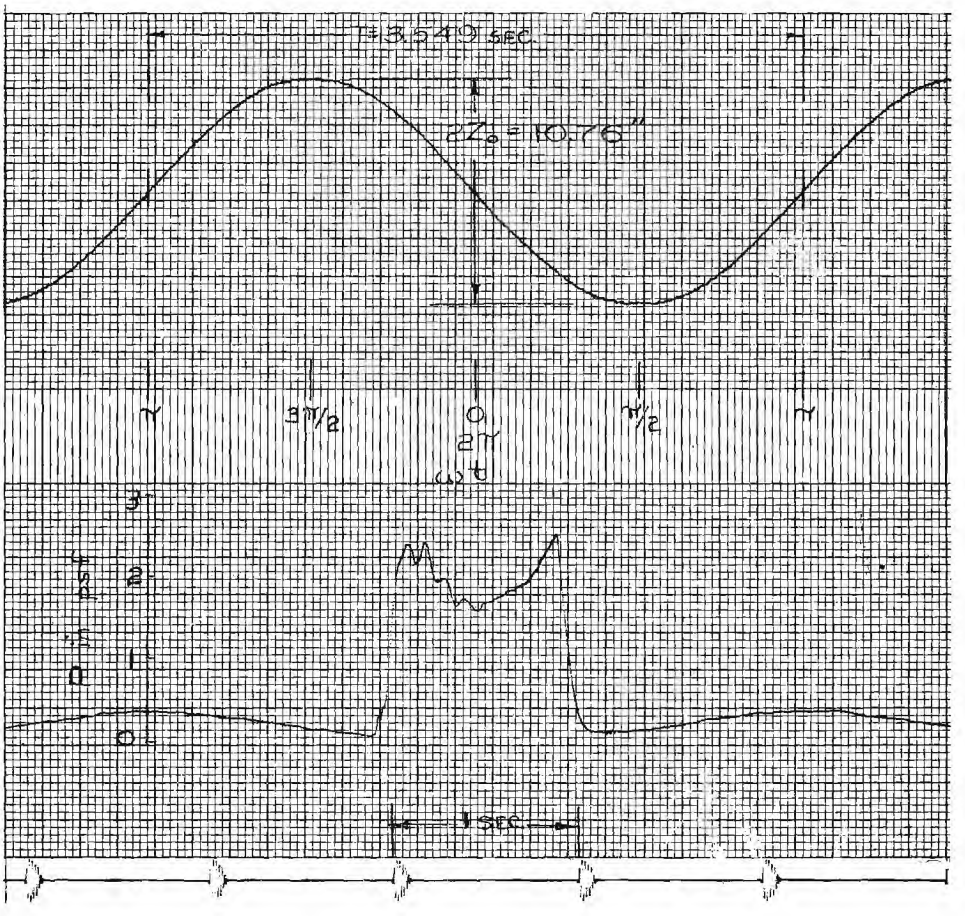

Figure 3. Record of Motion, Pressure Input, and Time.

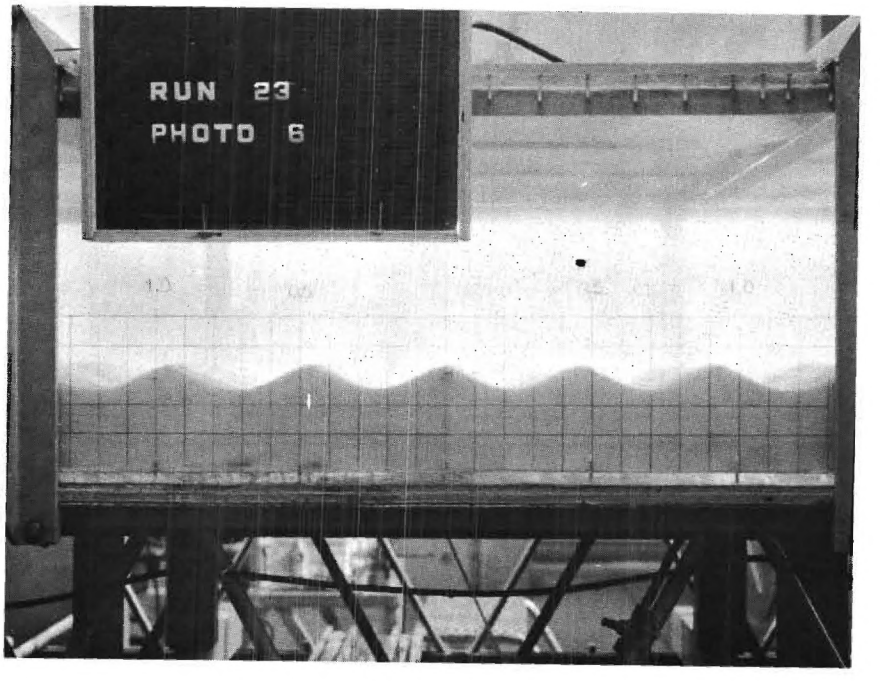

Figure 4. Dune Pattern.

Back Cover Blank

FINAL REPORT

PROJECT A-770

PART II - LOCALIZED SCOUR AROUND A HORIZONTAL CYLINDER

By
M. R. CARSTENS

Contract No. N600(24)-59885

Prepared for
U. S. Navy
Mine Defense Laboratory
Panama City, Florida

30 June 1967

Engineering Experiment Station
GEORGIA INSTITUTE OF TECHNOLOGY
Atlanta, Georgia

ERRATA

The following corrections are applicable to the Final Report, Part II, Project A-770:

Page 42:

The equation number should be 13.

Pages 52, 53, 54, 55, and 56:

The dimensionless time parameter should be $t\, D_g \sqrt{(s-1)gD_g}/D^2$

GEORGIA INSTITUTE OF TECHNOLOGY

School of Civil Engineering

Atlanta, Georgia

FINAL REPORT

PROJECT A-770

PART II - LOCALIZED SCOUR AROUND A HORIZONTAL CYLINDER

by

M. R. CARSTENS

Contract No. N600(24)-59885

30 June 1967

Prepared for
U. S. NAVY
MINE DEFENSE LABORATORY
PANAMA CITY, FLORIDA

FOREWORD

This report is PART II of a Final Report of Project A-770 of the Engineering Experiment Station of the Georgia Institute of Technology, Atlanta, Georgia. The project is being conducted for the U. S. Navy Mine Defense Laboratory, Panama City, Florida as a task under Contract No. N600(24)-59885. Most of the pertinent material contained in PART I, "The Effect of Dunes Upon Localized Scour," has been repeated in PART II. Most of the information contained in Chapter II was obtained in another study being sponsored by the Department of the Army, Coastal Engineering Research Center under Contract No. DA-49-055-CIVENG-65-1.

Appreciation is expressed to the staff of the U. S. Navy Mine Defense Laboratory for their continued help throughout the study. In fact, the initial interest of the staff of the U. S. Mine Defense Laboratory provided the impetus for the design and the construction of the oscillatory-flow water tunnel.

Appreciation is also expressed to the following persons that have aided in furthering the study of localized scour: Messrs. C. S. Martin; F. M. Neilson; H. Majumdar; L. DeJarnette; H. D. Altinbilek; and K. Watanakun.

ABSTRACT

A method of analyzing localized scour is proposed and is demonstrated for localized scour and subsequent settling of a horizontal cylinder into the bed under the action of oscillatory flow above the bed. Scour depth as a function of time is derived by integration of the equation of continuity of sediment in the scour hole. The differential equation involves three distinct functions, that is, (a) a mathematical function for the scour-hole geometry, (b) a mathematical function for the rate of sediment transport out of the scour hole, and (c) a mathematical function for the rate of sediment transport into the scour hole.

A mathematical function for the geometry of the scour hole requires the preparation of a topographic map of the scour hole from either a model test or a field survey since the geometry of the scour hole is dependent upon the geometry of the object around which scour occurs.

A rational function for the rate of sediment transport out of the scour hole is presented. Two model tests are required. One is to determine the incipient-scour condition. The other is to determine a constant in the transport equation. This latter test must be conducted without sediment transport into the scour hole in order to eliminate one of the three terms of the sediment-continuity equation.

Rational functions for the rate of sediment transport into the scour hole are presented for transport by oscillatory flow.

Results of an extensive model-test program are presented. Four cylinders of different size were tested. Two different bed materials were used. The period of the oscillatory flow was essentially constant but the total amplitude

of the water motion was varied from one foot to about three feet. Three of the model tests were used to evaluate constants in the transport functions. Measured settlement is compared with predicted settlement for 35 model tests.

Bed-form geometry, bed-form development, and the influence of bed forms upon model tests and upon sediment transport are discussed.

Key words: scour, sedimentation, dunes, hydraulic models.

TABLE OF CONTENTS

TABLE OF CONTENTS (Continued)

LIST OF FIGURES

LIST OF TABLES

GLOSSARY

Symbol	Definition
B	width of scour hole
C_D	coefficient of drag on a particle
D	cylinder diameter
D_g	geometric-mean sediment diameter
D_1	reference length
$f(\ )$	function of
f_b	boundary-drag coefficient
g	acceleration of gravity
K_2, K_3, K_4	dimensionless coefficients
L	length of cylinder
N_s	sediment number $(U_m/\sqrt{(s-1)g\ D_g})$
N_{sc}	critical sediment number
Q_{si}	sediment discharge into scour hole (solids plus void)
Q_{so}	sediment discharge out of scour hole (solids plus voids)
Q_s'	sediment discharge (solids)
q_s'	sediment discharge (solids) per unit width of bed
S	scour depth
S_i	initial depression of bottom of cylinder below mean bed level
S_T	terminal scour depth
s	ratio of solids density to water density
s.f.	particle shape factor
T	period of oscillation
t	time
t_d	time to develop an equilibrium duned bed from an initially flat bed

(Continued)

GLOSSARY (Continued)

Symbol	Definition
U_m	maximum velocity of oscillatory flow above the bed
u	velocity of oscillatory flow, $u(y,t)$
u_i	fluid velocity at particle level at incipient motion
u_{max}	maximum velocity of oscillatory flow, $u_{max}(y)$
V	mean velocity of unidirectional flow
$\forall$	volume of scour hole
y	vertical distance above bed
y_o	depth of unidirectional flow
α	inclination of bed from horizontal
γ	specific weight of water
η	amplitude of dunes
λ	wave length of dunes
ν	kinematic viscosity of water
ρ	density of water
σ_g	geometric standard deviation of bed material in regard to size
τ_o	boundary-shear stress
ϕ	angle of repose of the bed material

I. INTRODUCTION

The Georgia Institute of Technology Hydraulics Laboratory has been pursuing a program concerning localized scour around and subsequent burial of objects lying on the sea bed. The program at the Georgia Tech Hydraulics Laboratory involved the settlement of cylindrical objects into the sand bed of the test section of an oscillating-flow water tunnel. The principal objective of the hydraulic-laboratory program was to study the scouring process in order to be able to predict settlement as a function of time. In other words, similarity relations for localized scour were to be established as a result of the hydraulic-laboratory studies.

A. Hydraulic-Laboratory Experiments

Scour beneath a right-circular cylinder and subsequent settlement into the scour hole has been extensively studied in an oscillatory-flow water tunnel located in the Georgia Tech Hydraulics Laboratory. The test section is the bottom leg of a large U-tube. The test section is 10-ft. long, 1-ft. high, and 4-ft. wide. The central section of the floor is depressed in order to form a container for the erodible bed material. The sidewalls and top of the test section are made of transparent plastic in order to obtain settlement data by optical methods. Water is made to oscillate through the test section with simple-harmonic motion. Amplitude of the water motion is a controlled variable. The period of oscillation is essentially constant ($T = 3.6$ sec) during all runs

inasmuch as the water mass is oscillated at resonant frequency in the U-tube. The flow condition is a close approximation to the flow at the sea bed beneath first-order Stokian waves. A more complete description of the water-tunnel is given elsewhere 1/.

Two different bed materials were used. The coarser bed material was "flint shot" sand obtained from the Ottawa Silica Company. The finer bed material was glass beads obtained from the Minnesota Mining and Manufacturing Company. Pertinent properties of the bed materials are given in table I.

TABLE I

PROPERTIES OF BED MATERIALS

Property	Ottawa Sand	Glass Beads
Geometric mean diameter, D_g, in. mm	0.585	0.297
Geometric standard deviation, σ_g	1.16	1.06
Specific gravity, s	2.62	2.47
Angle of repose*, ϕ, in degrees	32.5	24

*Approximate value since ϕ is also a function of porosity.

The right-circular cylinders were fabricated from aluminum. The diameters are 0.501 in., 1.002 in., 1.702 in., and 3.450 in. The majority of the tests were performed with cylinders having a length-to-diameter ratio, L/D, of 4. A few tests were performed with larger ratios of L/D. One test was performed with a cylinder having hemispherical ends.

1. 1962-1963 Tests

The first series of tests had as objectives (a) to obtain settlement-time data, (b) to observe the phenomenon, (c) to determine the effect of orientation

of the cylinder with the wave crest, and (d) to determine the effect of initial burial. The scope of the 1962-1963 tests is shown in table II.

TABLE II

SCOPE OF 1962-1963 TESTS

Model Test No.	D (in)	Initial Orientation (deg)	Initial Burial S_i/D	L/D	D_g (mm)	Water Temperature (°F)	Total Amplitude (in)	Period (sec)	N_s
5	1.702	15	0.13	4	0.297	65.0	32.60	3.63	11.0
6	1.702	30	0.03	4	0.297	64.0	33.30	3.63	11.2
7	1.702	60	0.06	4	0.297	64.0	33.55		
8*	1.702	0	0.04	4	0.297	67.0	34.20	3.66	11.4
9	3.450	14	0.06	4	0.297	67.2	34.10	3.66	11.4
10	3.450	60	0.08	4	0.297	69.0	34.00	3.65	11.4
11	3.450	30	0.08	4	0.297	70.0	33.70		
12	3.450	15	0.08	4	0.297	67.0	33.80	3.64	11.4
13	3.450	0	0.08	4	0.297	70.0	33.60		
14	3.450	90	0.08	4	0.297	64.2	33.70	3.65	11.3
15	3.450	75	0.09	4	0.297	65.2	34.00	3.65	11.4
16	3.450	80	0.07	4	0.297	66.0	33.80	3.64	11.4
17	1.702	75	0.15	4	0.297	65.5	34.40	3.66	11.5
18	1.702	89.5	0.10	4	0.297	66.0	34.05	3.65	11.4
24	0.501	0	0.08	4	0.585	74.3	12.15	3.59	2.80
25	0.501	0	0.03	4	0.585	73.5	12.09	3.59	2.78
26	0.501	0		4	0.585	77.0	11.90	3.57	2.76
27	0.501	0	0.08	4	0.585	78.4	12.14	3.58	2.80
28	0.501	0	0.27	4	0.585	79.5	12.23	3.57	2.84
29	0.501	0	0.36	4	0.585	78.5	12.16	3.57	2.82
30	0.501	0	0.55	4	0.585	78.0	12.00	3.58	2.78
31	1.002	0	0.06	4	0.585	77.5	11.93		
32	0.501	0	0.06	8	0.585	76.5	12.25	3.58	2.83
33	0.501	0	0.15	12	0.585	76.5	12.23	3.59	2.82

(Continued)

TABLE II (Concluded)

SCOPE OF 1962-1963 TESTS

Model Test No.	D (in)	Initial Orientation (deg)	Initial Burial S_i/D	L/D	D_g (mm)	Water Temperature (°F)	Total Amplitude (in)	Period (sec)	N_s
34	0.501	0	0.06	16	0.585	76.0	12.12	3.58	2.80
37	0.501	0	0.02	4	0.585	75.0	11.99	3.57	2.78
38**	0.501	0	0.06	8	0.585	73.5	12.26	3.58	2.84
39	0.501	0	0.20	4	0.585	74.5	12.16	3.60	2.80
41	3.450	0	0.05	4	0.297	75.0	33.80	3.65	11.3
42	3.450	0	0.04	4	0.297	76.2	33.90	3.65	11.4
43*	3.450	0	0.21	4	0.297	74.5	33.80	3.65	11.3
44	3.450	0	0.20	4	0.297	75.0	33.50	3.66	11.2
45	3.450	0	0.27	4	0.297	75.8	33.60	3.66	11.2
46	3.450	0	0.50	4	0.297	75.5	33.40	3.66	11.2
47	1.702	0	0.21	4	0.297	76.8	33.60	3.65	11.3
50	1.702	0	0.06	4	0.297	76.6	34.10	3.57	11.7

*Settlement-time data determined from 16-mm motion pictures.

**Rounded ends.

The column labelled "Initial Orientation" is the angle in degrees between the axis of the cylinder and the wave crest (perpendicular to the direction of the water motion in the test section).

The column labelled "Initial Burial, S_i/D" is the ratio of the initial vertical displacement of the bottom of the cylinder from bed level to the cylinder diameter. The cylinder would settle slightly into the bed even though the cylinder was carefully lowered.

The column labelled "N_s" is the value of a flow parameter hereafter called the sediment number. The sediment number is $U_m/\sqrt{(s-1)g\ D_g}$ in which U_m is the maximum water velocity at bed level; s is the ratio of the specific weight of the sand, γ_s, to the specific weight of the water, γ; g is the scalar magnitude of the acceleration of gravity; and D_g is the geometric mean diameter of the sand. The sediment number, N_s, is a form of Froude number 2/ being proportional to the square root of the ratio of the fluid inertial force per unit volume to the buoyant weight (gravity force) of the sand per unit volume. The sediment number is the sole flow variable used in the sediment-transport functions which are developed subsequently in Chapter V. In addition, the geometry of the bed is characterized by the value of the sediment number as shown subsequently in Chapter II.

Settlement was obtained by maintaining a cathetometer-telescope focused on the top of the cylinder during settlement. A second observer read the cathetometer-telescope elevation at specified time intervals upon a signal from a third observer who also recorded the data.

The bed was screeded to be flat as an initial condition for all tests.

The cylinder settles into the scour hole in a stepwise manner. Scour holes develop at each end of the cylinder as shown in Figure 1. The scour holes enlarge around and under each end of the cylinder. The enlargement continues under the cylinder until the central support is insufficient at which time the cylinder drops suddenly. The process is repetitive. Because the central support becomes quite narrow prior to dropping, the cylinder can pivot on the central support. Cylinders which are initially oriented other than parallel to the wave crest pivot in steps until the cylinder axis is parallel

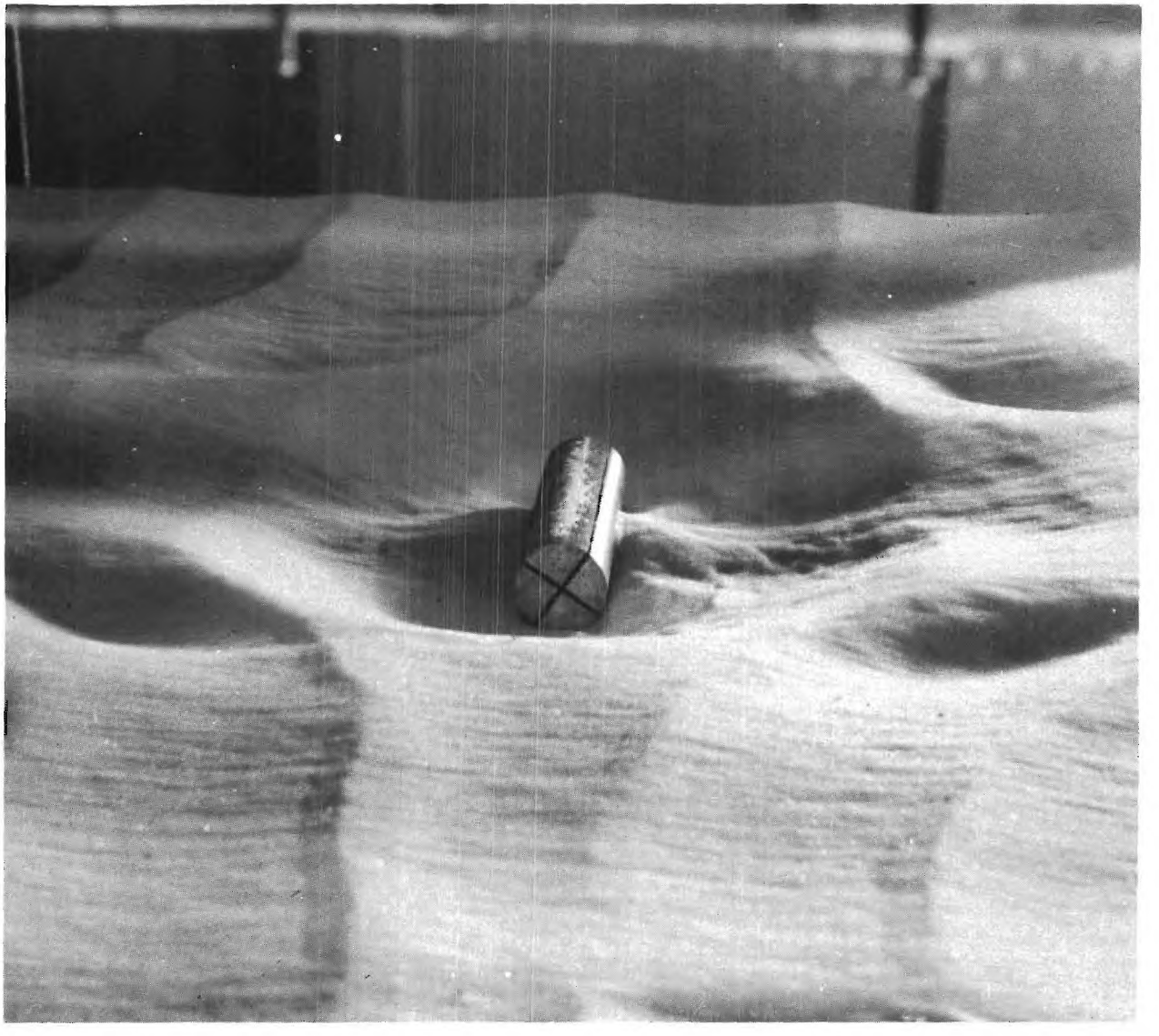

Figure 1. Scour Hole (N_s = 11.2).

to the direction of the wave crest. No difference in the settlement-time function could be detected if the initial orientation angle was less than 60 degrees.

In addition to the tests as listed in Table II a few exploratory tests were performed to determine whether piping under the cylinder was significant in the settlement process. A two-dimensional cylindrical model was constructed with a sand bed beneath the cylinder. Differential pressure was applied to the water on either side of the cylinder until piping under the cylinder developed. On the basis of these tests and observation of cylinder settlement, the conclusion was reached that settlement resulted from localized scour at the ends of the cylinder and that the effect of piping was insignificant.

2. 1964-1965 Tests

A second series of tests was conducted to determine the effect of dunes upon localized scour which occurs around a right-circular cylinder placed upon the bed under oscillatory flow.

During the 1962-1963 series of tests, dunes were observed to greatly influence the settlement of the model cylinders. When the dune amplitude was of the same order of magnitude as the cylinder diameter, the cylinder joined the dune system with axis of the cylinder coinciding with a ripple crest. This condition is shown in Figure 2 for which the value of N_s was 5.9. When the cylinder acted as a pseudo dune, the flow pattern around the cylinder was entirely changed. Scour holes did not develop at the ends of the cylinder and settlement appeared to cease.

The scope of the 1964-1965 tests is shown in Table III. In all tests the ratio, L/D, was four; the cylinder axis was oriented parallel to the wave

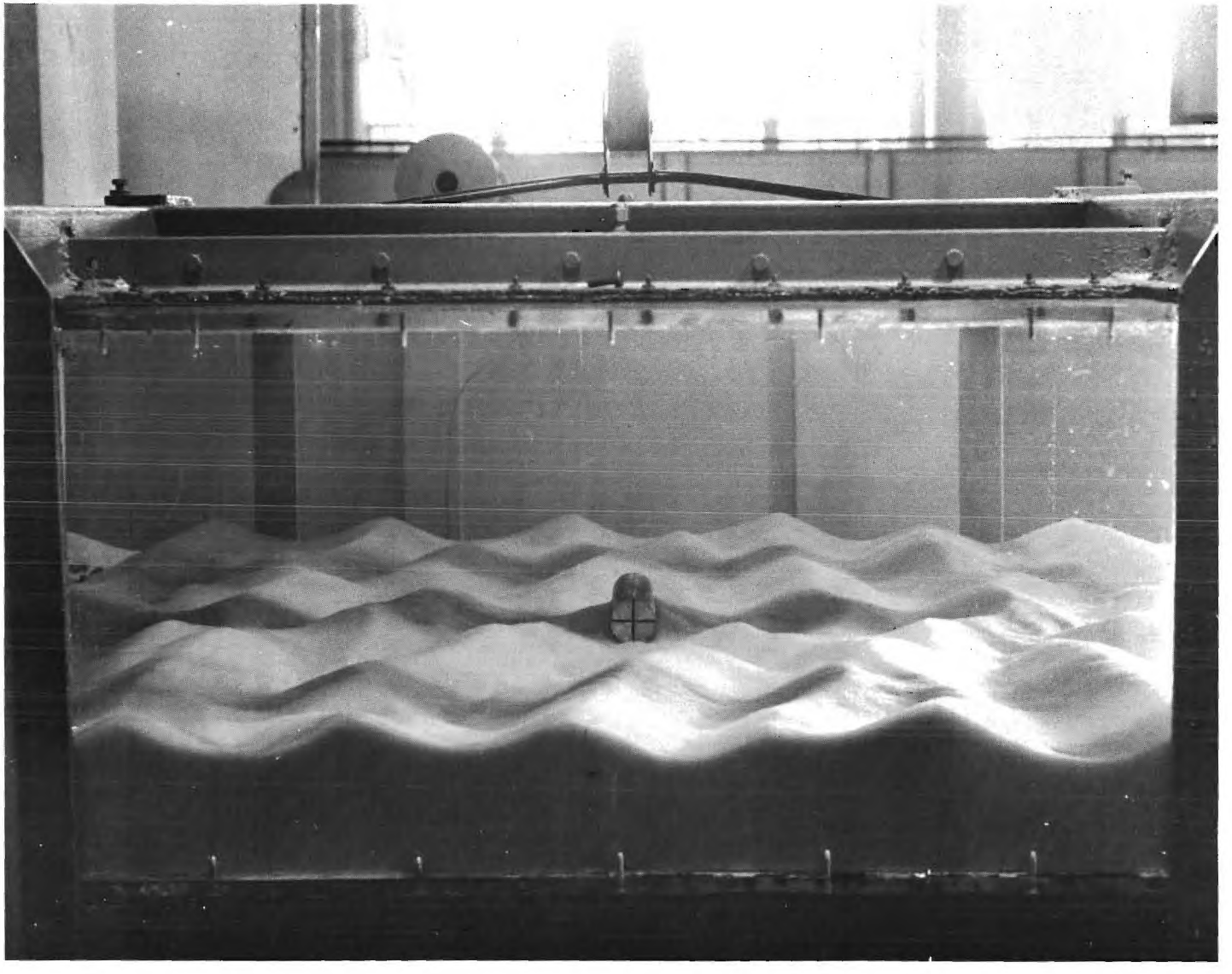

Figure 2. Model Incorporated Into Dune System (N_s = 5.9).

crest; the bed material was 0.297-mm diameter, glass beads; and the bed was flattened prior to each test. The procedure for obtaining settlement data was the same as in the earlier tests with the exception that vertical position of the cathetometer-telescope was sensed and recorded using the electronic equipment described in Part I 1/.

TABLE III

SCOPE OF 1964-1965 TESTS

Model Test No.	D (in)	Initial Burial S_i/D	Water Temperature (°F)	Total Amplitude (in)	Period (sec)	N_s
6	3.450	0.07	65	22.8	3.70	7.45
7	3.450	0.05	60	17.8	3.55	6.10
8	3.450	0.06	67	24.5	3.72	7.99
9	3.450	0.06	62	26.6	3.51	9.20
10	3.450	0.04	64	29.4	3.55	10.08
11	3.450	0.07	63	31.4	3.60	10.60
12	3.450	0.05	64	35.0	3.64	11.67
13	3.450	0.02	62	15.3	3.52	5.25
14	3.450	0.09	64	33.6	3.43	11.90
15	3.450	0.07	62	27.7	3.54	9.47
16	3.450	0.27	62	28.4	3.56	9.67
17	3.450	0.06	67	32.2	3.54	11.05
18	1.702	0.01	66	32.1	3.53	11.00
19	1.702	0.09	64	29.6	3.54	10.15
20	1.702	0.05	72	25.1	3.54	8.58
21	1.702	0.15	75	21.0	3.54	7.16
22	1.702	0.15	77	24.5	3.63	8.17
23	1.702	0.14	75	29.3	3.58	9.97

(Continued)

TABLE III (Concluded)

SCOPE OF 1964-1965 TESTS

Model Test No.	D (in)	Initial Burial S_i/D	Water Temperature (°F)	Total Amplitude (in)	Period (sec)	N_s
24	1.002	0.26	76	29.0	3.58	9.81
25	1.002	0.19	77	30.0	3.54	10.30
26	1.002	0.29	77	26.3	3.57	8.91
27	1.002	0.29	77	15.0	3.54	5.14
28	1.002	0.23	77	21.6	3.57	7.32
29	1.002	0.18	77	24.4	3.57	8.29
30	3.450	0.06	76	15.0	3.57	5.10
31	3.450	0.10	77	19.5	3.57	6.60
32	3.450	0.10	76	22.8	3.57	7.75
33	3.450	0.14	76	25.5	3.57	8.65
34	1.702	0.09	77	14.7	3.55	5.00
35	1.702	0.14	77	19.0	3.55	6.50
36	3.450	0.22	78	26.0	3.53	8.92
37	3.450	0.52	77	26.0	3.53	8.92
38	3.450	0.27	76	31.7	3.55	10.80
39	3.450	0.50	76	31.6	3.52	11.00
40	3.450	0.76	77	31.7	3.54	10.85

The recorded data of Test No. 12 is shown in Figure 3. The upper trace is that of water-motion displacement. Initial transients are eliminated by blowing down the water surface in one of the vertical legs in the U-tube. Upon release of the excess pressure over the water surface the oscillatory motion starts and continues at equilibrium amplitude as shown in Figure 3. Final transients are

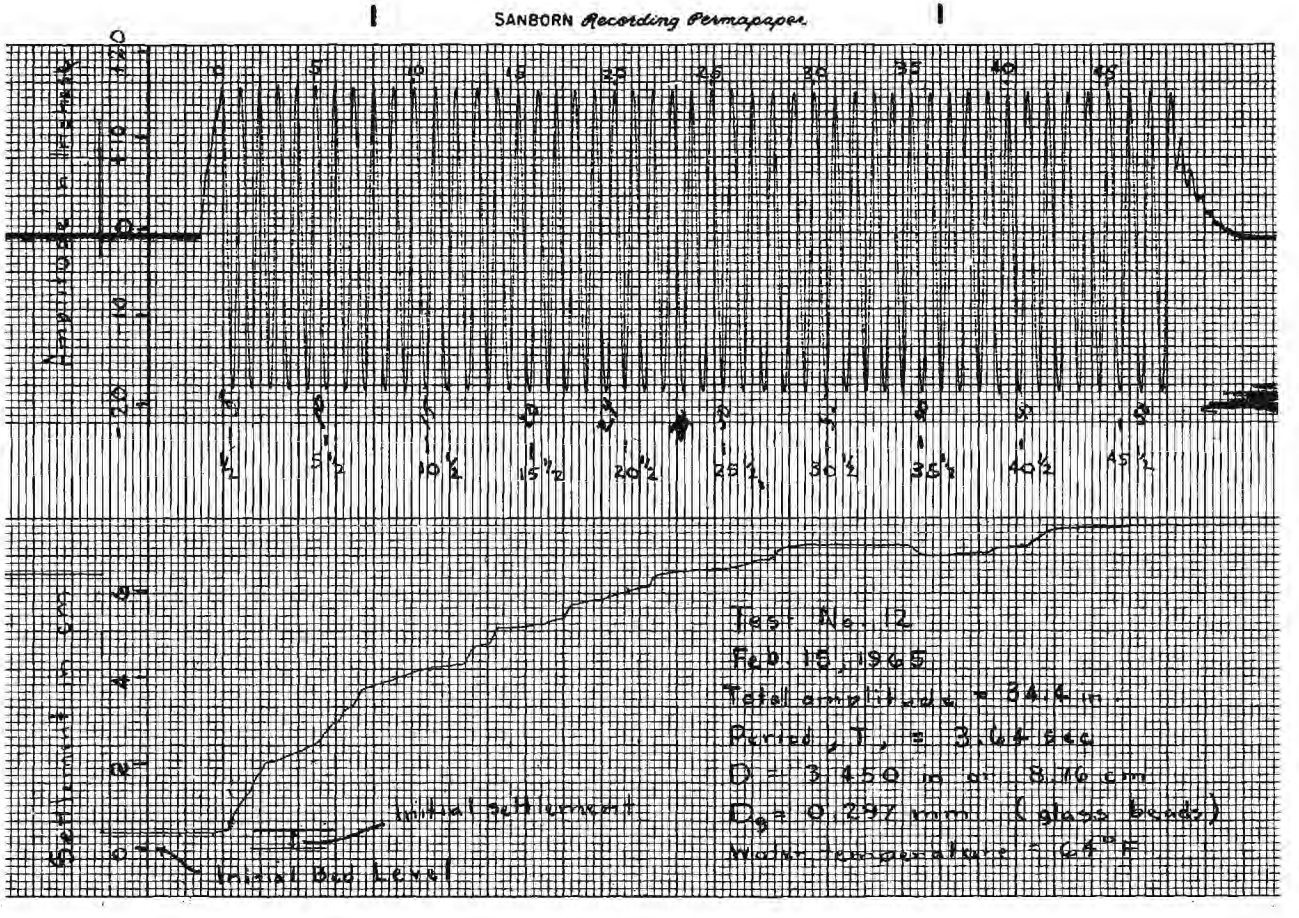

Figure 3. Recorded Data of Test No. 12 (1964-1965 Series).

eliminated by sealing the air space above the water in one of the vertical legs. The motion is rapidly but gently damped as shown in Figure 3. The middle trace is that of settlement, S, which is measured from the initial bed level to the bottom of the cylinder. The bottom trace is a timing mark with a pip being produced every cycle. Settlement by sudden drops is clearly shown in the middle trace. The first drop is the largest and occurs as soon as the water begins to oscillate. Succeeding drops decrease in magnitude and occur with an increasing time interval between drops. Tipping of the cylinder occurs at 36 cycles as shown in Figure 3.

Settlement of the cylinders was demonstrated to be influenced by dunes--even with the largest model. In other words, the minimum diameter for a cylinder to develop a typical scour hole as shown in Figure 1, irrespective of dune development, was not established. On the other hand, settlement did not appear to be influenced by dunes if the value of N_s were greater than 9.5, irrespective of the size of the model. Interpretation of the experimental results was complicated by simultaneous development of a dune system and development of the scour holes under the ends of the cylinder since each test was begun with a flat bed. A further complicating factor was that dunes obscured the view of the top of the cylinder when amplitude of the dunes was about equal to the protrusion of the cylinder. When the view of the cylinder was obscured no further data could be obtained to determine whether settlement continued. Settlement appeared to cease when the top of the cylinder was at dune crest height except when the value of the sediment number, N_s, was greater than 9.5.

Settlement as a function of time is shown graphically in the APPENDIX for each of the 1964-1965 tests.

B. Analysis of Settlement

As in all sediment problems, a reduced scale model of a prototype situation is virtually impossible. The flow obstruction (cylinder) can, of course, be reduced in scale. On the other hand, a similar scale reduction of the bed material would result in a great reduction in settling velocity of the bed material. As a consequence large quantities of the bed material would be picked up from the bed and would remain in suspension quite unlike the prototype situation in which the sand is scoured and is transported a short distance before being redeposited on the bed. For example, a 1/10 scale model of 0.3-mm sand would be 0.03-mm silt for which settling-velocity ratio would be of the order of 1/100, whereas the Froude criterion is indicative that the settling-velocity ratio should be 1/3.16. In these studies the Froude criterion was followed in that values of N_s of the model tests covered the same range as those of the prototype. The result is that the sediment diameter is outsize in the model.

A second difficulty is the scale effect of dunes. With a reduced-scale model the dunes will be of the same order of magnitude in size as the model. The flow pattern over the dunes will be a significant influence on the flow pattern around the reduced-scale model. Conversely, the flow pattern over the dunes will be an insignificant influence on the flow pattern around the prototype object provided that the pertinent length of the prototype object is greater than the dune wave length.

Because of these difficulties, the decision was made to formulate a rational settlement function using the model-test results for the determination of various constants. Further, the decision was made to formulate the rational settlement function by integration of sediment-transport functions. The

formulation of a settlement function involved the following steps:

(a) measuring the scour hole;

(b) devising a mathematical expression to represent the volume of the scour hole;

(c) differentiating the mathematical expression for scour-hole volume in order to obtain a mathematical equation for the time rate of change of scour-hole volume;

(d) formulating a volume rate function for sediment being transported out of the hole using experimentally determined results;

(e) formulating volume rate functions for sediment being transported into the hole from the surrounding bed;

(f) combining the volume-rate functions of steps (c), (d), and (e) into a differential equation using the principle of conservation of mass; and

(g) integrating the differential equation of step (f) in order to obtain the desired settlement-time function.

In the earlier work 3/, the rate of sediment transport into the scour hole from the surrounding bed, step (e), was omitted. One of the principal objectives of this report is to present a more complete and rational analysis by correcting the earlier omission.

II. BED FORMS

One objective of this analysis is to formulate a rational transport function for the rate that sediment is transported into the scour hole from the surrounding bed. Unfortunately not one but three distinct transport functions are required inasmuch as bed-form geometry is characterized by four distinct stages. The successive stages of bed-form development with increasing velocity are as follows: (a) No movement of bed material, (b) two-dimensional dunes, (c) three-dimensional dunes, and (d) flat bed with sediment transport. Since the bed has a different geometric configuration in each of the stages of development, different sediment transport functions exist in each stage in which transport occurs, that is, stages (b), (c), and (d). The formulation of these sediment-transport functions is discussed in Chapter VI. In this chapter the four different stages of bed-form development are discussed with particular attention being given to the limits of each stage.

A. No Movement of Bed Material

The upper limit of a stationary bed is defined by the initial-motion condition or the incipient-motion condition. The incipient-motion condition is traditionally defined as the flow condition at which an appreciable number of particles lying on the surface of a flat bed are in motion. Flat-bed incipient motion is traditionally expressed in terms of the value of the Shields parameter which is a function of a Reynolds number using the shear velocity as the velocity term as follows.

$$\frac{\tau_o}{(s-1)\gamma D_g} = f\left(\frac{D_g \sqrt{\tau_o/\rho}}{\nu} \right) \qquad (1)$$

in which τ_o is the boundary-shear stress, ϱ is the fluid density (mass), and ν is the kinematic viscosity of the fluid. Vanoni 4/ has recently published a thorough discussion of flat-bed incipient motion including an excellent bibliography containing thirty-four entries. For flow over a hydraulically rough boundary, the value of $\tau_o/(s-1)\gamma D_g$ has a critical value of about 0.06.

An alternative analysis is to analyze the stability of protruding surface grains by considering the hydrodynamic surface forces (lift and drag) and the gravity force (submerged weight) on a typical protruding surface grain 5/. Using the force analysis with experimental results for evaluation of constants, the writer has proposed the following criterion at initial motion

$$\frac{u_i^2}{(s-1)g\ D_g} = \left[\frac{\tan \phi \cos \alpha + \sin \alpha}{1 + \tan \phi} \right] \frac{8.2}{C_D} \qquad (2)$$

in which u_i is the fluid velocity at particle level, α is the angle of the bed from the horizontal in the direction of flow, and C_D is the coefficient of drag of the sand grains falling in an infinite fluid. Values of C_D for sand grains with a shape factor of 0.7 are given by Albertson, Barton, and Simons 6/. Advantages of the force analysis, culminating in Equation 2, are (a) the inclusion of the bed slope, α, and (b) the inclusion of particle angularity as reflected in the value of the angle of repose, ϕ, and the coefficient of drag, C_D.

1. Flat-Bed, Incipient-Motion Condition

Force analysis, Equation 2, can be utilized for the prediction of the flat-bed, incipient-motion condition for oscillatory flow with a laminar boundary layer. For a flat bed, the value of α is zero in Equation 2. The velocity distribution 7/ is given by the following expression

$$\frac{u}{U_m} = \sin \frac{2\pi t}{T} - e^{-y\sqrt{\pi/\nu T}} \sin\left(\frac{2\pi t}{T} - y\sqrt{\frac{\pi}{\nu T}}\right) \qquad (3)$$

in which u is the velocity at a distance y above the bed, T is the period of the simple-harmonic oscillatory flow, t is time and ν is the kinematic viscosity. By determining the velocity, u_i, in Equation 2 from Equation 3, u can be eliminated resulting in a solution for the flat-bed, incipient-motion condition in terms of a critical sediment number, N_{sc}.

The maximum velocity, u_{max}, during a cycle can be determined from Equation 3 for use in Equation 2. The maximum velocity occurs when

$$\tan \frac{2\pi t}{T} = \frac{e^{y\sqrt{\pi/\nu T}} - \cos y\sqrt{\pi/\nu T}}{\sin y\sqrt{\pi/\nu T}} \qquad (4)$$

The vertical distance y above the bed level at which u_{max} should be determined must be evaluated from experimental results. Flat-bed, incipient-motion experiments have been performed in the oscillatory-flow water tunnel with three different sands. Amplitude of the water motion was gradually increased until some of the surface grains were rolling back and forth. The results of these subjective experiments are shown in Table IV.

TABLE IV

EXPERIMENTALLY DETERMINED VALUES OF THE OSCILLATORY-FLOW, FLAT-BED, INCIPIENT-MOTION CONDITION

D_g (mm)	σ_g	s	Water Temp. (°F)	T (sec)	N_{sc} Measured	N_{sc} Computed
0.190	1.32	2.62	69.5	3.57	4.69	4.15
0.297	1.06	2.47	67	3.56	3.77	3.74
0.585	1.16	2.62	72	3.58	3.02	2.96

Values of N_{sc} were computed using y as 0.6 D_g in Equation 3 in order to determine N_{sc} from Equation 2. Considering the subjective nature of incipient-motion tests, the agreement between the measured values and the computed values is reasonable. Certainly the trend of the variation of N_{sc} with D_g is correctly predicted by Equations 2 and 3.

Values of the critical sediment number, N_{sc}, for the flat-bed, incipient-motion condition for oscillatory flow with a laminar boundary layer were computed using Equations 2 and 3. Computed values are shown as the upper three curves in Figure 4. The velocity was evaluated at a vertical distance y of 0.6 D_g. The water temperature was taken as being 60 degrees Fahrenheit. The bed material was assumed to have a shape factor, s.f., of 0.7. Curves were computed for first-order Stokian waves having periods of 3, 6, and 9 seconds.

2. Deformed-Bed, Incipient-Motion Condition

A deformed-bed, incipient-motion condition occurs on a previously duned bed or when a flow disturbance is placed on the bed. If a flow disturbance is placed on the bed under oscillatory flow, a dune system will propagate outward from the disturbance. Propagation of a dune system from a disturbance is accomplished by the formation of a new dune beyond the last one formed. The formation of a new dune appears to occur when the previously formed dune attains sufficient amplitude. In other words each new dune acts as a flow disturbance resulting in the formation of yet another dune.

The effect of a flow disturbance is to create a non-uniform flow zone adjacent to the bed. In a region of acceleration, such as on the upstream face of a dune, boundary layers can be expected to be of negligible thickness. The velocity at bed level will be much higher than that predicted from Equation 3. On the basis of tests in the oscillatory-flow water tunnel, the velocity at the

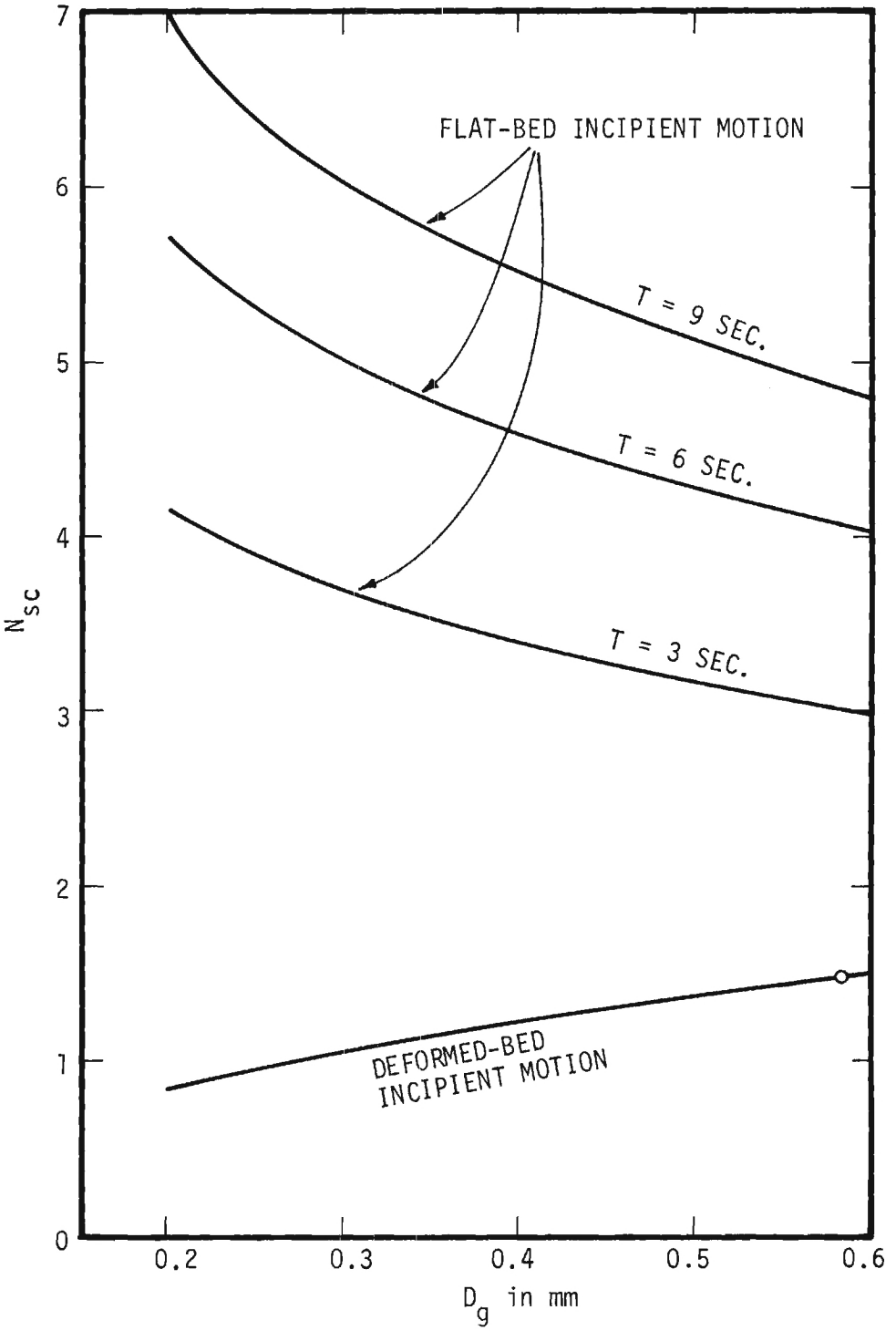

Figure 4. N_{sc} at Incipient Motion for Oscillatory Flow (Water at 60°F, s.f. = 0.7).

crest of a dune appears to be about 1.2 U_m [5,8,9]. At the crest of a dune, the angle α at the bed is about equal to the angle of repose, ϕ, of the bed material. By substituting 1.2 U_m for u_i and ϕ for α in Equation 2 an expression for N_{sc} at the deformed-bed, incipient-motion condition is obtained as follows,

$$N_{sc} = \left(\frac{2 \sin \phi}{1 + \tan \phi} \right) \frac{5.7}{C_D} \qquad (5)$$

Values of the critical sediment number, N_{sc} for the deformed-bed, incipient-motion condition with oscillatory flow over a duned bed were computed using Equation 5. Computed values are shown as the lowest curve in Figure 4. The water temperature was taken as being 60 degrees Fahrenheit. The bed material was assumed to have a shape factor, s.f., of 0.7. Wave period is immaterial. The one experimentally determined value shown in Figure 4 for the lower limit of dune propagation from a flow disturbance was obtained with the 0.585-mm Ottawa sand [5,9].

B. Two-Dimensional Dunes

1. Oscillatory Flow

If the value of N_s is less than approximately 6.5, the dune system is two-dimensional. The crests of the dunes are unbroken and are essentially constant in elevation. The crests of the dunes are perpendicular to the direction of the water motion at bed level. The fluid motion is two-dimensional with line vortices being formed in the lee of the dune crests. Two vortices are formed each cycle in the trough between a pair of adjacent crests. On reversal of motion the previously formed vortex is moved back toward the crest on which it was formed and is ejected into the main flow above the dune system. Being a symmetrical and cyclic motion, the dunes are essentially symmetrical

with the crests moving slightly back and forth as scour and deposition occur alternately on each side of the crest.

Geometry of equilibrium dunes has been determined in the oscillating-flow water tunnel 10/ using the 0.297-mm glass beads and the 0.585-mm Ottawa sand (Table I). Dune geometry was determined from photographs as shown in Figure 5. Coordinate scales were marked on the test-section wall as a means of scaling the dunes.

Amplitude of the dunes as a function of N_s is shown in Figure 6. On the extreme left of Figure 6, the limit labelled "no movement" is the deformed-bed incipient-motion condition as shown in Figure 4. At somewhat higher values of N_s, a dune system can be induced to form by placing an obstruction on the bed. With values of N_s slightly greater than the flat-bed, incipient-motion condition (Table IV) a dune system will develop spontaneously without a flow disturbance on the bed. The geometry of the equilibrium dune system does not appear to be a function of the manner in which that system is generated. In the range of two-dimensional dunes, dune amplitude is proportional to the value of N_s as shown in Figure 6.

The ratio of the amplitude-to-wave length of the dunes as a function of N_s is shown in Figure 7. The ratio, η/λ, is approximately constant for two-dimensional dunes, that for $N_s \leq 6.5$. The value of η/λ is about 0.18 for the 0.297-mm glass beads and is about 0.19 for the 0.585-mm Ottawa sand. The difference is probably the result of the larger angle of repose, ϕ, for the Ottawa sand. For example, if the trough of a dune were a circular arc with termini at the crests making angles with the bed of ϕ, the material with the larger angle of repose would obviously have a larger ratio of η/λ. However, the important point is that two-dimensional dunes are geometrically similar

Figure 5. Photograph of Two-dimensional Dunes.

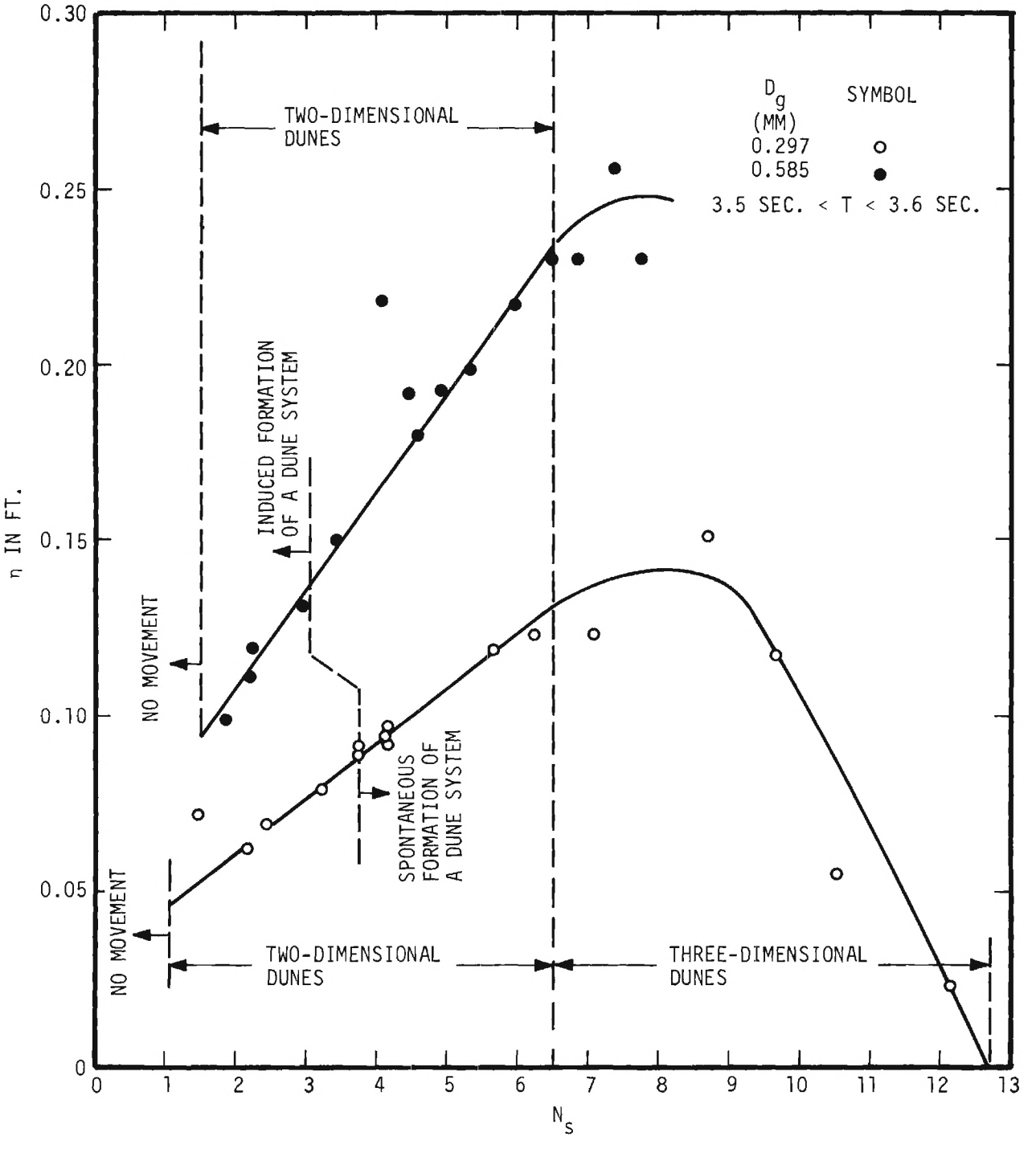

Figure 6. Dune Amplitude (Oscillatory Flow).

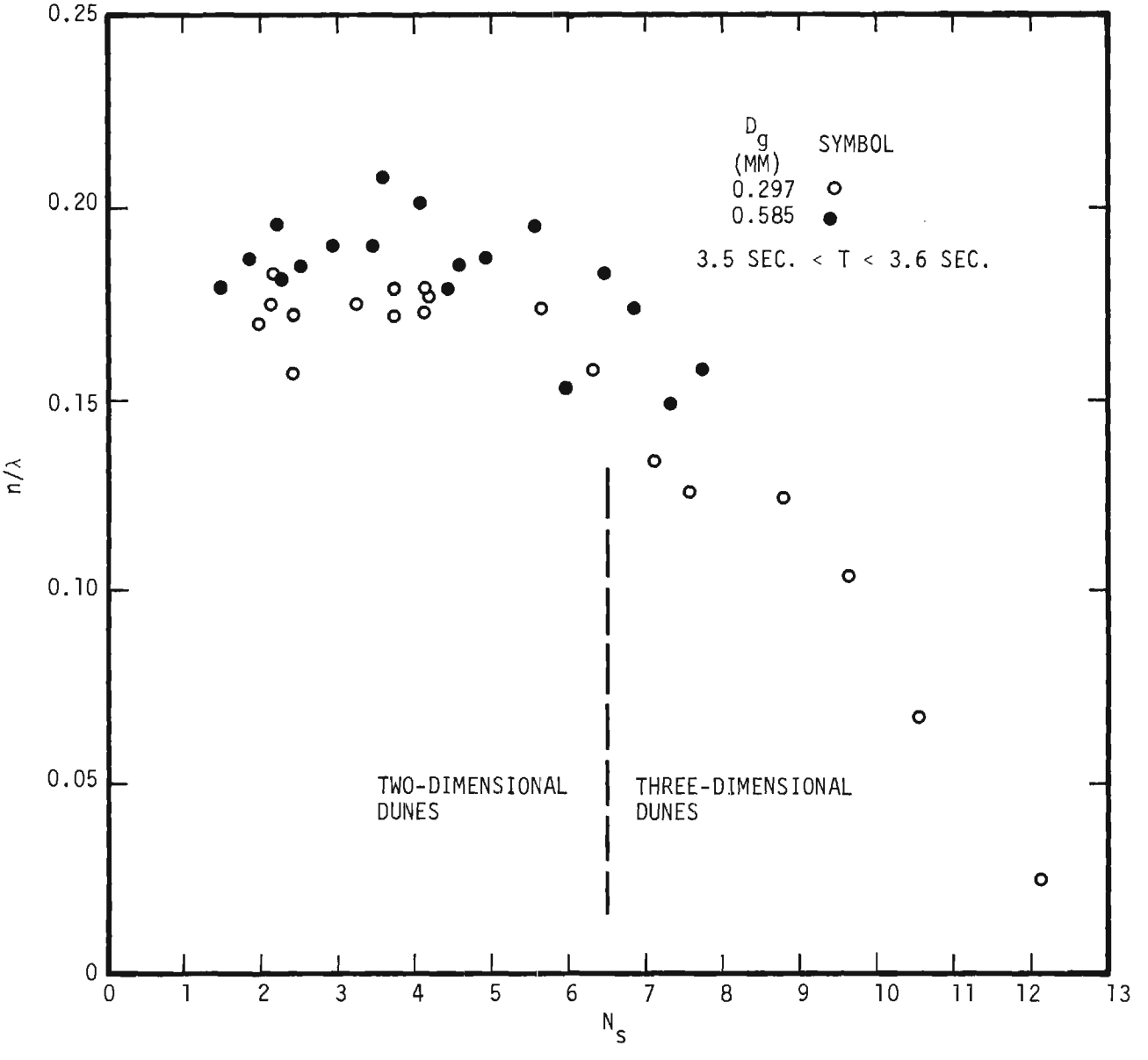

Figure 7. Ratio of Dune Amplitude to Wave Length (Oscillatory Flow).

as evidenced by the constancy of η/λ for values of N_s less than 6.5.

2. Unidirectional Flow

The dune systems of unidirectional flow are in some respects quite similar to those of oscillatory flow even though the shape of a dune is quite different. Similarity in regard to dune amplitude, η, as a function of N_s is shown by comparison of Figure 6 and Figure 8. Figure 8 was prepared from the data of Stein 11/. Stein's experiments were conducted in a 4-ft wide flume having a length of 100 ft. The bed material was sand having a mean diameter, D_g, of 0.40 mm and a geometric standard deviation, σ_g, of 1.50. The data shown in Figure 8 are from runs in which the depth of flow, y_o, was essentially constant, that is, 0.98 ft $< y_o <$ 1.02 ft. The mean velocity is used in computing the value of N_s. The linear variation of η with N_s is apparent in Figure 8. This characteristic was found with two-dimensional dunes in oscillatory flow. The boundary-drag coefficient of the bed, f_b, is shown in Figure 9. The maximum η, Figure 8, occurs at a larger value of N_s than the maximum value of f_b. Since the boundary-drag is primarily form drag of dunes, the change in f_b is indicative of a change in the dune geometry. The writer believes that this change in dune geometry of unidirectional flow is probably the same change that was observed in oscillatory flow, that is, a transition from two-dimensional dunes to three-dimensional dunes.

Graphs similar to Figures 8 and 9 of other experimental results were prepared in order to determine the upper limit of the region of two-dimensional dunes. Values of N_s near the limits of the various regions of bed geometry are listed in Table V.

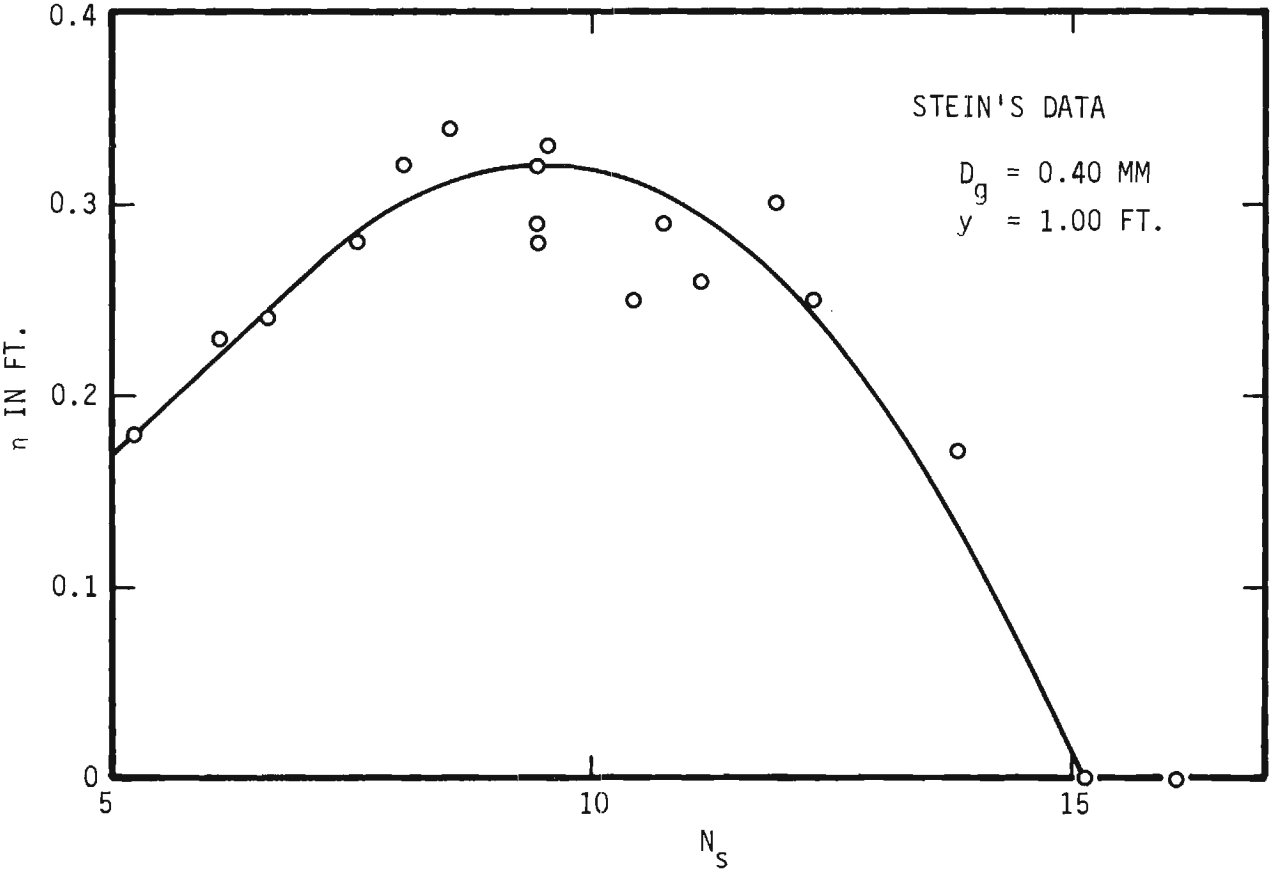

Figure 8. Dune Amplitude (Unidirectional Flow).

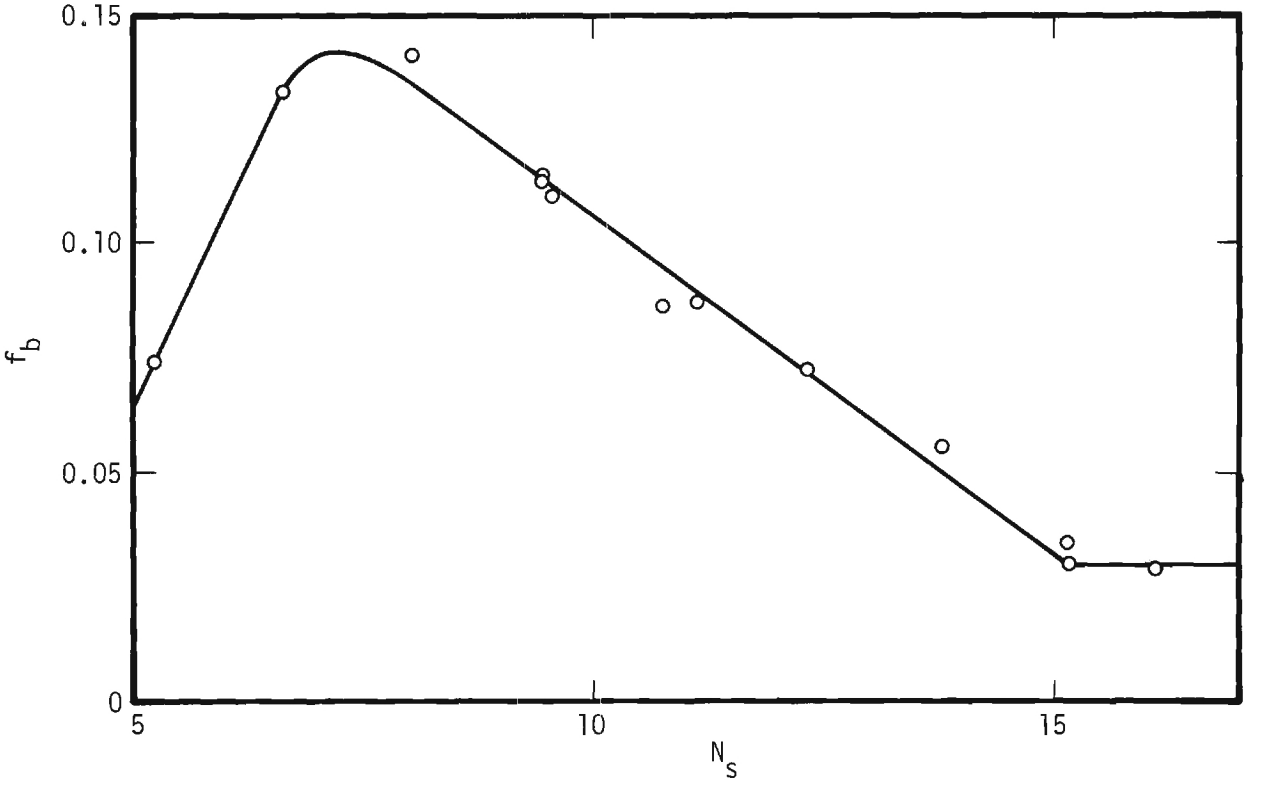

Figure 9. Boundary-drag Coefficient (Unidirectional Flow).

TABLE V

VALUES OF N_S WHICH DEFINE
BED GEOMETRY IN UNIDIRECTIONAL FLOW

Reference	D_g (mm)	σ_g	y_o (ft)	2-dim. to 3-dim. From f_b	2-dim. to 3-dim. From η	3 dim. to flat From f_b	3 dim. to flat From η
11/	0.40	1.50	1.00	6.8	8.0	15.2	15.2
	0.40	1.50	0.80	7.0	7.5	15.4	15.4
	0.40	1.50	0.60	6.0	7.7	12.8	13.4
	0.40	1.50	0.30	6.3	6.4	13.5	11.6
12/	0.152	1.76	0.24	<4.9	-	11.6	-
	0.137	1.38	0.24	6.2	-	12.0	-
	0.137	1.38	0.54	7.7	-	12.4	-
13/	0.142	1.38	0.23	-	-	13.5	-

The upper limit of two-dimensional dunes appears to occur at a value of N_s of 6.5 in unidirectional flow. The lower limit of two-dimensional dunes can not be determined from the experimental results used in compiling Table V 11,12,13/. Nevertheless, both the flat-bed incipient-motion condition and the deformed-bed, incipient-motion condition must exist.

C. Three-Dimensional Dunes

1. Oscillatory Flow

If the value of N_s is greater than approximately 6.5 the flow pattern is no longer two-dimensional. The breakdown of the two-dimensional dune system is progressive. If N_s is greater than 9 the dunes are sand hills with valleys both across and along the bed as shown in Figure 10. If N_s is greater than 10, the entire surface of the bed is in motion resembling a second fluid under the water.

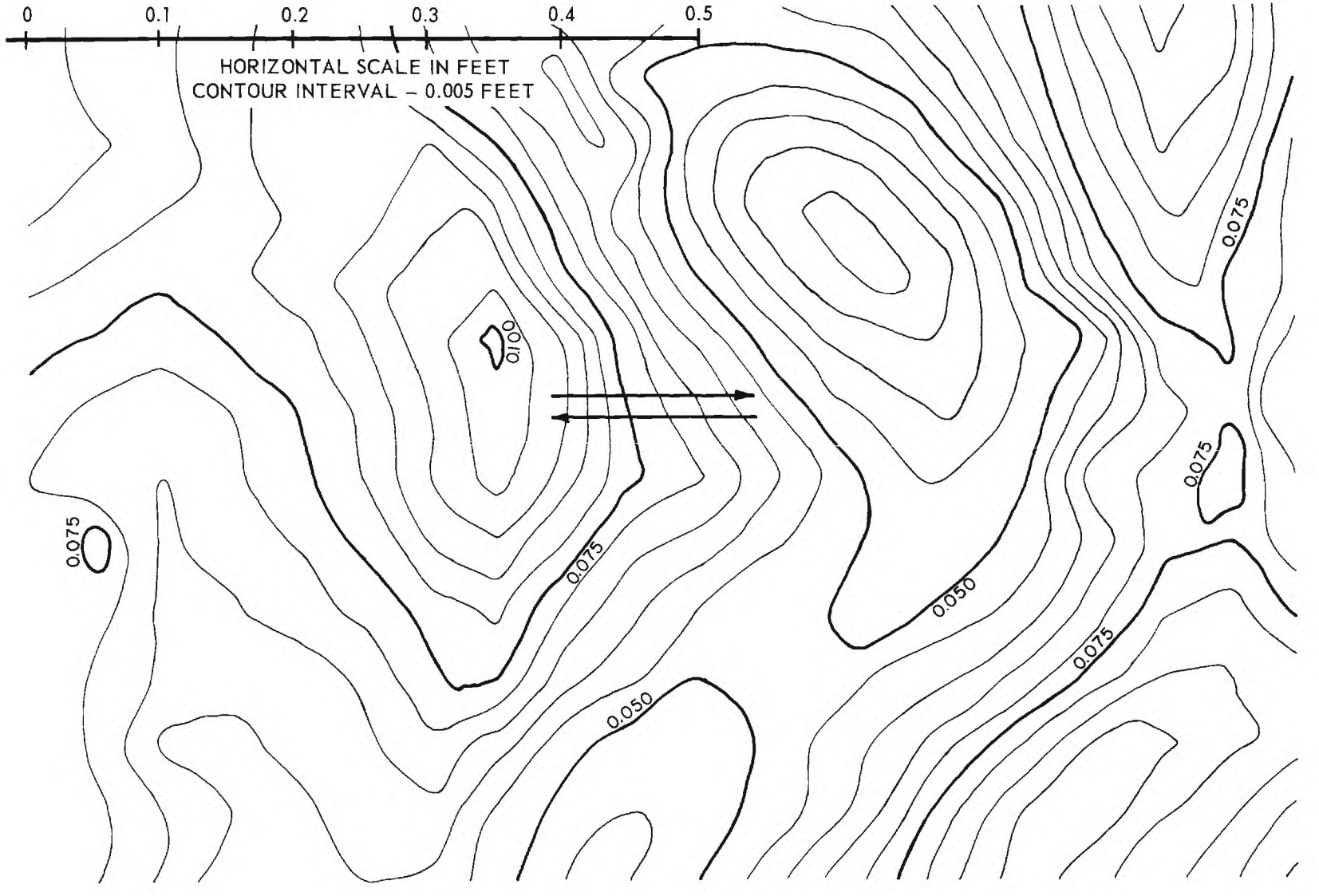

Figure 10. Topographic Map of Three-dimensional Dunes (N_s = 10.5).

The lower limit of the region of three-dimensional dunes is at an N_s value of 6.5. An observer has difficulty in precisely defining the limit between two-dimensional and three-dimensional dunes. The ratio of dune amplitude to wave length, η/λ, as shown in Figure 7 is a more sensitive measure of the change in dune geometry.

The upper limit of the region of three-dimensional dunes is a flat bed. As shown in Figures 6 and 7, the transition to flat bed occurred when N_s was 12.7 with the 0.297-mm glass beads. Because of a water-motion-amplitude limit of the oscillatory-flow water tunnel, the upper limit of the region of three-dimensional dunes could not be determined for the 0.585-mm bed material.

The important point is that three-dimensional dunes are not geometrically similar as evidenced by the decrease of η/λ with increasing values of N_s as shown in Figure 7.

2. Unidirectional Flow

The limits of the region of three-dimensional dunes for unidirectional flow are shown in Table V. The method of determining these limits from experimental results is shown in Figures 8 and 9. The lower limit was estimated to be 6.5 (II.B.2). The upper limit appears to be in the range $12 < N_s < 15$. The upper limit is in agreement with the value of 13 obtained from the oscillatory-flow experiments.

III. CONTINUITY EQUATION FOR SEDIMENT

The differential equation for cylinder settlement is based upon the principle of conservation of mass. The mass under consideration is the mass of sand removed from the scour hole. Since the cylinder settles into a scour hole which is enlarging with time, the rate form of the basic equation is required. For convenience a volume-rate equation is utilized rather than a mass-rate equation. A word statement of the transport equation is that the difference in the volume rate of excavation from the scour hole, Q_{so}, and in the volume rate of transport into the hole from the surrounding bed, Q_{si}, is equal to the time rate of change of scour-hole volume, $d\forall/dt$, or

$$Q_{so} - Q_{si} = d\forall/dt \tag{6}$$

In the following analysis, the assumption is made that the two transport processes involving (a) transport from the hole by localized scour and (b) transport into the hole from the surrounding bed are independent and that the net rate of transport is the sum of the two independent processes.

Since the flow conditions were constant during each model test and since Q_{so}, Q_{si}, and $\forall$ are functions of scour depth, S, Equation 6 is separable and integrable as follows

$$t = \int_0^S \frac{d\forall}{Q_{so} - Q_{si}} \tag{7}$$

with the initial condition that $S = 0$ when $t = 0$.

IV. THE SCOUR HOLE

Scour occurs at the ends of the cylinder forming a scour hole shown in Figure 1. Figure 11 is a topographic map of a typical scour hole. The scour hole is closely approximated by an inverted frustum of a right circular cone. The lower diameter is L + 0.24D. The side slope of the cone is the angle of repose, ϕ, of the bed material. The upper diameter of the frustum which is the width of the scour hole, B, is L + 0.24D + 2S cot ϕ.

The volume, $\forall$, of the scour hole is closely approximated as follows,

$$\forall = \frac{\pi}{3}\left[S^3 \cot^2 \phi + 1.5(L + 0.24D)S^2 \cot \phi + 0.25 (L + 0.24D)^2 S\right] \qquad (8)$$

The change in volume, $d\forall$, for use in Equation 6 is as follows,

$$d\forall = \pi D^3 \left[\left(\frac{S}{D}\right)^2 \cot^2\phi + \left(\frac{L}{D} + 0.24\right)\left(\frac{S}{D}\right) \cot \phi + \frac{1}{4}\left(\frac{L}{D} + 0.24\right)^2\right] d\left(\frac{S}{D}\right) \qquad (9)$$

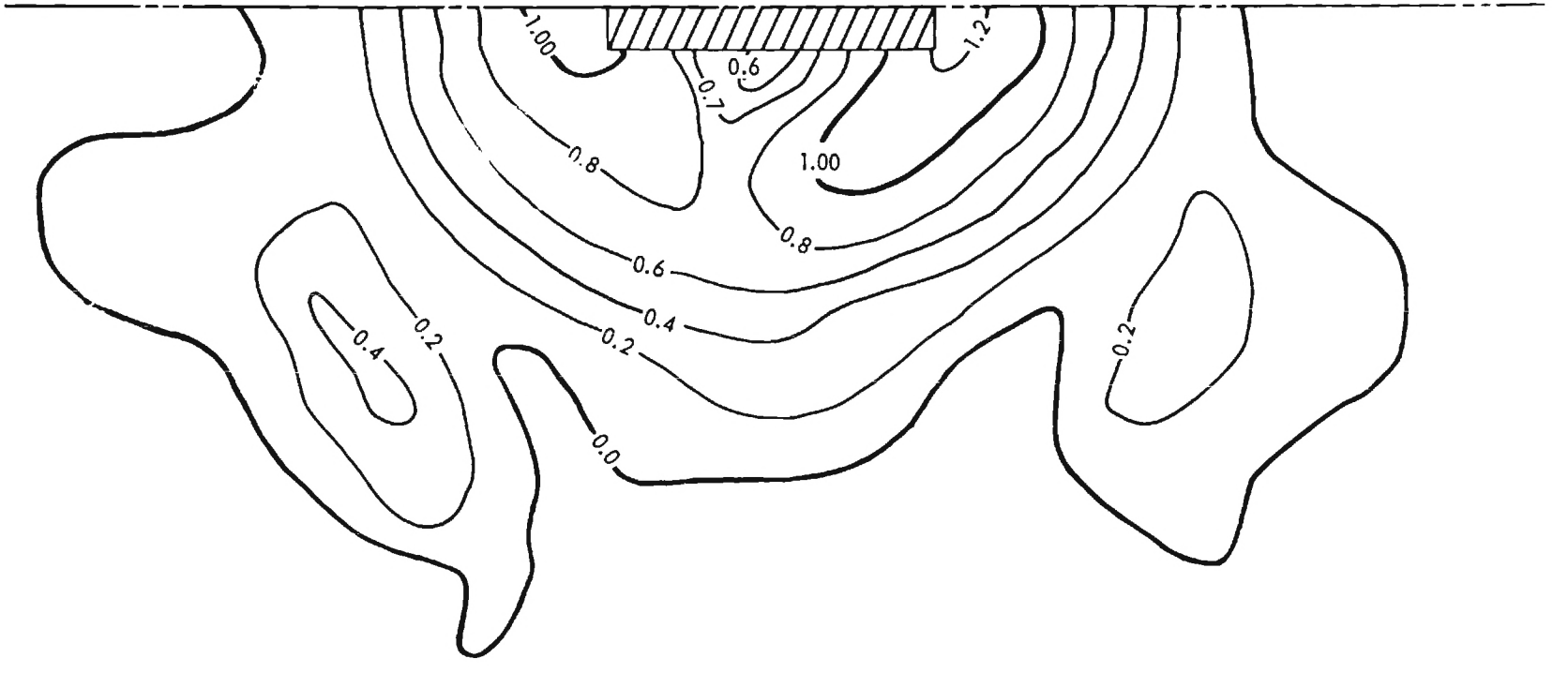

Figure 11. Topographic Map of a Typical Scour Hole (Contours in -D Units).

V. OUTPUT SEDIMENT-TRANSPORT FUNCTION

The formulation of an output sediment-transport function for the rate of transport out of the scour hole, Q_{so}, as a function of the sediment number, N_s, could not be determined from the model tests inasmuch as the presence of dunes influenced the flow pattern in the range of N_s from about 4 to about 9.5. As a consequence, data were obtained at values of N_s of about 2.8 and about 11.4 as shown in Table II. Furthermore, tests at the higher value of N_s are not similar to the tests at the lower. The dissimilarity is that the sediment-transport rate into the scour hole, Q_{si}, from the surrounding bed is insignificant when N_s is 2.8 but is significant when N_s is 11.5. This fundamental difference was <u>not</u> recognized in prior analysis 3/.

The mass-transport equation, Equation 7, is used to evaluate the output sediment-transport function. In order to evaluate Q_{so} from equation 7 only the model tests for which Q_{si} is zero could be utilized. Sediment transport into the scour hole was insignificant for Model Tests 24-39 (Table II), inclusive, for which the value of N_s was 2.8. Using the smallest model (D = 0.501 in.), localized scour around the model would occur without the formation of a dune system. In contrast, Model Test 31 (Table II) with the 1.002-in.-diameter cylinder had to be stopped because of the dune system which formed around the model. Another difficulty was that the smallest cylinder tended to tip as the cylinder settled into the bed. Tipping was negligible in all tests with the larger cylinders. Because of uneven settlement or tipping, only Model Test 39 (Table II) was judged to be representative of cylinder settlement.

In order to formulate an output sediment-transport function, Q_{so}, the work of others had to be utilized. Experimental studies were sought (a) in which Q_{si} was zero and (b) in which dunes did not influence the flow pattern in the scour hole. Scour holes resulting from two-dimensional jets were studied by Rouse[14] and Laursen[15]. Rouse's experiments involved a jet which flowed down a plane wall onto an initially flat bed of sand. Laursen's experiments involved a jet which flowed over an initially flat bed. The development of the scour holes was recorded from optical measurements. Both performed experiments with three sizes of sand and throughout a wide range of jet velocities. The writer reanalyzed the results of these two experiments and concluded that the sediment-transport rate out of the scour hole was proportional to N_s raised to the eighth or ninth power.

The problem in utilizing these experiments was that the flow situation was unsteady since the scour hole was enlarging with time. Two difficulties resulted from the unsteadiness. First the rate of change of scour-hole depth, dS/dt, had to be determined from experimentally determined graphs of S as a function of t in order to calculate Q_{so}. Second since the flow pattern is different at every value of scour depth, S, Q_{so} as a function of N_s had to be evaluated at constant values of S. Upon becoming aware of the lack of and the desirability of steady-state scour study, the writer pointed out this deficiency to one of his students.

Le Feuvre[16] studied sediment transport from a scour hole of fixed geometry. The top of the scour hole was the opening formed by the junction of a 2-in.-diameter, vertical, transparent, plastic pipe with the bottom of the horizontal, main-flow section which was a 3-in.-diameter, transparent, plastic pipe. A machined plastic wedge was fastened inside the vertical pipe forming a defined

scour hole with a sloping (60°) upstream face and with vertical sidewalls. Sediment was forced up into the bottom of the scour hole by means of a piston that was moved upward at a uniform rate by a system of gears powered by a synchronous motor. Using various combination of gears, the sediment-feed rate could be varied over a hundredfold range in finite increments. During a run, the water discharge through the main-flow section was adjusted by means of a downstream pinch valve until the horizontally oriented vortex within the scour hole could pick up and could transport the sediment being forced at a uniform rate into the bottom of the scour hole. In all runs the water discharge was adjusted until the sediment bed was stabilized at the same equilibrium level as noted on a reference mark on the vertical transparent pipe. A total of 148 runs was made involving variation of sediment-transport rate, Q_{so}, and using six different sediments. The properties of the particulate material used by Le Feuvre is given in Table VI.

TABLE VI.

PROPERTIES OF SEDIMENT USED BY LE FEUVRE 16/

Sediment	Material	Specific Gravity	D_g (mm)	Geometric Standard Deviation
1	Nickel	8.75	0.570	1.10
2	Sand	2.62	0.585	1.16
3	Sand	2.63	0.185	1.24
4	Glass	2.47	0.297	1.06
5	Glass	2.46	0.106	1.05
6	Lucite	1.20	0.250	1.31

Le Feuvre's data 16/ were considered to be of sufficient accuracy to permit the formulation of an empirical sediment-transport function for Q_{so}. In Le Feuvre's experiments the sediment discharge, Q_{so}, was very accurately determined since the value of Q_{so} was simply the product of the upward velocity of the piston and the cross-sectional area of the one-inch diameter, copper, water tube in which the piston was placed. Furthermore these experiments were ideal in that (a) dunes were nonexistent; (b) no sediment was transported into the scour hole from upstream; and (c) the scour-hole was invariant both in geometry and time. The writer discarded the fluid viscosity and the sediment density (mass) prior to attempting a correlation of the data. The fluid viscosity was discarded as a significant variable on the basis that localized scour, occurs in non-uniform flow regions where laminar boundary layers or sublayers are not developed. The mass density of the sediment was omitted on the basis that the inertial reaction of the sediment grains was negligible in relation to the submerged weight and the fluid-induced surface forces (lift and drag). Reasonable correlation of LeFeuvre's results was found with two parameters, that is,

$$\frac{Q_{so}}{D_1 D_g \sqrt{(s-1)g\, D_g}} \propto N_s^{\,4} \left\{ 1 - \left(\frac{N_{sc}}{N_s} \right)^2 \right\}^4 \qquad (10)$$

as shown in Figure 12. In Equation 10 the critical sediment number, N_{sc}, is the value of N_s at zero sediment transport. Le Feuvre determined the value of N_{sc} experimentally for each of the six sediments. The length term, D_1, on the left side of Equation 10 is the width of the scour hole (2 inches). A length term was required for dimensional homogeneity but not for data correlation. The writer reasoned that the length term must be proportional to the size of the

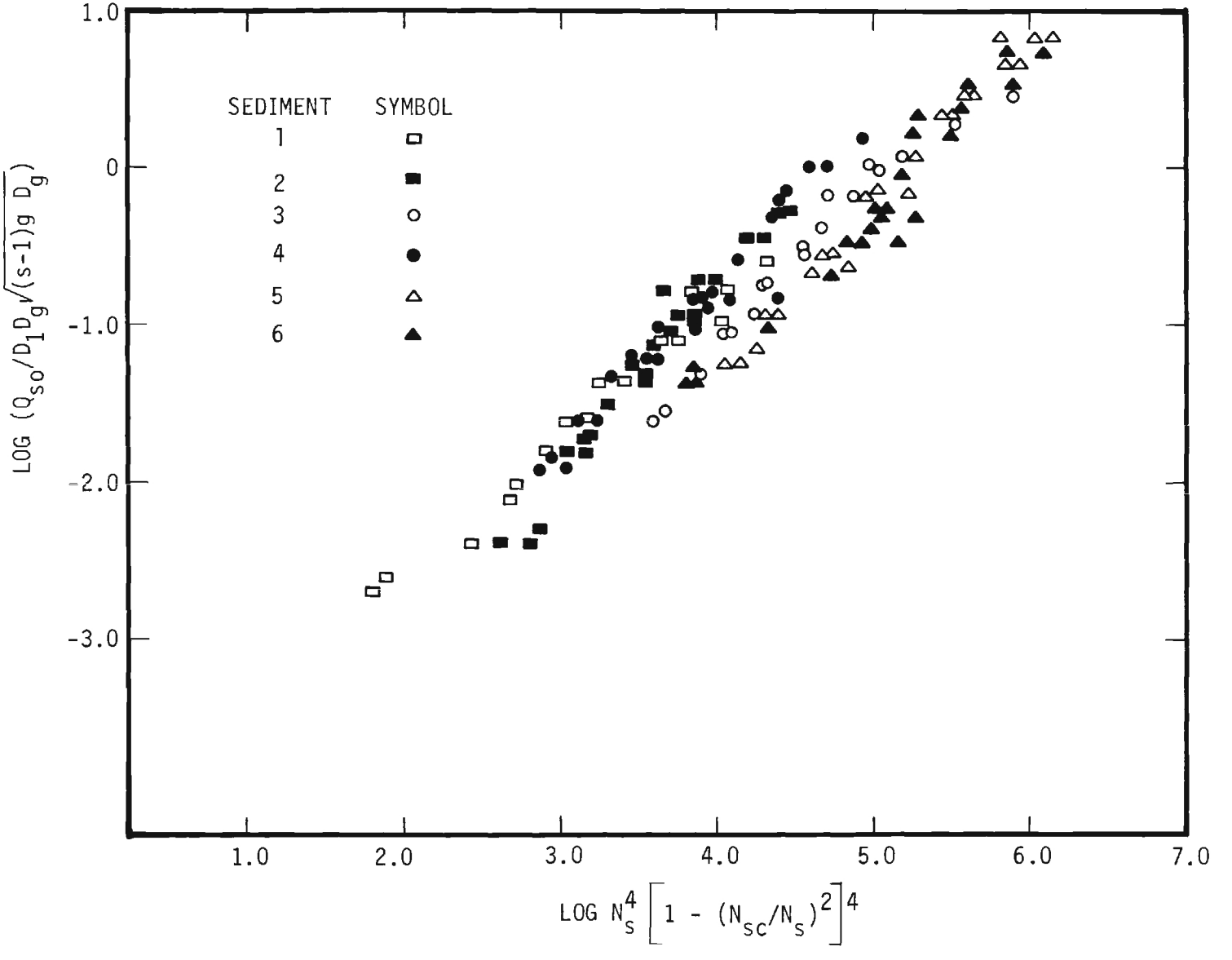

Figure 12. LeFeuvrés Data 16/ for Sediment Transport.

vortex which scoured the particles from the bed. Since the vortex size and geometry were constant, any length term of the vortex could be used. For cylinder burial, the logical length term would be the cylinder diameter, D, which determines the scale of the flow pattern around the ends of the cylinder where localized scour occurs.

Because of the fundamental similarity of all localized-scouring situations, the arrangement of the variables as given in Equation 10 can be expected to be quite general even though values of N_{sc} and the constant of proportionality will differ from one localized-scour situation to another depending upon the obstruction geometry, reference velocity used in evaluating N_s, and length term representing the scale of the flow pattern. The output sediment-transport function for Q_{so} to be used in Equation 7 can be formulated as

$$Q_{so} = D\, D_g \sqrt{(s-1)g\, D_g}\; N_s^4 \left\{1 - \left(\frac{N_{sc}}{N_s}\right)^2\right\}^4 \left\{f\left(\frac{S}{D}\right)\right\} \qquad (11)$$

Since the scour-hole size changes in relation to the cylinder with depth of scour, S, the function, f(S/D) is required in Equation 11.

Model Test 41 (1964-1965 series) was performed for the specific purpose of determining the critical sediment number, N_{sc}. The bed material was the 0.297-mm glass beads. The cylinder was the 1.702-in.-diameter cylinder. The bed was initially flattened. The cylinder was carefully lowered onto the bed. The run was performed by increasing the water-motion amplitude in small increments until particle movement was observed at the ends of the cylinder. A few particles were observed to move with a total water-motion amplitude of 3.12 inches. The corresponding value of the sediment number is 1.07. This value is only slightly larger than the value, 1.04, for the deformed-bed

incipient-motion condition as shown in Figure 4. On the basis of this measurement, the value of N_{sc} for flow around a cylinder is taken to be the same as the value of N_{sc} at incipient motion with a deformed bed as given by Equation 5 and shown in Figure 4. Hence the values of N_{sc} to be used in Equation 10 are 1.04 for the 0.297-mm glass beads and 1.49 for the 0.585 mm Ottawa sand.

Settlement-time data of Model Test 39 (1962-1963 series) are shown in Figure 13. The time scale is number of cycles from the beginning of the test. The data points designated by the open circles are settlement at one end of the cylinder and the solid circles are for the other end. Some tipping occurred throughout the test but subsequent scour relevelled the cylinder until about 250 cycles when tipping became excessive. As mentioned previously Model Test 39 was the best test with the smallest cylinder from the standpoint of tipping. For this reason the data of Model Test 39 were used to determine the function, f (S/D), in Equation 10.

The output sediment-transport function was determined by substituting Equation 11 into Equation 7 and integrating. Since Q_{si} is zero for Model Test 39 the integral is an elementary integral if f (S/D) is assumed to be proportional to a power of S/D. The integral of Equation 7 after substitution of Equations 9 and 11 is a settlement-time function. The function f (S/D) was systematically varied until the integral of Equation 7 matched the experimentally determined settlement function. The continuous curve shown in Figure 13 was deemed to be a satisfactory fit to the measured settlement function. The continuous curve of Figure 13 was obtained by using

$$f\ (S/D) = 2.38(10^{-3})/(S/D) \qquad (12)$$

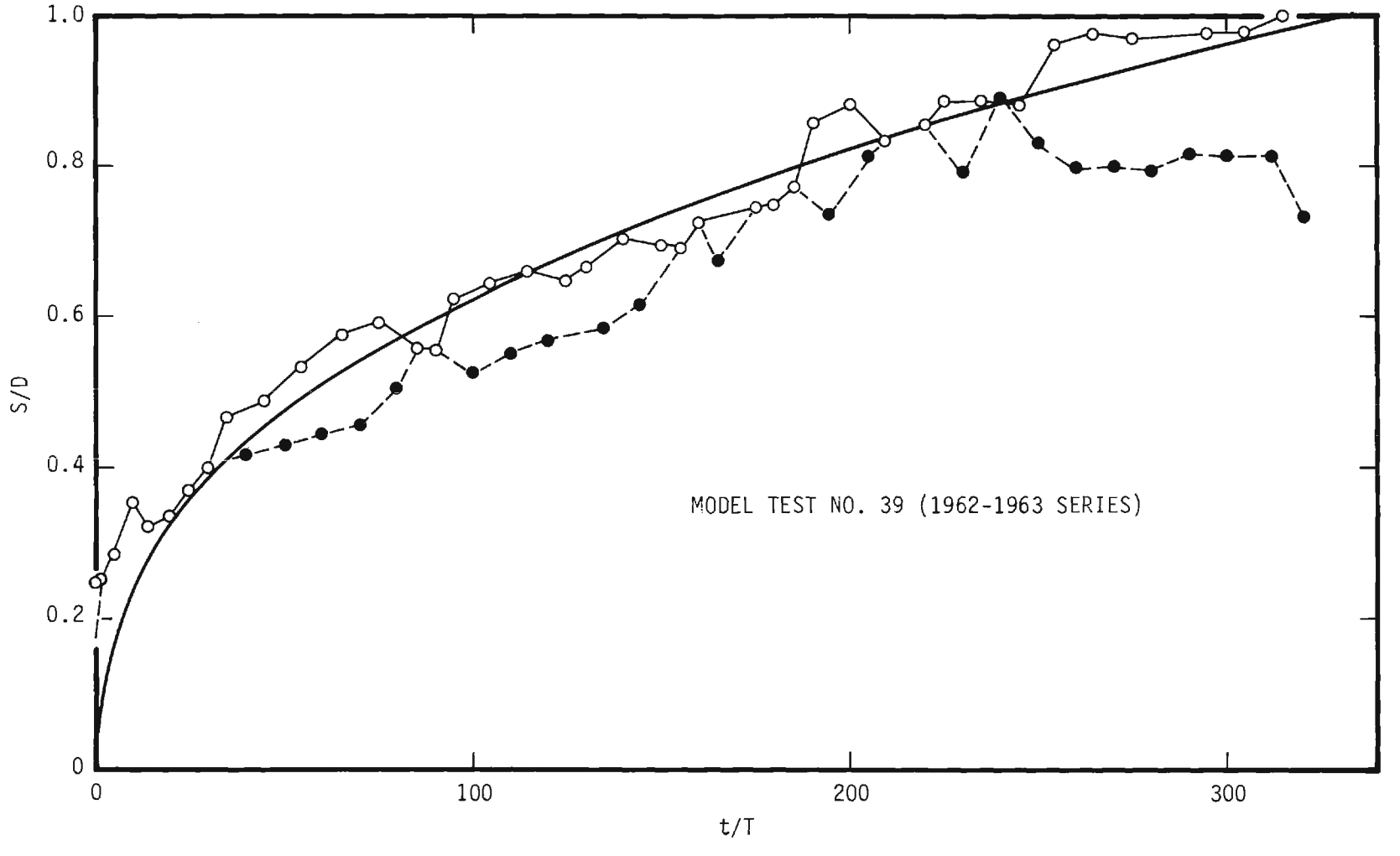

Figure 13. Settlement Versus Time of Model Test 39 (1962-1963 Series).

in Equation 7. Thus the output sediment-transport function to be utilized in subsequent integrations of Equation 7 is as follows

$$Q_{so} = 2.38(10^{-3})\ D\ D_g \sqrt{(s-1)g\,D_g}\ N_s^{\,4} \left\{1-\left(\frac{N_{sc}}{N_s}\right)^2\right\}^4 \left(\frac{S}{D}\right)^{-1} \qquad (12)$$

VI. INPUT SEDIMENT-TRANSPORT FUNCTIONS

The formulation of input sediment-transport functions for the rate that sediment is transported into a scour hole, of necessity, must be based upon the transport functions which are experimentally determined for unidirectional flow. The net rate of sediment transport is zero with oscillatory flow over a homogeneous bed. A scour hole is a discontinuity in an otherwise homogeneous bed. Natural processes of scour and deposition tend to eliminate the inhomogeneous area - the scour hole. Either the bed must be inhomogeneous or the water-motion must be asymmetric for a net transport of sediment to occur with oscillatory flow. Manohar 17/ performed some experiments with asymmetric water oscillation in which sediment transport was measured. Asymmetrical motion was achieved by making different time durations in each half cycle. Apparently no experiments have been performed with oscillatory flow which involve sediment transport into an inhomogeneous area of the bed, such as into a hole. In view of this deficiency of experimental information and in view of the similarity of bed-form characteristics as demonstrated in Chapter II, experiments involving sediment transport with unidirectional flow will be used as a guide in formulating input sediment-transport functions for oscillatory flow.

A. Transport Functions of Unidirectional Flow

As a guide to the formulation of input sediment-transport functions, the experimental results of Stein 11/ were chosen because of the care with which the experiments were performed. Using LeFeuvre's results 16/ as a model for correlation, Stein's results are shown in Figure 14.

A shown in Chapter II, two-dimensional dunes are geometrically similar. For geometrically similar flow situations, the transport function, Equation 10, by which LeFeuvre's data 16/ were correlated is applicable. The function shown

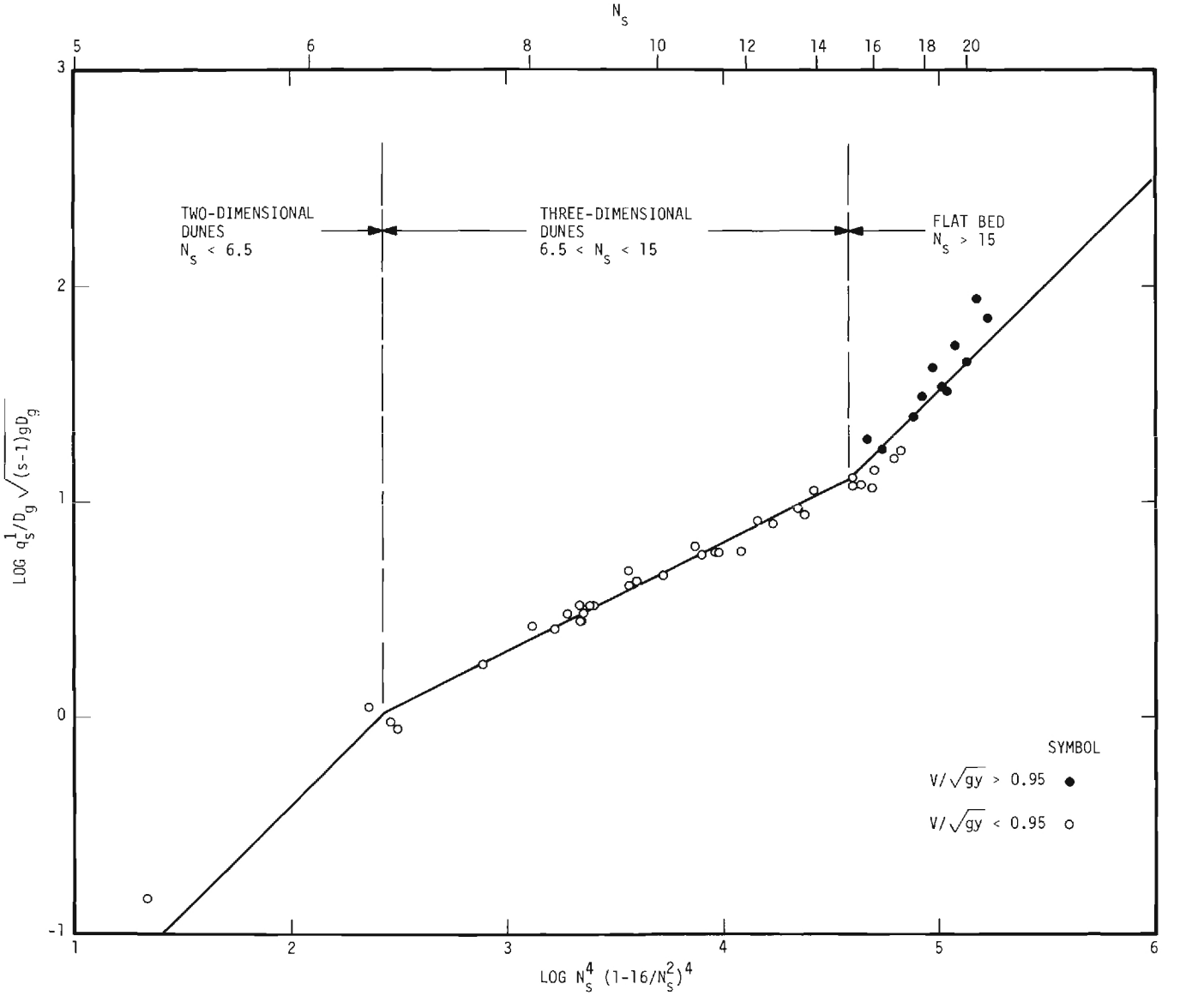

Figure 14. Stein's Data 11/ for Sediment Transport (D_g = 0.4 mm).

as a solid line in Figure 14 in the region of two-dimensional dunes is as follows

$$\frac{q_s{}^1}{D_g \sqrt{(s-1)g\, D_g}} \propto N_s{}^4 \left(1 - \frac{16}{N_s{}^2} \right)^4 \qquad (14)$$

in which $q_s{}^1$ is the volume rate of solids transport per unit width of bed. Equation 14 is a variation of Equation 10. The length term, D_1, is simply the length of the vortices in the lee of the crests. The volume rate of solids transport, Q_s^1, divided by the width of bed (length of the vortices) is simply $q_s{}^1$. Stein states that a mean velocity of 1.1 ft/sec represents the critical velocity for the beginning of dune formation. Stein determined the critical velocity indirectly. Using the value of 1.1 ft/sec, the value of N_{sc} in Equation 10 would be 4.2. Recognizing the lack of precision of determining the critical velocity, the writer used an integer value, 4, for the value of N_{sc} in Equation 14 and Figure 14.

Most of Stein's data were taken in the region of three-dimensional dunes, that is, $6.5 < N_s < 15$ as shown in Figure 14. As discussed in Chapter II, the region of three-dimensional dunes is characterized by a different dune geometry at every value of N_s. Hence, Equation 10 would not be expected to be applicable in this region. Fortuitiously, Stein's data in this region are correlated by the same parameters which are in Equation 10. The function shown in Figure 14 in the region of three-dimensional dunes is as follows

$$\frac{q_s{}^1}{D_g \sqrt{(s-1)g\, D_g}} \propto N_s{}^2 \left(1 - \frac{16}{N_s{}^2} \right)^2 \qquad (15)$$

The upper limit of the region, $N_s = 15$, was selected from Table V. Greater credence was given to the data obtained with the larger depths of flow, y_o.

The flat-bed region, $N_s > 15$, is complicated in laboratory flume experiments by the appearance of antidunes. Antidunes are bed forms that occur in trains that are in phase with and strongly interact with gravity water-surface waves 18/. The strong interaction between the waves on the bed and the surface waves occurs when the Froude number, $V/\sqrt{gy_o}$, is in the vicinity of unity. Stein's data points for which antidunes are suspected are shown as solid circles in Figure 14. Antidunes would not exist with oscillatory flow at the sea bed which is generated by a train of moving surface waves. Rather, in oscillatory flow, the bed can be expected to be flat for values of N_s, in excess of 13 as indicated in Figures 6 and 7. Since a flat bed is geometrically similar to every other flat bed, Equation 10 is presumed to be applicable. The transport function shown in Figure 14 is the same as Equations 10 and 14.

B. Transport Functions of Oscillatory Flow Into a Scour Hole

The input sediment-transport functions can now be written for sediment transport into a scour hole by using the analogous functions of unidirectional flow, as follows. For $N_s < 4$

$$Q_{si} = 0 \tag{16}$$

For $4 < N_s < 6.5$

$$Q_{si} = K_2 \, B \, D_g \sqrt{(s-1)g \, D_g} \; N_s^4 \left(1 - \frac{16}{N_s^2} \right)^4 \tag{17}$$

For $6.5 < N_s < 13$

$$Q_{si} = K_3 \, B \, D_g \sqrt{(s-1)g \, D_g} \; N_s^2 \left(1 - \frac{16}{N_s^2} \right)^2 \tag{18}$$

and for $N_s > 13$

$$Q_{si} = K_4 \, B \, D_g \sqrt{(s-1)g \, D_g} \; N_s^{\,4} \left(1 - \frac{16}{N_s^{\,2}} \right)^4 \qquad (19)$$

In Equations 17, 18, and 19, B is the width of the scour hole. The width of the scour hole around the right circular cylinder can be approximated as

$$B = L + 0.24D + 2S \cot \phi \qquad (20)$$

The selection of a value of 4 for N_{sc} in Equations 17, 18, and 19 is a simplifying assumption. As shown in Figure 4, the value of N_{sc} for flat-bed incipient motion is a function of sediment diameter, wave period, and water temperature. The flat-bed, incipient-motion criterion was chosen for the reason that if dunes are generated and propagate away from a flow disturbance, the sediment transport is away from the flow disturbance. In the problem under consideration, the concern is with the sediment transport toward the flow disturbance from the sourrounding bed. Only if dunes are generated away from the flow disturbance, that is, spontaneous formation of a dune system (Figure 6), will sediment be transported into the scour hole.

The constants, K_2, K_3, and K_4, have to be determined indirectly from Equation 7 utilizing the cylinder-settlement data obtained during the model-test program. Because of the scale effect of dunes upon the flow pattern around the models, the only usable data is that with sediment inflow but without the effect of dunes. These requirements limit the usable data to those tests for which N_s was greater than 9.5 (Tables II and III) as discussed in I.A.2. Since the maximum value of N_s was 11.9, Model Test No. 14, Table III, and since the minimum N_s is 9.5, the input sediment-transport function is Equation 18, from which K_3 can be determined. Values of K_3 were systematically varied

until the integral of Equation 7 was a reasonable fit to measured settlement-time data. By this procedure the value of K_3 was found to be $2.0(10^{-2})$. Comparison of the integral of Equation 7 and experimental results is shown in Figure 15. After the value of K_3 was determined, the values of K_2 and K_4 of Equations 17 and 19 could be computed. Values and ranges are summarized in Table VII, below

TABLE VII

COEFFICIENTS OF THE INPUT SEDIMENT-TRANSPORT FUNCTIONS

Equation	Range of N_s		K
	From	To	
16	N_{sc}	4	0
17	4	6.5	$1.22(10^{-3})$
18	6.5	13	$2.0\ (10^{-2})$
19	13	-	$1.44(10^{-4})$

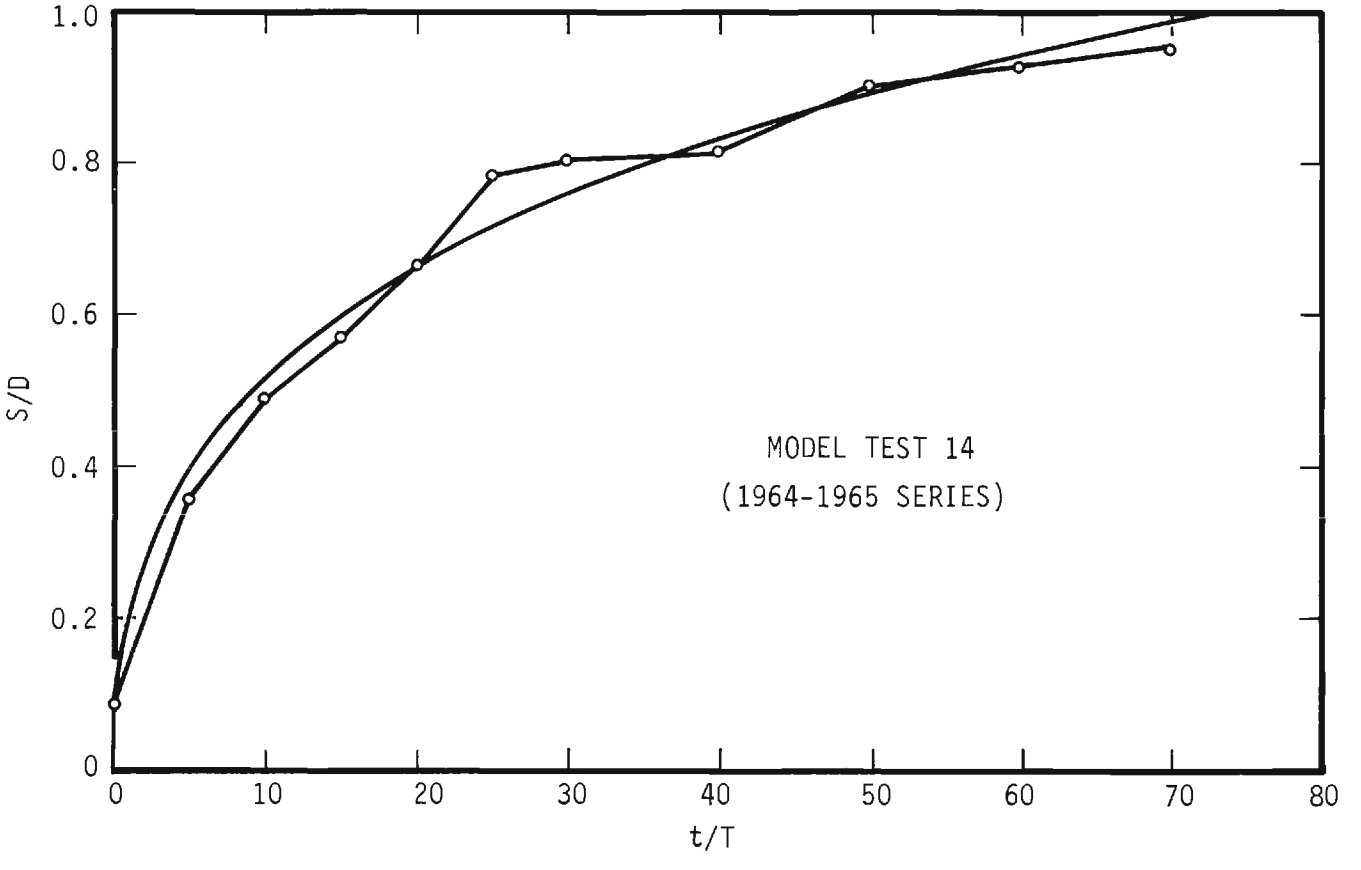

Figure 15. Settlement Versus Time of Model Test 14 (1964-1965 Series).

VII. THE SETTLEMENT FUNCTION

Settlement of cylinder into the bed resulting from scour induced by oscillatory flow is given by the integral of the sediment continuity equation, Equation 7. For a steady cyclic water motion, the volume of the scour hole, $\forall$, the rate of removal of sediment by localized scour, Q_{so}, and the rate of deposition of sediment into the scour hole from the surrounding bed, Q_{si}, have been presumed to be functions of the scour-hole depth, S, and time-invariant flow variables. With this presumption, Equation 7, can be integrated by substituting the right-hand side of Equation 9 for $d\forall$, by substituting the right-hand side of Equation 13 for Q_{so}, and by substituting the right-hand side of either Equations 16, 17, 18, or 19 for Q_{si}. This method accounts for change in bed-form geometry in that different input sediment-transport functions are utilized for different stages of bed-form development. In contrast, this method is based on the assumption that localized scour around the cylinder is independent of the geometry of the surrounding bed in that the same output sediment-transport function is utilized for all stages of bed-form development. The reasoning here is that the prototype body and scour-hole will be large enough that the smaller bed forms (dunes) will be negligible in respect to the flow pattern around the object in the bottom of the scour hole.

In the model tests, dunes on the bed did influence the flow pattern. This influence was negligible for the model tests in which N_s was greater than 9.5. The surrounding bed remained flat for model tests with the smallest cylinder, D = 0.501 in. and with N_s equal to 2.8. Since bed forms did not influence the flow pattern, these tests were utilized to evaluate the transport functions.

For prototype cylinders large enough so that the flow pattern around the

cylinder is not influenced by dunes, integration of Equation 7 with the appropriate transport functions constitutes the goal of the hydraulic-laboratory program.

A. Model-Test Results

Comparison of measured settlement-time functions with those obtained by integration of Equation 7 are shown in Figure 13 and Figure 15. Similar comparisons for all other model tests of the 1964-1965 series are contained in the APPENDIX. Each graph is indexed by the model test number. Information about each model test is contained in Table III. Since each model test was begun with a flat bed, dunes were developing simultaneously with the development of the scour hole around the cylinder. The number of cycles required to develop an equilibrium dune system is marked on the graphs of APPENDIX B by a vertical dashed line marked t_d/T. The lack of such a mark on the graphs indicates that t_d/T is greater than the largest value of t/T shown on the graph.

As discussed in I.A.2, the cylinder would stop settling and join the dune system when the dune amplitude was the same order of magnitude as the cylinder diameter. This condition is shown in Figure 2. The cessation of settlement from this cause is clearly shown by the settlement data of Model Tests 31, 32, and 33 in the APPENDIX. Some of the earlier model tests, for example, Model Test 8, were terminated as soon as the observers noted the cessation of settlement. If Model Test 8 had been continued, the settlement curve would have undoubtedly been similar to that of Model Test 32.

Settlement of a cylinder into the bed resulting from oscillatory flow over the bed is predictable by the integral of the sediment continuity equation, Equation 7. Since the integral is not an elementary integral, numerical methods have to be used to evaluate the integral at various values of scour

depth, S. Numerical integrations were performed using the physical variables of each model test of the 1964-1965 series of tests. The computed settlement-time curves are shown by the continuous curves in the graphs in the APPENDIX.

B. General Settlement-Time Curves

General settlement-time functions can be determined by repeated numerical integration of the dimensionless form of Equation 7. The dimensionless form used is as follows

$$\frac{t\, D_g \sqrt{(s-1) g\, D_g}}{D^2} = \int_0^{S/D} \frac{d\left(\frac{\forall}{D^3}\right)}{\frac{Q_{so}}{D\, D_g \sqrt{(s-1) g\, D_g}} - \frac{Q_{si}}{D\, D_g \sqrt{(s-1) g\, D_g}}} \qquad (21)$$

The expression under the integral sign is a function of the dimensionless variables of Equations 9, 13, 17, 18, and 19. Dimensionless settlement-time functions are shown in Figures 16-19, inclusive. Since sea sands are "well-rounded" the value of the angle of repose, ϕ, will be about 30 degrees 19/. Settlement or scour depth, S/D, is shown as a function of N_s and $t\, D_g \sqrt{(s-1) g\, D_g}$ in each figure. Separate figures have been prepared for different values of N_{sc}. The effect of the critical sediment number upon time for settlement to occur is significant only for values of N_s less than 8.

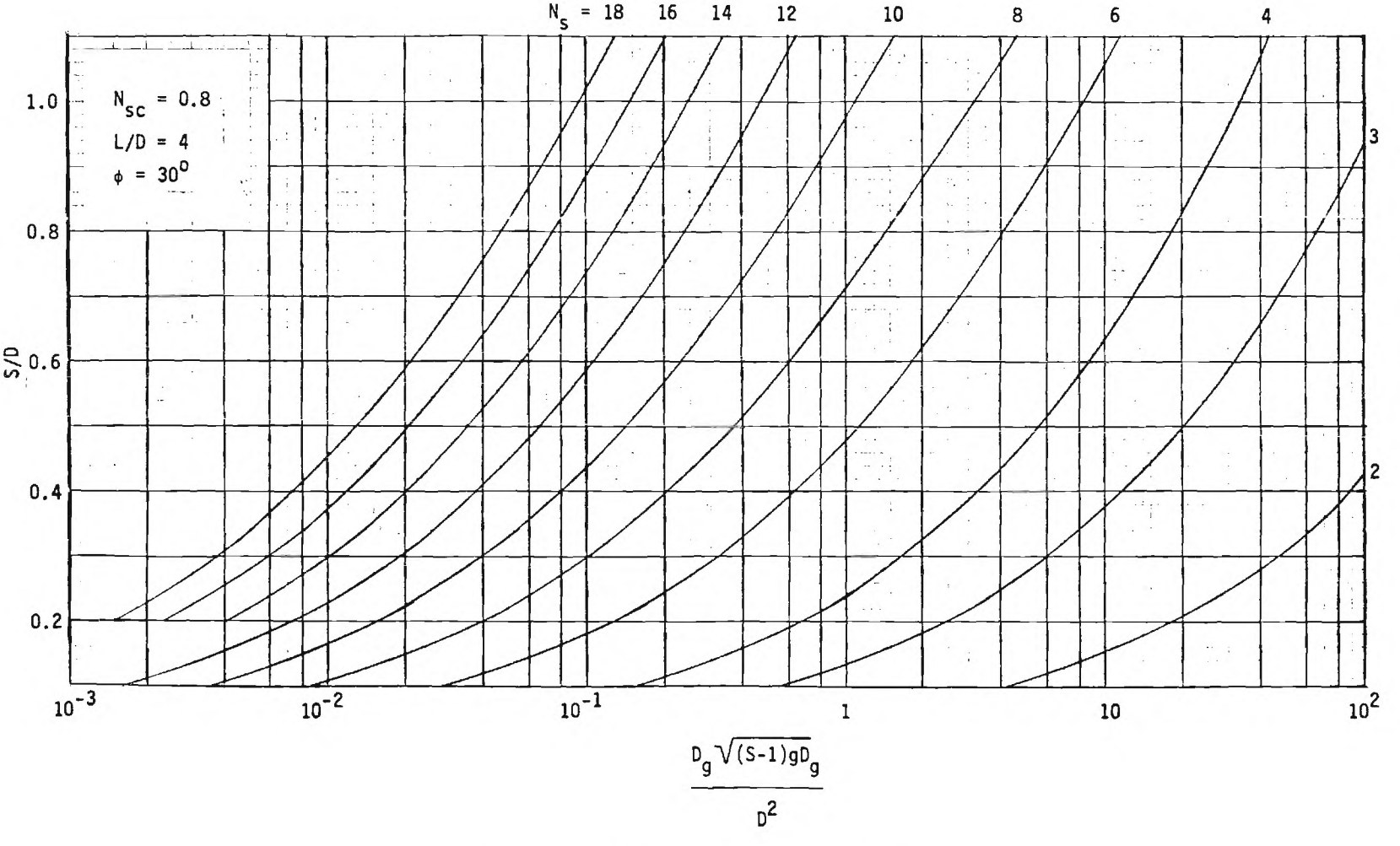

Figure 16. Settlement Curves (N_{sc} = 0.8).

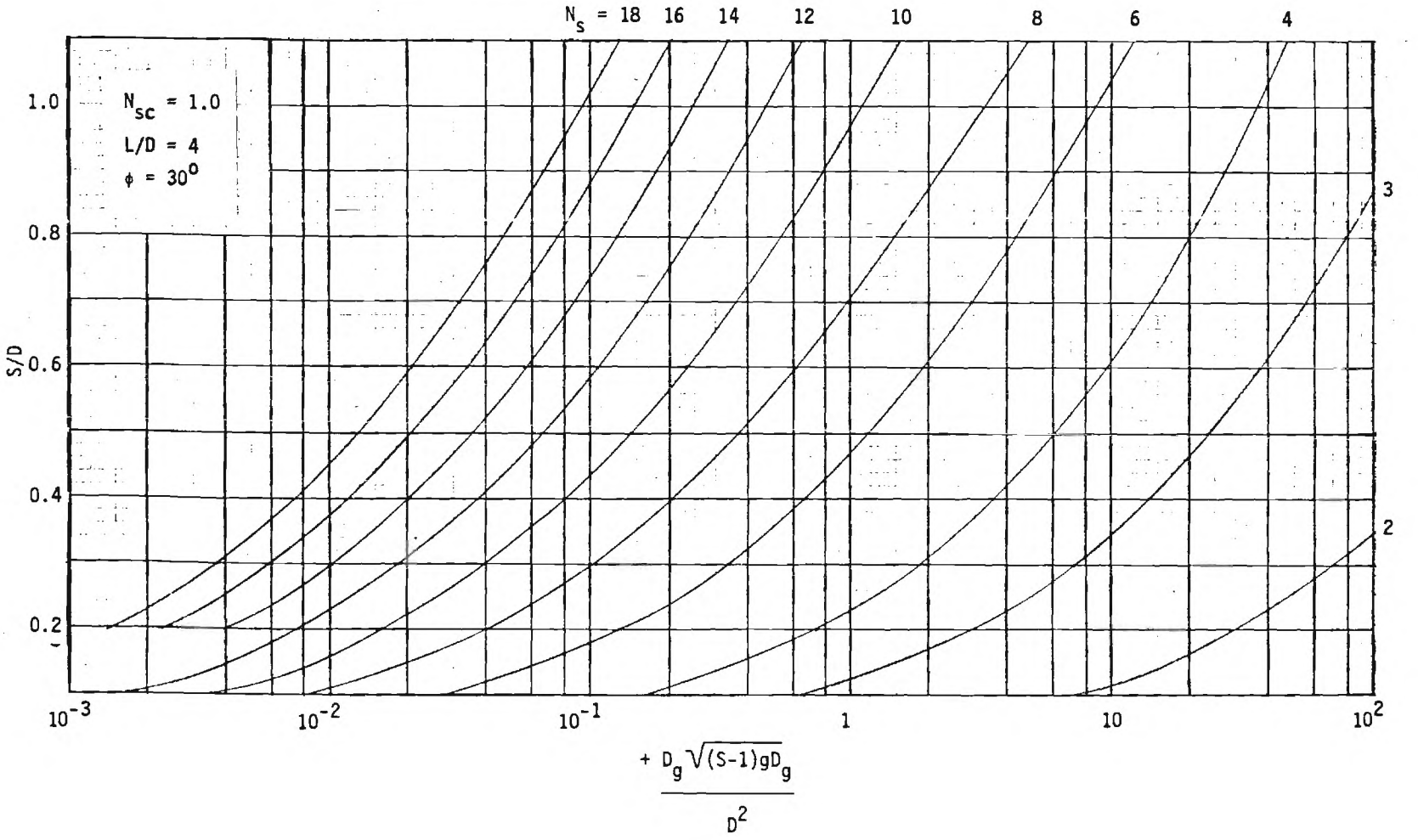

Figure 17. Settlement Curves (N_{sc} = 1.0).

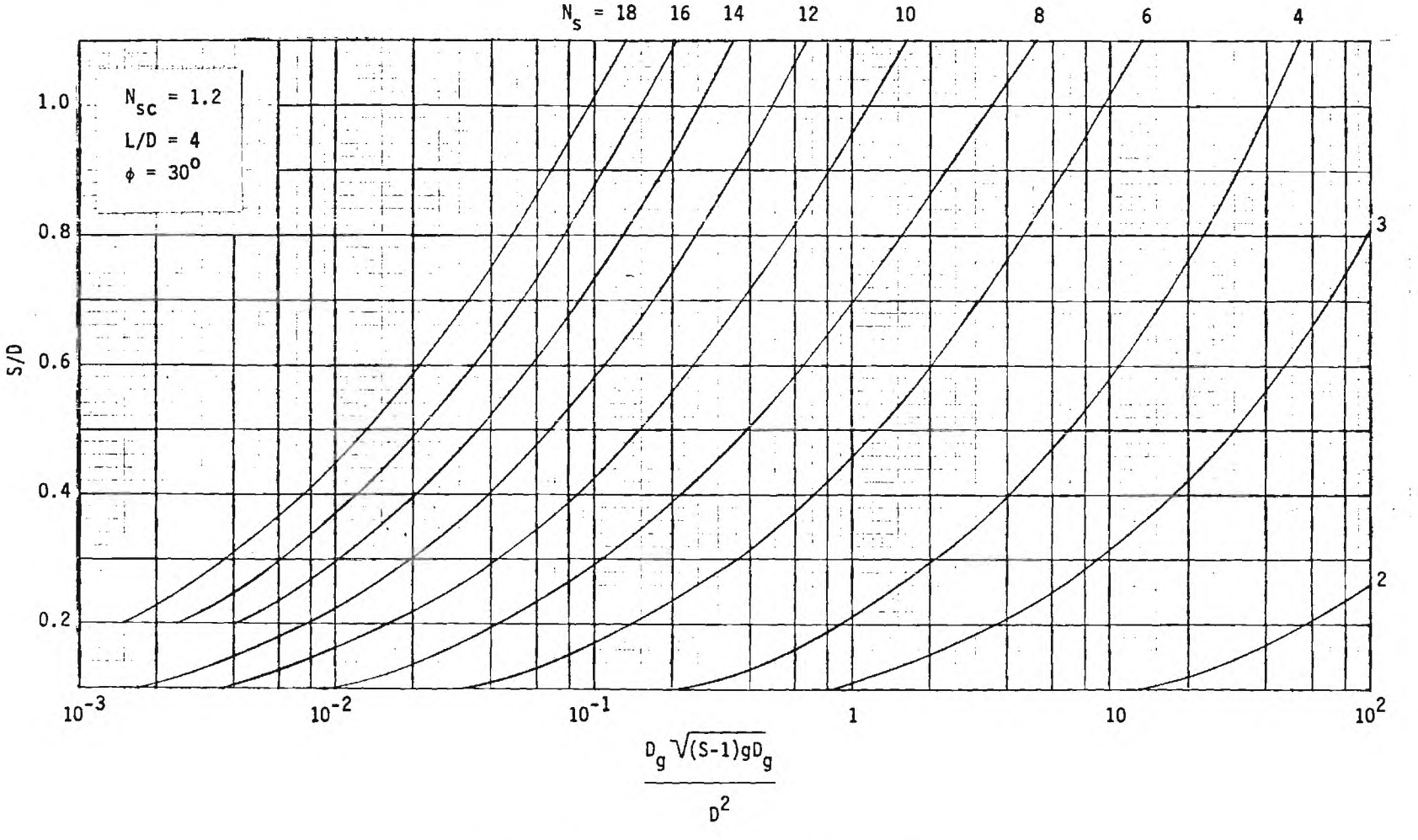

Figure 18. Settlement Curves (N_{sc} = 1.2).

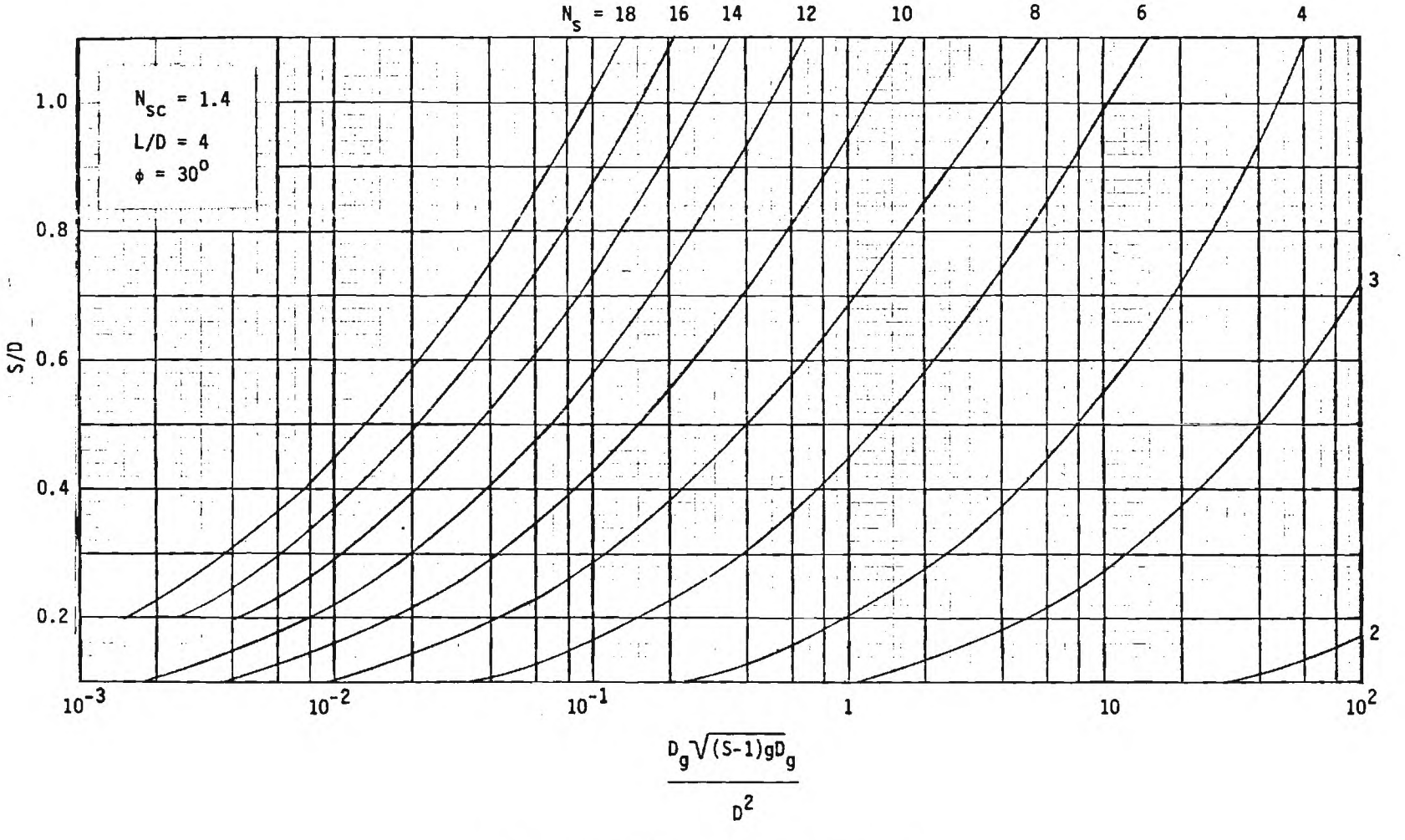

Figure 19. Settlement Curves (N_{sc} = 1.4).

C. Terminal scour depth

When the rate of sediment transport into the scour hole equals the rate of sediment transport out of the scour hole, a terminal depth, S_T, is attained. Terminal depth is approached assymptotically with increasing time. The theoretical limit, S_T, is attained when the denominator of the integral, equation 21, is zero. Values of the terminal depth of scour, S_T, were computed throughout a range of N_s for two values of N_{sc}, 0.8 and 1.4, for L/D of 4, and for ϕ of 30 degrees. The computed results are shown in Figure 20. Discontinuities in Figure 20 occur at N_s values of 4, 6.5, and 13 corresponding to changes in the input sediment-transport function.

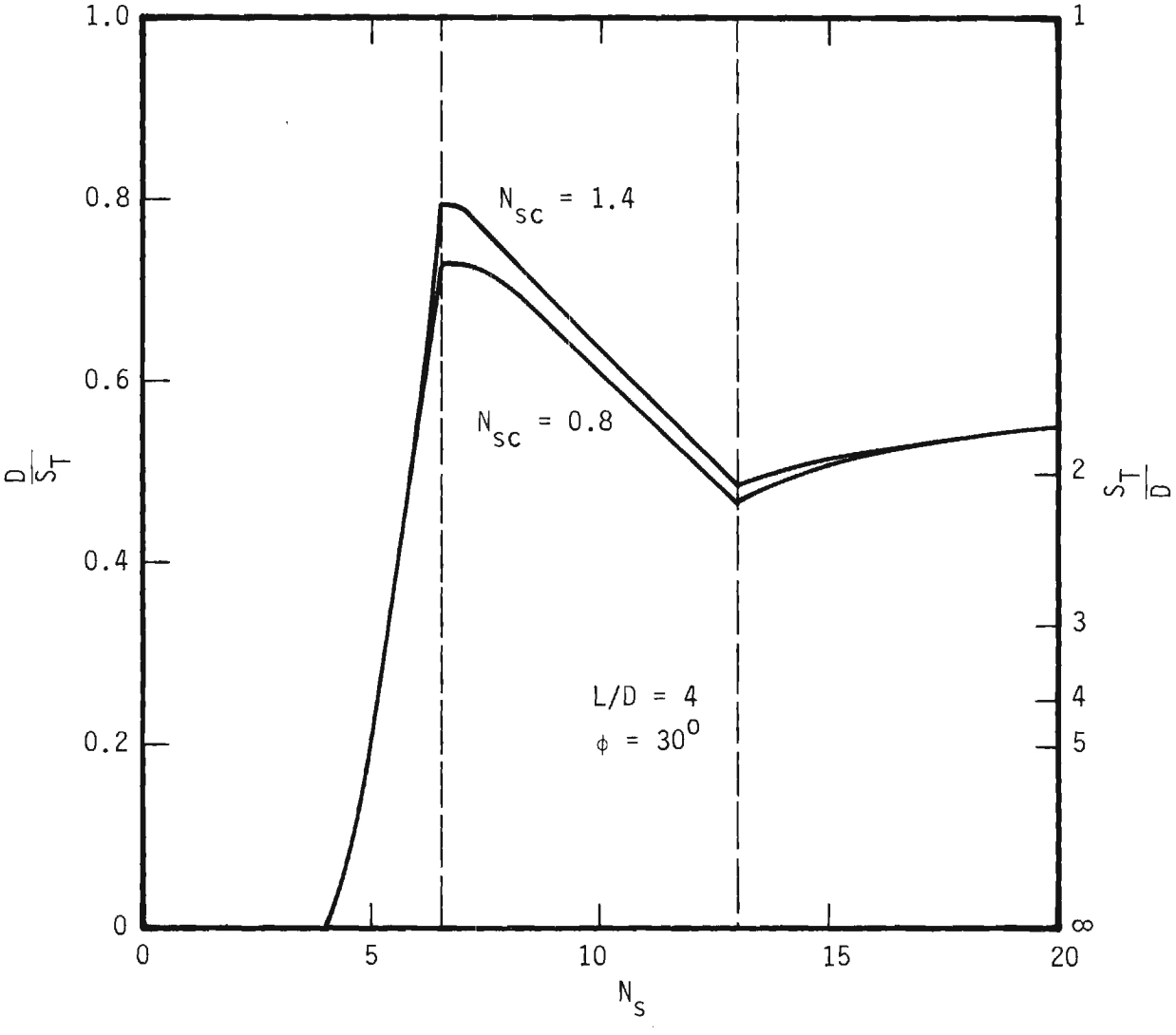

Figure 20. Terminal Scour Depth.

VIII. SUMMARY

Settlement of a cylinder into a bed under the action of oscillatory flow has been analyzed by means of the equation of continuity in the scour hole. This equation of continuity involves three terms -- (a) rate of change of scour hole volume (b) rate of sediment transport out of the hole, and (c) rate of sediment transport into the hole from the surrounding bed. Each of the terms was analyzed separately. Prediction of settlement as a function of time involves integration of the equation of continuity of sediment in the scour hole.

Scour holes developed during model tests were studied and mapped in order to formulate a mathematical function relating scour depth to scour-hole volume.

A mathematical function was formulated for the sediment-transport rate out of the scour hole. The work of LeFeuvre 16/ was used to determine the arrangement of variables. Model-test results were used to determine the value of numerical constants.

Mathematical functions were formulated for the sediment-transport rate into the scour hole from the surrounding bed. The work of others, principally Stein 11/ and LeFeuvre 16/, was used to determine the arrangement of variables. Model-test results were used to determine the value of a numerical constant.

The procedure summarized above permitted a detailed separate analysis of three simpler problems which were then recombined in the prediction of settlement of a circular cylinder. This procedure was not optional because the scale effect of dunes precluded valid model tests throughout the range of interest. By utilizing the parts to synthesize the whole, the region in which dunes spoiled the model tests could be bridged. In the writer's opinion, the procedure used in this study can be applied to a variety of localized scour

problems in which the scale effect of dunes is an obstacle to reduced-scale model tests.

IX. REFERENCES CITED

1. M. R. Carstens, Part I -- The Effect of Dunes upon Localized Scour, Final Report, Project A770, Engineering Experiment Station of the Georgia Institute of Technology, Atlanta, Georgia, December 31, 1965, 111 pages.

2. A. M. Z. Alam, T. F. Cheyer, and John F. Kennedy, Friction Factors for Flow in Sand Bed Channels, Report No. 78, Hydrodynamics Laboratory, Massachusetts Institute of Technology, Cambridge, Massachusetts, June 1966, 97 pages.

3. M. R. Carstens, "Similarity Laws for Localized Scour," Proc. ASCE, Journal of the Hydraulics Division, Vol. 92, No. HY3, 13-36 (May 1966).

4. Vito A. Vanoni, "Sediment-Transportation Mechanics: Initiation of Motion," Proc. ASCE, Journal of the Hydraulics Division, Vol. 92, No. HY2, 291-314, (March 1966)

5. M. R. Carstens, Initiation of Motion of Sediment Particles, Quarterly Report 9, Project A-798, School of Civil Engineering of the Georgia Institute of Technology, Atlanta, Georgia, September, 1966, 26 pages.

6. Maurice L. Albertson, James R. Barton, and Daryl B. Simons, Fluid Mechanics for Engineers, Prentice-Hall, Inc., Englewood Cliffs, New Jersey, 1960, Fig. 9-2, p. 399.

7. Charles S. Martin, The Role of a Permeable Bed in Incipient Sediment Motion, Ph.D. thesis, Georgia Institute of Technology, Atlanta, Georgia, 1964, 150 pages.

8. M. R. Carstens and F. M. Neilson, Evolution of a Duned Bed under Oscillatory Flow, Quarterly Report 7, Project A-798, Engineering Experiment Station of the Georgia Institute of Technology, Atlanta, Georgia, March 1966, 18 pages.

9. M. R. Carstens, A Different Interpretation of Incipient Motion, Quarterly Report 8, Project A-798, School of Civil Engineering of the Georgia Institute of Technology, Atlanta, Georgia, June, 1966, 12 pages.

10. F. M. Neilson and M. R. Carstens, Geometry of Dunes, Quarterly Report 6, Project A-798, Engineering Experiment Station of the Georgia Institute of Technology, Atlanta, Georgia, December, 1965, 18 pages.

11. Richard A. Stein, "Laboratory Studies of Total Load and Apparent Bed Loads," Journal of Geophysical Research, Vol. 70, No. 8, April 15, 1965 (1831-1842).

12. Vito A. Vanoni and Norman H. Brooks, Laboratory Studies of the Roughness and Suspended Load of Alluvial Streams, Report No. E-68, Sedimentation Laboratory, California Institute of Technology, Pasadena, California, December, 1957, 121 pages.

13. John F. Kennedy, Further Laboratory Studies of the Roughness and Suspended Load of Alluvial Streams, Report No. KH-R-3, California Institute of Technology, Pasadena, California, April, 1961, 36 pages.

14. H. Rouse, "Criteria for Similarity in the Transportation of Sediment," Proceedings, 1st Hydraulic Conference, University of Iowa Studies in Engineering, Bulletin 20, 1940, 33-49.

15. E. M. Laursen, "Observations on the Nature of Scour," Proceedings, 5th Hydraulic Conference, University of Iowa Studies in Engineering, Bulletin 34, 1952, 179-197.

16. A. R. LeFeuvre, Sediment Transport Functions with Special Emphasis on Localized Scour, Ph.D. thesis, Georgia Institute of Technology, Atlanta, Georgia, 1965, 93 pages.

17. Madhav Manohar, Mechanics of Bottom Sediment Movement Due to Wave Action, Technical Memorandum No. 75, Beach Erosion Board, Corps of Engineers, Department of the Army, June, 1955, 121 pages.

18. "Nomenclature for Bed Forms in Alluvial Channels," Proc. ASCE, Journal of the Hydraulics Division, Vol. 92, No. HY3, 51-64 (May 1966).

19. Daryl B. Simons and Maurice L. Albertson, "Uniform Water Conveyance Channels in Alluvial Material," Transactions, ASCE, Vol. 128, Part I, 1963, Fig. 12, p. 97.

X. APPENDIX

Model Test Results (1964-1965 Series)

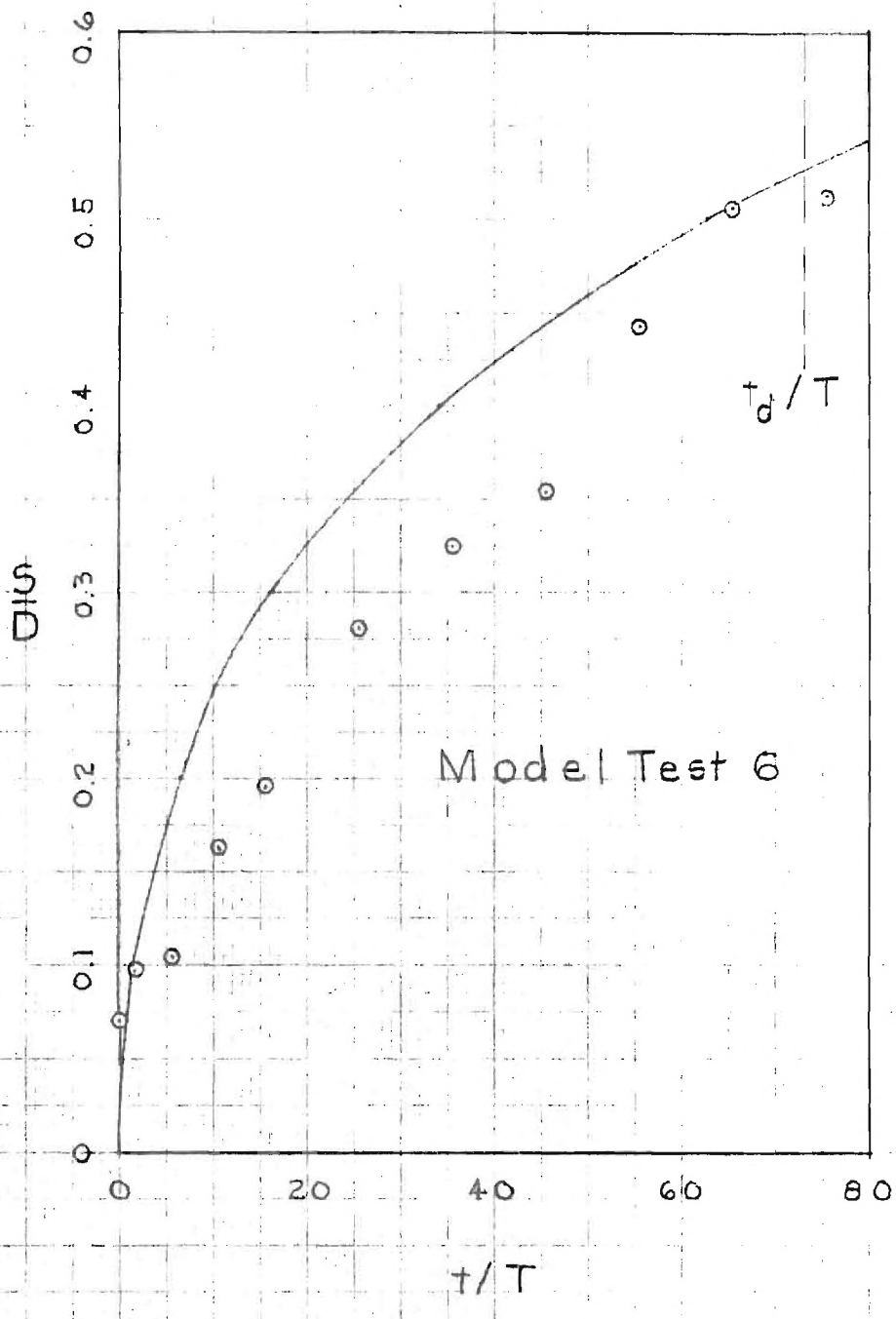
0.6
0.5
0.4
0.3
0.2
0.1
0
DHS
0
20
40
60
80
t/T
t_d/T
Model Test 6

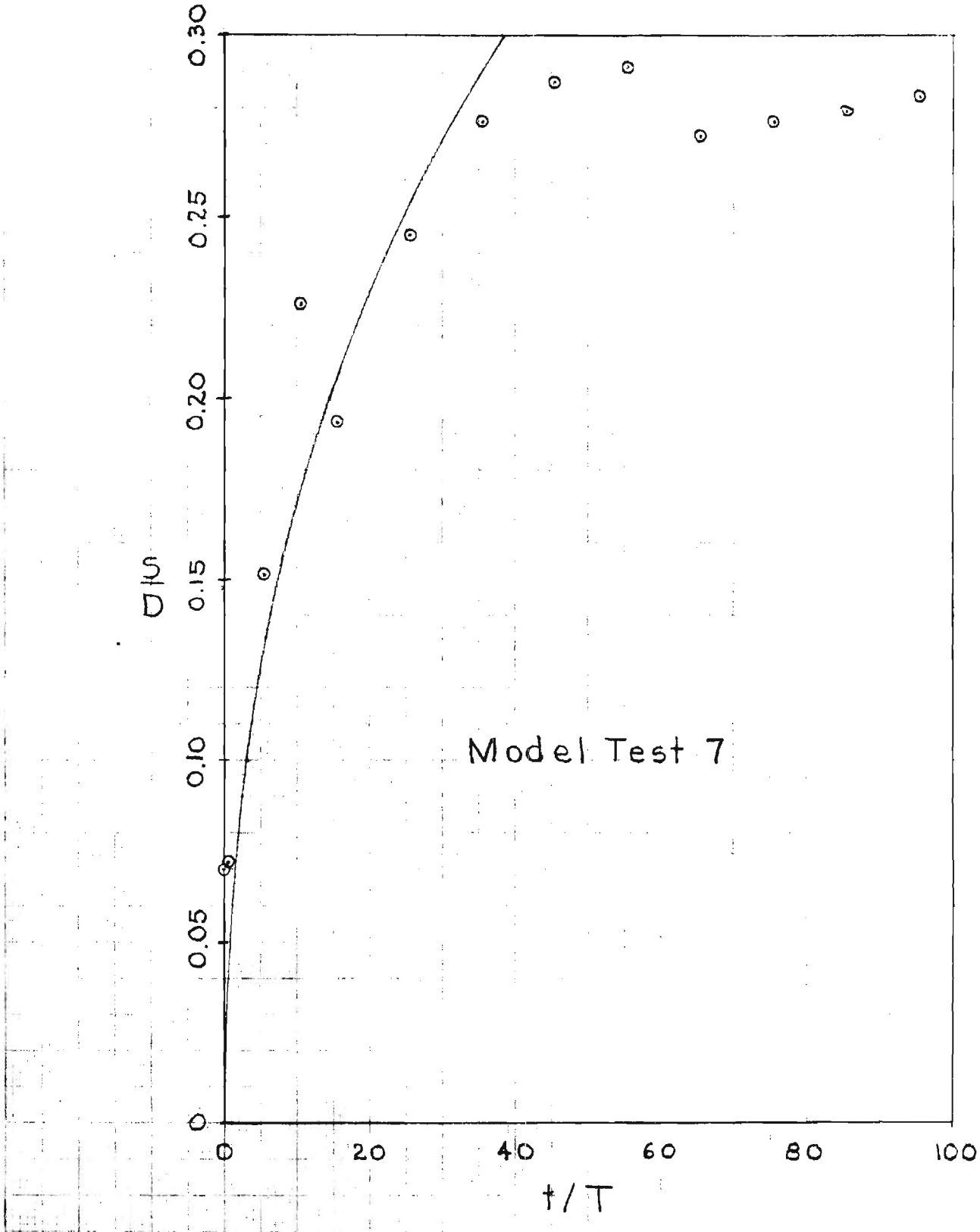
0.30
0.25
0.20
0.15
0.10
0.05
0
D/S
0
20
40
60
80
100
t/T
Model Test 7

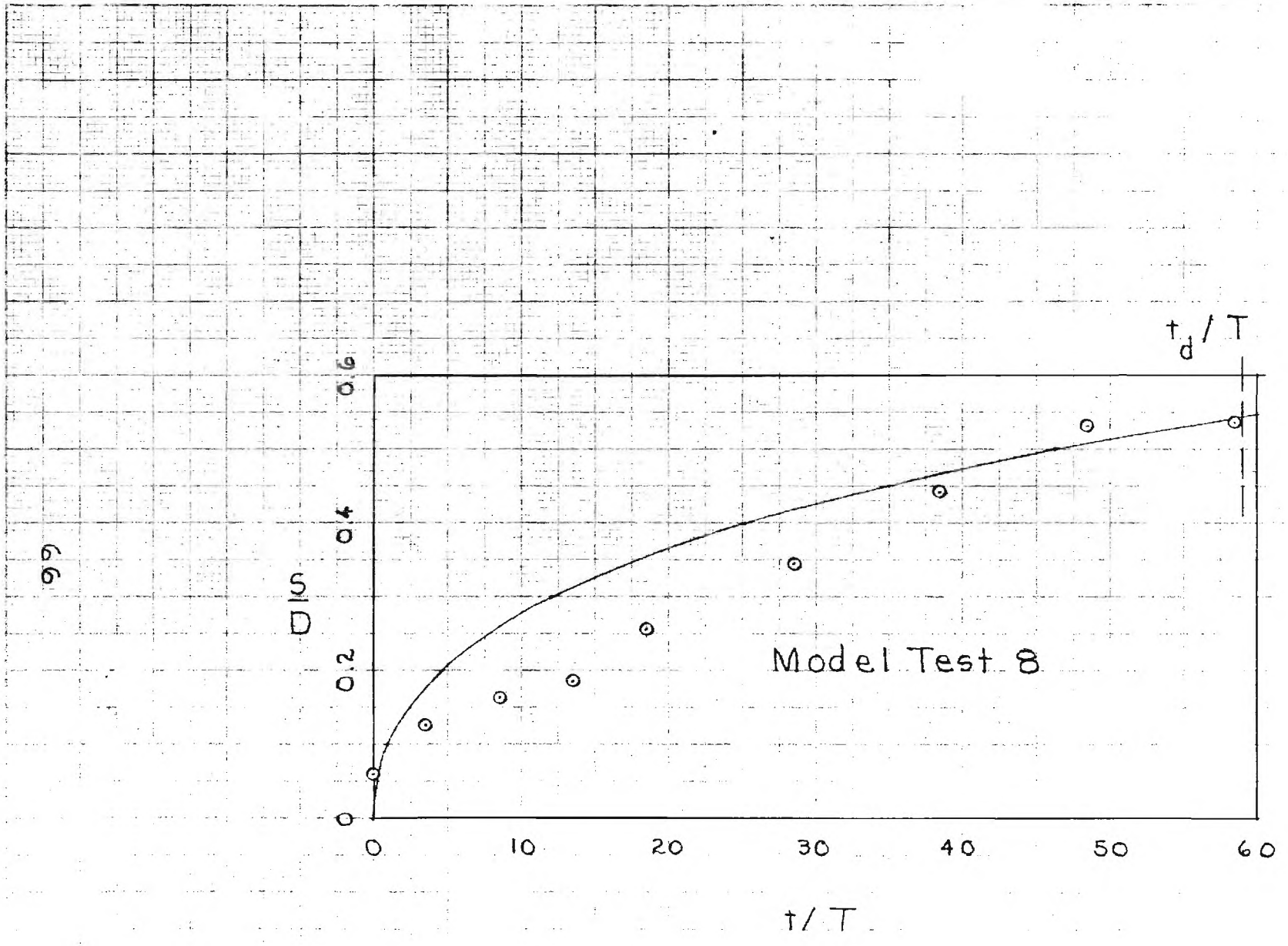
t_d / T
D/S
0.6
0.4
0.2
0
Model Test 8
0
10
20
30
40
50
60
t/T

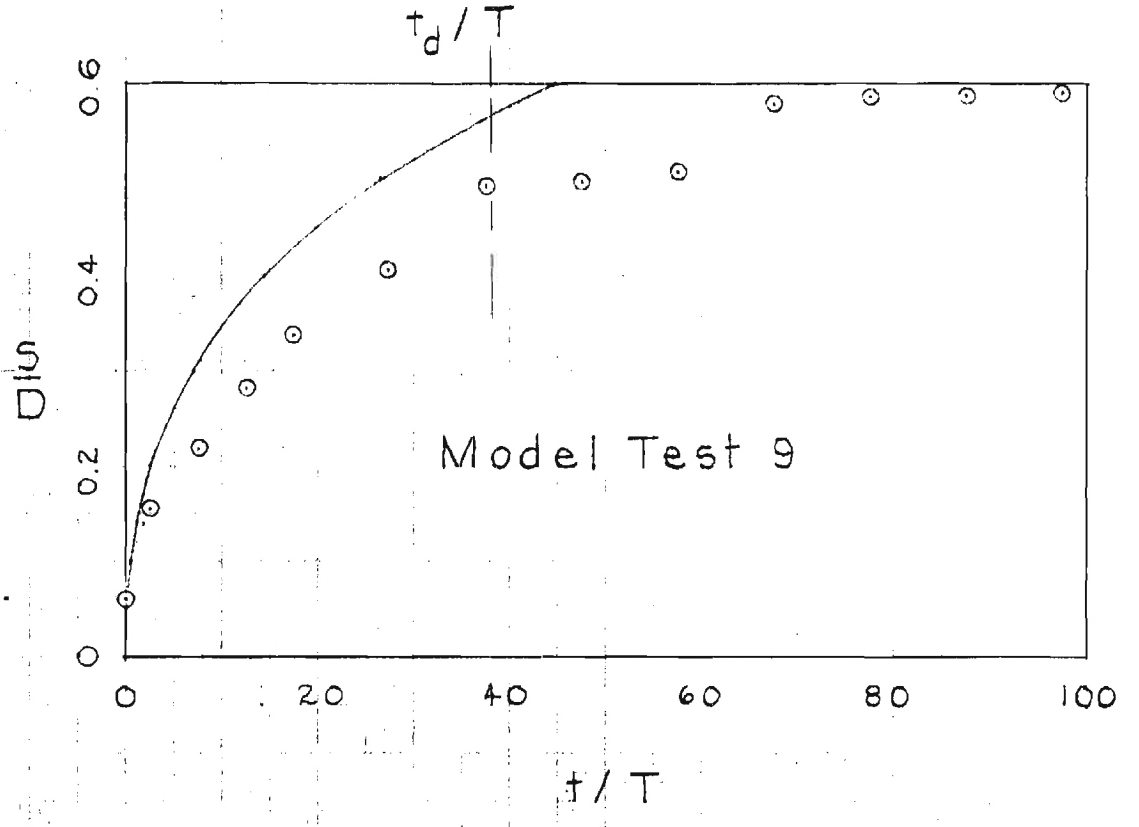
t_d / T
0.6
0.4
0.2
0
Dits
Model Test 9
0
20
40
60
80
100
t / T

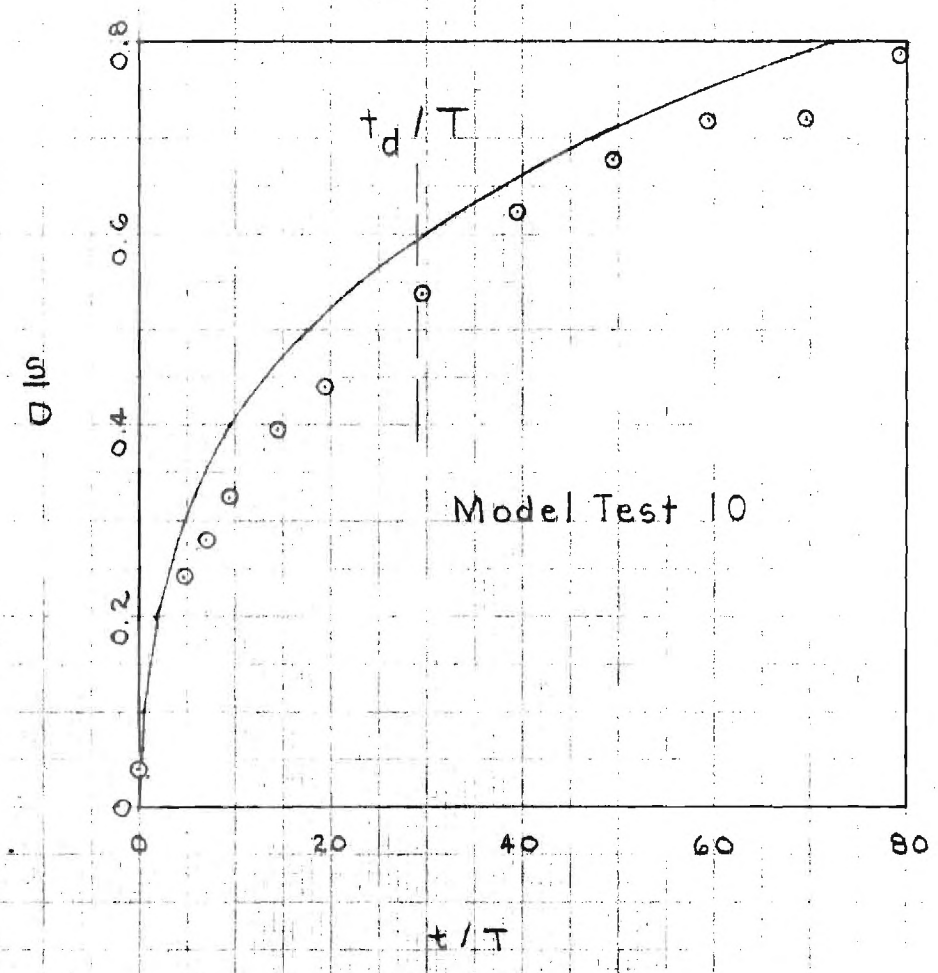
t_d / T
Model Test 10
U/U∞
0
0.2
0.4
0.6
0.8
0
20
40
60
80
t / T

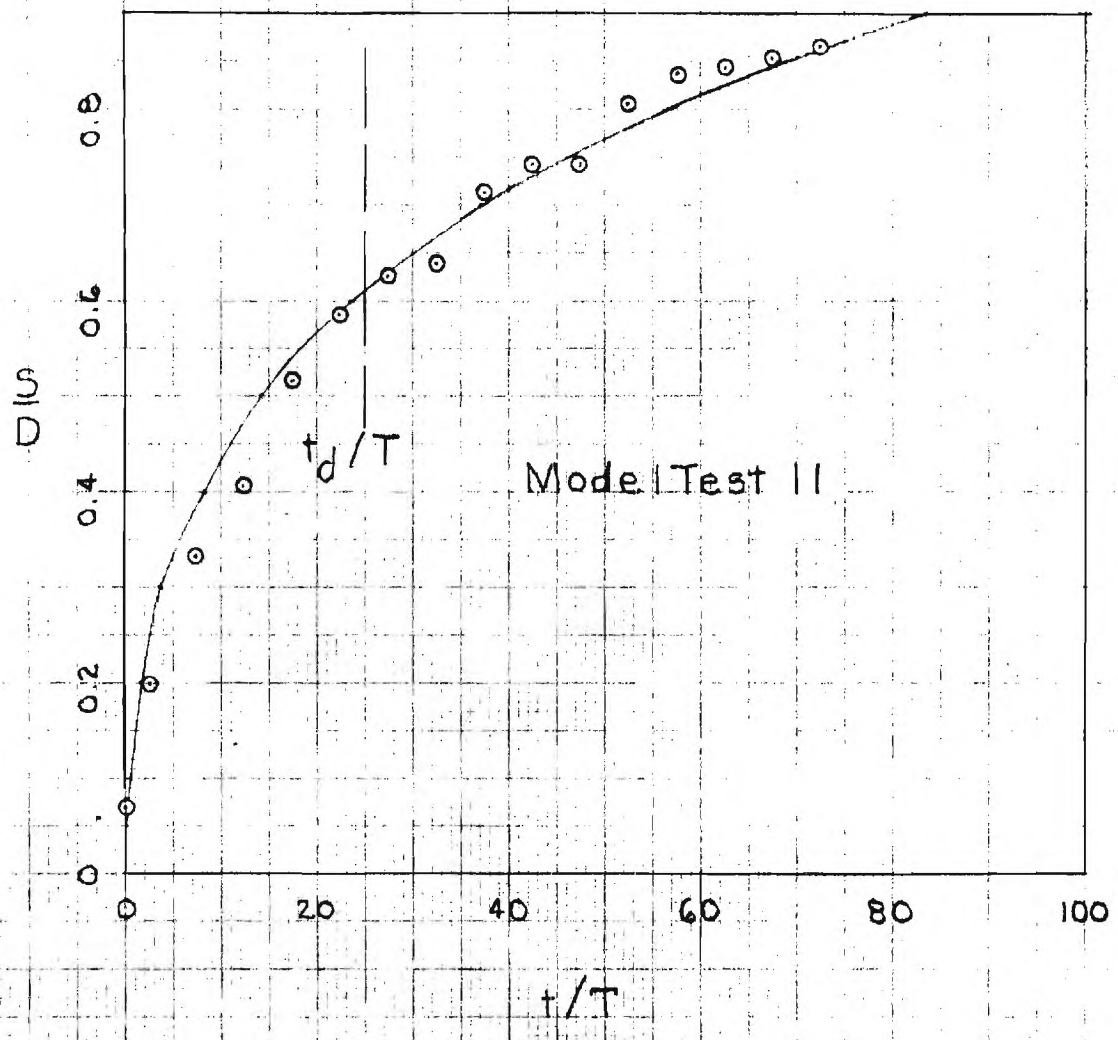
S/D
0.8
0.6
0.4
0.2
0
t_d/T
Model Test 11
0
20
40
60
80
100
t/T

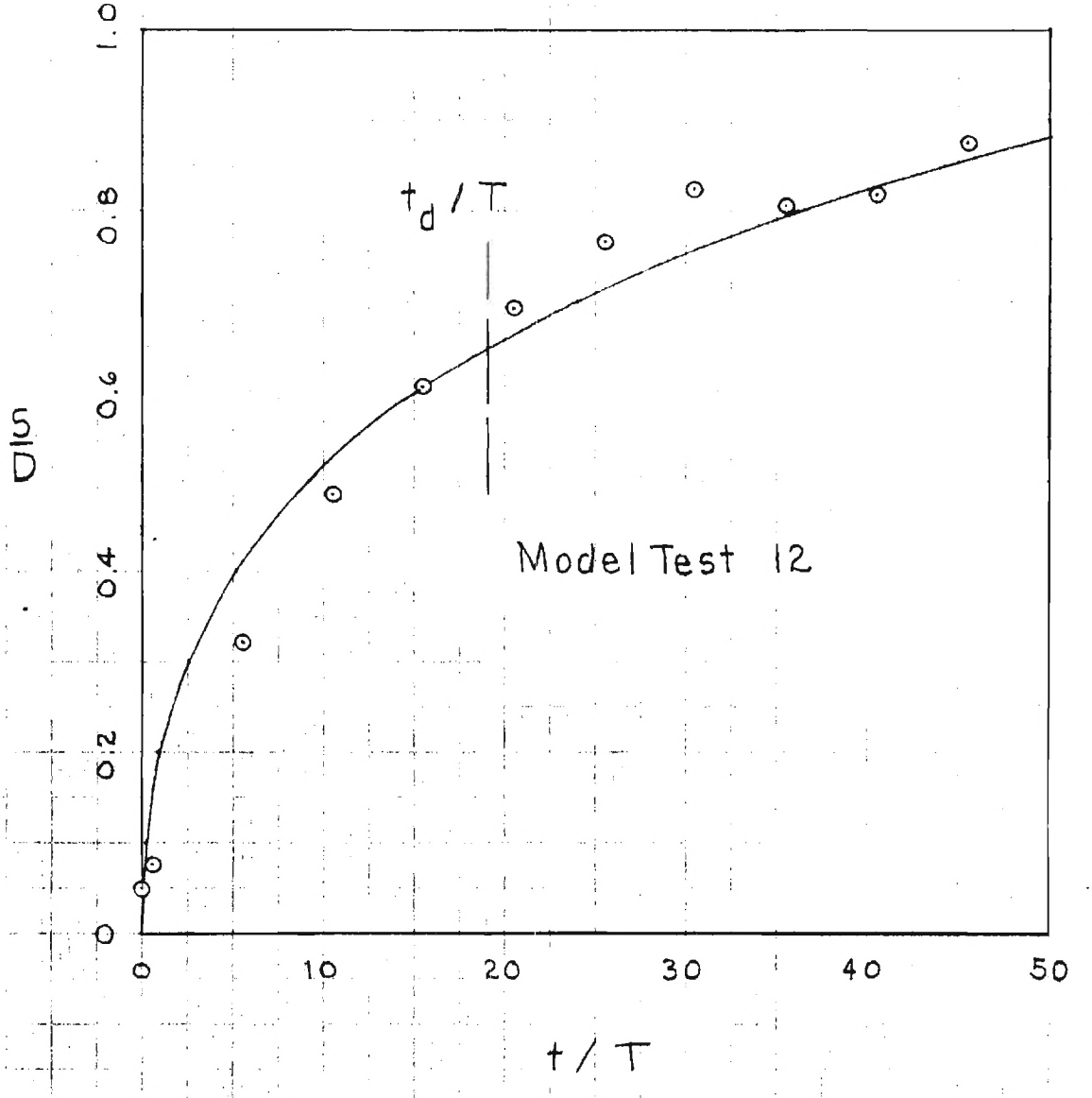
1.0
0.8
0.6
0.4
0.2
0
D/S
t_d / T
Model Test 12
0
10
20
30
40
50
t / T

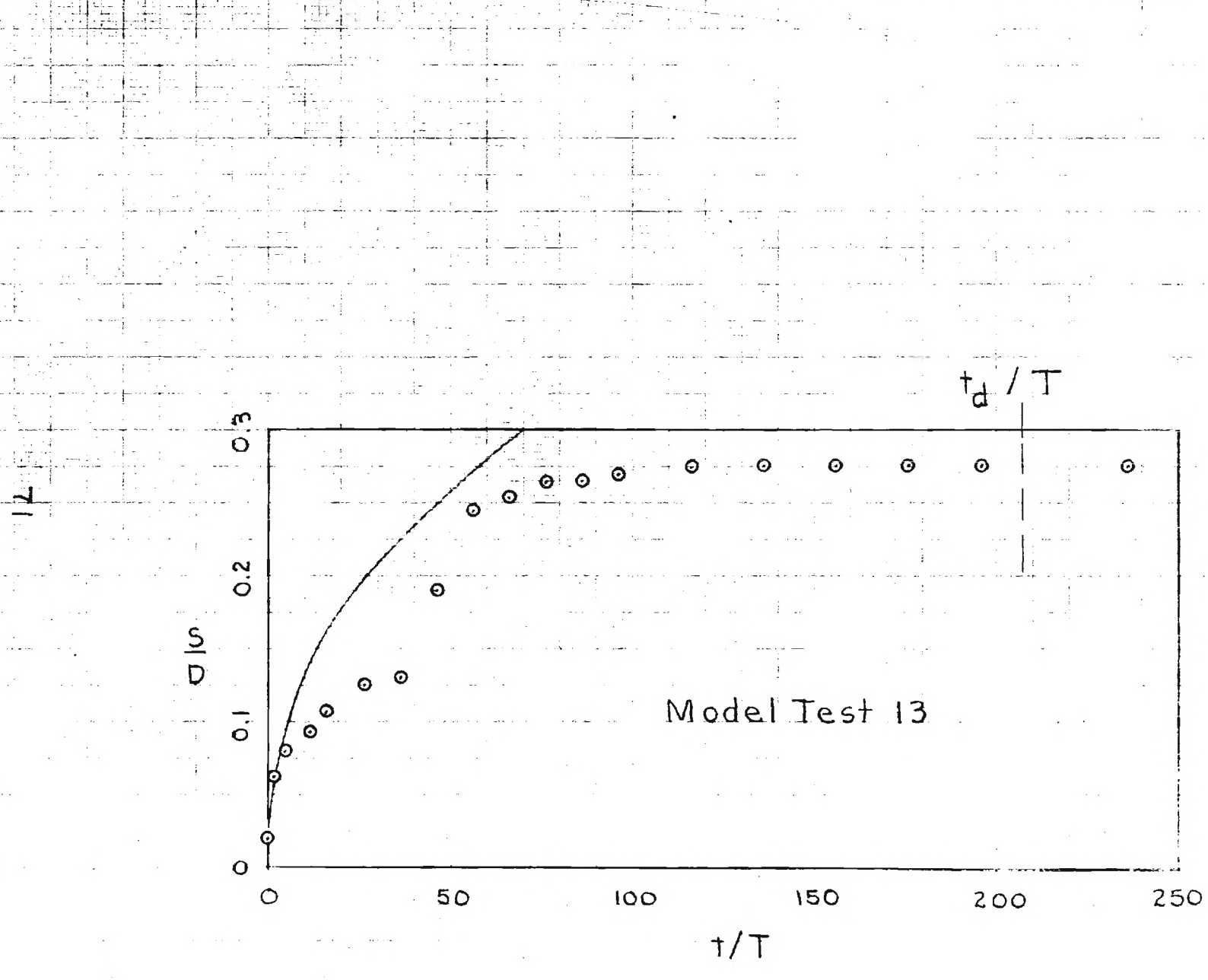
t_d / T
0.3
0.2
0.1
0
S/D
Model Test 13
0
50
100
150
200
250
t/T

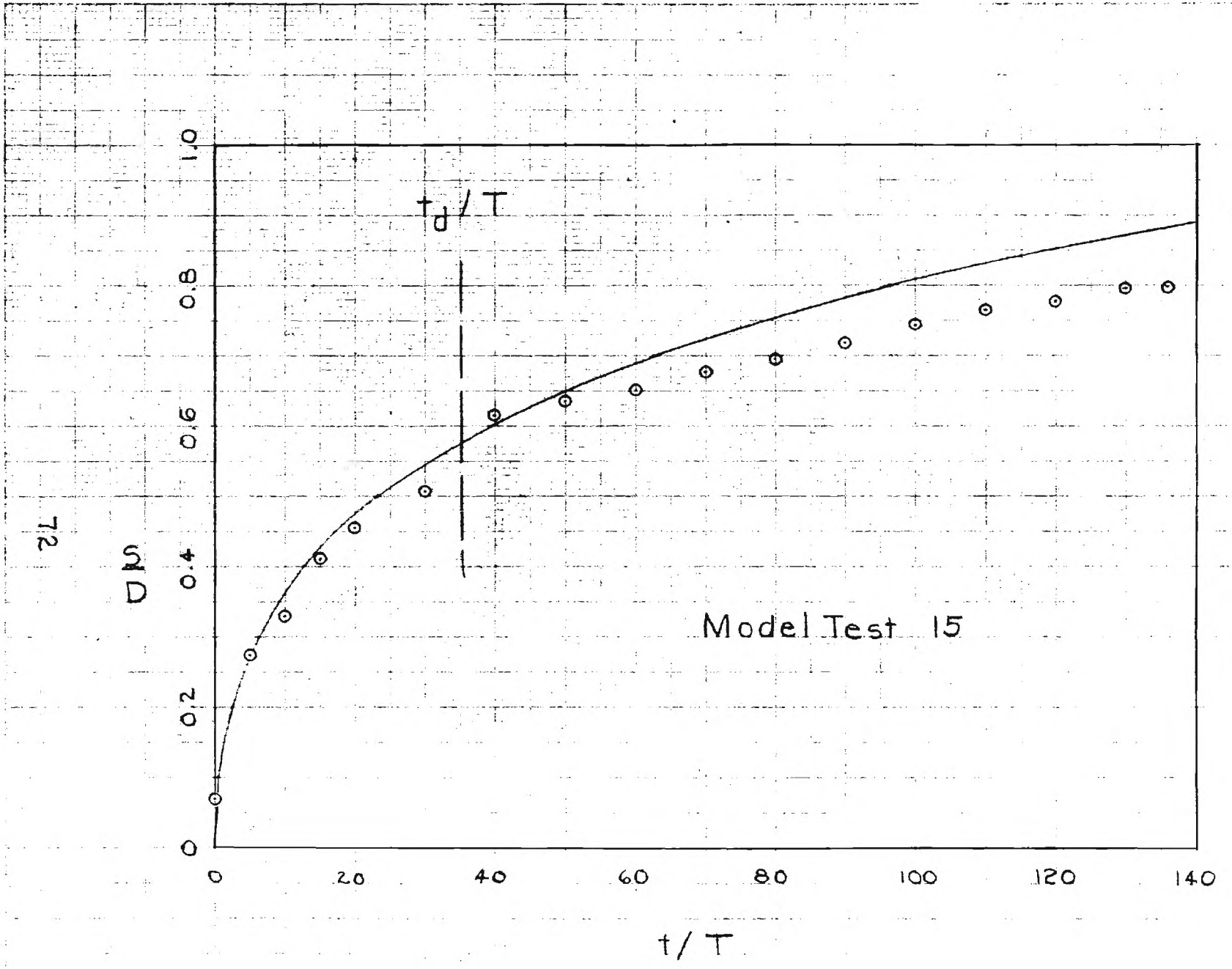
t_d / T
Model Test 15
D/2
0
0.2
0.4
0.6
0.8
1.0
0
20
40
60
80
100
120
140
t / T

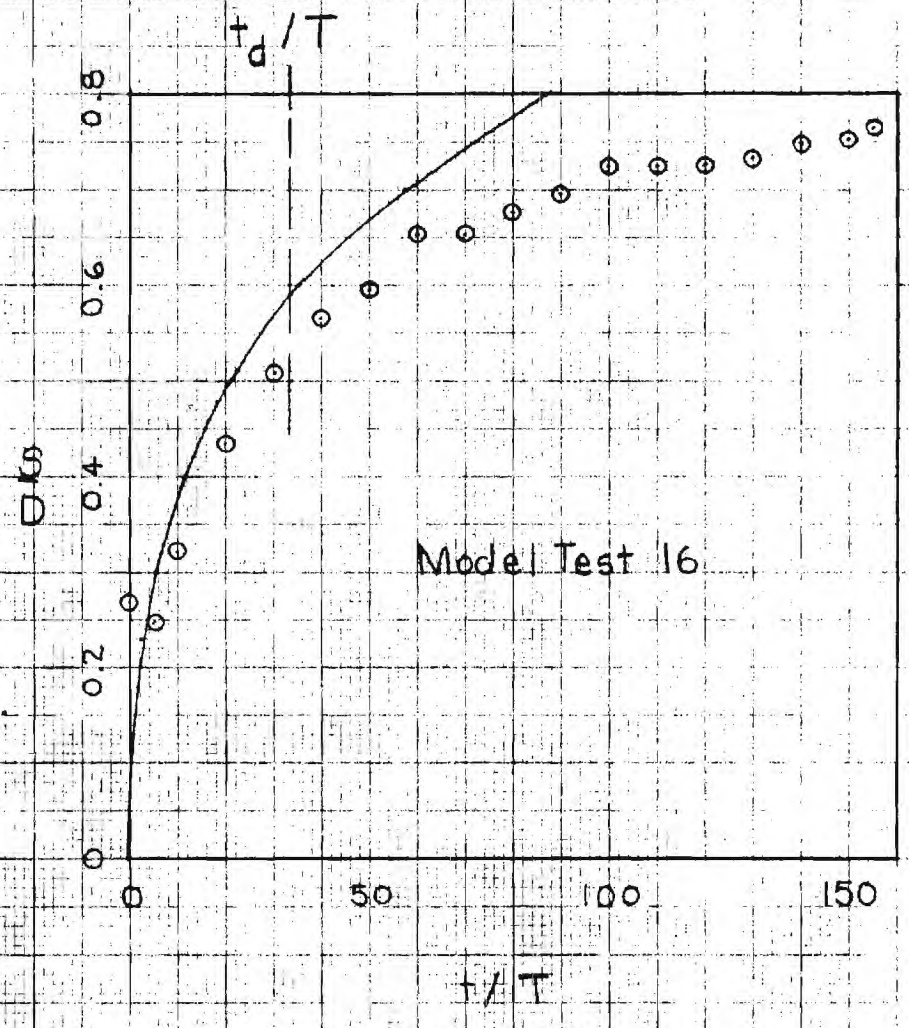
t_d / T
0.8
0.6
0.4
0.2
0
D/s
Model Test 16
0
50
100
150
t / T

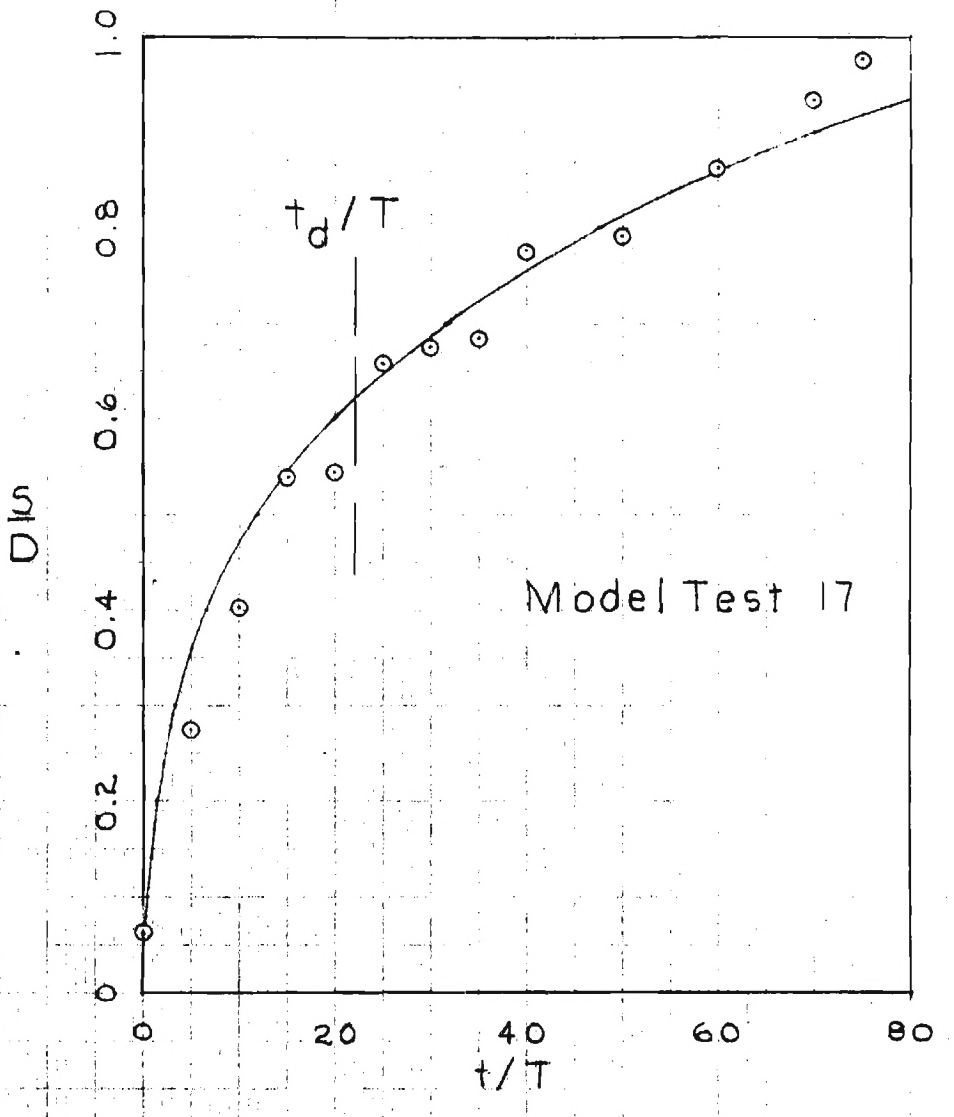
D/S
1.0
0.8
0.6
0.4
0.2
0
t_d/T
Model Test 17
0
20
40
60
80
t/T

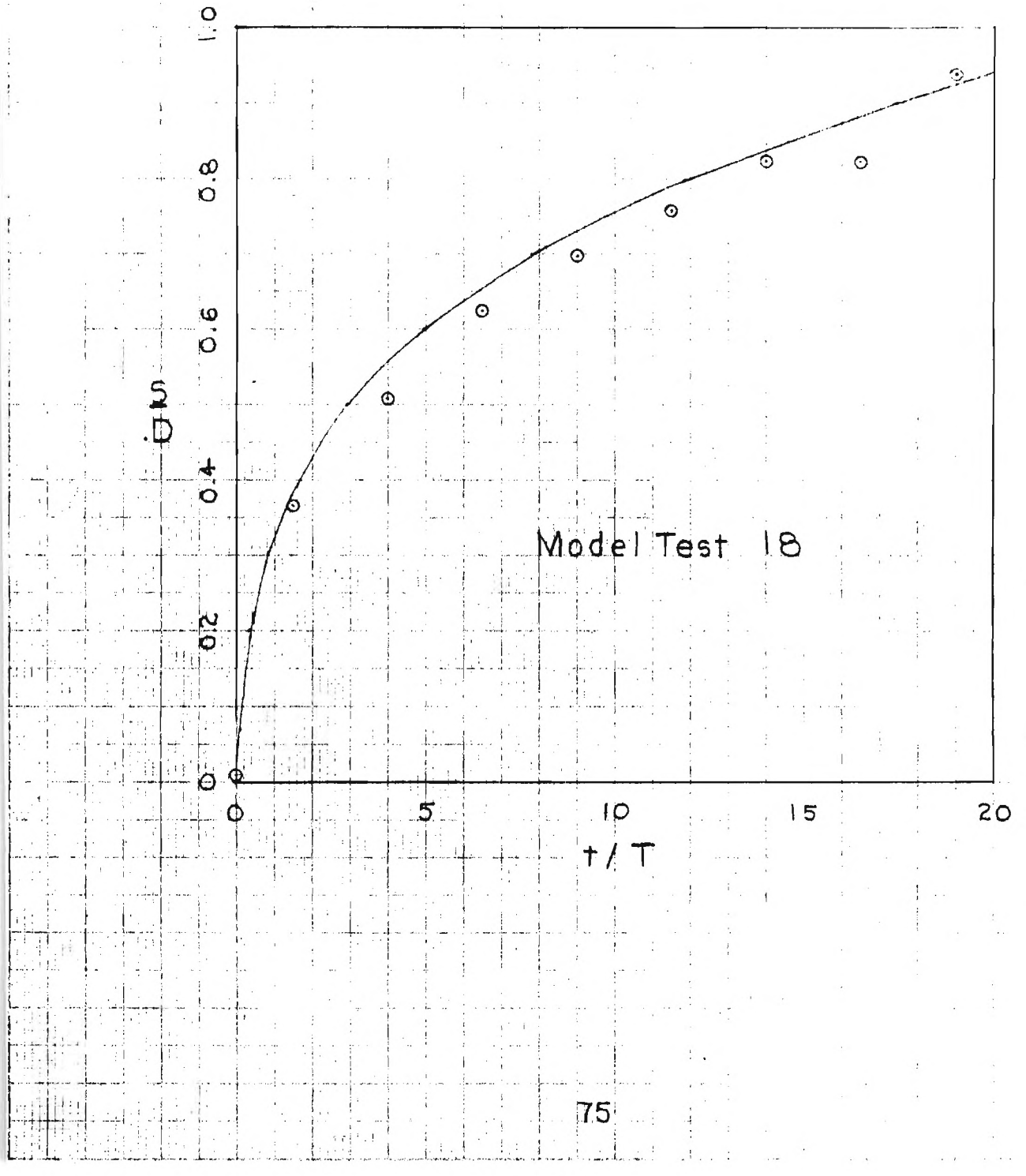
1.0
0.8
0.6
0.4
0.2
0
D
0
5
10
15
20
t / T
Model Test 18

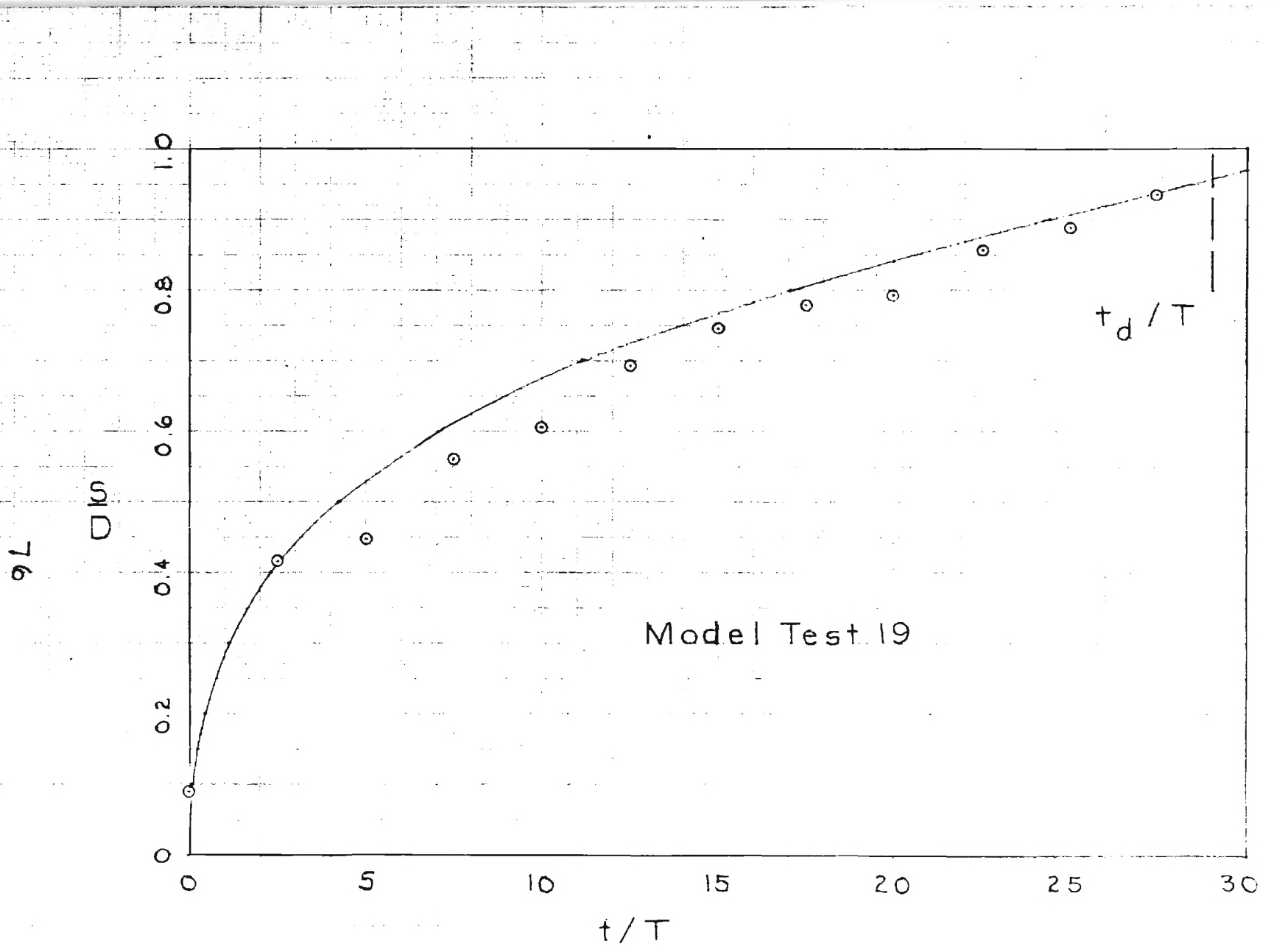
1.0
0.8
0.6
0.4
0.2
0
0
5
10
15
20
25
30
t / T
η_L
$\square_{KS}$
t_d / T
Model Test 19

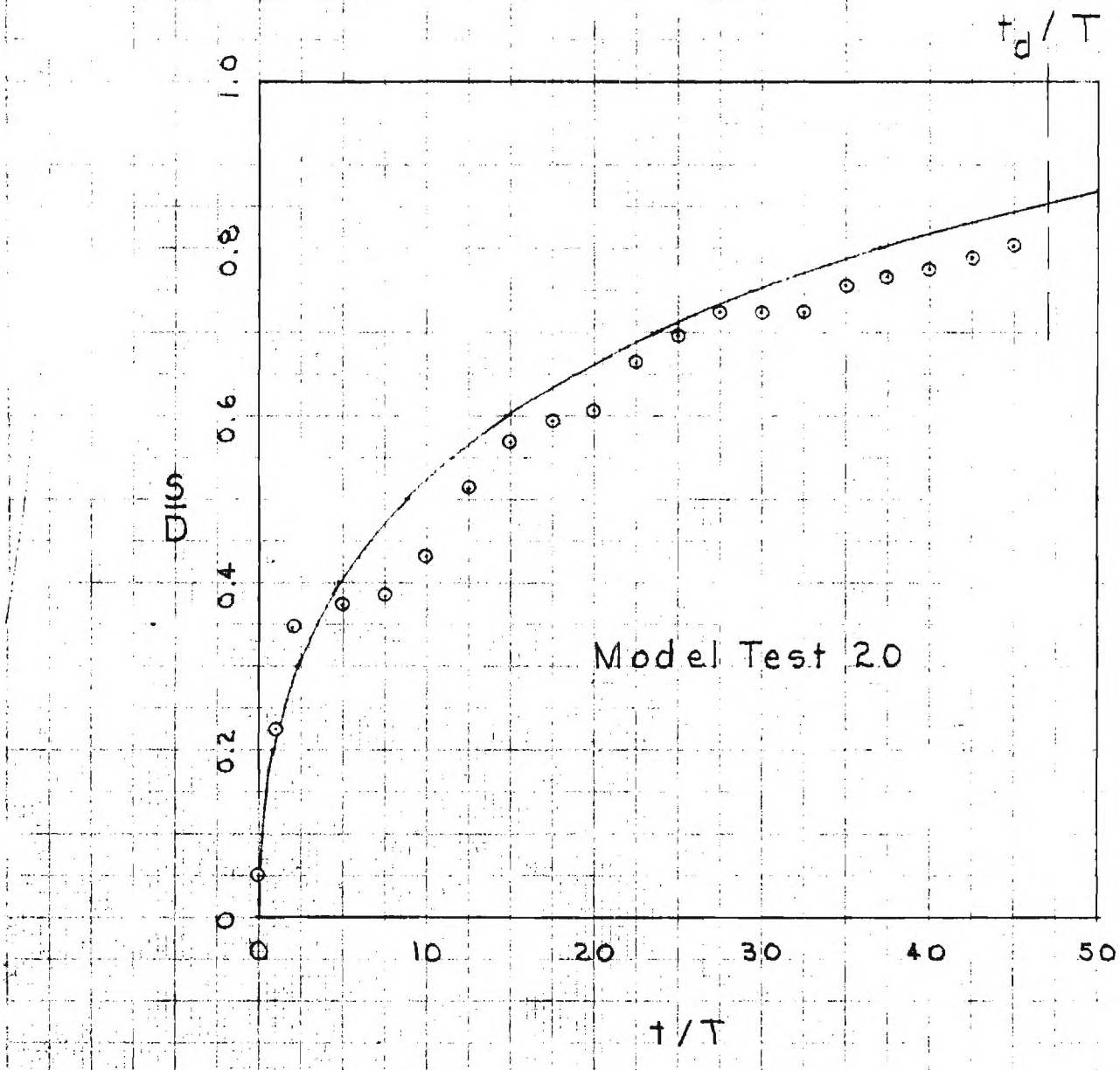
t_d / T
1.0
0.8
0.6
0.4
0.2
0
D/S
Model Test 20
0
10
20
30
40
50
t/T

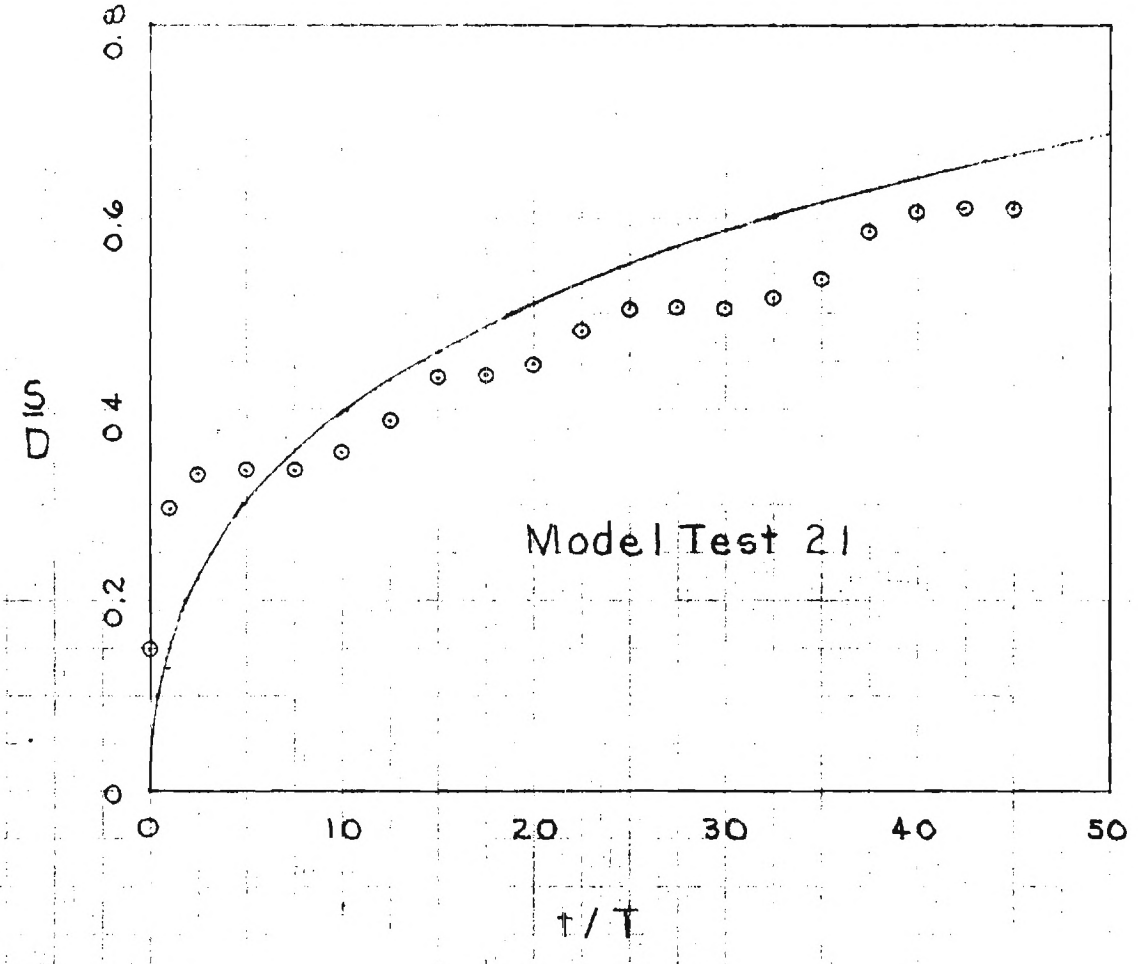
0.8
0.6
0.4
0.2
0
DIS
Model Test 21
0
10
20
30
40
50
t / T

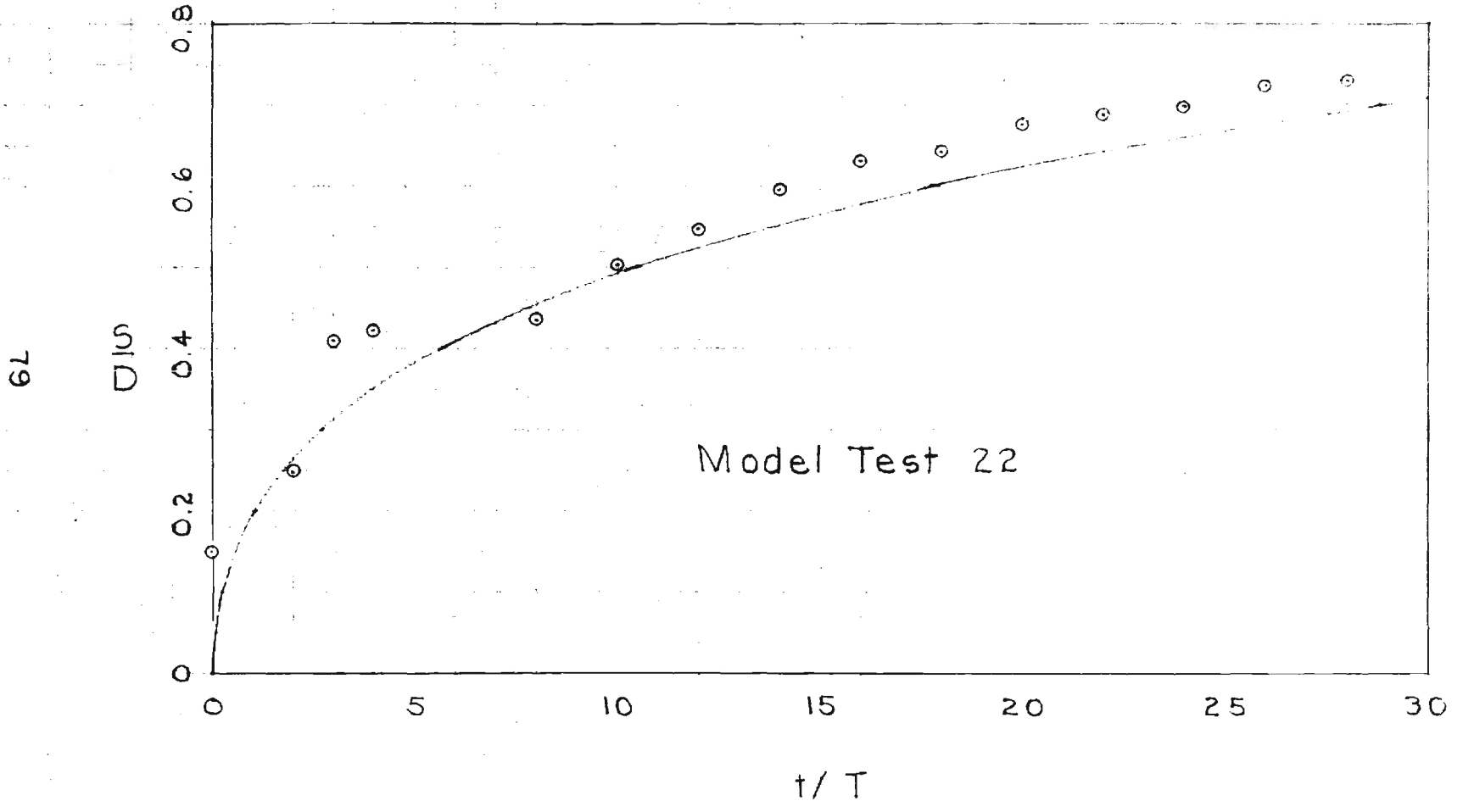
D/S
0.8
0.6
0.4
0.2
0
0
5
10
15
20
25
30
t/ T
Model Test 22

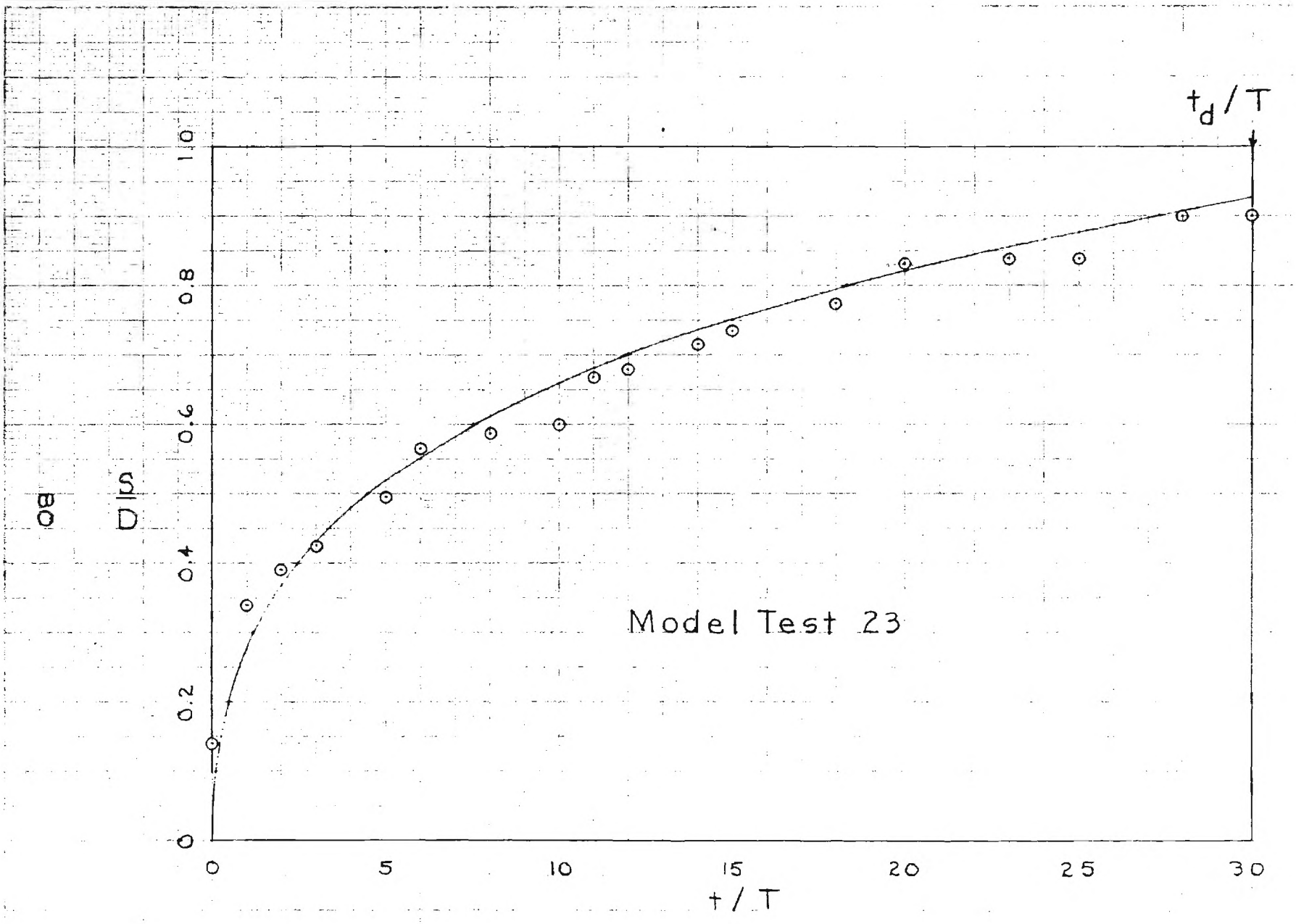
t_d / T
1.0
0.8
0.6
0.4
0.2
0
$\frac{S}{D}$
Model Test 23
0
5
10
15
20
25
30
t / T

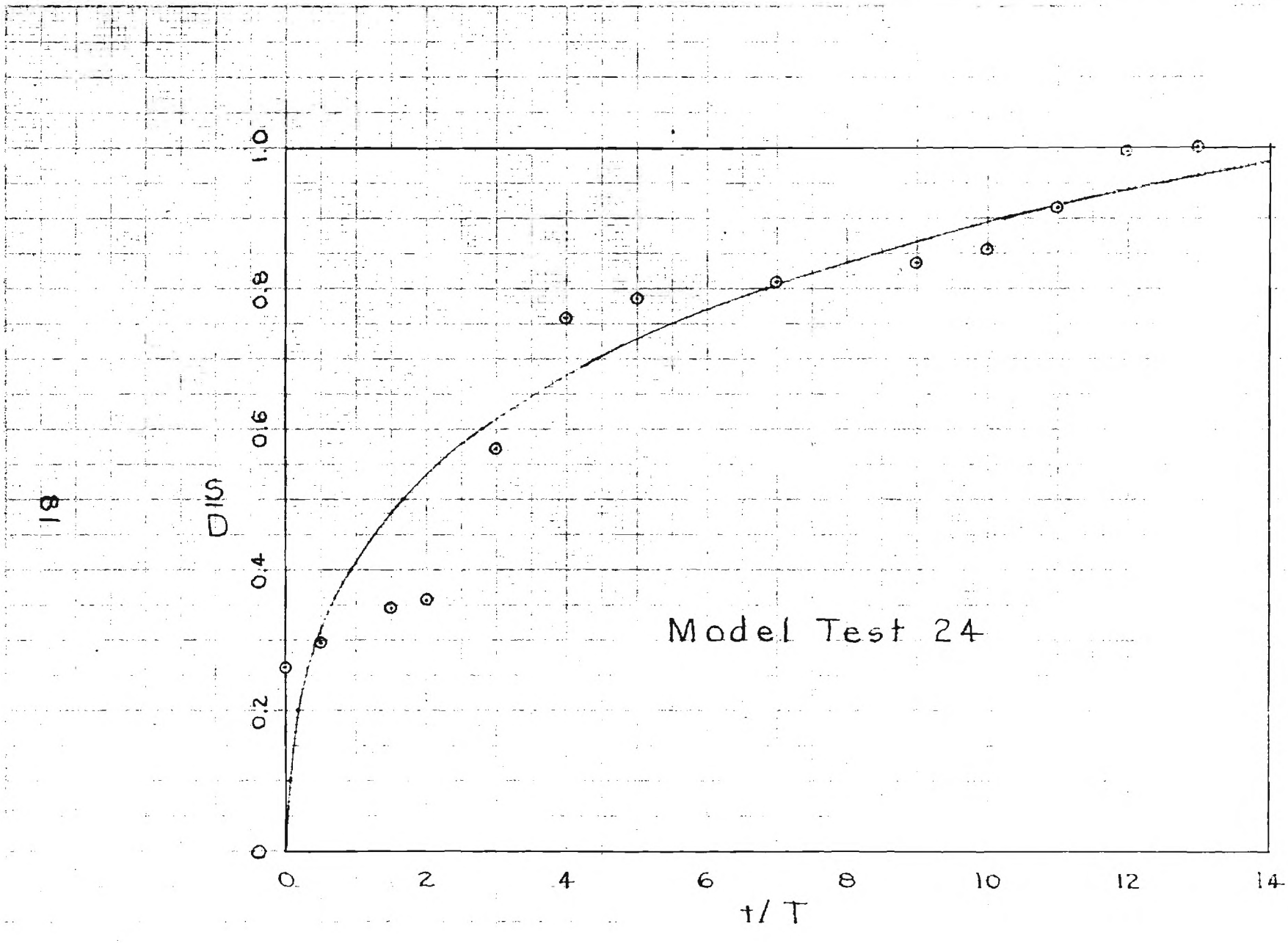
DIS
1.0
0.8
0.6
0.4
0.2
0
0
2
4
6
8
10
12
14
t/T
Model Test 24

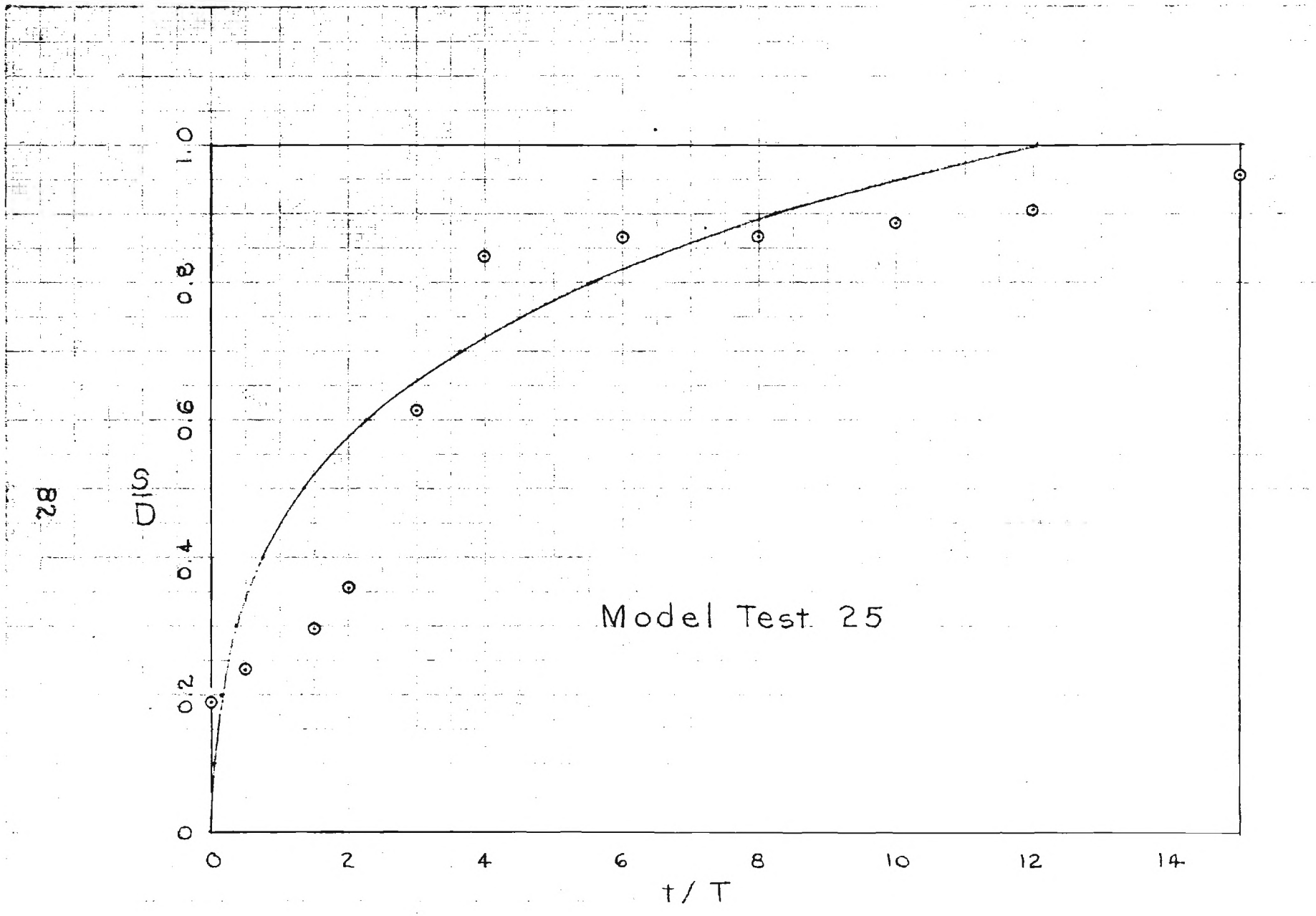
Model Test 25
D/S
t/T
0
0.2
0.4
0.6
0.8
1.0
0
2
4
6
8
10
12
14

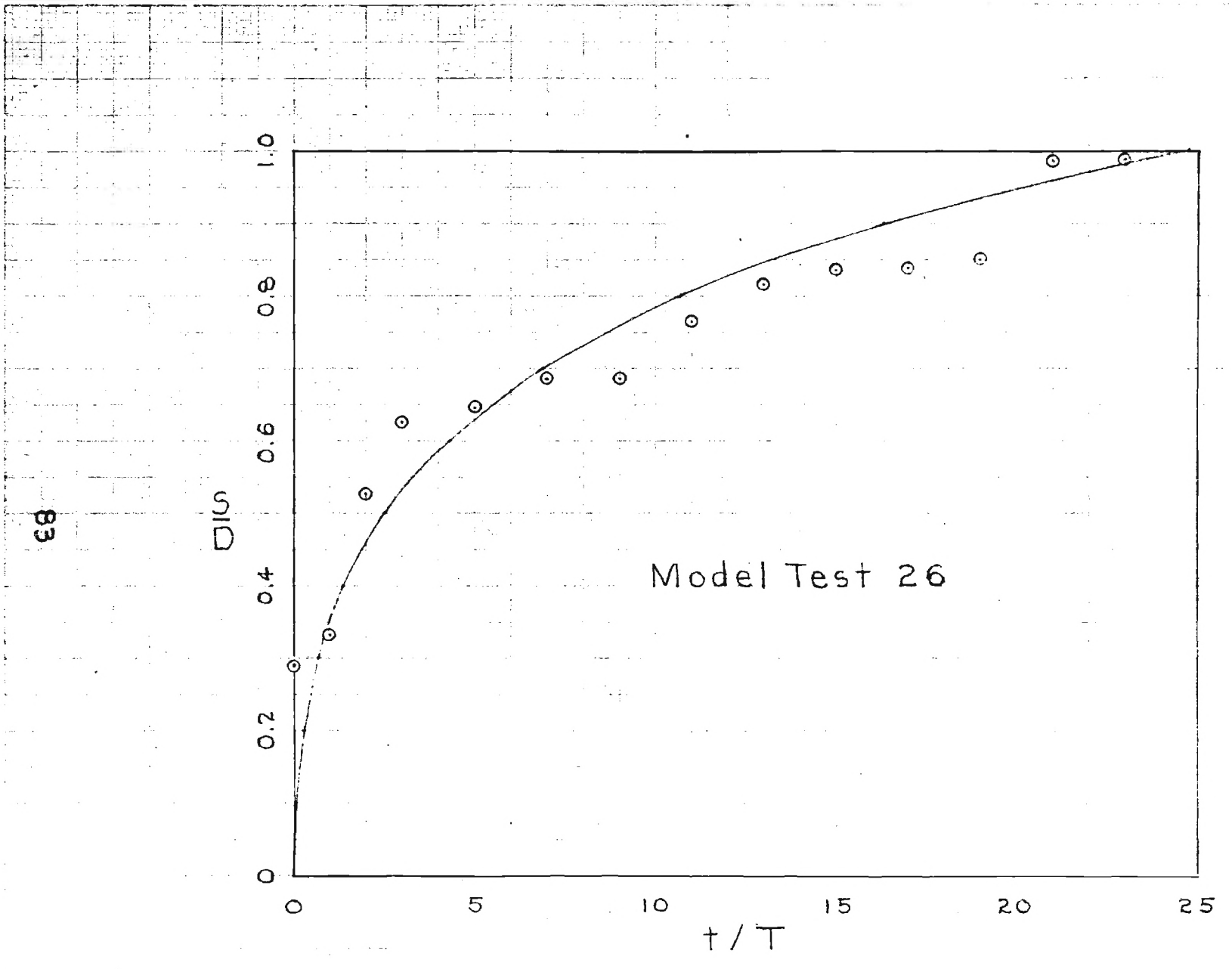
Model Test 26
DIS
t / T
0
0.2
0.4
0.6
0.8
1.0
0
5
10
15
20
25

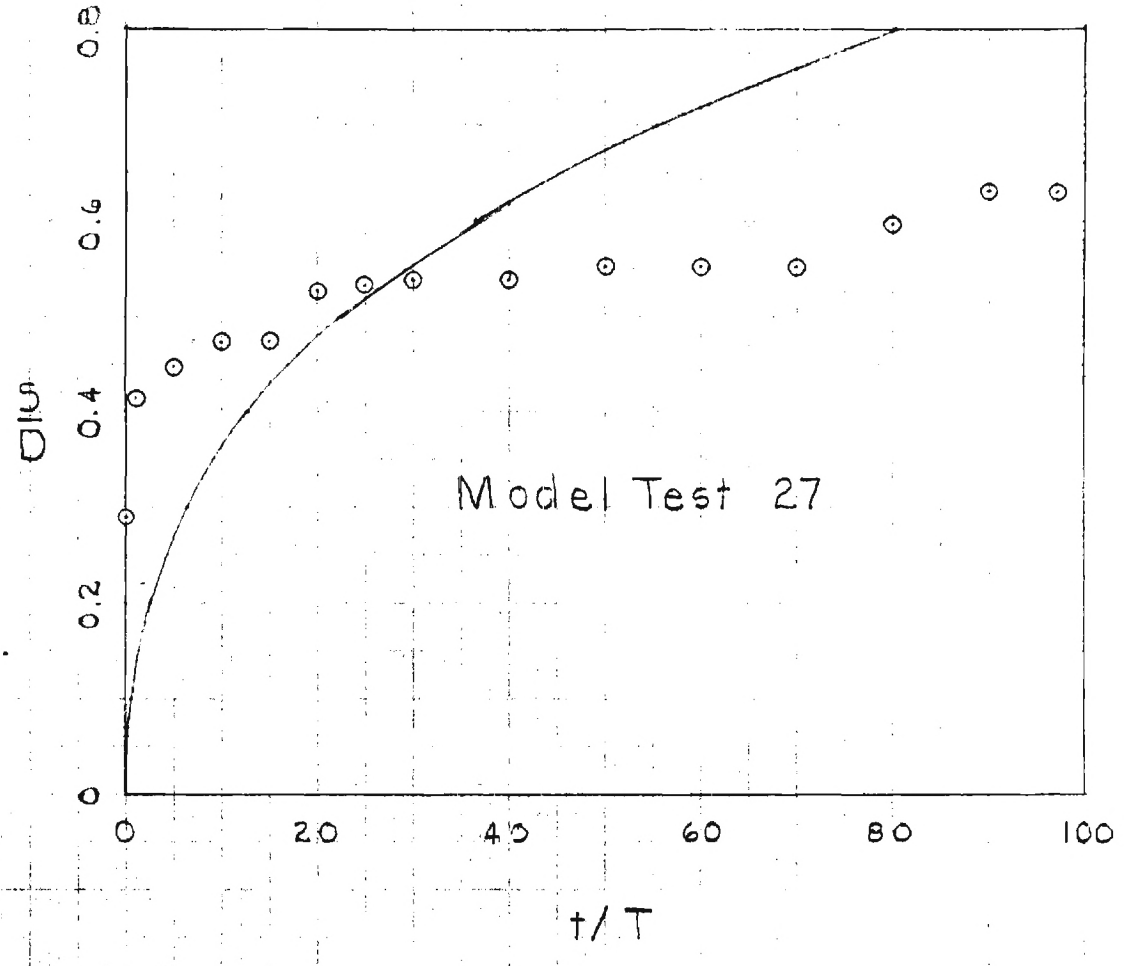
0.8
0.6
0.4
0.2
0
Q/Qs
Model Test 27
0
20
40
60
80
100
t/T

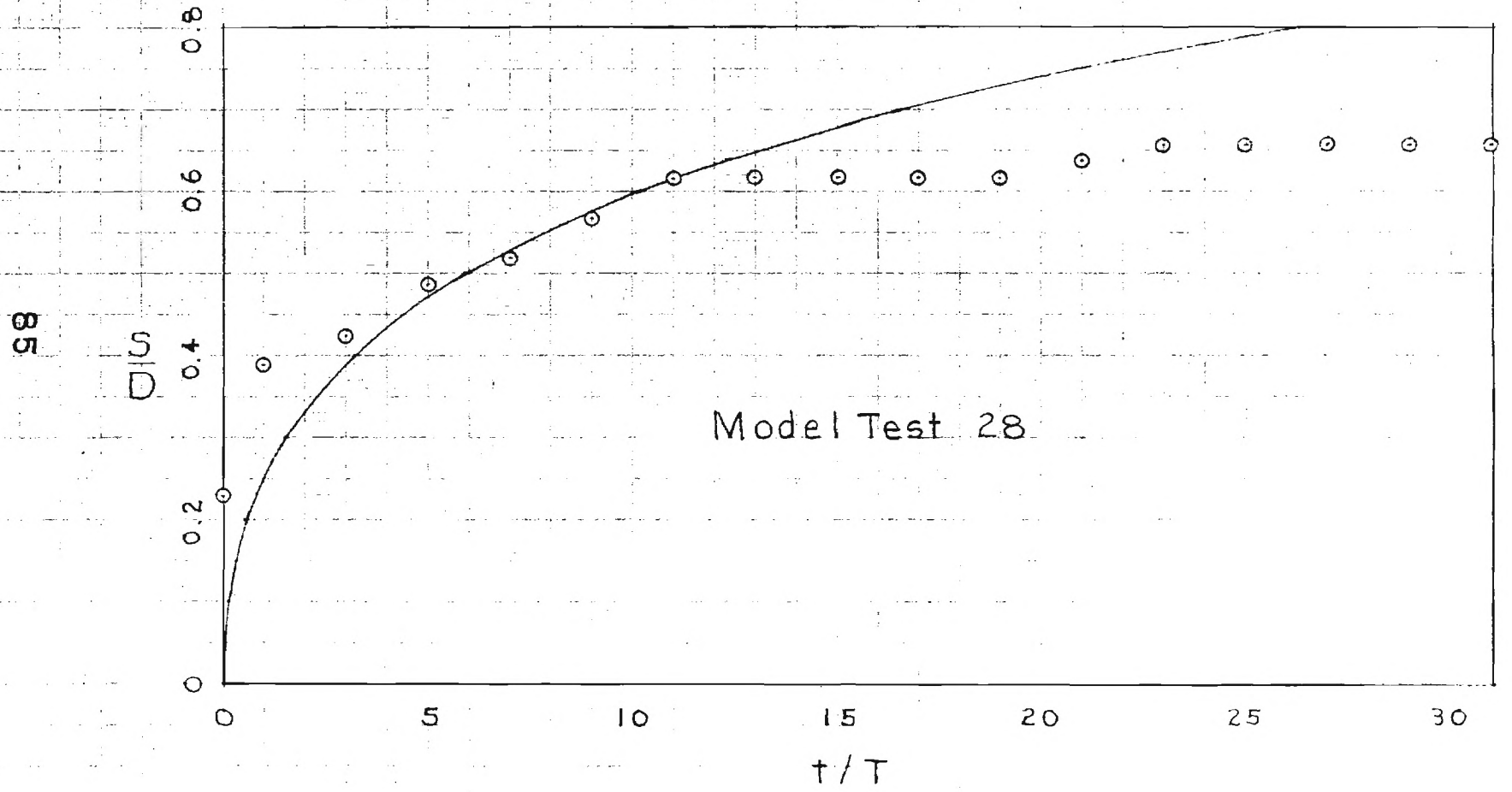
0.8
0.6
0.4
0.2
0
D/S
0
5
10
15
20
25
30
t/T
Model Test 28

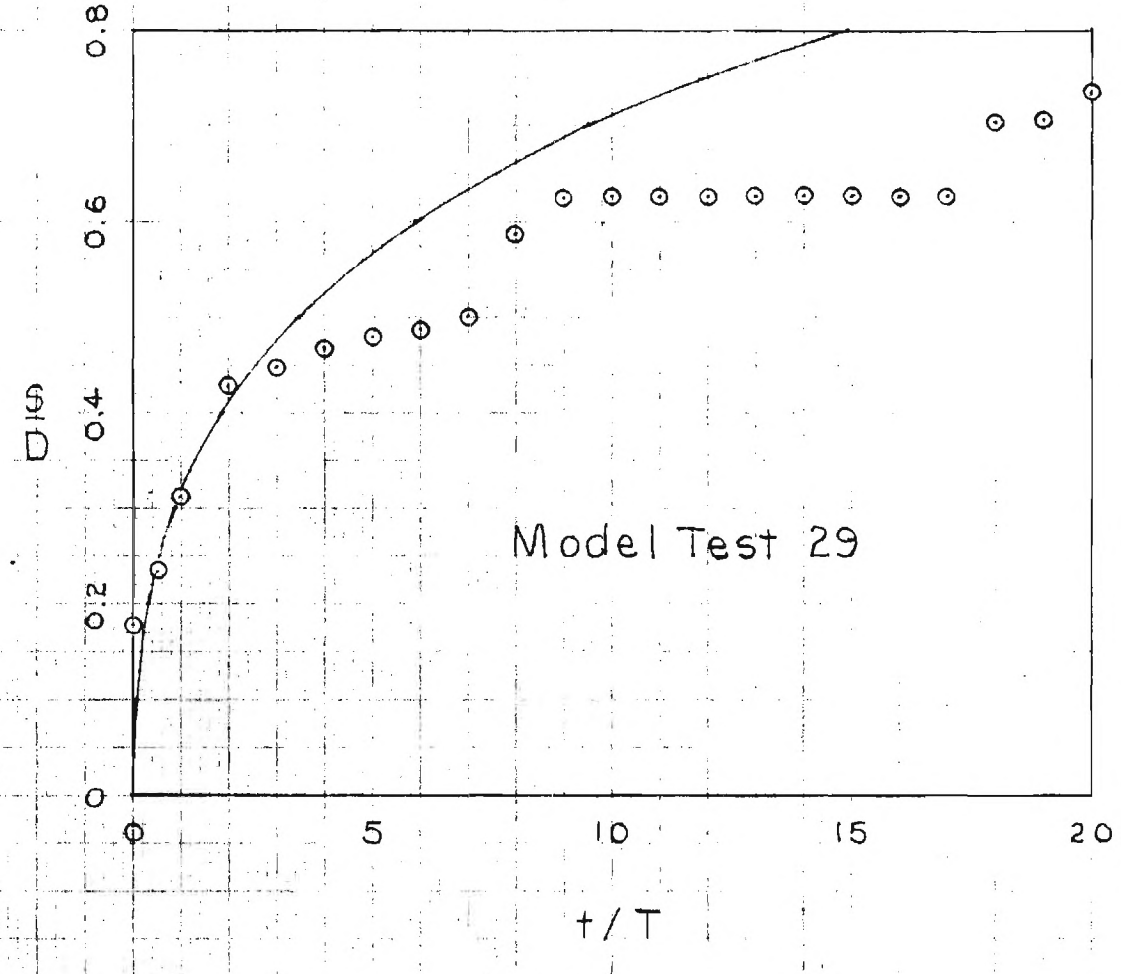
0.8
0.6
0.4
0.2
0
D/S
0
5
10
15
20
t/T
Model Test 29

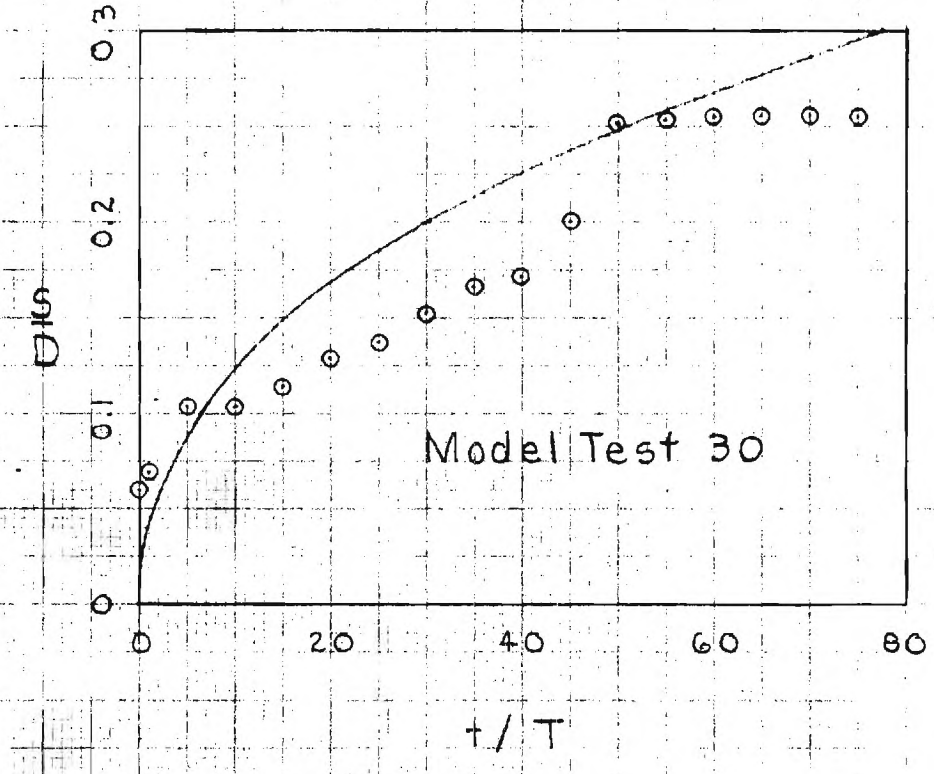
0.3
0.2
0.1
0
Dis
Model Test 30
0
20
40
60
80
t / T

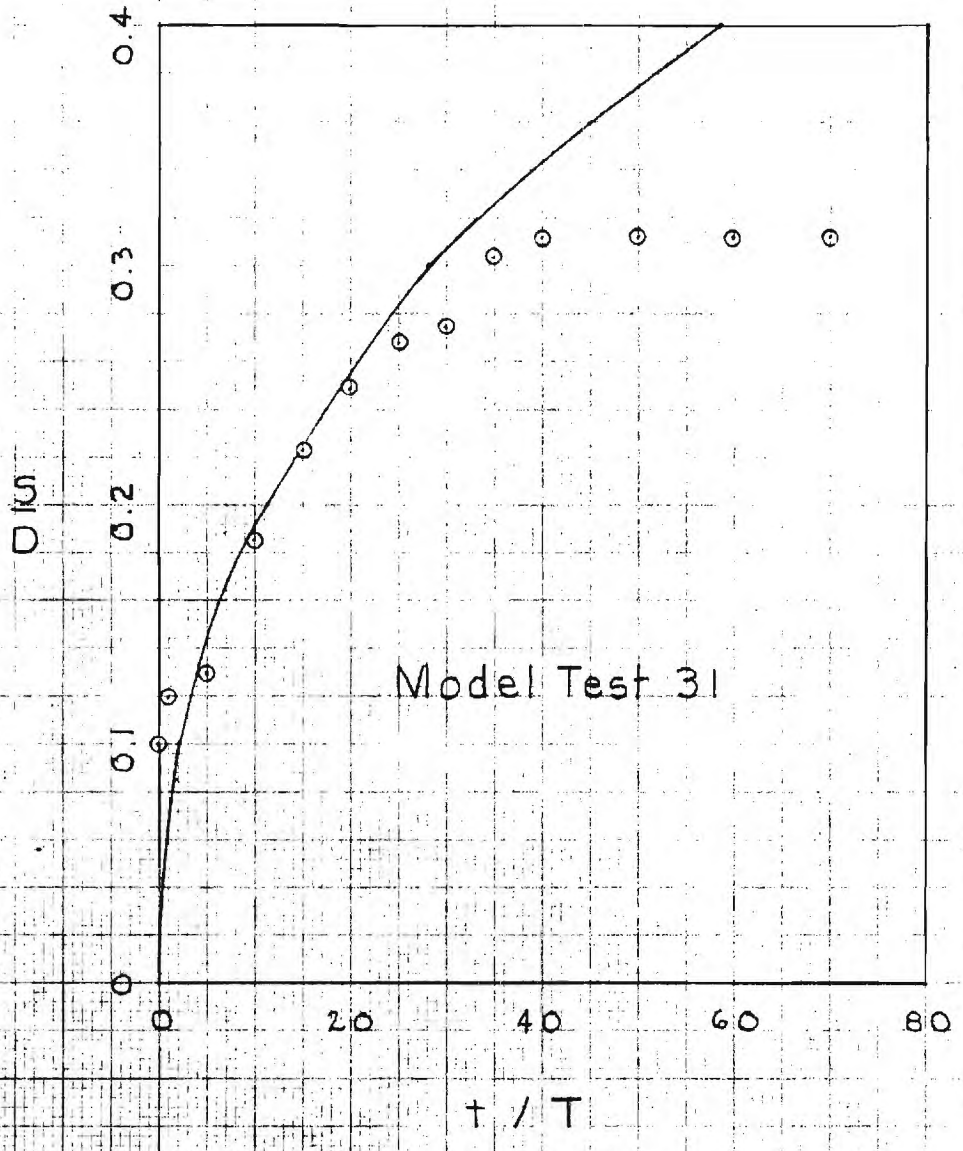
0.4
0.3
0.2
0.1
0
Ds
Model Test 31
0
20
40
60
80
t / T

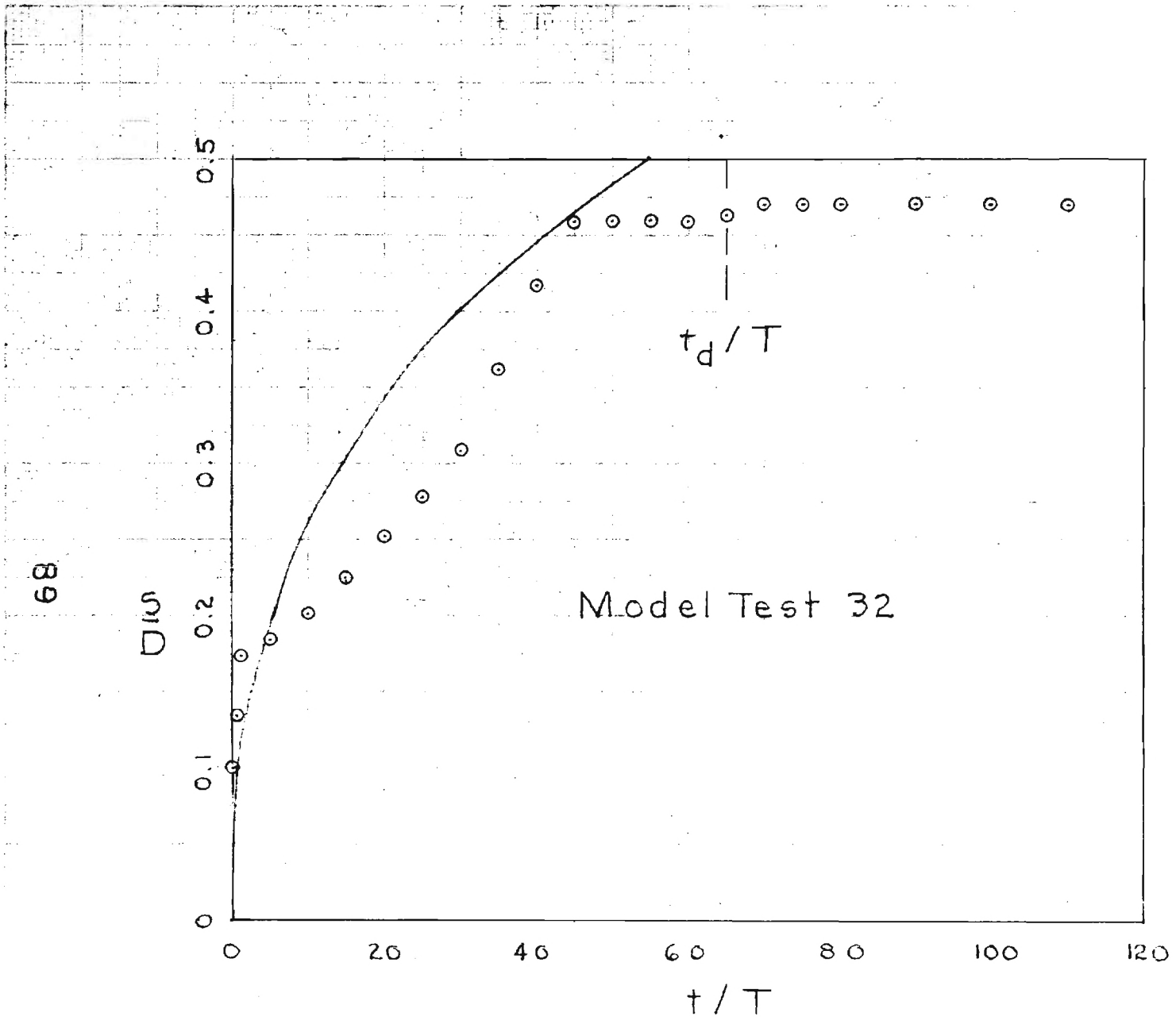
0.5
0.4
0.3
0.2
0.1
0
D/S
t_d / T
Model Test 32
0
20
40
60
80
100
120
t / T

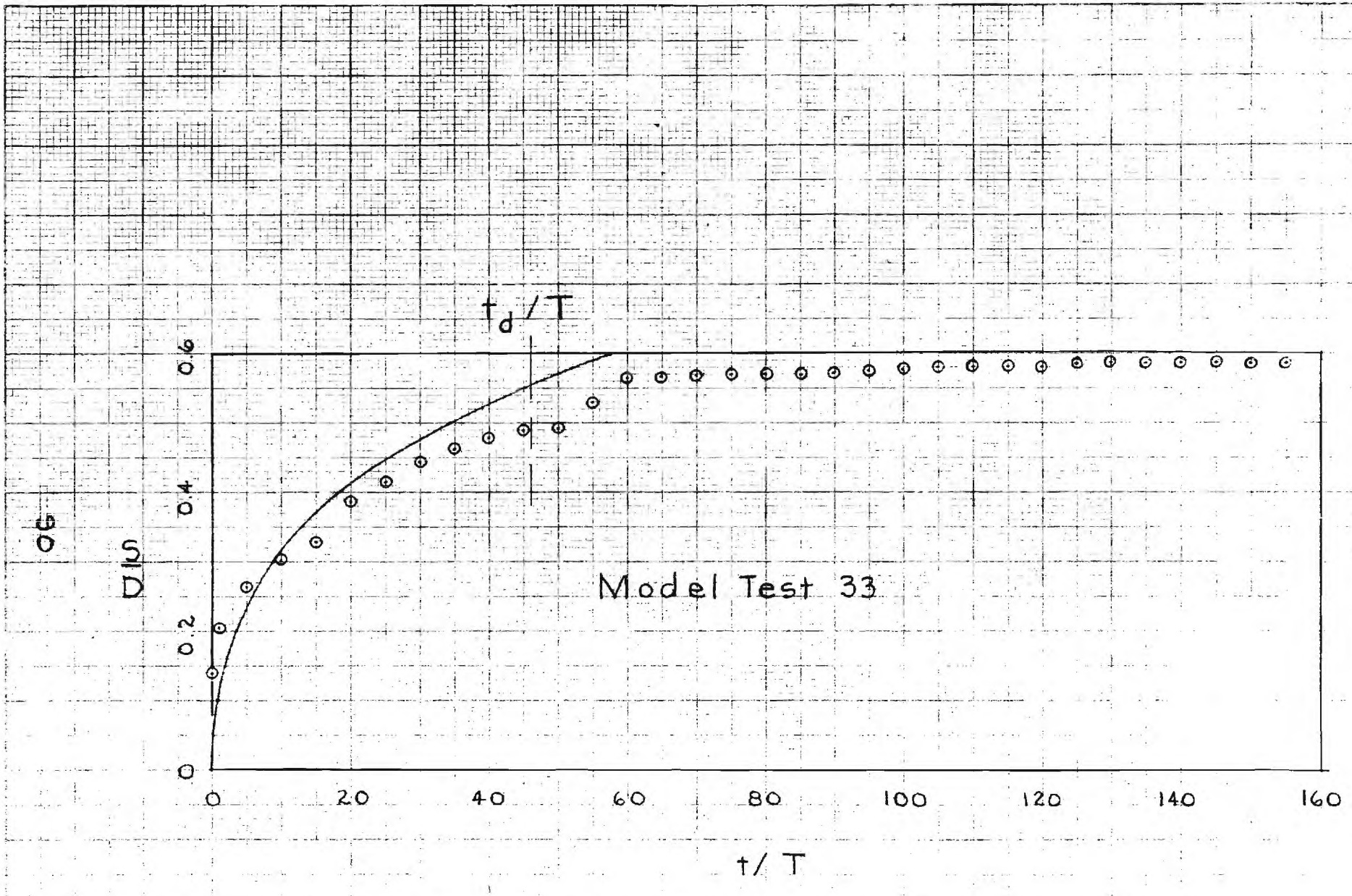
t_d/T
0.6
0.4
0.2
0
DIS
Model Test 33
0
20
40
60
80
100
120
140
160
t/T

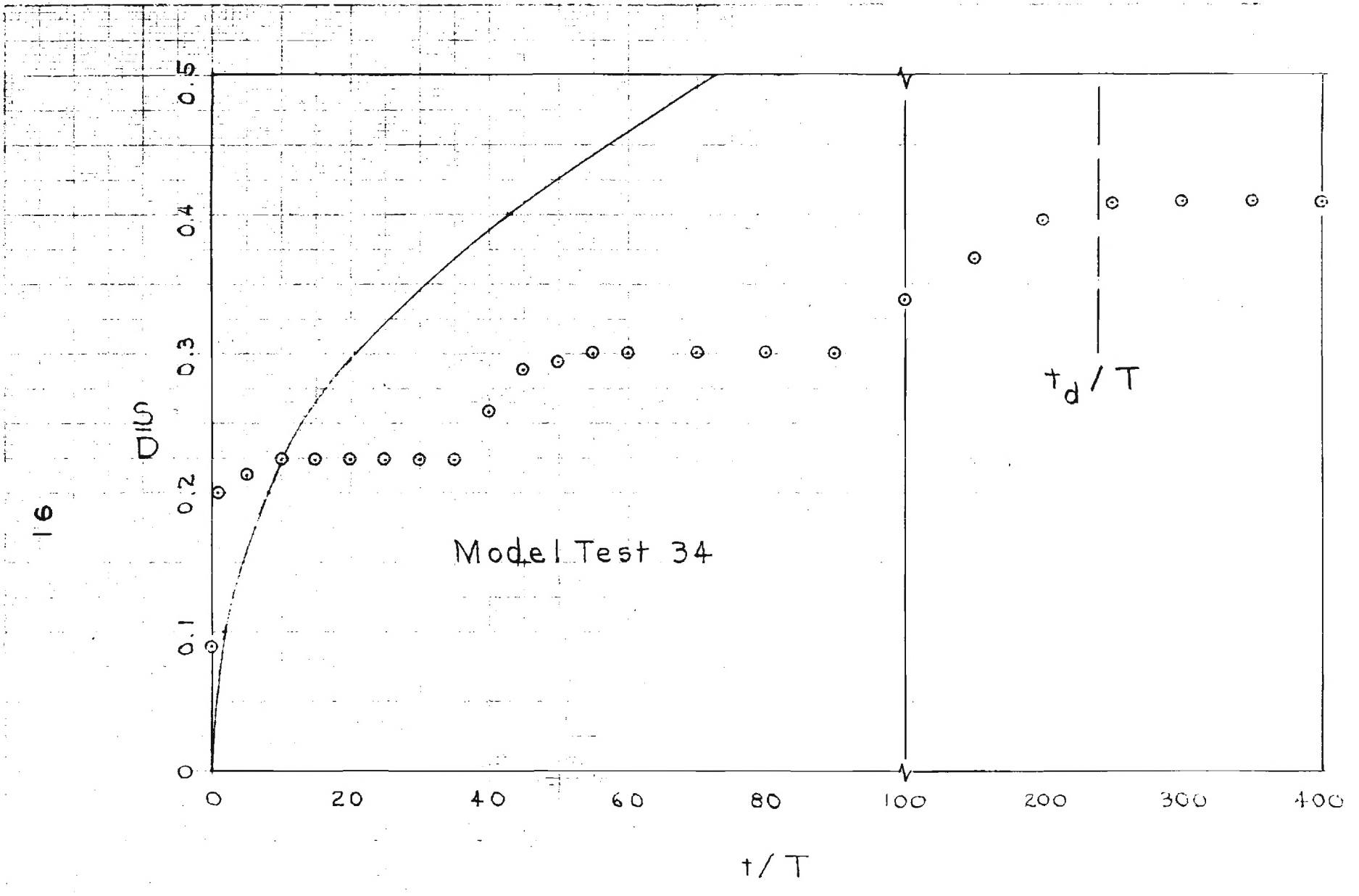
0.5
0.4
0.3
0.2
0.1
0
D/S
0
20
40
60
80
100
200
300
400
t/T
t_d/T
Model Test 34

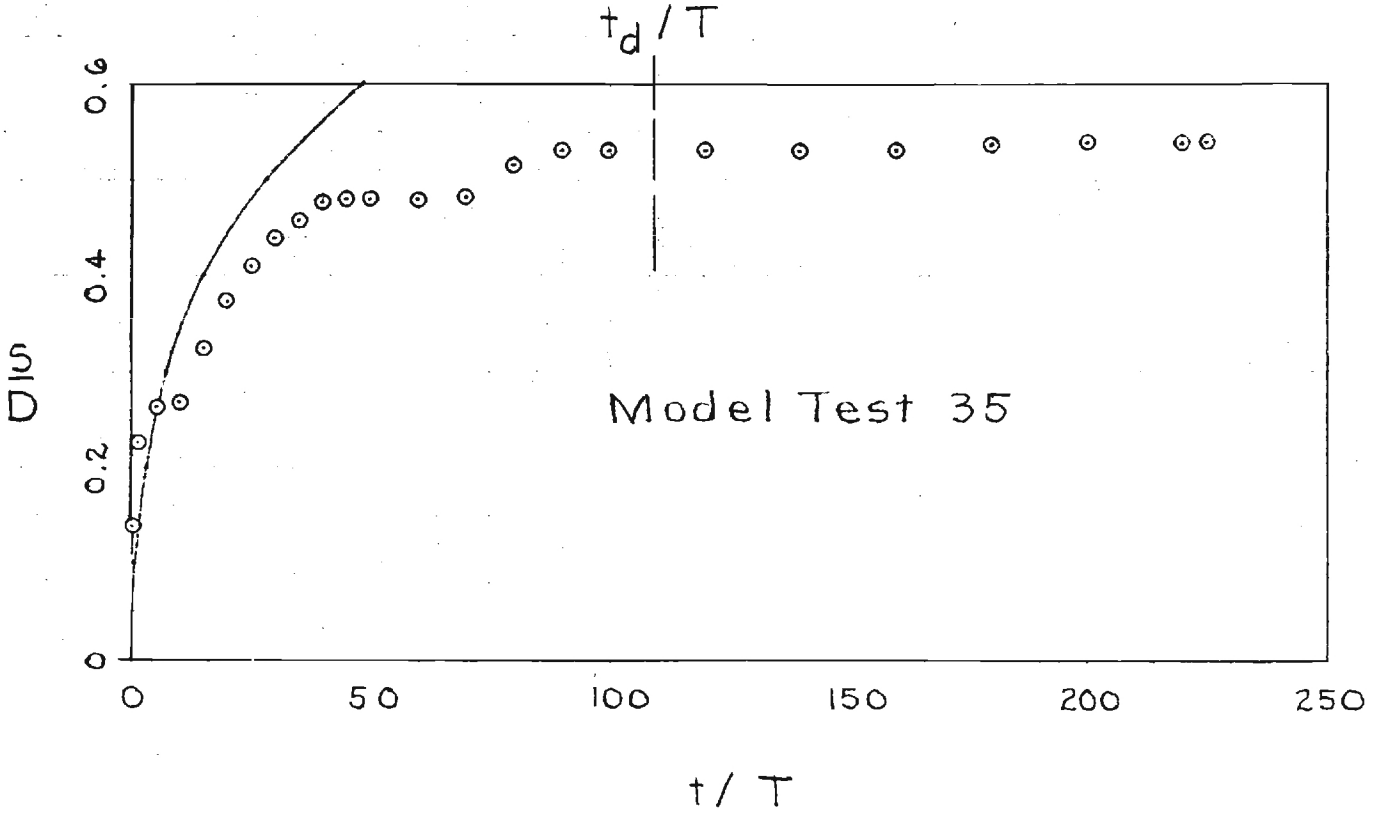
t_d / T
0.6
0.4
0.2
0
DIS
Model Test 35
0
50
100
150
200
250
t / T

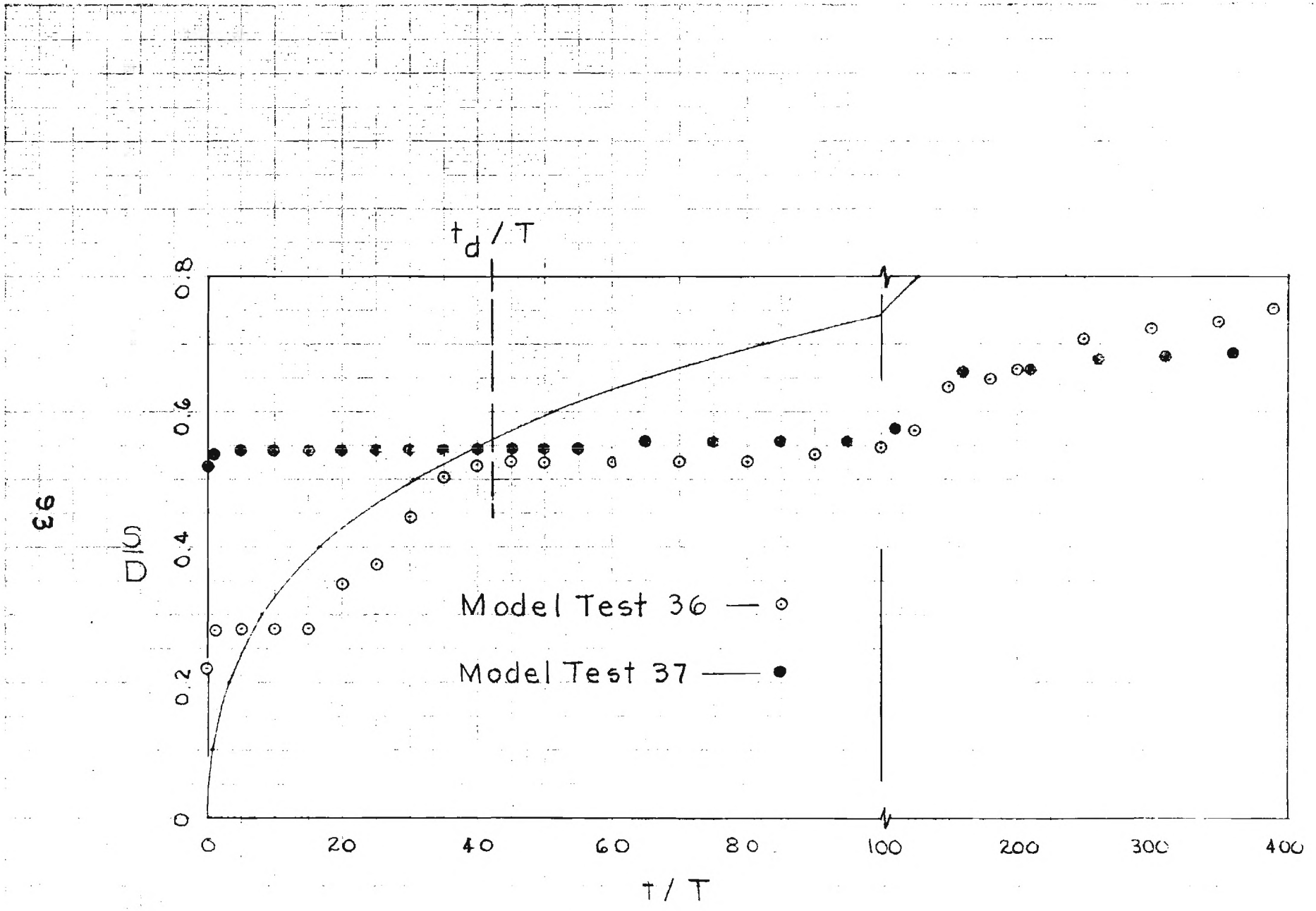
t_d / T
D/S
0.8
0.6
0.4
0.2
0
0
20
40
60
80
100
200
300
400
T / T
Model Test 36
Model Test 37

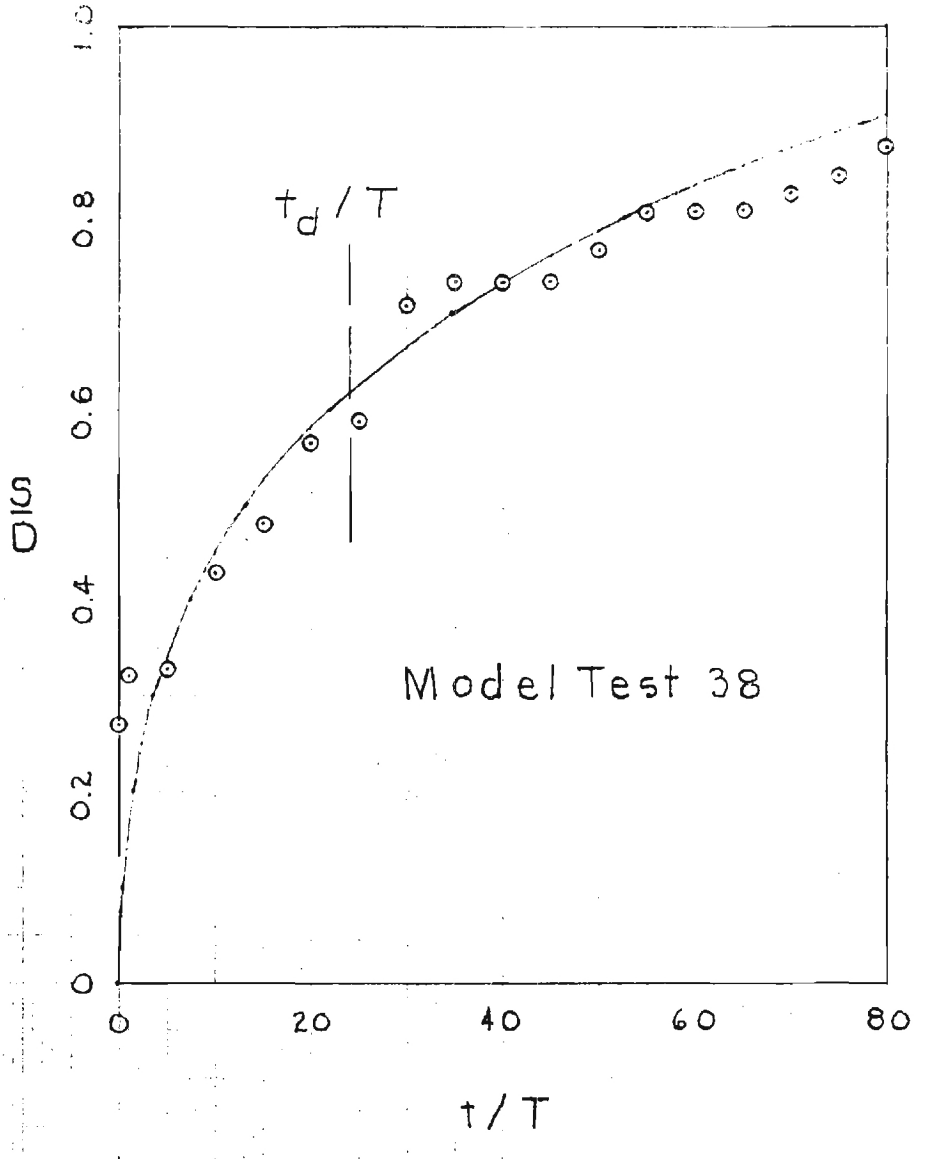
t_d / T
Model Test 38
0
0.2
0.4
0.6
0.8
1.0
0
20
40
60
80
t / T

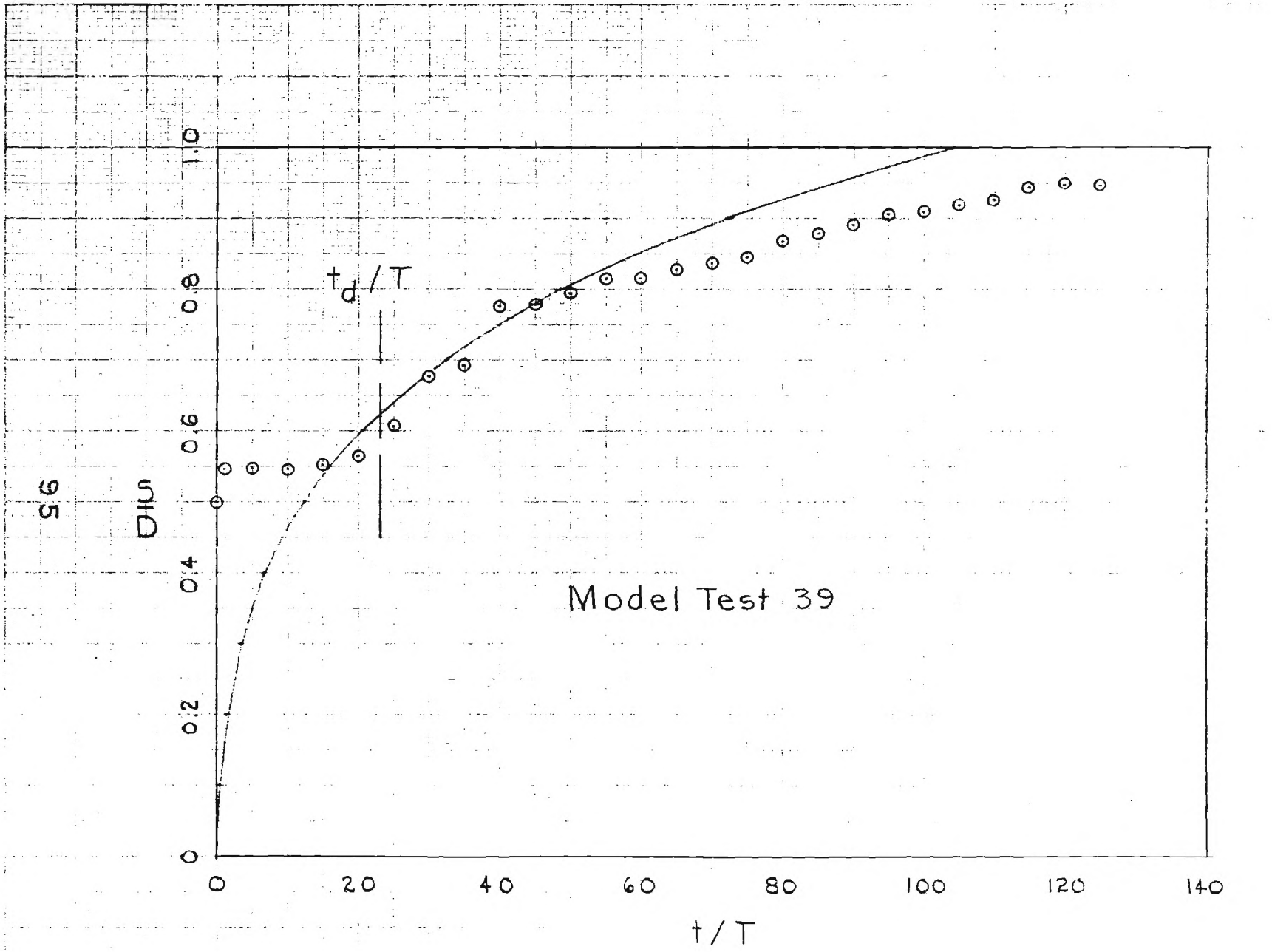
1.0
0.8
0.6
0.4
0.2
0
D/D95
t_d/T
Model Test 39
0
20
40
60
80
100
120
140
t/T

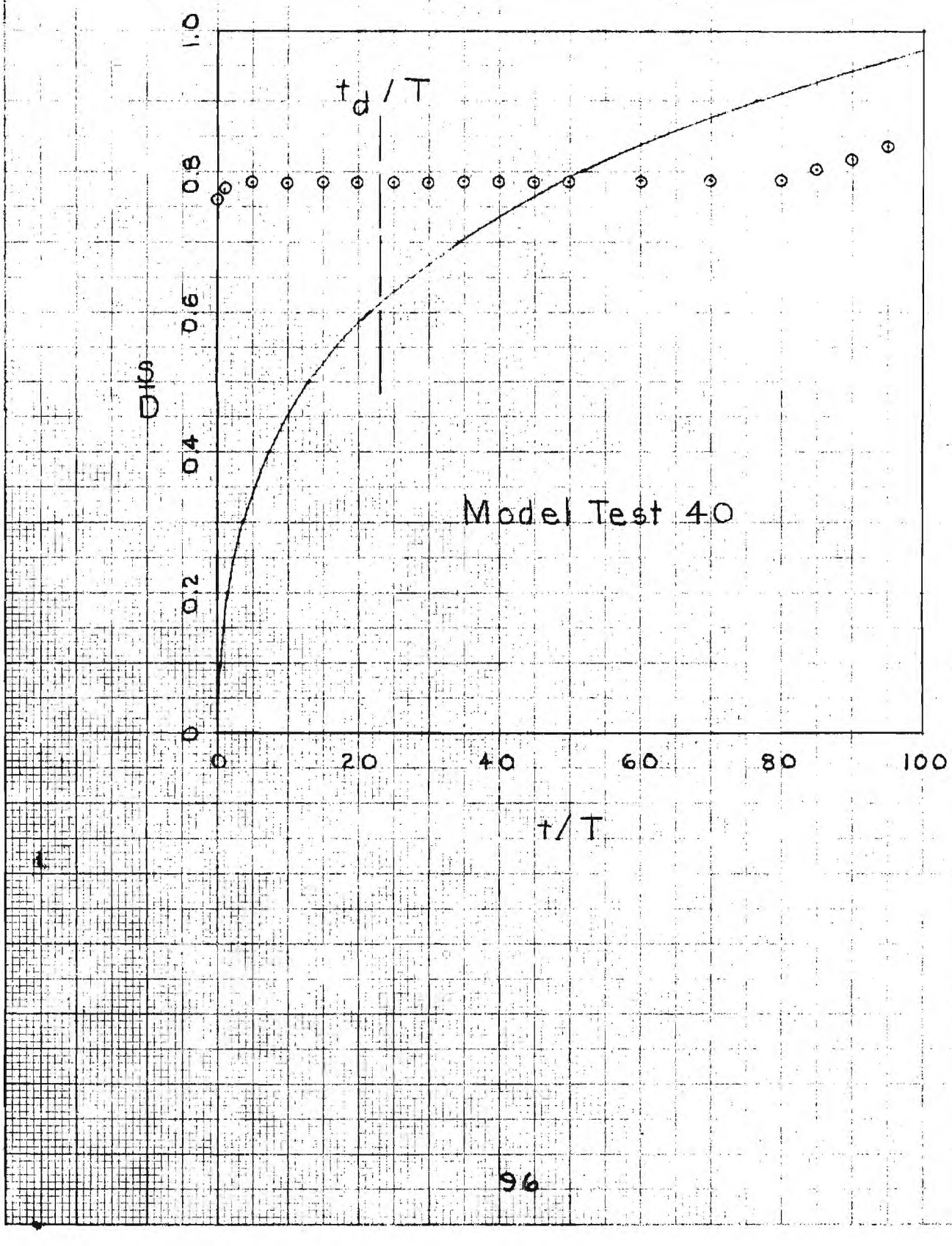
1.0
0.8
0.6
0.4
0.2
0
t_d / T
Ots
Model Test 40
0
20
40
60
80
100
t/T